



01 Jan 2004

Opportunities for Undergraduate Research Experiences (OURE) Research Papers 2004-2005 Volume II

Natalie Davidson

Rachel Dilly

James Duehning

Vanessa L. Eckhoff

et. al. For a complete list of authors, see <https://scholarsmine.mst.edu/oure/208>

Follow this and additional works at: <https://scholarsmine.mst.edu/oure>

Recommended Citation

Davidson, Natalie; Dilly, Rachel; Duehning, James; Eckhoff, Vanessa L.; Elmer, Jacob James; Fennewald, Tom; Ferrari, Gaston E.; Golden, Nicole; Grondin, Sarah; Hall, Jason; Heeszal, David; Hunter, Reanea; Hyzer, Kylee; Keeven, John; Kothari, Rahul; Kuligowski, M.; Lopez, Jorge; Mattson, Tricia; McEllen, Andrew; Miller, Justin; Moss, Benjamin; Munson, Justin; Naeger, Jacob; Naruka, Vaishalee; Nguyen, Nguyet; O'Berry, Moya; and Parish, Ryan, "Opportunities for Undergraduate Research Experiences (OURE) Research Papers 2004-2005 Volume II" (2004). *Opportunities for Undergraduate Research Experience Program (OURE)*. 208.

<https://scholarsmine.mst.edu/oure/208>

This Presentation is brought to you for free and open access by Scholars' Mine. It has been accepted for inclusion in Opportunities for Undergraduate Research Experience Program (OURE) by an authorized administrator of Scholars' Mine. This work is protected by U. S. Copyright Law. Unauthorized use including reproduction for redistribution requires the permission of the copyright holder. For more information, please contact scholarsmine@mst.edu.



Opportunities for Undergraduate Research Experiences (OURE)

Research Papers

2004 -2005

Volume II

(Da – Pa)

Opportunities for Undergraduate Research Experience (OURE)
Research Papers – 2004-2005
Volume- II
INDEX (Da - Pa)

This volume includes 2004-2005 OURE research papers authored by the following students (listed alphabetically by student's last name)

Davidson, Natalie
Dilly, Rachel
Duehning, James
Eckhoff, Vanessa L.
Elmer, Jacob James
Fennewald, Tom
Ferrari, Gaston E.
Golden, Nicole
Grondin, Sara
Hall, Jason
Heeszel, David
Hunter, Reanea
Hyzer, Kylee
Keeven, John
Kothari, Rahul
Kuligowski, M.
Lopez, Jorge
Mattson, Tricia
McEllen, Andrew
Miller, Justin
Moss, Benjamin
Munson, Justin
Naeger, Jacob
Naruka, Vaishalee
Nguyen, Nguyet
O'Berry, Moya
Parish, Ryan

Tundra Orbit Constellation
Natalie Davidson
University of Missouri-Rolla
Professor Hank Pernicka

Abstract

The popular geostationary orbit has become overcrowded with satellites. To remedy this problem, Tundra Orbit Constellations have been proposed. A Tundra Orbit is a constellation of three or more satellites orbiting in an inclined eccentric orbit. The purpose of this study is to provide an alternative to the geostationary belt and supply continuous coverage for the Northern Hemisphere, in particular the United States. To ensure the most economical configuration of satellites, an analysis of the benefits of number of satellites in such orbits and the change in coverage they provide must be performed. During analysis, it was discovered that comparisons between current and previous results produced dissimilarities. An evaluation of the software code was performed to determine errors. After an intensive assessment of the software code, errors continue to be sought and the comparisons of results were analyzed.

Introduction

A Tundra Orbit Constellation is a collection of three or more satellites orbiting in an inclined eccentric orbit¹. A Tundra orbit, as defined by Bruno², consists of the following orbital elements displayed in Table A.

Table A: Orbital Elements

Parameter	Value
Semimajor Axis (a)	42164.16 km
Inclination (i)	63.4°
Eccentricity (e)	0.2684
Argument of Perigee (ω)	270°

The above orbital elements were used to perform this study. Particular values for the Right Ascension of the Ascending Node (ω) were defined by Bruno, but adjusted for this analysis using

$$\Omega = -100.0^\circ + (360^\circ/N)t \quad (1)$$

Where N is the number of satellites in the constellation and t is each satellite in sequence. For example t would be one for the first satellite, two for the second satellite, etc.

Objective

Due to the low elevation of satellites traveling in the geostationary orbit belt, there are many perturbations that affect the satellite signal. Examples might include mountains or tall buildings. Ideally, an elevation of 90 degrees would prevent virtually any obstruction from having an effect on the signal. For example, as one drives around town, there are certain locations in which one cannot receive certain radio stations. As one examines the surroundings, one finds that buildings are common. These buildings block the signal coming from geostationary satellites because they

orbit at a low elevation (for users in northern latitudes such as the U.S. and Europe). Therefore, if a satellite is orbiting at an elevation of 90 degrees, it will pass straight above the receiver, removing all possibilities of interference of the signal. If a satellite in a highly inclined eccentric orbit is created with a perigee in the Southern Hemisphere, it will travel quickly throughout that hemisphere and very slowly throughout the Northern Hemisphere, the target region, as it passes through apogee. By transforming that single satellite into a constellation of three or more satellites, they can be staggered so that as one satellite declines in elevation another is rising above the horizon to take its place. To determine the best configuration of satellites, several factors needed to be taken into account. Cost and effectiveness of the satellite coverage were the most important factors. The more satellites in the constellation, the greater the coverage is and a greater population can receive coverage from the satellite. However, more satellites also lead to a greater cost. So, the objective was to optimize cost and effectiveness of the satellite coverage at the same time.

Approach

The previously written software code first needed to be verified. This was done by obtaining the code that plots several different parameters such as time, elevation of the satellites, number of satellites used in the constellation, and latitude and longitude points for the satellites crossing between North America and South America. This code was written using the MATLAB software.

The first plot to verify for accuracy was a time verses elevation plot. This plot proved to be accurate with previous results. Figure 1 shows the elevation verses time for 24 hours for a constellation of just three satellites as seen from Rolla, Missouri. The three satellites are phased evenly and the three peaks represent the maximum points of elevation, which correspond to the apogee of each respective satellite. The lowest points of elevation represent where one satellite sets and the next rises above the horizon. On this graph, the low point is approximately 61 degrees.

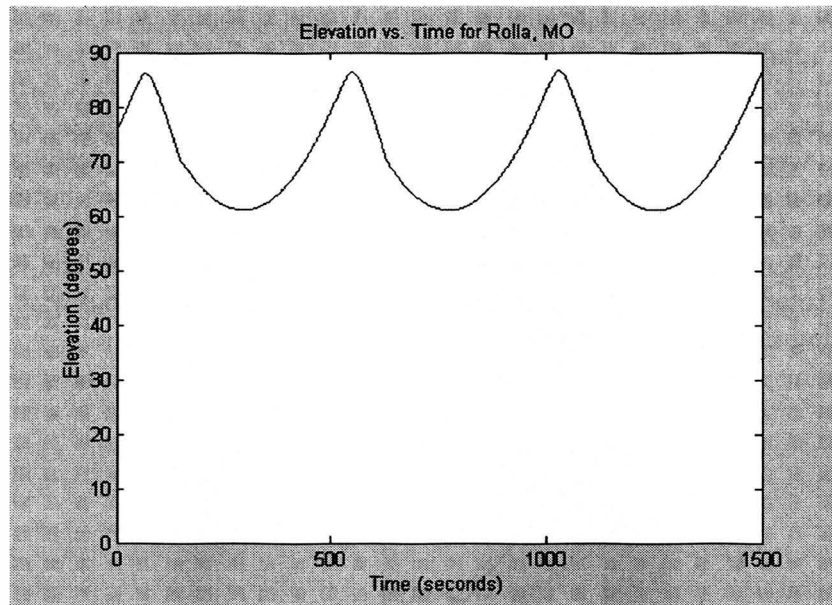


Figure 1: Three Satellites over Rolla, Missouri

A second plot to be verified was also a time versus elevation plot, but with a constellation of nine satellites instead of just three. This plot also proved to be accurate with previous results. The effect of tripling the number of satellites is shown in Figure 2. By increasing the number of satellites to nine the minimum elevation is increased to 73 degrees. However, increasing the number of satellites also increases the cost. Therefore, it would need to be determined if an increase in minimum elevation is worth triple the cost.

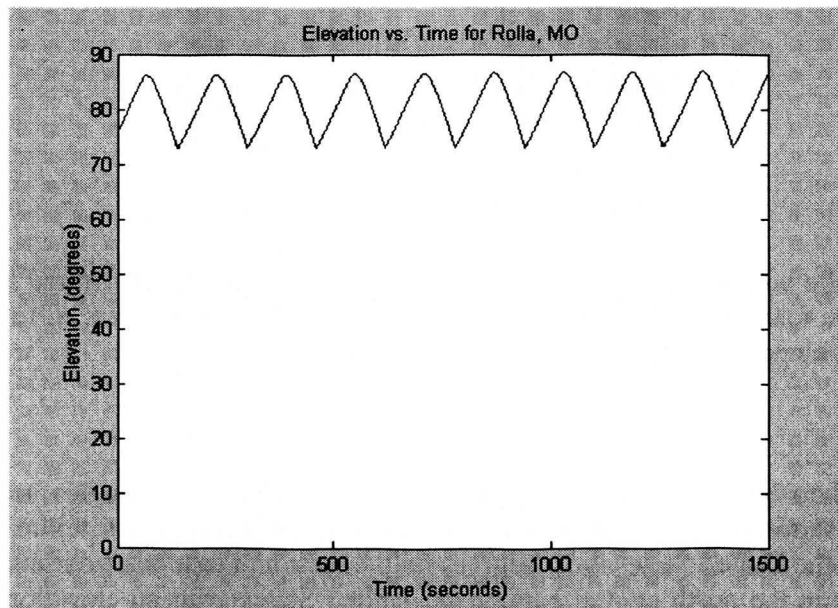


Figure 2: Nine satellites over Rolla, Missouri

Another plot to be verified was a latitude vs. longitude plot (ground track) over North and South America. When compared with previous results, this plot was found to be accurate. Figure 3 shows the pattern of the satellites with respect to latitude and longitude coordinates over North and South America. The graph ranges from 65 degrees south to 65 degrees north latitude, and from 130 degrees west to 45 degrees west. The point at which the satellite crosses over its path is where the elevation increases again. This point is at about 17.3 degrees north. The satellites' pattern is a figure eight due to the slow motion at apogee. The lower portion of the pattern is a clockwise motion because the satellite speeds up to pass through perigee and is traveling faster than the Earth's rotation. The upper portion of the pattern is a counterclockwise motion because the Earth is rotating faster than the satellite.

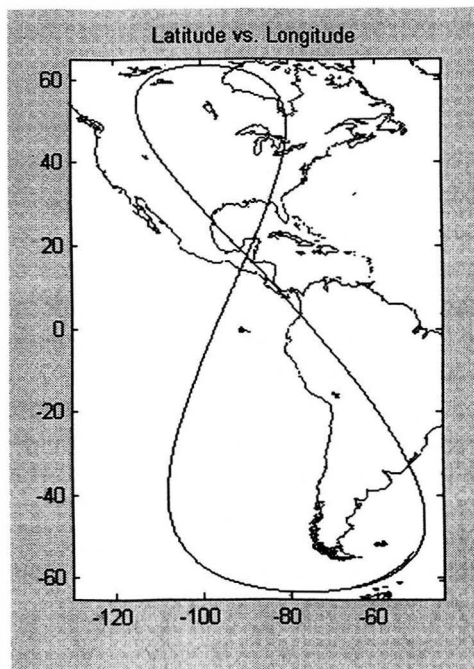


Figure 3: Tundra Ground Track

The last plot to be verified was a minimum elevation angle plot of the United States. This plot was proven to be inaccurate with previous results. Therefore, an analysis of the software code for errors was to be performed.

Current Status

The plots found to be inaccurate displayed the minimum elevation angles across the United States. Figure 4 shows the previous results using a constellation of three satellites. The minimum elevation across the United States is 55 degrees on the west and east coast oceans. The maximum elevation occurs in the north central part of the United States with an elevation of 75 degrees. This plot ranges from 125 degrees west to 65 degrees west longitude (x-axis) and 24 degrees north to 50 degrees north latitude (y-axis). This is the same range used in Figures 5, 6 and 7 as

well. It is clear that coverage would be more effective at higher latitudes towards the center of the United States according to this plot.

In comparison with the previous results, Figure 5 displays the current results for a constellation of three satellites over the United States as well. According to this plot, minimum elevation angles consistently increase northward. The minimum elevation across the United States is 62 degrees in the southeast part of the United States. The maximum elevation is 70 degrees at the northwest part of the United States. Due to differences in software code, Figures 4 and 5 fail to produce the same results. An in-depth analysis of the code has been performed throughout the course of this research with a final resolution still being sought. A further analysis and examination of the code is in progress to ensure correct and accurate results.

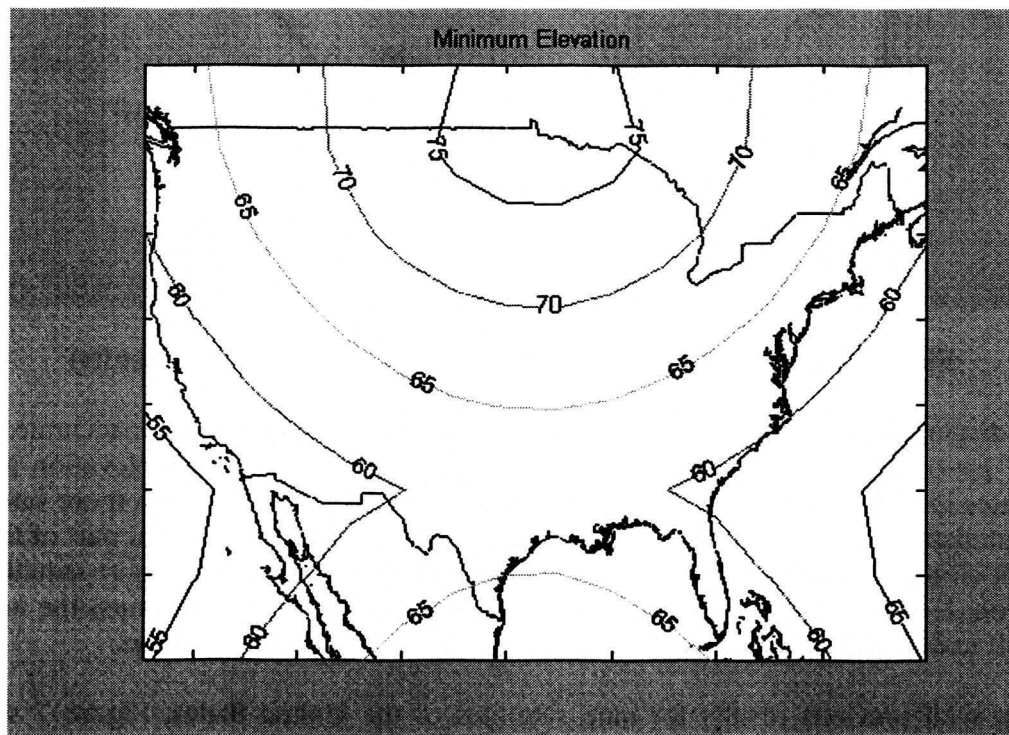


Figure 4: Three Satellites over the United States (previous results)

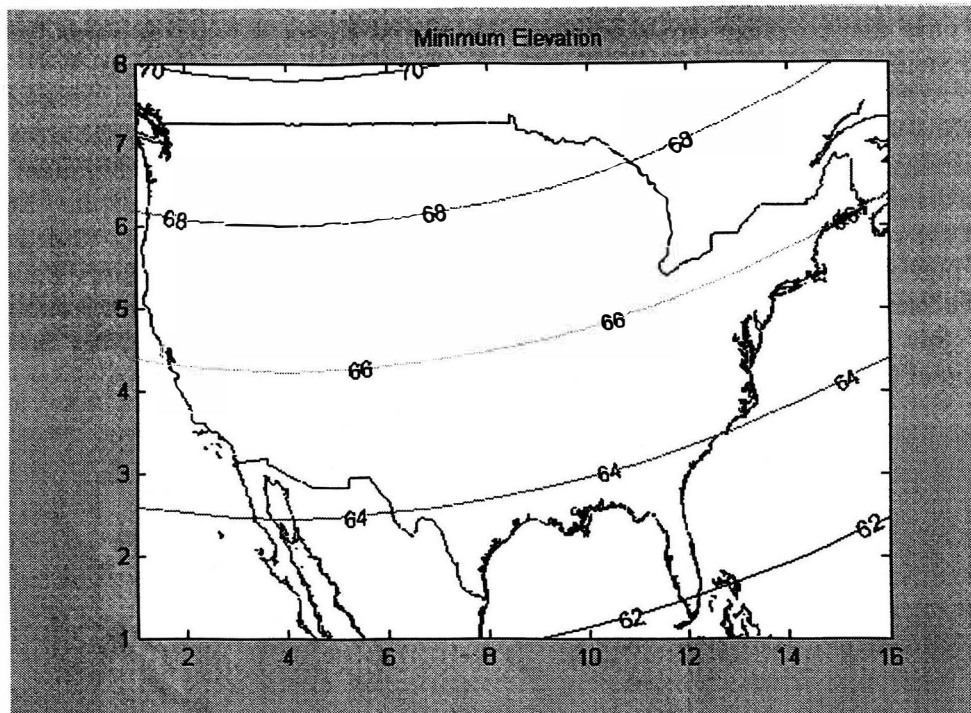


Figure 5: Three Satellites over the United States (current results)

The plots displaying a constellation of nine satellites were also found to be inaccurate. Figure 6 shows the previous results using this number of satellites. The minimum elevation across the United States increases to 65 degrees on the west and east coast oceans when more satellites are in the constellation. The maximum increases to 80 degrees in the north central part of the United States. It is clear that an improvement in reception can be seen when using more satellites in the constellation. However, this improvement in reception must be weighed against the increase in cost as well to determine the number of satellites to be used in the constellation.

In contrast with previous results for nine satellites of the United States, Figure 7 shows the current results for a constellation having this amount of satellites. According to this plot, symmetry is not seen for elevation angles. Figure 6 showed an equal representation of elevation angles on the west side of the United States as well as the east side. However in this plot, the symmetry does not begin in the center of the United States but in the west central part. Also, the minimum and maximum elevations disagree with Figure 6. In Figure 7, a minimum elevation of 74 can be found in the southern part of the United States. A maximum elevation of 78 can be found in the northwestern part. On account of dissimilarities in software code once again, Figures 6 and 7 fail to produce similar results. Another in-depth analysis of the code has been conducted with a final resolution still pending. A further analysis of this code is in progress to ensure correct results for future Tundra orbit constellation designs.

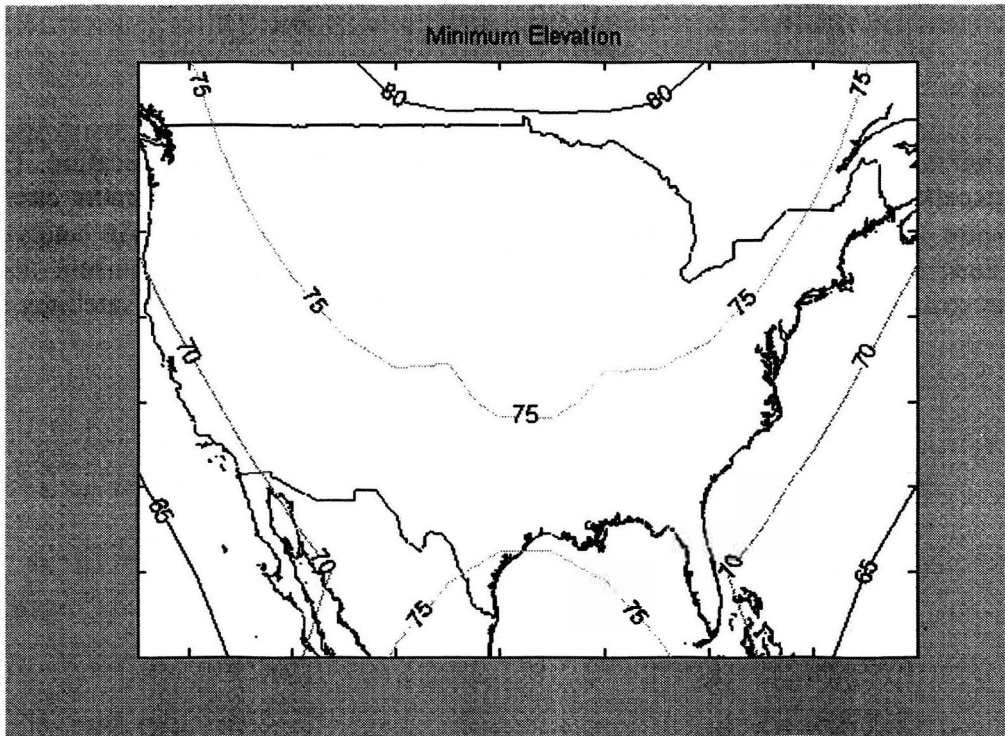


Figure 6: Nine Satellites over the United States (previous results)

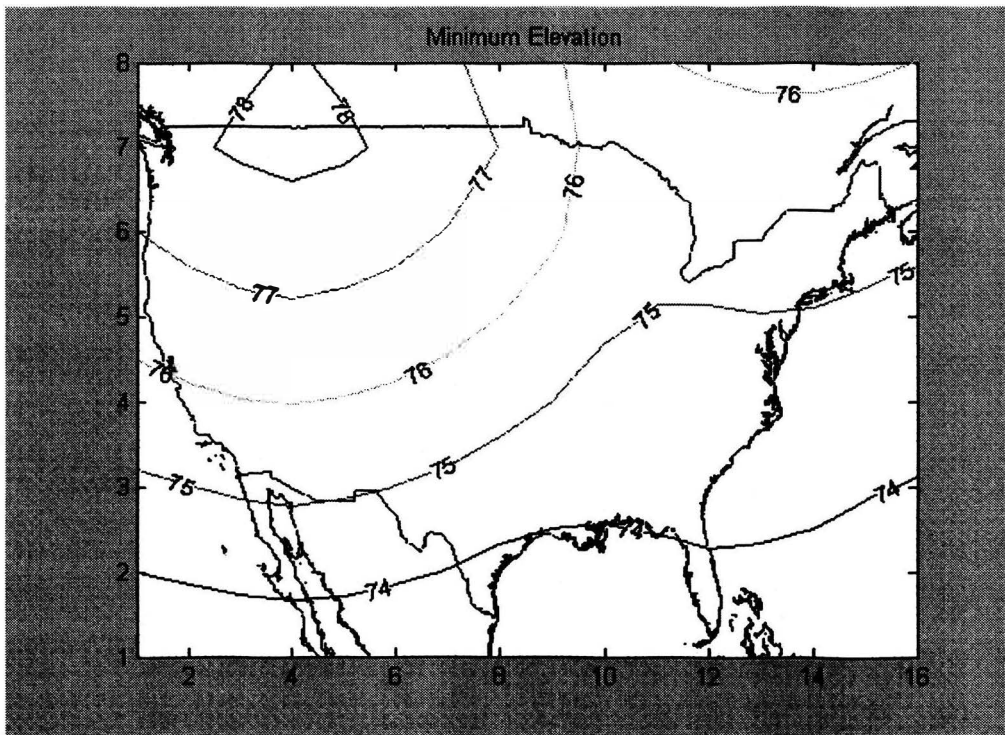


Figure 7: Nine Satellites over the United States (current results)

Conclusion

At higher latitudes, Tundra orbit constellations are ideal for satellite communication. They prove to be an excellent alternative to the overcrowded geostationary belt. Customers can expect to receive better reception from satellites in a Tundra orbit constellation. An analysis of the software code continues to correct dissimilarities between previous and current data. In the future, this software will be utilized to design an effective constellation of satellites in Tundra orbit.

References

1. Rondinelli, G.; Cramarossa, A.; Graziani, F.; “Orbit Control Strategy for a Constellation of Three Satellites in Tundra Orbits,” AAS paper AAS89-411, August 1989.
2. Bruno, M.J. and Pernicka, H.J., “Mission Design Considerations for the Tundra Constellation,” presented at the AIAA/AAS Astrodynamics Specialist Conference, Monterey, California, August 5-8, 2002.

High Pressure Water Jet Contaminant Remediation of Intertidal Sediment via Distributed Granular Activated Carbon

**Rachel Dilly
March 30,2005**

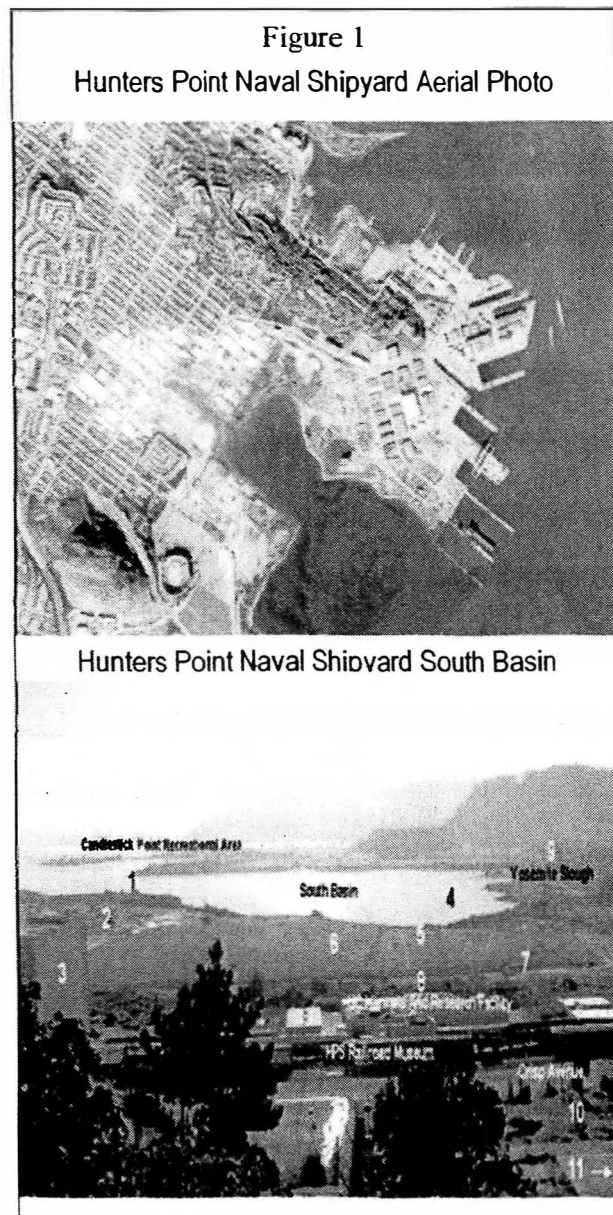
ABSTRACT

Hunters Point Naval Shipyard lies on western intertidal coastline and is designated as a Superfund site. Studies indicate sediment dwelling organisms that usually thrive in this intertidal area are now suffering and dying from PCB toxins. Experts have discovered that PCBs adsorb onto Granular Activated Carbon (GAC) particles, a material commonly used for contaminant remediation. Using a water jet, the GAC can be distributed in situ throughout the top 10 cm. of sediment. Research measures will include reproducing the natural, intertidal habitat in the UMR High Pressure Water Jet Laboratory. Specifically, to realize optimal benefits from the remediation process, a mixture of 2% (by dry weight) surrogate material to the sediment must be attained.

The United States Department of Defense (DoD), Department of Energy (DOE), and Environmental Protection Agency (EPA) have stated that approximately 1 billion cubic yards of sediment underlying the nation's surface water is sufficiently polluted with toxins and has the potential to injure fish, wildlife and humans. (Ghosh, et al.) "Sediment serves as a contaminant reservoir from which aquatic organism can accumulate toxic compounds like PCBs and DDT that are passed up the food chain." (Stanford University) Scientists and engineers have proposed various methods to remediate these contaminated habitats. Marine and estuary sites pose great obstacles for remediation because equipment is difficult to maneuver in situ, therefore a combination of remedial approaches are necessary. One proposed method uses high pressure waterjets to inject remediation material into the contaminated aquatic sediment. This method eliminates the need to relocate the sediment and minimizes the risk to the environment of the local organisms. In situ treatment of the sediment via the water jet treatment is the best method of remediation for this habitat so that minimal risk is posed to indigenous life forms. An additional benefit of this approach is that the costs are relatively low when compared to other remediation options.

BACKGROUND: HUNTERS POINT NAVAL SHIPYARD

Hunters Point Naval Shipyard is a 936 acre property located in San Francisco Bay, California.(1) From 1869 through 1987 this property was used by the Navy and its leasees for ship building repair, servicing and testing. By 1987, the Environmental Protection Agency (EPA) confirmed unacceptable levels of contamination including polychlorinated biphenyls (PCBs), trichloroethylene, pesticides, lead, and other contaminants. In 1989, the EPA listed Hunters Point Naval Shipyard (HPNS) on the



National Priorities List for Superfund sites. This site was separated into 6 parcels, labeled A through F, to optimize remediation efforts. In at least 5 of these parcels, PCBs and other contaminants remain on site and require remediation.

The main intertidal zone of PCB contamination lies in the awkwardly accessible South Basin area. (Figure 1) Clams, worms, and amphipods live in approximately the top 10 centimeters of this contaminated sediment. During the few hours of low tide in this area, access is restrictive because sediment is spongy, can reach far past the ankle and thus limits remediation options.

GRANULAR ACTIVATED CARBON

Granular Activated Carbon (GAC) is a common water filtration material and contaminant remediation substrate. It is an adsorbent material with a somewhat corrugated sheet structure, which gives it an increased surface area compared to other materials. The surface area per gram can be as high as 2500 m².(2) PCBs and other

contaminants readily adsorb to GAC not only because of the high surface area, but also due to its high porosity. (3)

HIGH PRESSURE WATER JETS

High Pressure Waterjets have been used for decades to cut rock and other material. They are the ideal tool for many applications because they are precise, produce little byproduct, and are versatile. Waterjets cut materials by combining high pressure water and an abrasive sand, usually garnet. An amendment of xanthan gum or guar is used to suspend the abrasive in a mixture which is then transported through the waterjet delivery system.

EXPERIMENT

Remediation of the South Basin using High Pressure Waterjets with a surrogate abrasive, specifically the Granular Activated Carbon, is possible if we use lower pressures to target the top 5-10 centimeters of sediment where the majority of the contaminants reside. A target concentration of 2% GAC by dry weight for optimal remediation is accomplished by applying waterjet technology. Approximately 400 grams of kaolinite is used per sample, therefore the GAC content must be greater than or equal to 8 grams. A slurry of 90% water, 9.91% GAC, and 0.09% xanthan gum was determined by experimental analysis.

SEDIMENT MODELLING

Sample sediment was retrieved from a surface water source that mimicked similar conditions as the South Basin. Analysis of this sample revealed the density of the sediment, $\rho=0.91 \text{ g/cm}^3$, and a water content of approximately 30%. In the lab, kaolinite

is utilized as the surrogate sediment using these characteristics. A total of 64 mason jars were prepared to contain the sediment slurry samples.

NOZZLE DESIGN AND SELECTION

The optimal waterjet configuration to deliver the GAC consists of a pump, reactor system, hose, and nozzle. (Figure 2)

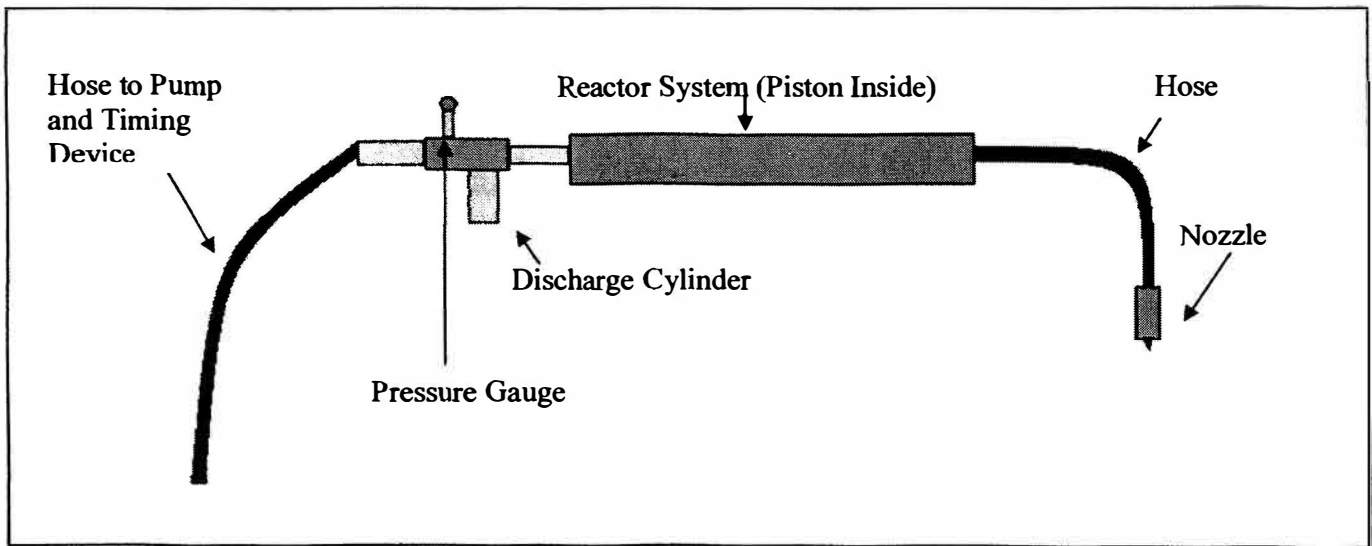


Figure 2

When the timing device is begun, the pump pressurizes the assembly; the high pressure water moves the piston within the reactor tube and pushes the GAC slurry out through the hose and nozzle apparatus.

The nozzle diameter used is directly related to the flow rate with the corresponding equation:

$$Q = \frac{(C_d)(\pi R^2)(12\sqrt{P})(12 * 60)}{231}$$

Where Q is the flow rate in gallons per minute, C_d is the discharge coefficient using a constant value of 0.85, and P is pressure measured in psi. (Appendix A) Nozzle diameters used in this experiment are 0.030 in., 0.040 in., 0.050 in., and 0.060 inches. These diameters are commonly used in waterjet applications. In using these specific diameters, the amount of GAC injected into the surrogate sediment can be estimated. These numbers are estimations only because pump pressures can spike and injection times can be delayed due to air compression within the reactor tube.

The project has been conducted as a factorial experiment using 64 samples of surrogate sediment subjected to varying time periods, pressures, and nozzle diameters. (Appendix B) Factorial experiments eliminate redundancy and reduce the number of samples necessary to obtain optimal data points. This layout provides only one sample for a given set of parameters, whereas other layouts develop several samples for the same information.

After the GAC was injected into the surrogate material, the samples were cooked in an oven between 150° F and 175° F for at least two weeks. Drying the samples over a long period of time minimized fracturing and allowed for a cleaner removal of the sample from the mason jar, resulting in more accurate analysis. Foam was inserted into the jars after they were dry to enable a waterjet to cut off the top of each.

The target of 2% GAC by dry weight is the goal so that an optimal pressure, nozzle diameter, and time period may be determined. The 64 core drill samples were analyzed utilizing a grey scale gradient. (Appendix C) A comparison of each sample to the gray gradient has been performed to determine the concentration of GAC achieved.

A qualitative analysis of the samples using a grey scale gradient was performed. Nozzle diameters of 0.03, 0.03, 0.05, and 0.06 inches were used, although use of the 0.03 inch nozzle yielded no results due to the high viscosity of the GAC slurry. Therefore, experiments using the 0.06 inch nozzle were duplicated with differing back pressures to determine if there is any difference in results. From calculations, the 0.06 inch nozzle was the only diameter to have the capacity to achieve 8 grams within the 400 gram surrogate sediment, specifically 2% by dry weight. The differing back pressures were determined to make little or no difference in the results.

Within the 0.06 diameter nozzle range, samples using 1200, 1500, and 1800 PSI for time ranges of 0.7 to 1.3 seconds attained optimal GAC saturation. (Appendix D) The specific combinations of pressures and time intervals are as listed in Table 1.

Nozzle Diameter, inches	Pressure, PSI	Time Interval, seconds
0.06	1500	0.7
0.06	1200	1.3
0.06	1800	0.7
0.06	1200	0.7
0.06	1200	1

Table 1

Although several sample colors appear to be within the required range, these samples were deemed inadmissible. This is because some of the original kaolinite was displaced from the jar upon penetration by the waterjet, and therefore achieved the target concentration by subtraction of sediment rather than the addition of carbon.

After experimental analysis reviewed, field experimentation by established professionals will be conducted; it is outside the scope of this experiment. When experimental results are available, possible field equipment that utilizes waterjet technologies include:

- Low ground pressure vehicles that can drag injectors such as the ArgoATV
- Dry solid injection tools such as the Dryject which uses waterjets to blast a holes in soil and inject sand, but may be adaptable to this application and
- Slurry injection normally used for soil/sediment stabilization with cement mortar

If High Pressure waterjets can be used to deliver granular activated carbon, then they can be used to deliver a wider range of materials for soil remediation. In fact, one project already in progress models an unconsolidated aquifer and will utilize waterjets to deliver other remediation substances such as EHC, a combination of cellulose and iron, and zero valent iron into soil.

LEARNING EXPERIENCE

Performing research in the field of geological engineering has given me a more realistic perspective of the work involved in research and development. In this discipline, one must be physically and mentally prepared to meet the challenges required to solve problems of today. Although the internet, library, and school books were important informational resources, my advisor, colleagues, and fellow students have become my best informational resources that I have developed. I have learned some fundamentals of qualitative, quantitative, and mixed methods experimental design. This research experiment used qualitative analysis with a grey-scale gradient.

REFERENCES

1. Environmental Protection Agency. "Hunters Point Naval Shipyard." (February 27,2004) n. pag. Online. Internet. EPA Region 9 ID # 1170090087 <http://yosemite.epa.gov/r9/sfund/overview.nsf/o/...>
2. Ghosh, Dr. Upal, et al. "In Situ Bioavailability Reduction of PCBs in Sediments: From Bench-Scale to Field Demonstration." Strategic Environmental Research and Development Program, DoD, DOE, EPA. February 18-19, 2004. Remediation Technology Development Forum. Baltimore, Maryland.
3. Stanford University. "Contaminated Sediment Processes and Bioavailability." (February 25, 2004) n. pag. Online. Internet. <http://www-ce.stanford.edu/faculty/luthy/LuthyResearch.html>

ACRONYMS

DoD – Department of Defense

DOE – Department of Energy

EPA – Environmental Protection Agency

GAC – Granular Activated Carbon

HPNS – Hunters Point Naval Shipyard

PCB – Polychlorinated Biphenyls

PSI – Pounds per Square Inch

ZVI – Zero Valent Iron

GLOSSARY

Discharge Coefficient – (C_d) The ratio of the actual rate of flow of a fluid through a meter to the rate computed by a theoretically derived equation or by empirical equation

EHC – a remediation product used for the in situ treatment of groundwater and saturated soil impacted by heavy metals and persistent organic compounds such as chlorinated solvents, pesticides and energetics.

Factorial Experiment – an experiment in which the effects of multiple factors are investigated simultaneously

Granular Activated Carbon - A highly porous adsorbent material, produced by heating organic matter, such as coal, wood and coconut shell, in the absence of air, which is then crushed into granules. Activated carbon is positively charged and therefore able to remove negative ions from water.

Guar - drought-tolerant herb grown for forage and for its seed which yield a gum used as a thickening agent or sizing material

Intertidal – a shore area above low-tide mark

PCB - any of several compounds that are produced by replacing hydrogen atoms in biphenyl with chlorine, have various industrial applications, and are poisonous environmental pollutants which tend to accumulate in animal tissues

Xanthan Gum - a thickening and suspending agent used especially in pharmaceuticals and prepared foods

Zero Valent Iron – used for in situ remediation of selected metals in groundwater

ACKNOWLEDGEMENTS

Elmore, Dr. Curt. Assistant Professor, Research Advisor. University of Missouri – Rolla

Summers, Dr. David. Curators' Professor, University of Missouri – Rolla Rock

Mechanics and Explosives Laboratory

Fossey, Robert. Research Specialist, University of Missouri – Rolla Rock Mechanics and

Explosives Laboratory

Tyler, John. Research Engineer, University of Missouri – Rolla Rock Mechanics and

Explosives Laboratory

Poppa, Kerry. Student, University of Missouri – Rolla

Meyer, Mark Andrew. Student, University of Missouri - Rolla

APPENDIX A

Flow Rate of Injected Granular Activated Carbon

Size (Inches)	PSI	Rate (GPM)	Duration (seconds)	% GAC Concentration	GAC Delivered (grams)
0.03	1000	0.710646	0.5	0.091	0
0.03	1500	0.870360	0.7	0.091	0
0.03	1800	0.953431	1.0	0.091	0
0.03	1200	0.778473	1.3	0.091	0
0.04	1000	1.263370	0.5	0.091	1.668070547
0.04	1500	1.547306	0.7	0.091	2.860145187
0.04	1800	1.694989	1.0	0.091	4.475902961
0.04	1200	1.383952	1.3	0.091	4.750927304
0.05	1000	1.974016	0.5	0.091	2.60636023
0.05	1500	2.417665	0.7	0.091	4.468976854
0.05	1800	2.648420	1.0	0.091	6.993598377
0.05	1200	2.162426	1.3	0.091	7.423323912
0.06	1000	2.842582	0.5	0.091	3.753158731
0.06	1500	3.481438	0.7	0.091	6.43532667
0.06	1800	3.813725	1.0	0.091	10.07078166
0.06	1200	3.113893	1.3	0.091	10.68958643

$$Q = C_d \cdot \pi \cdot r^2 \cdot [12 \cdot \sqrt{P}] \cdot 12 \cdot 60 / 231$$

APPENDIX B

Intertidal PCB Remediation via Water Jet Distribution Data Factorial Sheets

T ₁	0.5	P ₁	P ₂	P ₃	P ₄
0.5		1000	1500	1200	1800
D ₁	0.04	1	5	9	13
D ₂	0.05	17	21	25	29
D ₃	0.06	33	37	41	45
D ₄	0.06	49	53	57	61

T ₂	0.7	P ₁	P ₂	P ₃	P ₄
0.7		1000	1500	1200	1800
D ₁	0.04	2	6	10	14
D ₂	0.05	18	22	26	30
D ₃	0.06	34	38	42	46
D ₄	0.06	50	54	58	62

T ₃	1	P ₁	P ₂	P ₃	P ₄
1		1000	1500	1200	1800
D ₁	0.04	3	7	11	15
D ₂	0.05	19	23	27	31
D ₃	0.06	35	39	43	47
D ₄	0.06	51	55	59	63

T ₄	1.3	P ₁	P ₂	P ₃	P ₄
1.3		1000	1500	1200	1800
D ₁	0.04	4	8	12	16
D ₂	0.05	20	24	28	32
D ₃	0.06	36	40	44	48
D ₄	0.06	52	56	60	64

Basfont = Sample Number

P ₁ = 1000	D ₁ = 0.04	T ₁ = 0.5
P ₂ = 1500	D ₂ = 0.05	T ₂ = 0.7
P ₃ = 1200	D ₃ = 0.06	T ₃ = 1
P ₄ = 1800	D ₄ = 0.06	T ₄ = 1.3

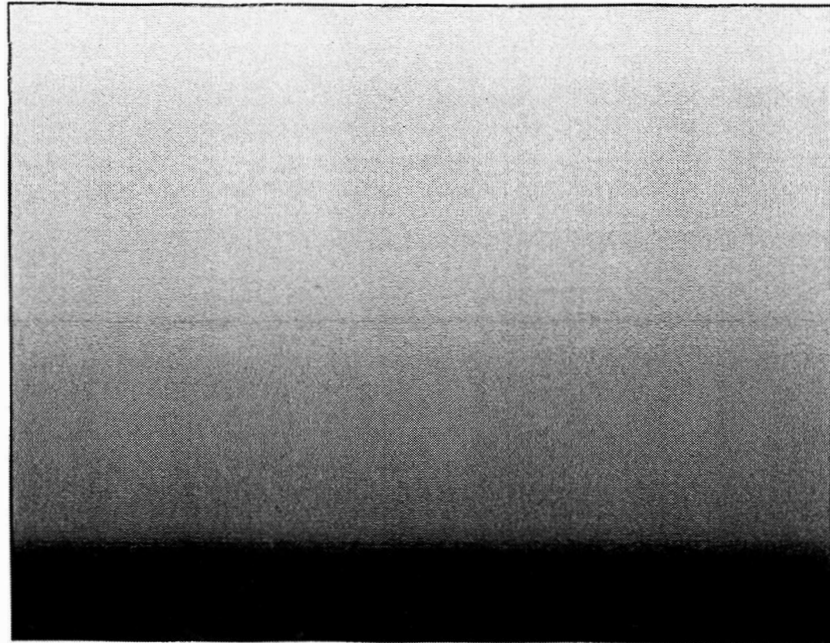
APPENDIX C

Grey Scale Gradient Analysis





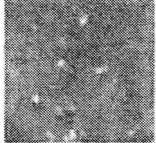
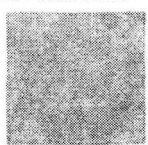



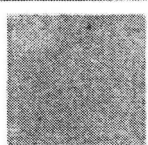

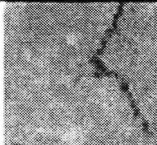

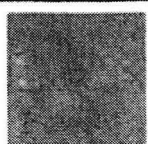



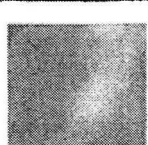







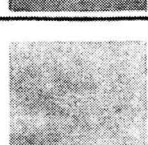







Kaolinite-----

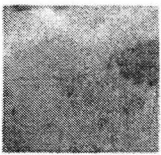
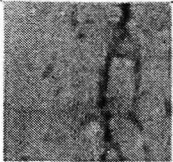
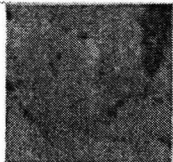
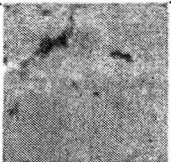
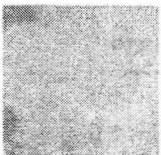
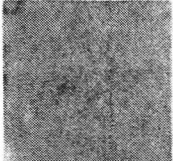
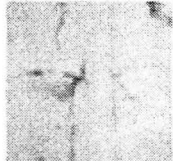

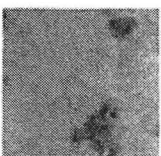
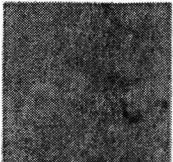
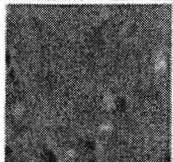
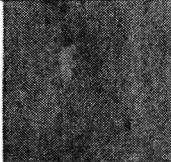
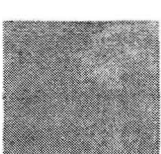

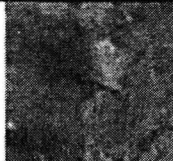
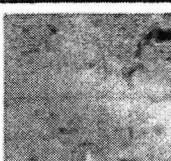
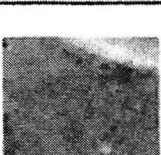
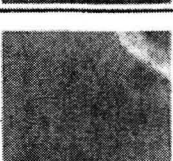
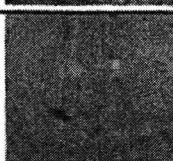
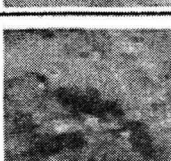
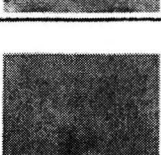
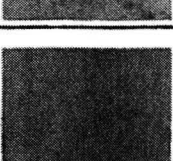
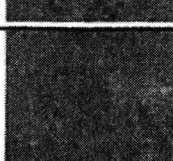

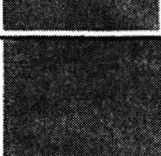
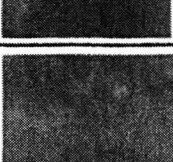
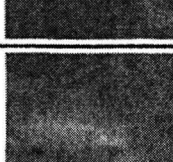

2% GAC-----

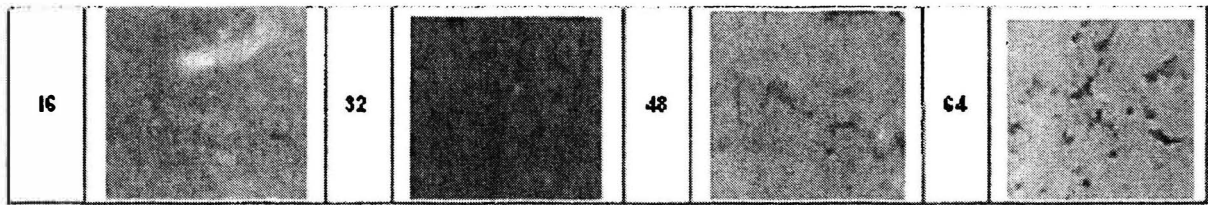
>2% GAC-----



Appendix D

2% GAC							
1		17		33		49	
2		18		34		50	
3		19		35		51	
4		20		36		52	
5		21		37		53	
6		22		38		54	
7		23		39		55	
8		24		40		56	

9		25		41		57	
10		26		42		58	
11		27		43		59	
12		28		44		60	
13		29		45		61	
14		30		46		62	
15		31		47		63	



Text in blue = target concentration and distribution has been achieved.



Final Submittal - Opportunities for Undergraduate Research Experience (OURE)

Miniature Shear Vane Testing on Compacted Silts

Prepared By:

**James Duehning
Undergraduate Student**

**Department of Civil, Architectural and Environmental Engineering
University of Missouri-Rolla
Rolla, MO 65401**

Date Submitted: December 2004

TABLE OF CONTENTS

Section	Page
1. Introduction.....	1
2. Historical Overview.....	2
3. Materials.....	6
4.0 Methods.....	8
5.0 Results.....	10
5.1 Laboratory.....	10
5.2 Field Experience.....	13
6.0 Conclusion.....	13
7.0 Recommendations.....	14
8.0 Works Cited.....	15
Appendices	
A. Laboratory Data Sheets.....	17
B. Laboratory Data Graphs.....	27

1.0 Introduction

Geotechnical Engineering is a branch of Civil Engineering that deals with soil, rock, ground water and their relationship with the design, construction, and operation of engineering projects (Coduto, 1998). As early as the Middle Ages builders found out through trial and error that the soils stratum underneath their structures had to be competent enough to withstand the stresses induced by these structures. The trial and error method continued through the Renaissance and into the Industrial Revolution. (Coduto, 1998) The trial and error method turned out to be a very tedious and expensive way of learning.

In 1922 the first comprehensive geotechnical report was spawned by landslides in Sweden. A commission was established to determine the properties of the soils in question and determine field test and lab test so future generations could determine if a soil was unstable before the soil failed and took human lives. During the conception of the report many landslides continued to take lives which further emphasized the importance of the Commission's work. The report was published by the Geotechnical Commission of the Swedish State Railways and presented methods of investigation and analyses and contained recommendations on how to avoid future landslides. (Coduto, 1998). Since 1922 many improvements have been made to understand the soil beneath us.

The subject of this paper originated from a research project by The United States Bureau of Reclamation (USBR) conducted at the University of Missouri - Rolla to determine the strength of silts under different loadings (Amelia Toellner, personal communication, October 18, 2004). The particular research section that spawned this

OURE – Miniature Shear Vane Testing on Compacted Silts

paper was the testing of the silt by a mini Cone Penetrometer Test (CPT) and a mini Laboratory Shear Vane Test, and the correlation between the two testing systems. This paper takes a look at the advantages of using the laboratory shear vane when silts are compacted with different water contents. With the conclusion of all the lab test and this paper I was able to complete one hour of CE 390.

2.0 Historical Overview

The first Field Shear Vane (field vane) was designed by John Olson, the Secretary of the Geotechnical Commission. The vane was used in 1919 during the construction of the Lidingö Bridge in Stockholm, Sweden built between 1917 and 1926 (Nordendahl, 1928). One of the major problems of the project was the buckling of long piles needed to support the bridge. The soil consisted of very soft clay with a thickness of up to 40m. Olson was given the task to determine the coefficient of horizontal sub-grade reaction of the clay. Olson came up with the vane borer which consisted of two blades attached to a system of pipes the end of the pipes which was above ground level and attached to a torque wrench. A needle above a protractor showed the actual rotation of the vane. The rotation of the vane, in degrees, represented the coefficient of sub-grade reaction in-situ under conditions which were closely related to those of a pile.(Floodin and Broms, 1981) Olsson's test also determined that the rotation rate was an important factor and that the displacements could be larger if the load was applied very slowly (Nordendahl, 1928) "The apparatus was found to be very well suited for it's purpose and it is highly desirable that further investigations of the strength of the clay should be performed with the

OURE – Miniature Shear Vane Testing on Compacted Silts

method now described by a similar method”(Flodin and Broms, 1981). The vane borer (figure 1.1) as it is used today was presented in 1948 by Lyman Cadling at the Second International Conference in Rotterdam (Flodin and Broms, 1981).

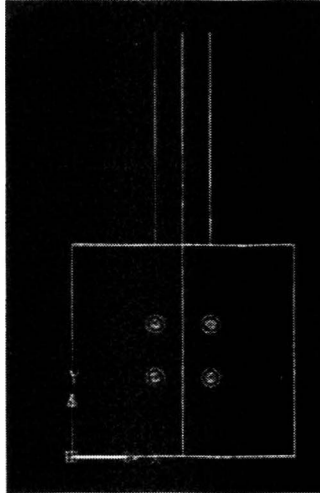


Fig. 2.1 AutoCAD drawing of original field vane

Two years later a report on a more advanced device was published (Cadling & Odenstad, 1950). Since the developments of the pioneers mentioned above, the use of the vane is used and the current configuration of the vane has been standardized in the United States by the American Society of Testing and Materials (ASTM) ASTM designation D 2573-01. ASTM D 2573-01 gives some guidelines as to how the standard field vane should be configured the maximum blade thickness as .118 in. the average thickness should be .0787 in. the blade edges can be tapered to decrease disturbance from insertion into the soil sample. The ASTM also states that the vane shaft diameter should not exceed .551 in. at the center of the vane. A field vane borrowed from Mr. Richard Frueh of Shannon and Wilson is shown in Figure 1.2. Some comments about this vane are that the vane shaft diameter is .75 in. which means that this vane was not with in ASTM standard.

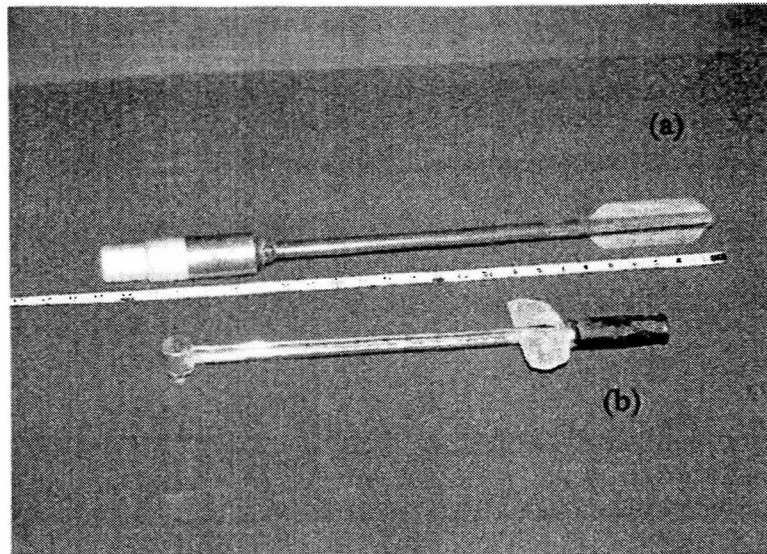


Fig. 2.2 (a) Field Vane and (b) torque Meter

In the early 1940's the Army Operational Research Group (AORG) was assigned to carry out some investigations into the cross-country performance of tracked vehicles (Evans, Sherratt, 1948). The AORG came up with a much smaller vane similar to the field vane mentioned above except the smaller vane was used for laboratory purposes only. The 'Miniature Vane' has proved useful for measuring the shearing resistance of clays and especially for very soft clays (Evans, Sherratt, 1948). Figure 1.3 shows a picture of the 'Miniature Vane' used by the University of Missouri – Rolla. This vane has been used to determine test and results used in association with this paper. Some simple elements on the laboratory vane are that the crank handle on the bottom controls the vertical movement of the vane. The other crank handle located on the top of the vane block controls the rate of rotation that the vane is subjected to. This crank handle is connected to the torque spring that as the handle is rotated the spring induces more torque to the rod which is connected to the vane. On top of the vane block there is a 360° protractor that displays the rotation of the vane through the spring this measurement is in degrees.

OURE – Miniature Shear Vane Testing on Compacted Silts

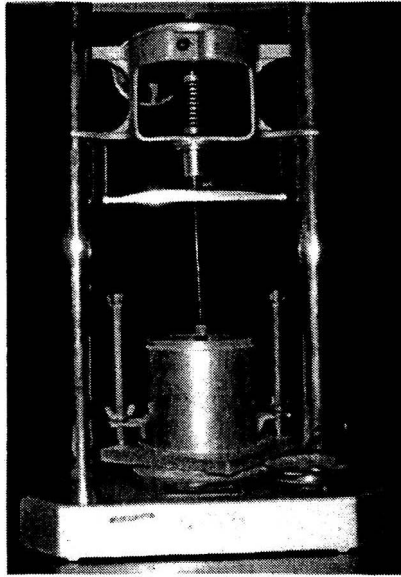


Fig. 2.3 ‘Miniature Laboratory Shear Vane’

As mentioned above both the field and laboratory vane’s have been standardized in America the ASTM for the laboratory vane is designated D-4648 Standard Test Method for Laboratory Miniature Vane Shear Test for Saturated Fine Grained Clayey Soil. This ASTM states that the vane assembly shall consist of four rectangular bladed vanes, and recommends that the vane have a height twice the diameter or equal to the diameter the vane used for all test in this paper had a ratio of 1:1 for height and diameter. The vane should also be rotated at a constant rate of 60 to 90°/min. This is commonly achieved using a motorized vane visually represented in Figure 1.4 this vane shows the same setup described above. The ‘Miniature Vanes’ used in labs today have transducers connected on the vane as well as one substituted in for the spring. This setup will provide much more accurate data because instead of unsteady readings (usually one to 10) the transducers are able to obtain constant readings.

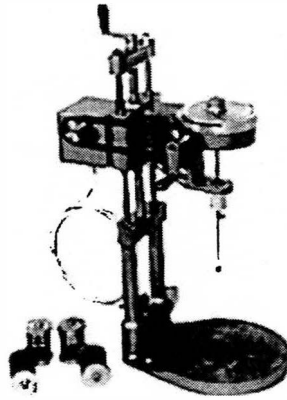


Fig. 2.4 Motorized Laboratory Vane (2004)

3.0 MATERIALS

The material discussed and used in association with this paper consists of brown silt with trace amounts of sand and gravel. The silt was obtained from a borrow site at an SCI construction site in Collinsville, Illinois as illustrated in figure 3.1. Figure 3.1 illustrates that the silt was taken from the pile to the left of the backhoe and due to recent construction the silt is loose and has been disturbed.

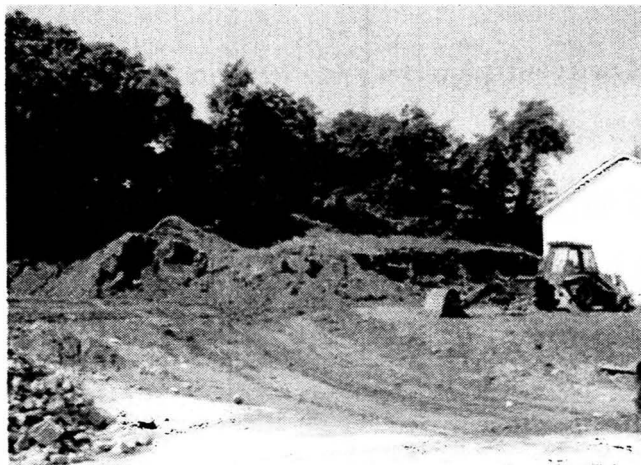


Fig. 3.1 Soil Borrow Site in Collinsville, IL (Toellner, 04)

OURE – Miniature Shear Vane Testing on Compacted Silts

The silt was determined to be deposited by a method known as alluvium. Alluvium deposits are transported by water and slowly build up of thousands of years in a report published by the Missouri Department of Natural Resources Division of geology and Land Survey the silt in question is Peoria loess and consists of a well sorted medium to coarse grained silt (Thompson, 1995).

The silt is described by Madison County Illinois soil survey as a loessial deposit. The Unified Soil Classification System (USCS) classifies this silt as a ML, M stands for a predominantly silt and L stands for a low plasticity. To determine the Liquid Limit and Plasticity Index, Atterberg limits were determined through a series of lab test; using the equipment in the Civil Engineering undergraduate soils lab. Figure 3.1 graphically represents the Plasticity chart which is used to determine the type of soil that is used according to USCS. Those soils that plot above the A-line are clays and those that plot below the A-line are silts. It was found that the Liquid Limit of the silt was 29% and the Plasticity Index was 6%.

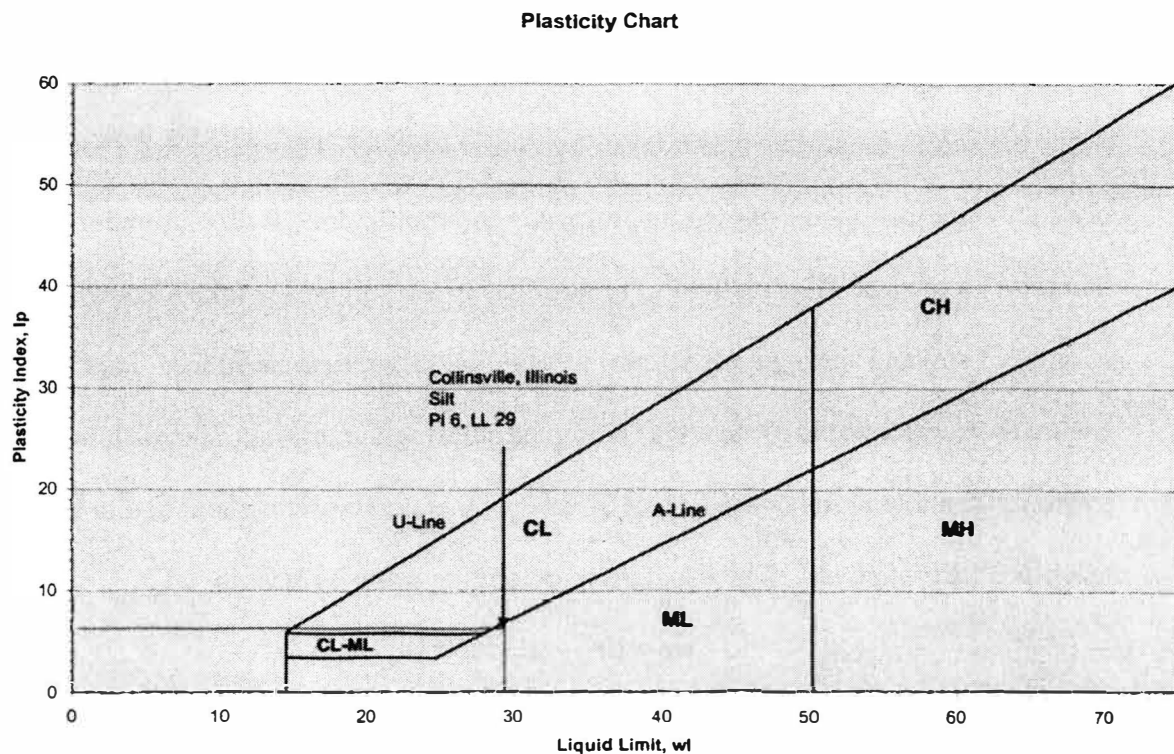


Fig. 3.2 Plasticity Chart for Silt used in OURE

OURE – Miniature Shear Vane Testing on Compacted Silts

Since the soil was disturbed due to construction activity no in-situ testing could be done and the natural water content could not be determined. The lab water content was determined through lab test to be 9.2 %. The silt used in all test was ground and sieved to the minus #40 sieve. This was done to ensure that the vane was not broken due to small rocks, coarse sand or any other material that could be within the large clumps of soil used in association of such tests.

Table 3.1 shows the soil properties that were found and used in association with calculations and conclusions in this paper.

Laboratory Soil Properties	
Clay Content	16.5%
Liquid Limit	28.5
Plastic Limit	22.5
Plasticity Index	6
Max Dry Density	108.5 lb/ft ³

4.0 Methods

Since the soil in question was not taken by optimal means of sampling there was a need for a reconstituted sample this process is commonly done for the miniature laboratory vane test. The method of reconstituting the soil was to take a known amount of soil and adding a predetermined amount of water to be added. This would ensure the correct water content was being used during the testing. Since silt is a very hydrophilic material meaning it attracts water. A pretest water content had to be taken for the ground silt. The equation to determine water content is

$$wc = (m_2 - m_1) / (m_2 - m_c)$$

m_2 = the weight of the soil wet + can (gm)

m_1 = the weight of the soil oven dried + can (gm)

m_c = the weight of the can empty (gm)

wc is in % to do this multiply the above equation by 100%

OURE – Miniature Shear Vane Testing on Compacted Silts

This pretest water content was used to determine the weight of silt needed to obtain the desired water content. The equation to determine the weight of silt needed to achieve the desired water content is:

$$wc+1 = Wt/Ws$$

$$Ws = Wt / (wc+1)$$

Where

wc = desired water content – pretest water content

Wt = 2100gm the amount of soil specified by the standard compaction test

Ws = the amount of soil needed to achieve the desired water content

Once the weight of soil was determined the amount of water is determined using the equation: $Ws * wc = Ww$. In the interest of time and illustration a spreadsheet was set up with all the above calculations and can be seen in appendix A1.

Once the weight of soil is weighed out on a scale and the amount of water needed is weighed the two are mixed in a mixing bowl. To achieve the best possible results water is added at a slow rate during the mixing process this is done to ensure that the soil specimen has the desired wc throughout. The mixing process was carried out using a mechanical mixer. The first step was to use bread mixers so that the soil and water did not leave the aluminum bowl. The second step in the mixing process was use typical mixing beaters. Mixing was done for about 2-3 minutes until the soil looked to be hydrated.

Once the mixing process was completed the soil was transferred to a standard proctor mold. The mold had to be filled up in three lifts this insured adequate compaction. Compaction was achieved through means of a mechanical hammer that

OURE – Miniature Shear Vane Testing on Compacted Silts

weighed 25lbs and was dropped from a height of 12 in. The mold was rotated at a rate of 20 cycles per minute and the number of hammer blows was 25 per layer.

Once the compaction process was completed the specimen was trimmed at the top of the mold and placed in the miniature laboratory vane directly under the vane. The vane was slowly lowered and entered the soil at a height of 14 in. The vane was lowered to a height of 13 in. this was done to ensure adequate coverage on all sides of the vane. An initial reading was taken and then the crank controlling the rotation of the vane was rotated at a rate of 5°/sec this rate is specified by ASTM. Once the soil started to take load readings were taken about every 10 degrees. Once the specimen failed the vane was lowered to a height of 12 in. and the soil was once again subjected to the same test. There were a total of 11 tests that were conducted on the silt in question. These test ranged in water contents from 17% to 22.5% these were the limits of the testing. These limits were determined since at 22.5% wc there was not enough soil in the mold to complete a specimen this was because at a high wc the soil acts as a liquid. At a wc of 17% the soil was compacted so well that the vane could not be pushed in to the soil without damaging the vane.

5.0 Results

5.1 Laboratory

Once all the lab trials were completed the data from each test was compiled in an excel spreadsheet these spreadsheets are available in the reference section.

OURE – Miniature Shear Vane Testing on Compacted Silts

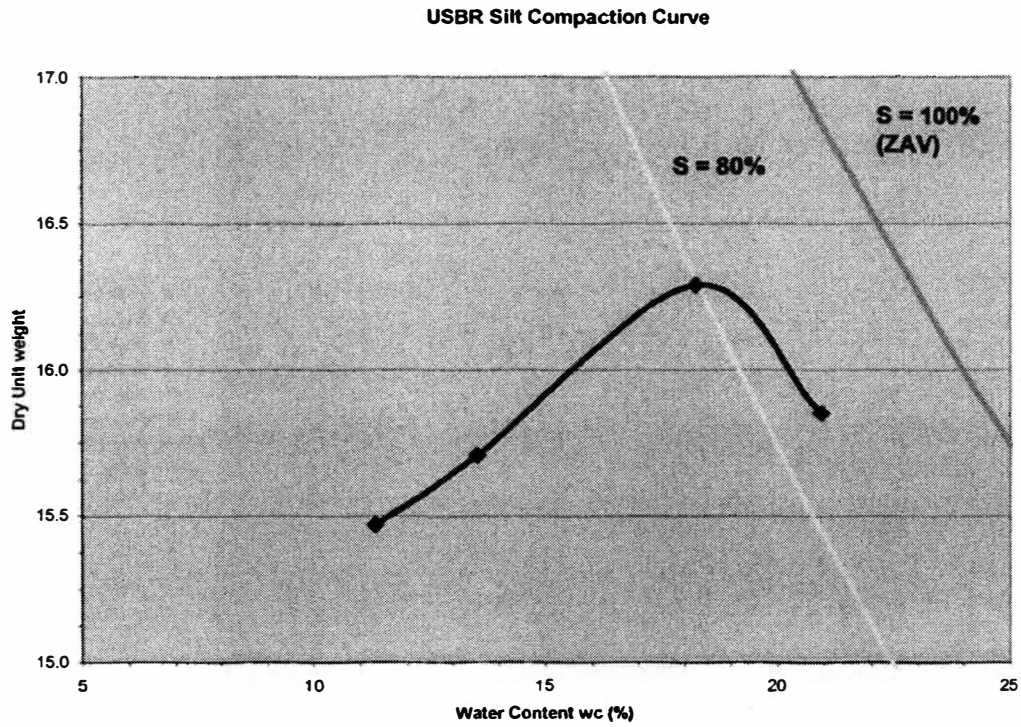


Fig. 5.1 USBR Compaction Curve

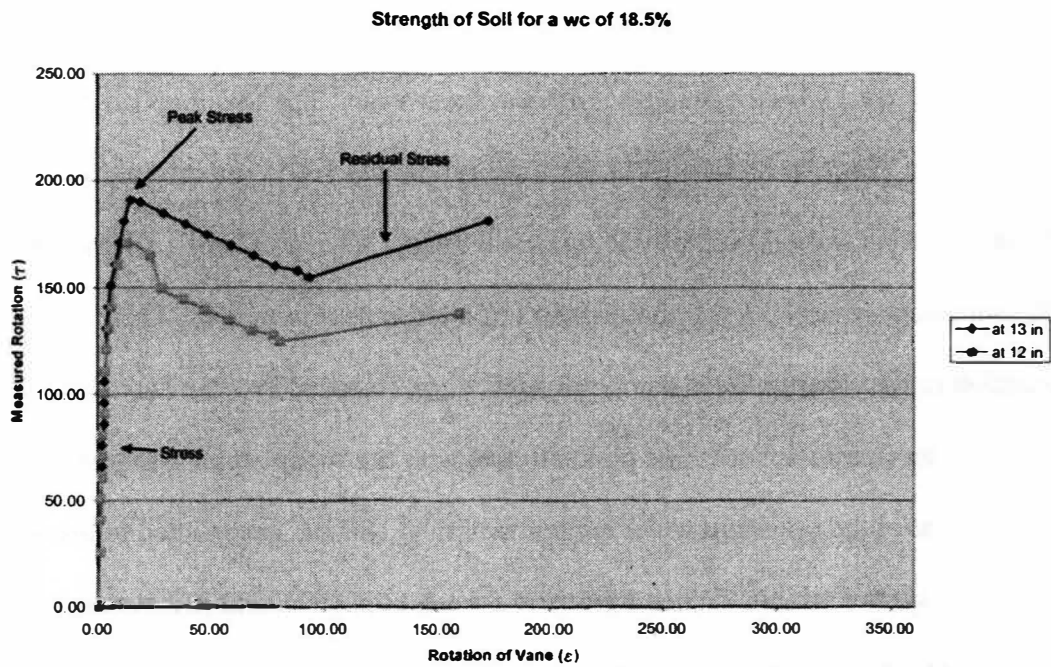


Fig. 5.1 Graph of Shear Strength vs. Strain

OURE – Miniature Shear Vane Testing on Compacted Silts

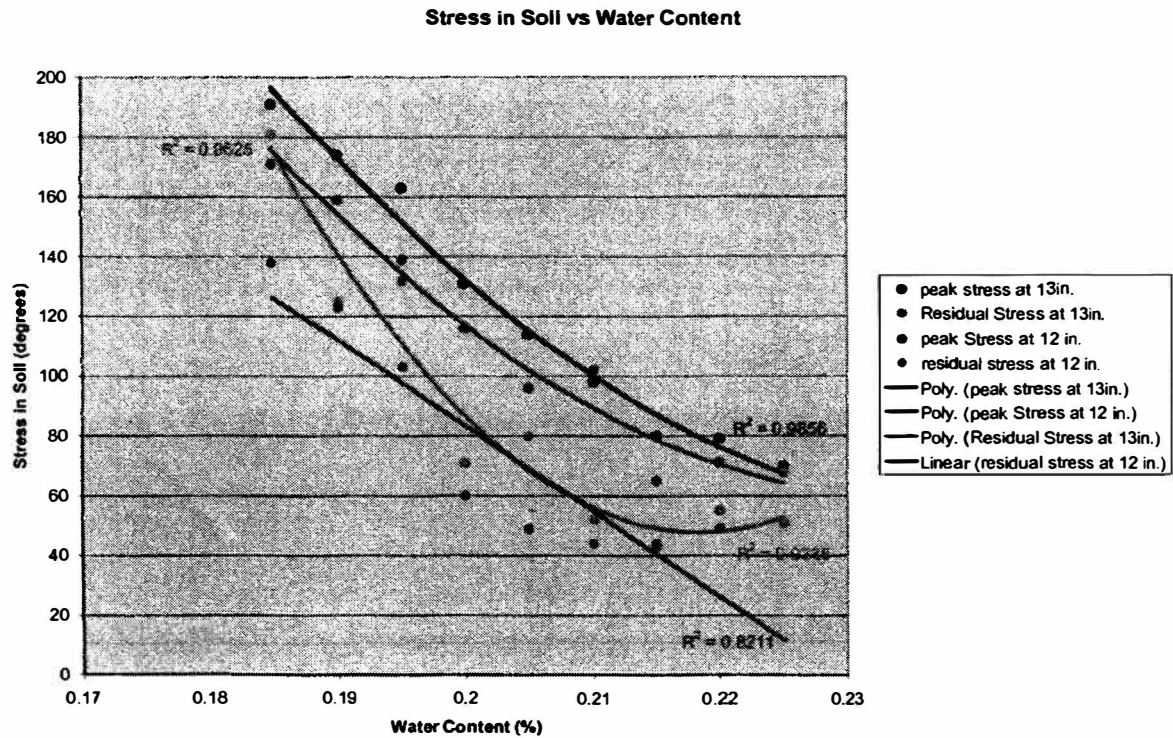


Fig. 5.1 Plot of Stresses vs. wc

Figure 5.1 is an illustration of the Compaction curve that was used to determine what water content I would use to test with the shear vane. The two lines on the graph represent Zero Air Void lines at 80% saturation and 100% saturation. Since the 100% saturation is what is typically found in the field. An example of a silt that is at 100% saturation would be a soil that is a part of a levee next to a river. This compaction curve was produced using the ASTM for Standard Proctor Test. Using the compaction curve I set up some points to test with the shear vane. The first point I looked at was at the optimum water content which is 18.5%. I continued to test silt using higher water contents. When I reached a water content of 22.5% I stopped testing the silt since at that water content the silt was too soft to compact. This means that with each drop of the hammer the silt would not compact at a certain point. On

OURE – Miniature Shear Vane Testing on Compacted Silts

the other side of the compaction curve test were ended at 17.0% water content. At that water content the vane could not be pushed into the specimen without damaging the vane. The amount of silt and no matter how much I tried the specimen wouldn't take any load

Figure 5.2 is an illustration of the shear vs. strain of the silt at two different points one at 13 in. and 12 in. I choose both these heights to ensure adequate soil cover on all sides of the vane. There is a drop in the 12 in. stress compared to the 13 in. stress

Figure 5.3 illustrates that an increase in water content has a direct relation to the strength of the soil and causes a decrease in the amount of strength that compacted silts can resist. The light blue trend line has a low R^2 value because a reading was not taken for the 20% water content for the residual stress at 12 in. This was due to a miscommunication between my lab assistant and me.

5.2 Field Experience

With the vane that was borrowed from Shannon and Wilson a test was conducted on a saturated pond bank near the Rolla area. The pond bank consisted of a soft clay which was optimal for the borrowed vane since I didn't want to destroy the vane. The Field vane gave a reading of 40 foot-pounds for one trial.

6.0 Conclusion

This paper was put together in the hope that the research and results will be used to update current models of the laboratory vane. I hope that this paper will be used to develop new testing equipment for in-situ testing. This new testing equipment will

OURE – Miniature Shear Vane Testing on Compacted Silts

hopefully be user friendly and helpful to determine the strength of soil before a failure occurs on a job site. When vane testing is carried out during the early phases of a construction project it is beneficial to the contractor and the owner to determine the shear strength of the soil that they are building on. With improvements to current testing equipment it is possible to decrease the amount of loss time or the loss of life due to failures. These failures occur when proper testing of soil and its properties are ignored due to the amount of time that it may take to complete them.

7.0 Recommendations

I recommend that in the future more care be taken in testing silts and clays with the shear vane. To do this I would keep the rotation of the vane a constant, this could be achieved by using a motor to induce the rotation of the vane. I also recommend that many different tests be done for each water content. This is to ensure that the results of one test are not a misrepresentation for the actual strength of a silt or clay at that water content.

I recommend conducting more field test on many different soils. This will help the person conducting the test a better understanding of the properties of the field vane. This would also give more data to correlate the laboratory vane and the field vane.

8.0 Works Cited

- Floodin, N., Broms, B. (1981). *Soft Clay Engineering*, Elsevier, Amsterdam
- Coduto, D. P. (1998). *Geotechnical Engineering principles and practices*, Prentice-Hall, New Jersey.
- Holtz, R. D., Kovacs, W. D. (1981). *An Introduction to Geotechnical Engineering*, Prentice-Hall, New Jersey.
- Chandler, R.J. (1988). *Vane Shear Strength Testing in Soils: Field and Laboratory Studies*, ASTM STP 1014, A.F. Richards Ed., Philadelphia, 13-44
- American Society for Testing Materials (1957). *Symposium on Vane Shear Testing of Soils*, ASTM STP 193. Philadelphia
- Gibbs H. J. (1957). "An apparatus and method of Vane Shear Testing of Soils." *Symposium on Vane Shear Testing of Soils*, ASTM STP 193 Philadelphia Pa., 9-15.
- Cadling L., Odenstad S. (1950). "The Vane Borer." *Proceedings, No. 2*, Royal Swedish Geotechnical Inst., Stockholm, Sweden 1-87
- Aas, G., Lacasse, S., Lunne, T., Hoeg, K. (1986). "Use of in-situ tests for foundation design on clay." *ASCE Specialty Conference in-situ*, ASCE, Blacksburg Va., 1-30.
- Thompson T., (1995). "The Stratigraphic Succession in Missouri." Missouri Department of Natural Resources Division of Geology and Land Survey, Volume 40 (2nd Series) Revised, 148-149
- Evans, I., Sherratt, G.G., (1948) "A simple and Convenient Instrument for Measuring the Shearing Resistance of Clay Soils." Army Operational Research Group, War Office, Volume 25, 411-414.
- American Society for Testing Materials, (2004). "Standard Test Method for Field Vane Shear Test in Cohesive Soil." ASTM D 2573-01, 1-8
- American Society for Testing Materials, (2004). "Standard Test Method for Laboratory Miniature Vane Shear Test for Saturated Fine-Grained Clayey Soil." ASTM D 4648-00, 1-7
- Olsen, R.S. (1994). "The Field Vane Shear Web Page." <http://www.liquefaction.com/insitutests/vane> (Sept. 1, 2004)
- American Society of Civil Engineers, "Overview of Journals." <http://www.pubs.asce.org/authors/index.html-1> (October 18, 2004)

OURE – Miniature Shear Vane Testing on Compacted Silts

Geotest Instrument Corporation, "Product Catalog."

<http://www.geotestinst.com//index.phtml> (December 1, 2004)

Toellner, A., Personal Communication, (Fall Semester, 2004)

Mudd, R., Personal Communication, (Fall Semester, 2004)

Luna, R., Personal Communication, (Fall Semester, 2004)

Appendices A

Laboratory Data Sheets

Vane Shear Data for a water content of 18.5%

WATER CONTENT OF SPECIMEN

W _{WET-CROSS} (g) =	50.5
W _{WET-CROSS} (g) =	154
W _{DRY-CROSS} (g) =	138
WC _{ACTUAL} % =	0.183

WATER CONTENT OF SOIL IN LAB = 1.5

ADJUSTED WATER CONTENT = 18.9%

k = 19C where K = 0.001515 ft³ for a 5 x 5 vane

CALIBRATION LINE $E = Y \cdot M \cdot X + B$
 $M = 1632.7$ $Y = 1632.7 \times + 5.196$

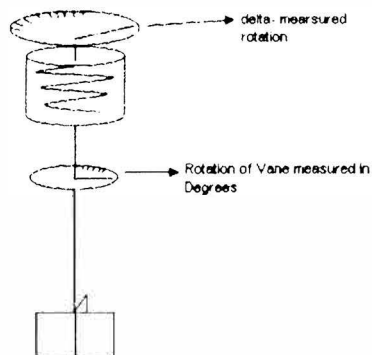
B = SLOPE OF CALIBRATION CURVE = M

CALIBRATION CURVE PERFORMED BY JEFF BRADSHAW OF THE CIVIL ENGINEERING DEPT

= residual stress

VANE AT TOP OF SPECIMEN = 14 IN

269						71						349						302					
13						12						12						12					
READINGS	MEASURED ROTATION FROM TOP OF MINUTARE VANE (Δ)	T = (Δ / (B X 12))	T = T X k	ACTUAL ROTATION OF VANE	ε = Actual Rotation of vane / 360°	READINGS	MEASURED ROTATION FROM TOP OF MINUTARE VANE (Δ)	T = (Δ / (B X 12))	T = T X k	ACTUAL ROTATION OF VANE	ε = Actual Rotation of vane / 360°	READINGS	MEASURED ROTATION FROM TOP OF MINUTARE VANE (Δ)	T = (Δ / (B X 12))	T = T X k	ACTUAL ROTATION OF VANE	ε = Actual Rotation of vane / 360°	READINGS	MEASURED ROTATION FROM TOP OF MINUTARE VANE (Δ)	T = (Δ / (B X 12))	T = T X k	ACTUAL ROTATION OF VANE	ε = Actual Rotation of vane / 360°
1	0.00	0.0000	0.00E+00	0.00	0.00E+00	1	0.00	0.0000	0.00E+00	0.00	0.00E+00	1	0.00	0.0000	0.00E+00	0.00	0.00E+00	1	0.00	0.0000	0.00E+00	0.00	0.00E+00
2	41.00	0.0021	3.17E-07	1.00	2.78E-03	2	26.00	0.0013	2.01E-07	1.00	2.78E-03	2	26.00	0.0013	2.01E-07	1.00	2.78E-03	3	41.00	0.0021	3.17E-07	1.00	2.78E-03
3	68.00	0.0034	5.10E-07	2.00	5.56E-03	3	41.00	0.0021	3.17E-07	1.00	2.78E-03	3	41.00	0.0021	3.17E-07	1.00	2.78E-03	4	51.00	0.0026	3.94E-07	1.00	2.78E-03
4	78.00	0.0039	5.85E-07	2.00	5.56E-03	4	51.00	0.0026	3.94E-07	1.00	2.78E-03	4	51.00	0.0026	3.94E-07	1.00	2.78E-03	5	61.00	0.0031	4.72E-07	2.00	5.56E-03
5	86.00	0.0044	6.85E-07	3.00	8.33E-03	5	61.00	0.0031	4.72E-07	2.00	5.56E-03	5	61.00	0.0031	4.72E-07	2.00	5.56E-03	6	71.00	0.0036	5.49E-07	2.00	5.56E-03
6	96.00	0.0049	7.42E-07	3.00	8.33E-03	6	71.00	0.0036	5.49E-07	2.00	5.56E-03	6	71.00	0.0036	5.49E-07	2.00	5.56E-03	7	81.00	0.0041	6.26E-07	2.00	5.56E-03
7	106.00	0.0054	8.20E-07	3.00	8.33E-03	7	81.00	0.0041	6.26E-07	2.00	5.56E-03	7	81.00	0.0041	6.26E-07	2.00	5.56E-03	8	91.00	0.0046	7.04E-07	3.00	8.33E-03
8	121.00	0.0062	9.35E-07	4.00	1.11E-02	8	91.00	0.0046	7.04E-07	3.00	8.33E-03	8	91.00	0.0046	7.04E-07	3.00	8.33E-03	9	101.00	0.0052	7.81E-07	3.00	8.33E-03
9	131.00	0.0067	1.01E-06	4.00	1.11E-02	9	101.00	0.0052	7.81E-07	3.00	8.33E-03	9	101.00	0.0052	7.81E-07	3.00	8.33E-03	10	111.00	0.0057	8.58E-07	3.00	8.33E-03
10	141.00	0.0072	1.09E-06	5.00	1.39E-02	10	111.00	0.0057	8.58E-07	3.00	8.33E-03	10	111.00	0.0057	8.58E-07	3.00	8.33E-03	11	121.00	0.0062	9.35E-07	4.00	1.11E-02
11	151.00	0.0077	1.17E-06	6.00	1.67E-02	11	121.00	0.0062	9.35E-07	4.00	1.11E-02	11	121.00	0.0062	9.35E-07	4.00	1.11E-02	12	131.00	0.0067	1.01E-06	5.00	1.39E-02
12	161.00	0.0082	1.24E-06	8.00	2.22E-02	12	131.00	0.0067	1.01E-06	5.00	1.39E-02	12	131.00	0.0067	1.01E-06	5.00	1.39E-02	13	141.00	0.0072	1.09E-06	6.00	1.67E-02
13	171.00	0.0087	1.32E-06	10.00	2.78E-02	13	141.00	0.0072	1.09E-06	6.00	1.67E-02	13	141.00	0.0072	1.09E-06	6.00	1.67E-02	14	161.00	0.0082	1.24E-06	9.00	2.50E-02
14	181.00	0.0092	1.40E-06	12.00	3.33E-02	14	161.00	0.0082	1.24E-06	9.00	2.50E-02	14	161.00	0.0082	1.24E-06	9.00	2.50E-02	15	171.00	0.0087	1.32E-06	13.00	3.61E-02
15	191.00	0.0097	1.48E-06	15.00	4.17E-02	15	171.00	0.0087	1.32E-06	13.00	3.61E-02	15	171.00	0.0087	1.32E-06	13.00	3.61E-02	16	181.00	0.0092	1.40E-06	23.00	6.39E-02
16	190.00	0.0097	1.47E-06	19.00	5.28E-02	16	165.00	0.0084	1.28E-06	23.00	6.39E-02	16	165.00	0.0084	1.28E-06	23.00	6.39E-02	17	185.00	0.0094	1.43E-06	28.00	7.78E-02
17	185.00	0.0094	1.43E-06	29.00	8.08E-02	17	150.00	0.0077	1.16E-06	28.00	7.78E-02	17	150.00	0.0077	1.16E-06	28.00	7.78E-02	18	180.00	0.0092	1.39E-06	39.00	1.06E-01
18	180.00	0.0092	1.39E-06	39.00	1.08E-01	18	145.00	0.0074	1.12E-06	38.00	1.06E-01	18	145.00	0.0074	1.12E-06	38.00	1.06E-01	19	175.00	0.0089	1.35E-06	49.00	1.33E-01
19	175.00	0.0089	1.35E-06	49.00	1.36E-01	19	140.00	0.0071	1.08E-06	48.00	1.33E-01	19	140.00	0.0071	1.08E-06	48.00	1.33E-01	20	170.00	0.0087	1.31E-06	59.00	1.61E-01
20	170.00	0.0087	1.31E-06	59.00	1.64E-01	20	135.00	0.0069	1.04E-06	58.00	1.61E-01	20	135.00	0.0069	1.04E-06	58.00	1.61E-01	21	165.00	0.0084	1.28E-06	68.00	1.89E-01
21	165.00	0.0084	1.28E-06	68.00	1.92E-01	21	130.00	0.0066	1.01E-06	68.00	1.89E-01	21	130.00	0.0066	1.01E-06	68.00	1.89E-01	22	160.00	0.0082	1.24E-06	79.00	2.17E-01
22	160.00	0.0082	1.24E-06	79.00	2.19E-01	22	128.00	0.0065	9.90E-07	78.00	2.17E-01	22	128.00	0.0065	9.90E-07	78.00	2.17E-01	23	158.00	0.0081	1.22E-06	89.00	2.25E-01
23	158.00	0.0081	1.22E-06	89.00	2.47E-01	23	125.00	0.0064	9.67E-07	81.00	2.25E-01	23	125.00	0.0064	9.67E-07	81.00	2.25E-01	24	155.00	0.0079	1.20E-06	94.00	2.61E-01
24	155.00	0.0079	1.20E-06	94.00	2.61E-01	24		0.0000	0.00E+00		0.00E+00	24		0.0000	0.00E+00		0.00E+00	25		0.0000	0.00E+00		0.00E+00
25		0.0000	0.00E+00		0.00E+00	25		0.0000	0.00E+00		0.00E+00	25		0.0000	0.00E+00		0.00E+00						
1	155.00			94.00	2.61E-01	1	125.00			81.00	2.25E-01	1	125.00			81.00	2.25E-01						
2	181.00			173.00	4.81E-01	2	138.00			160.00	4.44E-01	2	138.00			160.00	4.44E-01						



Vane Shear Data for a water content of 19.00%

WATER CONTENT OF SPECIMEN

W _{TARE} (g) =	52.4
W _{WET + GROSS} (g) =	216.3
W _{DRY + GROSS} (g) =	190
WC _{ACTUAL} % =	0.191

WATER CONTENT OF SOIL IN LAB = 1.6

ADJUSTED WATER CONTENT = 17.4%

k = 1/K where K = 0.0001515 ft³ for a 5 x 5 vane

CALIBRATION LINE = Y = MX + B = y = 1632.7x + 5.196

M = 1632.7

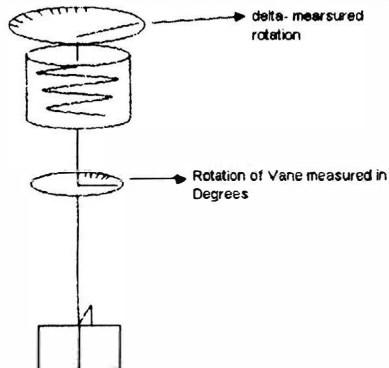
B = SLOPE OF CALIBRATION CURVE = M

CALIBRATION CURVE PERFORMED BY JEFF
BRADSHAW OF THE CIVIL ENGINEERING DEPT

= residual stress

VANE AT TOP OF SPECIMEN = 14 IN

270						264						315						121					
13						12						12						12					
READING S	MEASURED ROTATION FROM TOP OF MINITUAIRE VANE (Δ)	T = (Δ / (B X 12))	τ = T X k	ACTUAL ROTATION OF VANE	ε = Actual Rotation of vane / 360°	READING S	MEASURED ROTATION FROM TOP OF MINITUAIRE VANE (Δ)	T = (Δ / (B X 12))	τ = T X k	ACTUAL ROTATION OF VANE	ε = Actual Rotation of vane / 360°	READING S	MEASURED ROTATION FROM TOP OF MINITUAIRE VANE (Δ)	T = (Δ / (B X 12))	τ = T X k	ACTUAL ROTATION OF VANE	ε = Actual Rotation of vane / 360°	READING S	MEASURED ROTATION FROM TOP OF MINITUAIRE VANE (Δ)	T = (Δ / (B X 12))	τ = T X k	ACTUAL ROTATION OF VANE	ε = Actual Rotation of vane / 360°
1	0.00	0.0000	0.00E+00	0.00	0.00E+00	1	0.00	0.0000	0.00E+00	0.00	0.00E+00	1	0.00	0.0000	0.00E+00	0.00	0.00E+00	1	0.00	0.0000	0.00E+00	0.00	0.00E+00
2	50.00	0.0026	3.87E-07	1.00	2.78E-03	2	29.00	0.0015	2.24E-07	0.00	0.00E+00	2	29.00	0.0015	2.24E-07	0.00	0.00E+00	2	29.00	0.0015	2.24E-07	0.00	0.00E+00
3	65.00	0.0033	5.03E-07	2.00	5.58E-03	3	40.00	0.0020	3.09E-07	1.00	2.78E-03	3	40.00	0.0020	3.09E-07	1.00	2.78E-03	3	40.00	0.0020	3.09E-07	1.00	2.78E-03
4	75.00	0.0038	5.80E-07	3.00	8.33E-03	4	52.00	0.0027	4.02E-07	1.00	2.78E-03	4	52.00	0.0027	4.02E-07	1.00	2.78E-03	4	52.00	0.0027	4.02E-07	1.00	2.78E-03
5	85.00	0.0043	6.57E-07	4.00	1.11E-02	5	65.00	0.0033	5.03E-07	1.00	2.78E-03	5	65.00	0.0033	5.03E-07	1.00	2.78E-03	5	65.00	0.0033	5.03E-07	1.00	2.78E-03
6	95.00	0.0048	7.35E-07	5.00	1.39E-02	6	75.00	0.0038	5.80E-07	2.00	5.58E-03	6	75.00	0.0038	5.80E-07	2.00	5.58E-03	6	75.00	0.0038	5.80E-07	2.00	5.58E-03
7	110.00	0.0056	8.51E-07	7.00	1.94E-02	7	85.00	0.0043	6.57E-07	2.00	5.58E-03	7	85.00	0.0043	6.57E-07	2.00	5.58E-03	7	85.00	0.0043	6.57E-07	2.00	5.58E-03
8	120.00	0.0061	9.28E-07	7.00	1.94E-02	8	95.00	0.0048	7.35E-07	3.00	8.33E-03	8	95.00	0.0048	7.35E-07	3.00	8.33E-03	8	95.00	0.0048	7.35E-07	3.00	8.33E-03
9	130.00	0.0066	1.01E-06	10.00	2.78E-02	9	105.00	0.0054	8.12E-07	4.00	1.11E-02	9	105.00	0.0054	8.12E-07	4.00	1.11E-02	9	105.00	0.0054	8.12E-07	4.00	1.11E-02
10	140.00	0.0071	1.08E-06	13.00	3.61E-02	10	115.00	0.0059	8.89E-07	5.00	1.39E-02	10	115.00	0.0059	8.89E-07	5.00	1.39E-02	10	115.00	0.0059	8.89E-07	5.00	1.39E-02
11	150.00	0.0077	1.16E-06	18.00	5.00E-02	11	125.00	0.0064	9.67E-07	7.00	1.94E-02	11	125.00	0.0064	9.67E-07	7.00	1.94E-02	11	125.00	0.0064	9.67E-07	7.00	1.94E-02
12	160.00	0.0082	1.24E-06	24.00	6.67E-02	12	135.00	0.0069	1.04E-06	9.00	2.50E-02	12	135.00	0.0069	1.04E-06	9.00	2.50E-02	12	135.00	0.0069	1.04E-06	9.00	2.50E-02
13	170.00	0.0087	1.31E-06	28.00	7.22E-02	13	145.00	0.0074	1.12E-06	12.00	3.33E-02	13	145.00	0.0074	1.12E-06	12.00	3.33E-02	13	145.00	0.0074	1.12E-06	12.00	3.33E-02
14	174.00	0.0089	1.35E-06	36.00	1.00E-01	14	158.00	0.0081	1.22E-06	21.00	5.83E-02	14	158.00	0.0081	1.22E-06	21.00	5.83E-02	14	158.00	0.0081	1.22E-06	21.00	5.83E-02
15	165.00	0.0084	1.28E-06	46.00	1.28E-01	15	159.00	0.0081	1.23E-06	29.00	8.06E-02	15	159.00	0.0081	1.23E-06	29.00	8.06E-02	15	159.00	0.0081	1.23E-06	29.00	8.06E-02
16	158.00	0.0081	1.22E-06	56.00	1.56E-01	16	150.00	0.0077	1.16E-06	39.00	1.08E-01	16	150.00	0.0077	1.16E-06	39.00	1.08E-01	16	150.00	0.0077	1.16E-06	39.00	1.08E-01
17	145.00	0.0074	1.12E-06	66.00	1.83E-01	17	145.00	0.0074	1.12E-06	49.00	1.36E-01	17	145.00	0.0074	1.12E-06	49.00	1.36E-01	17	145.00	0.0074	1.12E-06	49.00	1.36E-01
18	130.00	0.0066	1.01E-06	76.00	2.11E-01	18	140.00	0.0071	1.08E-06	59.00	1.64E-01	18	140.00	0.0071	1.08E-06	59.00	1.64E-01	18	140.00	0.0071	1.08E-06	59.00	1.64E-01
19	128.00	0.0065	9.90E-07	86.00	2.39E-01	19	130.00	0.0066	1.01E-06	69.00	1.92E-01	19	130.00	0.0066	1.01E-06	69.00	1.92E-01	19	130.00	0.0066	1.01E-06	69.00	1.92E-01
20	120.00	0.0061	9.28E-07	96.00	2.67E-01	20	120.00	0.0061	9.28E-07	79.00	2.19E-01	20	120.00	0.0061	9.28E-07	79.00	2.19E-01	20	120.00	0.0061	9.28E-07	79.00	2.19E-01
21	111.00	0.0057	8.58E-07	103.00	2.86E-01	21	110.00	0.0056	8.51E-07	89.00	2.47E-01	21	110.00	0.0056	8.51E-07	89.00	2.47E-01	21	110.00	0.0056	8.51E-07	89.00	2.47E-01
22		0.0000	0.00E+00		0.00E+00	22	100.00	0.0051	7.73E-07	99.00	2.75E-01	22	100.00	0.0051	7.73E-07	99.00	2.75E-01	22	100.00	0.0051	7.73E-07	99.00	2.75E-01
23		0.0000	0.00E+00		0.00E+00	23	95.00	0.0048	7.35E-07	100.00	2.78E-01	23	95.00	0.0048	7.35E-07	100.00	2.78E-01	23	95.00	0.0048	7.35E-07	100.00	2.78E-01
24		0.0000	0.00E+00		0.00E+00	24		0.0000	0.00E+00		0.00E+00	24		0.0000	0.00E+00		0.00E+00	24		0.0000	0.00E+00		0.00E+00
25		0.0000	0.00E+00		0.00E+00	25		0.0000	0.00E+00		0.00E+00	25		0.0000	0.00E+00		0.00E+00	25		0.0000	0.00E+00		0.00E+00
1	111.00			103.00	2.86E-01	1	95.00			100.00	2.78E-01	1	95.00			100.00	2.78E-01	1	95.00			100.00	2.78E-01
2	125.00			186.00	4.67E-01	2	123.00			174.00	4.83E-01	2	123.00			174.00	4.83E-01	2	123.00			174.00	4.83E-01



Vane Shear Data for a water content of 19.5%

WATER CONTENT OF SPECIMEN

W _{TAKE} (g) =	42.7
W _{WET + GROSS} (g) =	149.5
W _{DRY + GROSS} (g) =	132.1
WC _{ACTUAL} % =	0.195

WATER CONTENT OF SOIL IN LAB = 1.6

ADJUSTED WATER CONTENT = 18.4%

VANE AT TOP OF SPECIMEN = 14 IN

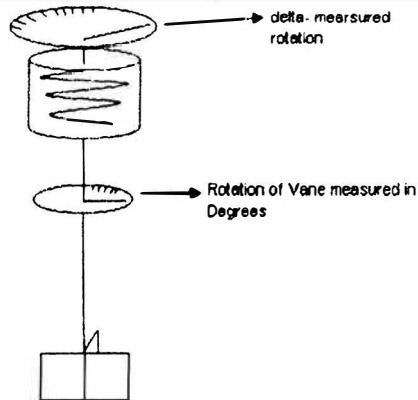
k = 1/K where K = 0.0001515 ft³ for a 5 x 5 vane

CALIBRATION LINE = Y = MX + B = y = 1632.7x + 5.196
M = 1632.7

B = SLOPE OF CALIBRATION CURVE = M
CALIBRATION CURVE PERFORMED BY JEFF BRADSHAW
OF THE CIVIL ENGINEERING DEPT

= residual stress

271							128							310							346						
13							12							12							12						
READINGS	MEASURED ROTATION FROM TOP OF MINITURE VANE (Δ)	T = (Δ / (B X 12))	τ = T X k	ACTUAL ROTATION OF VANE	ε = Actual Rotation of vane / 360°		READINGS	MEASURED ROTATION FROM TOP OF MINITURE VANE (Δ)	T = (Δ / (B X 12))	τ = T X k	ACTUAL ROTATION OF VANE	ε = Actual Rotation of vane / 360°		READINGS	MEASURED ROTATION FROM TOP OF MINITURE VANE (Δ)	T = (Δ / (B X 12))	τ = T X k	ACTUAL ROTATION OF VANE	ε = Actual Rotation of vane / 360°		READINGS	MEASURED ROTATION FROM TOP OF MINITURE VANE (Δ)	T = (Δ / (B X 12))	τ = T X k	ACTUAL ROTATION OF VANE	ε = Actual Rotation of vane / 360°	
1	0.00	0.0000	0.00E+00	0.00	0.00E+00		1	0.00	0.0000	0.00E+00	0.00	0.00E+00		1	0.00	0.0000	0.00E+00	0.00	0.00E+00		1	0.00	0.0000	0.00E+00	0.00	0.00E+00	
2	34.00	0.0017	2.63E-07	1.00	2.78E-03		2	25.00	0.0013	1.93E-07	1.00	2.78E-03		2	25.00	0.0013	1.93E-07	1.00	2.78E-03		2	25.00	0.0013	1.93E-07	1.00	2.78E-03	
3	46.00	0.0023	3.56E-07	1.00	2.78E-03		3	40.00	0.0020	3.09E-07	1.00	2.78E-03		3	40.00	0.0020	3.09E-07	1.00	2.78E-03		3	40.00	0.0020	3.09E-07	1.00	2.78E-03	
4	74.00	0.0038	5.72E-07	3.00	8.33E-03		4	65.00	0.0033	5.03E-07	2.00	5.56E-03		4	65.00	0.0033	5.03E-07	2.00	5.56E-03		4	65.00	0.0033	5.03E-07	2.00	5.56E-03	
5	94.00	0.0048	7.27E-07	4.00	1.11E-02		5	75.00	0.0038	5.80E-07	2.00	5.56E-03		5	75.00	0.0038	5.80E-07	2.00	5.56E-03		5	75.00	0.0038	5.80E-07	2.00	5.56E-03	
6	104.00	0.0053	8.04E-07	6.00	1.67E-02		6	85.00	0.0043	6.57E-07	3.00	8.33E-03		6	85.00	0.0043	6.57E-07	3.00	8.33E-03		6	85.00	0.0043	6.57E-07	3.00	8.33E-03	
7	114.00	0.0058	8.82E-07	8.00	2.22E-02		7	95.00	0.0048	7.35E-07	4.00	1.11E-02		7	95.00	0.0048	7.35E-07	4.00	1.11E-02		7	95.00	0.0048	7.35E-07	4.00	1.11E-02	
8	124.00	0.0063	9.59E-07	11.00	3.06E-02		8	105.00	0.0054	8.12E-07	6.00	1.67E-02		8	105.00	0.0054	8.12E-07	6.00	1.67E-02		8	105.00	0.0054	8.12E-07	6.00	1.67E-02	
9	134.00	0.0068	1.04E-06	14.00			9	115.00	0.0059	8.89E-07	9.00			9	115.00	0.0059	8.89E-07	9.00			9	115.00	0.0059	8.89E-07	9.00		
10	144.00	0.0073	1.11E-06	21.00			10	125.00	0.0064	9.67E-07	13.00			10	125.00	0.0064	9.67E-07	13.00			10	125.00	0.0064	9.67E-07	13.00		
11	154.00	0.0079	1.19E-06	22.00			11	135.00	0.0069	1.04E-06	21.00			11	135.00	0.0069	1.04E-06	21.00			11	135.00	0.0069	1.04E-06	21.00		
12	163.00	0.0083	1.26E-06	32.00			12	139.00	0.0071	1.07E-06	24.00			12	139.00	0.0071	1.07E-06	24.00			12	139.00	0.0071	1.07E-06	24.00		
13	150.00	0.0077	1.16E-06	42.00			13	132.00	0.0067	1.02E-06	34.00			13	132.00	0.0067	1.02E-06	34.00			13	132.00	0.0067	1.02E-06	34.00		
14	145.00	0.0074	1.12E-06	52.00			14	124.00	0.0063	9.59E-07	44.00			14	124.00	0.0063	9.59E-07	44.00			14	124.00	0.0063	9.59E-07	44.00		
15	135.00	0.0069	1.04E-06	62.00			15	118.00	0.0060	9.12E-07	54.00			15	118.00	0.0060	9.12E-07	54.00			15	118.00	0.0060	9.12E-07	54.00		
16	130.00	0.0066	1.01E-06	72.00			16	110.00	0.0056	8.51E-07	64.00			16	110.00	0.0056	8.51E-07	64.00			16	110.00	0.0056	8.51E-07	64.00		
17	128.00	0.0065	9.90E-07	82.00			17	103.00	0.0053	7.96E-07	74.00			17	103.00	0.0053	7.96E-07	74.00			17	103.00	0.0053	7.96E-07	74.00		
18	122.00	0.0062	9.43E-07	92.00			18	95.00	0.0048	7.35E-07	84.00			18	95.00	0.0048	7.35E-07	84.00			18	95.00	0.0048	7.35E-07	84.00		
19	118.00	0.0060	9.12E-07	102.00			19	90.00	0.0046	6.96E-07	84.00			19	90.00	0.0046	6.96E-07	84.00			19	90.00	0.0046	6.96E-07	84.00		
20	113.00	0.0056	8.74E-07	104.00			20	88.00	0.0045	6.80E-07	95.00			20	88.00	0.0045	6.80E-07	95.00			20	88.00	0.0045	6.80E-07	95.00		
21		0.0000	0.00E+00				21		0.0000	0.00E+00				21		0.0000	0.00E+00				21		0.0000	0.00E+00			
22		0.0000	0.00E+00				22		0.0000	0.00E+00				22		0.0000	0.00E+00				22		0.0000	0.00E+00			
23		0.0000	0.00E+00				23		0.0000	0.00E+00				23		0.0000	0.00E+00				23		0.0000	0.00E+00			
24		0.0000	0.00E+00				24		0.0000	0.00E+00				24		0.0000	0.00E+00				24		0.0000	0.00E+00			
25		0.0000	0.00E+00				25		0.0000	0.00E+00				25		0.0000	0.00E+00				25		0.0000	0.00E+00			
1	113.00			104.00			1	88.00			97.00			1	88.00			97.00			1	88.00			97.00		
2	132.00			171.00			2	100.00			163.00			2	100.00			163.00			2	100.00			163.00		



Vane Shear Data for a water content of 20%

WATER CONTENT OF SPECIMEN

W _{TARE} (g) =	11.6
W _{WET + GROSS} (g) =	35.72
W _{DRY + GROSS} (g) =	31.7
WC ACTUAL % =	0.200

WATER CONTENT OF SOIL IN LAB = 1.6

ADJUSTED WATER CONTENT = 18.4%

k = 1/K where K = 0.0001515 ft³ for a 5 x 5 vane

CALIBRATION CURVE = Y = MX + B = 1632.7x + 5.196

M = 1632.7

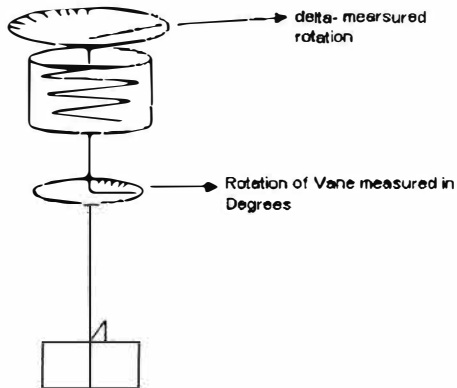
B = SLOPE OF CALIBRATION CURVE = M

CALIBRATION CURVE PERFORMED BY
JEFF BRADSHAW OF THE CIVIL
ENGINEERING DEPT.

residual
strength

VANE AT TOP OF SPECIMEN = 14 IN

274							DEPTH READING (IN)							300						
13							12													
READINGS	MEASURED ROTATION FROM TOP OF MINITUAIRE VANE (Δ)	T = (Δ / (B X 12))	τ = T X k	ACTUAL ROTATION OF VANE	ε = Actual Rotation of vane / 360°		READING S	MEASURED ROTATION FROM TOP OF MINITUAIRE VANE (Δ)	T = (Δ / (B X 12))	τ = T X k	ACTUAL ROTATION OF VANE	ε = Actual Rotation of vane / 360°		READING S	MEASURED ROTATION FROM TOP OF MINITUAIRE VANE (Δ)	T = (Δ / (B X 12))	τ = T X k	ACTUAL ROTATION OF VANE	ε = Actual Rotation of vane / 360°	
1	0.00	0.00000	0.0000E+00	0.00	0.000E+00		1.00	0.00	0.0000	0.0000E+00	0.00	0.000E+00		1.00	0.00	0.0000	0.0000E+00	0.00	0.000E+00	
2	66.00	0.00337	5.1035E-07	1.00	2.778E-03		2.00	25.00	0.0013	1.9331E-07	0.00	0.000E+00		2.00	25.00	0.0013	1.9331E-07	0.00	0.000E+00	
3	91.00	0.00464	7.0367E-07	2.00	5.556E-03		3.00	45.00	0.0023	3.4797E-07	0.00	0.000E+00		3.00	45.00	0.0023	3.4797E-07	0.00	0.000E+00	
4	107.00	0.00546	8.2739E-07	9.00	2.500E-02		4.00	65.00	0.0033	5.0262E-07	1.00	2.7778E-03		4.00	65.00	0.0033	5.0262E-07	1.00	2.7778E-03	
5	121.00	0.00618	9.3564E-07	13.00	3.611E-02		5.00	85.00	0.0043	8.5727E-07	4.00	1.1111E-02		5.00	85.00	0.0043	8.5727E-07	4.00	1.1111E-02	
6	130.00	0.00664	1.0052E-06	20.00	5.556E-02		6.00	95.00	0.0048	7.3460E-07	7.00	1.9444E-02		6.00	95.00	0.0048	7.3460E-07	7.00	1.9444E-02	
7	131.00	0.00669	1.0130E-06	27.00	7.500E-02		7.00	105.00	0.0054	8.1192E-07	10.00	2.7778E-02		7.00	105.00	0.0054	8.1192E-07	10.00	2.7778E-02	
8	120.00	0.00612	9.2791E-07	48.00	1.333E-01		8.00	110.00	0.0056	8.5058E-07	14.00	3.8889E-02		8.00	110.00	0.0056	8.5058E-07	14.00	3.8889E-02	
9	100.00	0.00510	7.7326E-07	58.00	1.811E-01		9.00	115.00	0.0059	8.8925E-07	21.00			9.00	115.00	0.0059	8.8925E-07	21.00		
10	80.00	0.00408	6.1861E-07	68.00	1.889E-01		10.00	116.00	0.0059	8.9698E-07	29.00			10.00	116.00	0.0059	8.9698E-07	29.00		
11	70.00	0.00357	5.4128E-07	78.00	2.167E-01		11.00	110.00	0.0056	8.5058E-07	39.00			11.00	110.00	0.0056	8.5058E-07	39.00		
12	66.00	0.00337	5.1035E-07	80.00	2.222E-01		12.00	100.00	0.0051	7.7326E-07	49.00			12.00	100.00	0.0051	7.7326E-07	49.00		
13		0.00000	0.0000E+00		0.000E+00		13.00	90.00	0.0046	6.9593E-07	59.00			13.00	90.00	0.0046	6.9593E-07	59.00		
14		0.00000	0.0000E+00		0.000E+00		14.00	80.00	0.0041	6.1861E-07	69.00			14.00	80.00	0.0041	6.1861E-07	69.00		
15		0.00000	0.0000E+00		0.000E+00		15.00	75.00	0.0038	5.7994E-07	79.00			15.00	75.00	0.0038	5.7994E-07	79.00		
16		0.00000	0.0000E+00		0.000E+00		16.00	70.00	0.0036	5.4128E-07	83.00			16.00	70.00	0.0036	5.4128E-07	83.00		
17		0.00000	0.0000E+00		0.000E+00		17.00		0.0000	0.0000E+00				17.00		0.0000	0.0000E+00			
18		0.00000	0.0000E+00		0.000E+00		18.00		0.0000	0.0000E+00				18.00		0.0000	0.0000E+00			
19		0.00000	0.0000E+00		0.000E+00		19.00		0.0000	0.0000E+00				19.00		0.0000	0.0000E+00			
20		0.00000	0.0000E+00		0.000E+00		20.00		0.0000	0.0000E+00				20.00		0.0000	0.0000E+00			
21		0.00000	0.0000E+00		0.000E+00		21.00		0.0000	0.0000E+00				21.00		0.0000	0.0000E+00			
22		0.00000	0.0000E+00		0.000E+00		22.00		0.0000	0.0000E+00				22.00		0.0000	0.0000E+00			
23		0.00000	0.0000E+00		0.000E+00		23.00		0.0000	0.0000E+00				23.00		0.0000	0.0000E+00			
24		0.00000	0.0000E+00		0.000E+00		24.00		0.0000	0.0000E+00				24.00		0.0000	0.0000E+00			
25		0.00000	0.0000E+00		0.000E+00		25.00		0.0000	0.0000E+00				25.00		0.0000	0.0000E+00			
1	66.00			80.00			1.00							1.00						
2	71.00			112.00			2.00							2.00						



Vane Shear Data for a water content of 20.5%

WATER CONTENT OF SPECIMEN

W _{WET + GROSS} (g) =	42.4
W _{DRY + GROSS} (g) =	128.5
WC _{ACTUAL} % =	113.9
WC _{ACTUAL} % =	0.204

WATER CONTENT OF SOIL IN LAB = 1.6

ADJUSTED WATER CONTENT = 18.9%

k = 1/K where K = 0.0001515 ft³ for a 5 x 5 vane

CALIBRATION LINE = Y = MX + B = y = 1632.7x + 5.196

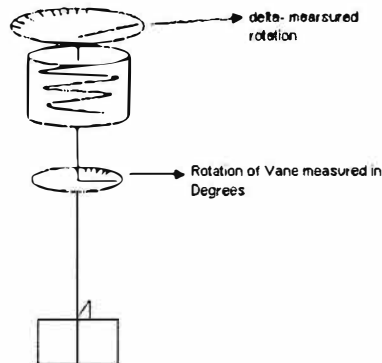
M = 1632.7

B = SLOPE OF CALIBRATION CURVE = M

CALIBRATION CURVE PERFORMED BY JEFF BRADSHAW OF THE CIVIL ENGINEERING DEPT

VANE AT TOP OF SPECIMEN = 14 IN.

270						295					
13						12					
READINGS	MEASURED ROTATION FROM TOP OF MINITURE VANE (Δ)	T = (Δ / (B X 12))	τ = T X k	ACTUAL ROTATION OF VANE	ε = Actual Rotation of vane / 360°	READINGS	MEASURED ROTATION FROM TOP OF MINITURE VANE (Δ)	T = (Δ / (B X 12))	τ = T X k	ACTUAL ROTATION OF VANE	ε = Actual Rotation of vane / 360°
1	0.00	0.00000	0.0000E+00	0.00	0.000E+00	1.00	0.00	0.0000	0.0000E+00	1.00	2.7778E-03
2	32.00	0.00163	2.4744E-07	1.00	2.778E-03	2.00	30.00	0.0015	2.3198E-07	2.00	5.5558E-03
3	56.00	0.00286	4.3303E-07	4.00	1.111E-02	3.00	55.00	0.0028	4.2529E-07	4.00	1.1111E-02
4	67.00	0.00342	5.1808E-07	6.00	1.667E-02	4.00	65.00	0.0033	5.0262E-07	8.00	1.6667E-02
5	80.00	0.00408	6.1861E-07	8.00	2.222E-02	5.00	75.00	0.0038	5.7994E-07	9.00	2.5000E-02
6	90.00	0.00459	6.9593E-07	16.00	4.444E-02	6.00	85.00	0.0043	6.5727E-07	22.00	6.1111E-02
7	101.00	0.00516	7.8099E-07	18.00	5.000E-02	7.00	95.00	0.0048	7.3460E-07	24.00	6.6667E-02
8	110.00	0.00561	8.5058E-07	28.00	7.776E-02	8.00	96.00	0.0049	7.4233E-07	34.00	9.4444E-02
9	114.00	0.00582	8.8152E-07	38.00	1.058E-01	9.00	94.00	0.0048	7.2686E-07	44.00	1.2222E-01
10	100.00	0.00510	7.7326E-07	48.00	1.333E-01	10.00	90.00	0.0046	6.9593E-07	54.00	1.5000E-01
11	90.00	0.00459	6.9593E-07	58.00	1.611E-01	11.00	88.00	0.0045	6.8047E-07	64.00	1.7778E-01
12	85.00	0.00434	6.5727E-07	68.00	1.889E-01	12.00	83.00	0.0042	6.4180E-07	74.00	2.0556E-01
13	80.00	0.00408	6.1861E-07	78.00	2.167E-01	13.00	80.00	0.0041	6.1861E-07	84.00	2.3333E-01
14	75.00	0.00383	5.7994E-07	85.00	2.381E-01	14.00	76.00	0.0039	5.8768E-07	89.00	2.4722E-01
15		0.00000	0.0000E+00		0.000E+00	15.00	72.00	0.0037	5.5675E-07	95.00	2.6389E-01
16		0.00000	0.0000E+00		0.000E+00	16.00	70.00	0.0036	5.4128E-07	110.00	3.0556E-01
17		0.00000	0.0000E+00		0.000E+00	17.00	68.00	0.0035	5.2582E-07	126.00	3.5000E-01
18		0.00000	0.0000E+00		0.000E+00	18.00	64.00	0.0033	4.9489E-07	138.00	3.8333E-01
19		0.00000	0.0000E+00		0.000E+00	19.00	62.00	0.0032	4.7842E-07	144.00	4.0000E-01
20		0.00000	0.0000E+00		0.000E+00	20.00	58.00	0.0030	4.4848E-07	152.00	4.2222E-01
21		0.00000	0.0000E+00		0.000E+00	21.00	55.00	0.0028	4.2529E-07	164.00	4.5556E-01
22		0.00000	0.0000E+00		0.000E+00	22.00	53.00	0.0027	4.0983E-07	172.00	4.7778E-01
23		0.00000	0.0000E+00		0.000E+00	23.00	51.00	0.0026	3.9436E-07	186.00	5.1667E-01
24		0.00000	0.0000E+00		0.000E+00	24.00		0.0000	0.0000E+00		0.0000E+00
25		0.00000	0.0000E+00		0.000E+00	25.00		0.0000	0.0000E+00		0.0000E+00
1	75.00	0.00383	5.7994E-07	86.00	2.389E-01	1.00	51.00	0.0026	3.9436E-07	186.00	5.1667E-01
2	80.00	0.00408	6.1861E-07	102.00	2.833E-01	2.00	60.00	0.0031	4.6396E-07	192.00	5.3333E-01



Vane Shear Data for a water content of 21%

WATER CONTENT OF SPECIMEN

W _{TARE} (g) =	11
W _{WET + GROSS} (g) =	41.7
W _{DRY + GROSS} (g) =	36.4
WC ACTUAL % =	0.21

WATER CONTENT OF SOIL IN LAB = 1.6

ADJUSTED WATER CONTENT = 19.4%

k = 1/K where K = 0.0001515 R³ for a 5 x 5 vane

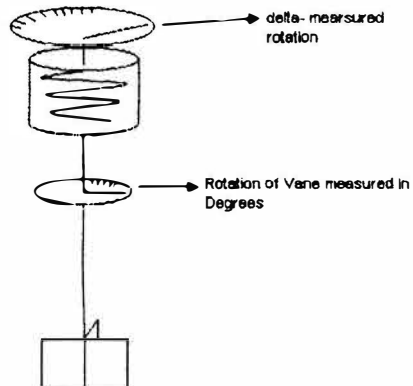
CALIBRATION LINE = Y = MX + B
M = 1632.7
B = 5.196

SLOPE OF CALIBRATION CURVE = M

CALIBRATION CURVE PERFORMED BY
JEFF BRADSHAW OF THE CIVIL
ENGINEERING DEPT.

VANE AT TOP OF SPECIMEN = 14 IN.

271						273						289						16					
13						12						12						16					
READINGS	MEASURED ROTATION FROM TOP OF MINUTUARE VANE (Δ)	T = (Δ / (B X 12))	τ = T X k	ACTUAL ROTATION OF VANE	ε = Actual Rotation of vane / 360°	READINGS	MEASURED ROTATION FROM TOP OF MINUTUARE VANE (Δ)	T = (Δ / (B X 12))	τ = T X k	ACTUAL ROTATION OF VANE	ε = Actual Rotation of vane / 360°	READINGS	MEASURED ROTATION FROM TOP OF MINUTUARE VANE (Δ)	T = (Δ / (B X 12))	τ = T X k	ACTUAL ROTATION OF VANE	ε = Actual Rotation of vane / 360°	READINGS	MEASURED ROTATION FROM TOP OF MINUTUARE VANE (Δ)	T = (Δ / (B X 12))	τ = T X k	ACTUAL ROTATION OF VANE	ε = Actual Rotation of vane / 360°
1	0.00	0.00000	0.0000E+00	0.00	0.000E+00	1.00	0.00	0.0000	0.0000E+00	0.00	0.000E+00	1.00	0.00	0.0000	0.0000E+00	0.00	0.000E+00	2.00	0.00	0.0000	0.0000E+00	0.00	0.000E+00
2	29.00	0.00148	2.2425E-07	0.00	0.000E+00	2.00	21.00	0.0011	1.6238E-07	1.00	2.777E-03	2.00	21.00	0.0011	1.6238E-07	1.00	2.777E-03	3.00	41.00	0.0021	3.1704E-07	5.00	1.388E-02
3	49.00	0.00250	3.7890E-07	2.00	5.556E-03	3.00	41.00	0.0021	3.1704E-07	5.00	1.388E-02	4.00	56.00	0.0029	4.3303E-07	9.00	2.5000E-02	5.00	56.00	0.0036	5.4901E-07	15.00	4.1867E-02
4	69.00	0.00352	5.3355E-07	7.00	1.944E-02	6.00	86.00	0.0044	6.8500E-07	24.00	6.667E-02	7.00	86.00	0.0049	7.4233E-07	34.00	9.4444E-02	8.00	101.00	0.0052	7.8099E-07	44.00	1.2222E-01
5	84.00	0.00429	6.4954E-07	13.00	3.611E-02	9.00	102.00	0.0052	7.8872E-07	54.00	1.5000E-01	10.00	90.00	0.0046	6.8503E-07	64.00	1.777E-01	11.00	82.00	0.0042	6.3407E-07	74.00	2.0556E-01
6	94.00	0.00480	7.2686E-07	22.00	6.111E-02	12.00	74.00	0.0038	5.7221E-07	84.00	2.3333E-01	13.00	62.00	0.0032	4.7842E-07	96.00	2.6389E-01	14.00	52.00	0.0027	4.0209E-07	125.00	3.4722E-01
7	98.00	0.00500	7.5779E-07	27.00	7.500E-02	15.00	45.00	0.0023	3.4797E-07	150.00	4.1667E-01	16.00	42.00	0.0021	3.2477E-07	175.00	4.8611E-01	17.00	39.00	0.0020	3.0157E-07	178.00	4.9444E-01
8	95.00	0.00485	7.3460E-07	37.00	1.028E-01	18.00		0.0000	0.0000E+00		0.000E+00	18.00		0.0000	0.0000E+00		0.000E+00	19.00		0.0000	0.0000E+00		0.000E+00
9	90.00	0.00459	6.9593E-07	47.00	1.308E-01	20.00		0.0000	0.0000E+00		0.000E+00	20.00		0.0000	0.0000E+00		0.000E+00	21.00		0.0000	0.0000E+00		0.000E+00
10	87.00	0.00444	6.7274E-07	57.00	1.583E-01	22.00		0.0000	0.0000E+00		0.000E+00	22.00		0.0000	0.0000E+00		0.000E+00	23.00		0.0000	0.0000E+00		0.000E+00
11	82.00	0.00419	6.3407E-07	67.00	1.861E-01	23.00		0.0000	0.0000E+00		0.000E+00	24.00		0.0000	0.0000E+00		0.000E+00	24.00		0.0000	0.0000E+00		0.000E+00
12	76.00	0.00388	5.8768E-07	77.00	2.139E-01	25.00		0.0000	0.0000E+00		0.000E+00	25.00		0.0000	0.0000E+00		0.000E+00	25.00		0.0000	0.0000E+00		0.000E+00
13	72.00	0.00367	5.5675E-07	87.00	2.417E-01																		
14	66.00	0.00337	5.1035E-07	99.00	2.750E-01																		
15	62.00	0.00316	4.7942E-07	100.00	2.778E-01																		
16	58.00	0.00296	4.4849E-07	125.00	3.472E-01																		
17	56.00	0.00286	4.3303E-07	150.00	4.167E-01																		
18	52.00	0.00265	4.0209E-07	186.00	5.167E-01																		
19		0.00000	0.0000E+00		0.000E+00																		
20		0.00000	0.0000E+00		0.000E+00																		
21		0.00000	0.0000E+00		0.000E+00																		
22		0.00000	0.0000E+00		0.000E+00																		
23		0.00000	0.0000E+00		0.000E+00																		
24		0.00000	0.0000E+00		0.000E+00																		
25		0.00000	0.0000E+00		0.000E+00																		
1	52.00			186.00		1.00	39.00			178.00		2.00	49.00			298.00							
2	52.00			297.00																			



Vane Shear Data for a water content of 21.5%

WATER CONTENT OF SPECIMEN	
W _{WET} (g) =	43.6
W _{WET + GROSS} (g) =	170
W _{DRY + GROSS} (g) =	147.8
WC ACTUAL % =	0213

WATER CONTENT OF SOIL IN LAB = 16

ADJUSTED WATER CONTENT = 19.9%

k = 1/K where K = 0.0001515 ft³ for a 5 x 5 vane

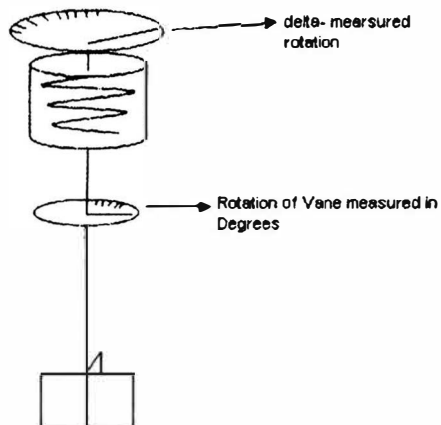
CALIBRATION LINE = Y = MX + B =
M = 1632.7 y = 1632.7x + 5.196

B = SLOPE OF CALIBRATION CURVE = M
CALIBRATION CURVE PERFORMED BY JEFF BRADSHAW
OF THE CIVIL ENGINEERING DEPT.

VANE AT TOP OF SPECIMEN = 14 IN.

= residual strength

275							7							285							64						
13							12							12							64						
READING S	MEASURED ROTATION FROM TOP OF MINITURE VANE (Δ)	T = (Δ / (B X 12))	τ = T X k	ACTUAL ROTATION OF VANE	ε = Actual Rotation of vane / 360°		READING S	MEASURED ROTATION FROM TOP OF MINITURE VANE (Δ)	T = (Δ / (B X 12))	τ = T X k	ACTUAL ROTATION OF VANE	ε = Actual Rotation of vane / 360°		READING S	MEASURED ROTATION FROM TOP OF MINITURE VANE (Δ)	T = (Δ / (B X 12))	τ = T X k	ACTUAL ROTATION OF VANE	ε = Actual Rotation of vane / 360°		READING S	MEASURED ROTATION FROM TOP OF MINITURE VANE (Δ)	T = (Δ / (B X 12))	τ = T X k	ACTUAL ROTATION OF VANE	ε = Actual Rotation of vane / 360°	
1	0.00	0.00000	0.0000E+00	0.00	0.0000E+00		1.00	0.00	0.0000	0.0000E+00	0.00	0.0000E+00		1.00	0.00	0.0000	0.0000E+00	0.00	0.0000E+00		1.00	0.00	0.0000	0.0000E+00	0.00	0.0000E+00	
2	20.00	0.00102	1.5465E-07	1.00	2.778E-03		2.00	30.00	0.0015	2.3198E-07	2.00	5.5556E-03		2.00	30.00	0.0015	2.3198E-07	2.00	5.5556E-03		2.00	30.00	0.0015	2.3198E-07	2.00	5.5556E-03	
3	40.00	0.00204	3.0930E-07	2.00	5.5556E-03		3.00	40.00	0.0020	3.0630E-07	2.00	5.5556E-03		3.00	40.00	0.0020	3.0630E-07	2.00	5.5556E-03		3.00	40.00	0.0020	3.0630E-07	2.00	5.5556E-03	
4	50.00	0.00255	3.8663E-07	5.00	1.389E-02		4.00	50.00	0.0026	3.8663E-07	4.00	1.1111E-02		4.00	50.00	0.0026	3.8663E-07	4.00	1.1111E-02		4.00	50.00	0.0026	3.8663E-07	4.00	1.1111E-02	
5	60.00	0.00306	4.6398E-07	9.00	2.500E-02		5.00	60.00	0.0031	4.6398E-07	7.00	1.9444E-02		5.00	60.00	0.0031	4.6398E-07	7.00	1.9444E-02		5.00	60.00	0.0031	4.6398E-07	7.00	1.9444E-02	
6	70.00	0.00357	5.4128E-07	22.00	6.111E-02		6.00	65.00	0.0033	5.0262E-07	11.00	3.0556E-02		6.00	65.00	0.0033	5.0262E-07	11.00	3.0556E-02		6.00	65.00	0.0033	5.0262E-07	11.00	3.0556E-02	
7	80.00	0.00408	6.1861E-07	34.00	9.444E-02		7.00	62.00	0.0032	4.7942E-07	26.00	7.2222E-02		7.00	62.00	0.0032	4.7942E-07	26.00	7.2222E-02		7.00	62.00	0.0032	4.7942E-07	26.00	7.2222E-02	
8	74.00	0.00378	5.7221E-07	49.00	1.361E-01		8.00	58.00	0.0030	4.4849E-07	38.00	1.0000E-01		8.00	58.00	0.0030	4.4849E-07	38.00	1.0000E-01		8.00	58.00	0.0030	4.4849E-07	38.00	1.0000E-01	
9	70.00	0.00357	5.4128E-07	53.00	1.472E-01		9.00	56.00	0.0029	4.3303E-07	48.00			9.00	56.00	0.0029	4.3303E-07	48.00			9.00	56.00	0.0029	4.3303E-07	48.00		
10	68.00	0.00347	5.2582E-07	63.00	1.750E-01		10.00	54.00	0.0028	4.1756E-07	46.00			10.00	54.00	0.0028	4.1756E-07	46.00			10.00	54.00	0.0028	4.1756E-07	46.00		
11	64.00	0.00327	4.8489E-07	73.00	2.028E-01		11.00	48.00	0.0024	3.7116E-07	56.00			11.00	48.00	0.0024	3.7116E-07	56.00			11.00	48.00	0.0024	3.7116E-07	56.00		
12	60.00	0.00306	4.6398E-07	83.00	2.308E-01		12.00	44.00	0.0022	3.4023E-07	66.00			12.00	44.00	0.0022	3.4023E-07	66.00			12.00	44.00	0.0022	3.4023E-07	66.00		
13	52.00	0.00265	4.0209E-07	88.00	2.444E-01		13.00	42.00	0.0021	3.2477E-07	76.00			13.00	42.00	0.0021	3.2477E-07	76.00			13.00	42.00	0.0021	3.2477E-07	76.00		
14	50.00	0.00255	3.8663E-07	90.00	2.500E-01		14.00	40.00	0.0020	3.0630E-07	86.00			14.00	40.00	0.0020	3.0630E-07	86.00			14.00	40.00	0.0020	3.0630E-07	86.00		
15	45.00	0.00230	3.4797E-07	150.00	4.167E-01		15.00	38.00	0.0019	2.9384E-07	88.00			15.00	38.00	0.0019	2.9384E-07	88.00			15.00	38.00	0.0019	2.9384E-07	88.00		
16	40.00	0.00204	3.0930E-07	200.00	5.556E-01		16.00	36.00	0.0018	2.7837E-07	90.00			16.00	36.00	0.0018	2.7837E-07	90.00			16.00	36.00	0.0018	2.7837E-07	90.00		
17	37.00	0.00189	2.8611E-07	204.00	5.667E-01		17.00	35.00	0.0018	2.7084E-07	131.00			17.00	35.00	0.0018	2.7084E-07	131.00			17.00	35.00	0.0018	2.7084E-07	131.00		
18		0.00000	0.0000E+00		0.000E+00		18.00		0.0000	0.0000E+00				18.00		0.0000	0.0000E+00				18.00		0.0000	0.0000E+00			
19		0.00000	0.0000E+00		0.000E+00		19.00		0.0000	0.0000E+00				19.00		0.0000	0.0000E+00				19.00		0.0000	0.0000E+00			
20		0.00000	0.0000E+00		0.000E+00		20.00		0.0000	0.0000E+00				20.00		0.0000	0.0000E+00				20.00		0.0000	0.0000E+00			
21		0.00000	0.0000E+00		0.000E+00		21.00		0.0000	0.0000E+00				21.00		0.0000	0.0000E+00				21.00		0.0000	0.0000E+00			
22		0.00000	0.0000E+00		0.000E+00		22.00		0.0000	0.0000E+00				22.00		0.0000	0.0000E+00				22.00		0.0000	0.0000E+00			
23		0.00000	0.0000E+00		0.000E+00		23.00		0.0000	0.0000E+00				23.00		0.0000	0.0000E+00				23.00		0.0000	0.0000E+00			
24		0.00000	0.0000E+00		0.000E+00		24.00		0.0000	0.0000E+00				24.00		0.0000	0.0000E+00				24.00		0.0000	0.0000E+00			
25		0.00000	0.0000E+00		0.000E+00		25.00		0.0000	0.0000E+00				25.00		0.0000	0.0000E+00				25.00		0.0000	0.0000E+00			
1	37.00			204.00			1.00	35.00			131.00			1.00	35.00			131.00			1.00	35.00			131.00		
2	43.00			323.00			2.00	44.00			220.00			2.00	44.00			220.00			2.00	44.00			220.00		



Vane Shear Data for a water content of 22.0%

WATER CONTENT OF SPECIMEN

W _{LAB} (g) =	53.7
W _{WET + GROSS} (g) =	158.4
W _{DRY + GROSS} (g) =	139.8
WC _{ACTUAL} % =	0.22

WATER CONTENT OF SOIL IN LAB = 1.8

ADJUSTED WATER CONTENT = 20.4%

k = 1/K where K = 0.0001515 ft³ for a 5 x 5 vane

CALIBRATION LINE = Y = MX + B = y = 1632.7x + 5.198

M = 1632.7

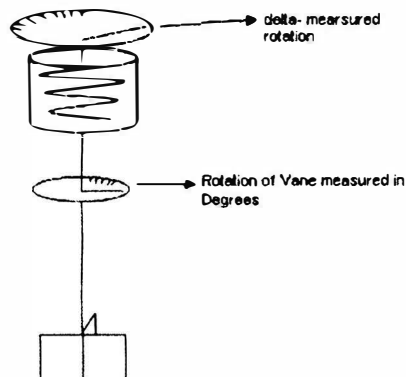
B = SLOPE OF CALIBRATION CURVE = M

CALIBRATION CURVE PERFORMED BY JEFF BRADSHAW OF THE CIVIL ENGINEERING DEPT.

= residual strength

VANE AT TOP OF SPECIMEN = 14 IN

271						322						264						211					
13						12						12						12					
READINGS	MEASURED ROTATION FROM TOP OF MINITURE VANE (Δ)	T = (Δ / (B X 12))	τ = T X k	ACTUAL ROTATION OF VANE	ε = Actual Rotation of Vane / 360°	READINGS	MEASURED ROTATION FROM TOP OF MINITURE VANE (Δ)	T = (Δ / (B X 12))	τ = T X k	ACTUAL ROTATION OF VANE	ε = Actual Rotation of Vane / 360°	READINGS	MEASURED ROTATION FROM TOP OF MINITURE VANE (Δ)	T = (Δ / (B X 12))	τ = T X k	ACTUAL ROTATION OF VANE	ε = Actual Rotation of Vane / 360°	READINGS	MEASURED ROTATION FROM TOP OF MINITURE VANE (Δ)	T = (Δ / (B X 12))	τ = T X k	ACTUAL ROTATION OF VANE	ε = Actual Rotation of Vane / 360°
1	0.00	0.00000	0.0000E+00	0.00	0.000E+00	1.00	0.00	0.0000	0.0000E+00	0.00	0.000E+00	1.00	0.00	0.0000	0.0000E+00	0.00	0.000E+00	1.00	0.00	0.0000	0.0000E+00	0.00	0.000E+00
2	28.00	0.00143	2.1851E-07	1.00	2.778E-03	2.00	23.00	0.0012	1.7785E-07	1.00	2.778E-03	2.00	23.00	0.0012	1.7785E-07	1.00	2.778E-03	2.00	23.00	0.0012	1.7785E-07	1.00	2.778E-03
3	39.00	0.00199	3.0157E-07	3.00	8.333E-03	3.00	40.50	0.0021	3.1317E-07	2.00	5.555E-03	3.00	40.50	0.0021	3.1317E-07	2.00	5.555E-03	3.00	40.50	0.0021	3.1317E-07	2.00	5.555E-03
4	55.00	0.00281	4.2529E-07	5.00	1.389E-02	4.00	51.00	0.0028	3.9436E-07	4.00	1.111E-02	4.00	51.00	0.0028	3.9436E-07	4.00	1.111E-02	4.00	51.00	0.0028	3.9436E-07	4.00	1.111E-02
5	68.00	0.00352	5.3355E-07	20.00	5.558E-02	5.00	61.00	0.0031	4.7186E-07	6.00	1.667E-02	5.00	61.00	0.0031	4.7186E-07	6.00	1.667E-02	5.00	61.00	0.0031	4.7186E-07	6.00	1.667E-02
6	79.00	0.00403	6.1087E-07	38.00	1.056E-01	6.00	71.00	0.0036	5.4901E-07	22.00	6.111E-02	6.00	71.00	0.0036	5.4901E-07	22.00	6.111E-02	6.00	71.00	0.0036	5.4901E-07	22.00	6.111E-02
7	75.00	0.00383	5.7994E-07	48.00	1.333E-01	7.00	65.00	0.0033	5.0262E-07	29.00	8.055E-02	7.00	65.00	0.0033	5.0262E-07	29.00	8.055E-02	7.00	65.00	0.0033	5.0262E-07	29.00	8.055E-02
8	70.00	0.00357	5.4128E-07	56.00	1.611E-01	8.00	60.00	0.0031	4.6396E-07	39.00	1.083E-01	8.00	60.00	0.0031	4.6396E-07	39.00	1.083E-01	8.00	60.00	0.0031	4.6396E-07	39.00	1.083E-01
9	65.00	0.00332	5.0262E-07	66.00	1.889E-01	9.00	58.00	0.0030	4.4849E-07	49.00	1.361E-01	9.00	58.00	0.0030	4.4849E-07	49.00	1.361E-01	9.00	58.00	0.0030	4.4849E-07	49.00	1.361E-01
10	60.00	0.00306	4.6396E-07	78.00	2.167E-01	10.00	55.00	0.0028	4.2529E-07	59.00	1.639E-01	10.00	55.00	0.0028	4.2529E-07	59.00	1.639E-01	10.00	55.00	0.0028	4.2529E-07	59.00	1.639E-01
11	55.00	0.00281	4.2529E-07	88.00	2.444E-01	11.00	53.00	0.0027	4.0983E-07	69.00	1.916E-01	11.00	53.00	0.0027	4.0983E-07	69.00	1.916E-01	11.00	53.00	0.0027	4.0983E-07	69.00	1.916E-01
12	50.00	0.00255	3.8663E-07	92.00	2.550E-01	12.00	50.00	0.0026	3.8663E-07	79.00	2.194E-01	12.00	50.00	0.0026	3.8663E-07	79.00	2.194E-01	12.00	50.00	0.0026	3.8663E-07	79.00	2.194E-01
13		0.00000	0.0000E+00		0.000E+00	13.00	48.00	0.0024	3.7116E-07	69.00	2.472E-01	13.00	48.00	0.0024	3.7116E-07	69.00	2.472E-01	13.00	48.00	0.0024	3.7116E-07	69.00	2.472E-01
14		0.00000	0.0000E+00		0.000E+00	14.00	44.00	0.0022	3.4023E-07	91.00	2.527E-01	14.00	44.00	0.0022	3.4023E-07	91.00	2.527E-01	14.00	44.00	0.0022	3.4023E-07	91.00	2.527E-01
15		0.00000	0.0000E+00		0.000E+00	15.00	41.00	0.0021	3.1704E-07	93.00	2.583E-01	15.00	41.00	0.0021	3.1704E-07	93.00	2.583E-01	15.00	41.00	0.0021	3.1704E-07	93.00	2.583E-01
16		0.00000	0.0000E+00		0.000E+00	16.00		0.0000	0.0000E+00		0.0000E+00	16.00		0.0000	0.0000E+00		0.0000E+00	16.00		0.0000	0.0000E+00		0.0000E+00
17		0.00000	0.0000E+00		0.000E+00	17.00		0.0000	0.0000E+00		0.0000E+00	17.00		0.0000	0.0000E+00		0.0000E+00	17.00		0.0000	0.0000E+00		0.0000E+00
18		0.00000	0.0000E+00		0.000E+00	18.00		0.0000	0.0000E+00		0.0000E+00	18.00		0.0000	0.0000E+00		0.0000E+00	18.00		0.0000	0.0000E+00		0.0000E+00
19		0.00000	0.0000E+00		0.000E+00	19.00		0.0000	0.0000E+00		0.0000E+00	19.00		0.0000	0.0000E+00		0.0000E+00	19.00		0.0000	0.0000E+00		0.0000E+00
20		0.00000	0.0000E+00		0.000E+00	20.00		0.0000	0.0000E+00		0.0000E+00	20.00		0.0000	0.0000E+00		0.0000E+00	20.00		0.0000	0.0000E+00		0.0000E+00
21		0.00000	0.0000E+00		0.000E+00	21.00		0.0000	0.0000E+00		0.0000E+00	21.00		0.0000	0.0000E+00		0.0000E+00	21.00		0.0000	0.0000E+00		0.0000E+00
22		0.00000	0.0000E+00		0.000E+00	22.00		0.0000	0.0000E+00		0.0000E+00	22.00		0.0000	0.0000E+00		0.0000E+00	22.00		0.0000	0.0000E+00		0.0000E+00
23		0.00000	0.0000E+00		0.000E+00	23.00		0.0000	0.0000E+00		0.0000E+00	23.00		0.0000	0.0000E+00		0.0000E+00	23.00		0.0000	0.0000E+00		0.0000E+00
24		0.00000	0.0000E+00		0.000E+00	24.00		0.0000	0.0000E+00		0.0000E+00	24.00		0.0000	0.0000E+00		0.0000E+00	24.00		0.0000	0.0000E+00		0.0000E+00
25		0.00000	0.0000E+00		0.000E+00	25.00		0.0000	0.0000E+00		0.0000E+00	25.00		0.0000	0.0000E+00		0.0000E+00	25.00		0.0000	0.0000E+00		0.0000E+00
1	50.00			92.00		1.00	41.00			93.00		1.00	41.00			93.00		1.00	41.00			93.00	
2	55.00			223.00		2.00	44.00			291.60		2.00	44.00			291.60		2.00	44.00			291.60	



Vane Shear Data for a water content of 22.5%

WATER CONTENT OF SPECIMEN	
$(W_{ATL} \%) =$	49.6
$W_{WET} + GROSS (g) =$	186.5
$W_{DRY} + GROSS (g) =$	161.6
$WC_{ACTUAL} \% =$	0.222

WATER CONTENT OF SOIL IN LAB = 1.0

ADJUSTED WATER CONTENT = 20.9%

$k = 1/K$ where $K =$ 0.0001515 R^3 for a 5 x 5 vane

CALIBRATION LINE = $Y = MX + B =$
 $M =$ 1632.7 $y = 1832.7x + 5.196$

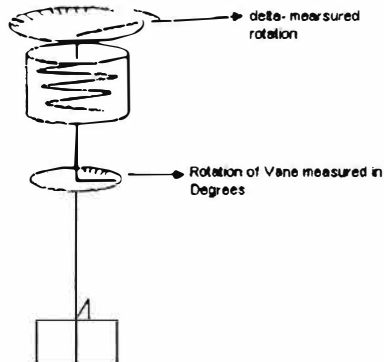
$B =$ SLOPE OF CALIBRATION CURVE = M

CALIBRATION CURVE PERFORMED BY JEFF
 BRADSHAW OF THE CIVIL ENGINEERING
 DEPT

= residual strength

VANE AT TOP OF SPECIMEN = 14 IN

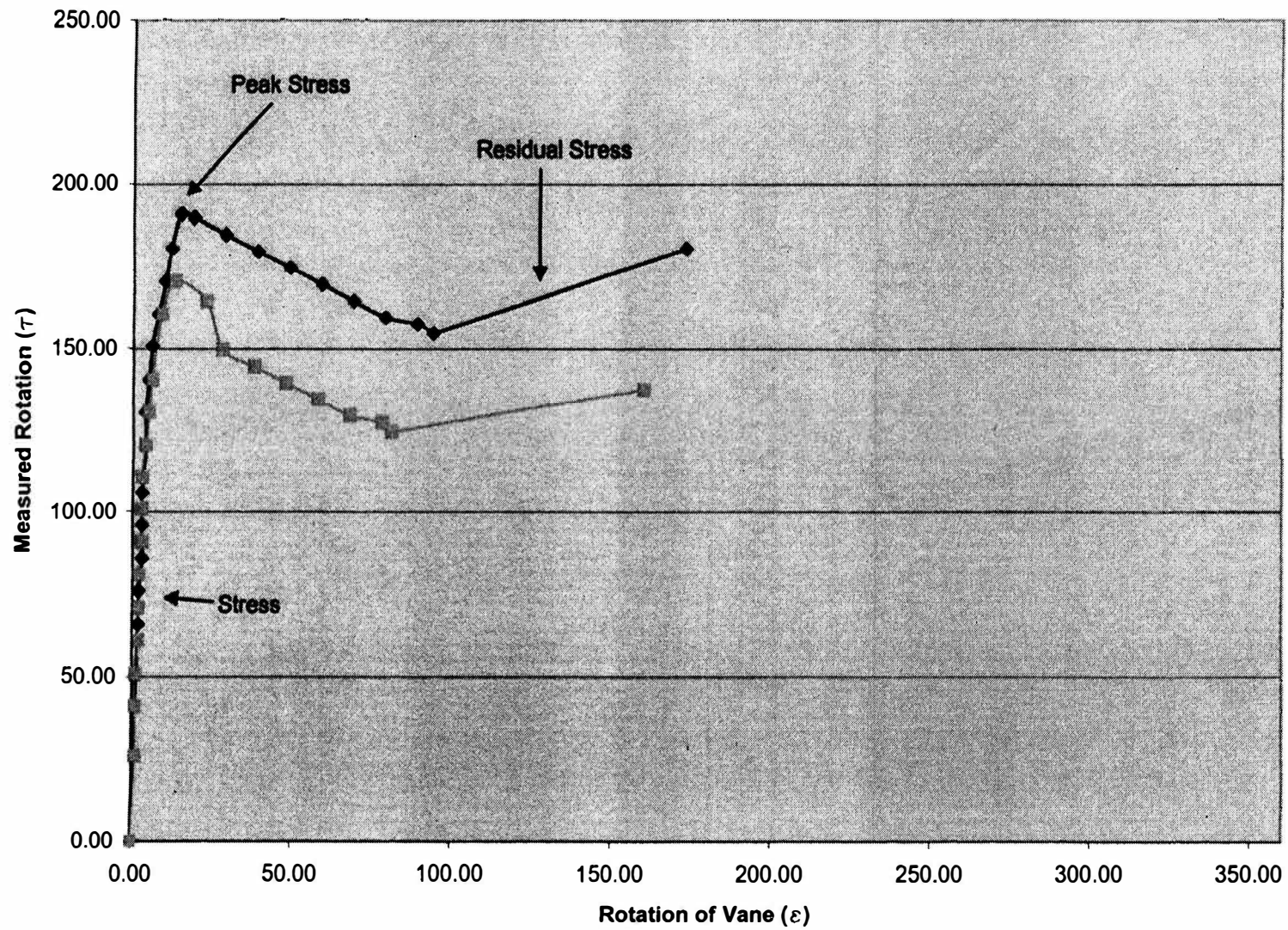
275						115						282						71					
13						12						12						71					
READINGS	MEASURED ROTATION FROM TOP OF MINITURE VANE (Δ)	$T = (\Delta / (B \times 12))$	$\tau = T \times k$	ACTUAL ROTATION OF VANE	$\epsilon = \text{Actual Rotation of vane} / 360^\circ$	READINGS	MEASURED ROTATION FROM TOP OF MINITURE VANE (Δ)	$T = (\Delta / (B \times 12))$	$\tau = T \times k$	ACTUAL ROTATION OF VANE	$\epsilon = \text{Actual Rotation of vane} / 360^\circ$	READINGS	MEASURED ROTATION FROM TOP OF MINITURE VANE (Δ)	$T = (\Delta / (B \times 12))$	$\tau = T \times k$	ACTUAL ROTATION OF VANE	$\epsilon = \text{Actual Rotation of vane} / 360^\circ$	READINGS	MEASURED ROTATION FROM TOP OF MINITURE VANE (Δ)	$T = (\Delta / (B \times 12))$	$\tau = T \times k$	ACTUAL ROTATION OF VANE	$\epsilon = \text{Actual Rotation of vane} / 360^\circ$
1	0.00	0.00000	0.0000E+00	1.00	2.778E-03	1	0.00	0.0000	0.0000E+00	0.00	0.0000E+00	1	0.00	0.0000	0.0000E+00	0.00	0.0000E+00	1	0.00	0.0000	0.0000E+00	0.00	0.0000E+00
2	25.00	0.00128	1.9331E-07	5.00	1.389E-02	2	21.00	0.0011	1.6238E-07	1.00	2.778E-03	2	21.00	0.0011	1.6238E-07	1.00	2.778E-03	3	32.00	0.0016	2.4744E-07	3.00	8.333E-03
3	46.00	0.00235	3.5570E-07	7.00	1.944E-02	3	32.00	0.0016	2.4744E-07	3.00	8.333E-03	4	48.00	0.0024	3.7116E-07	7.00	1.944E-02	5	58.00	0.0030	4.4849E-07	11.00	3.0556E-02
4	56.00	0.00288	4.3303E-07	15.00	4.167E-02	6	67.00	0.0034	5.1808E-07	14.00	3.889E-02	7	68.00	0.0035	5.2582E-07	17.00	4.7222E-02	8	68.00	0.0035	5.2582E-07	17.00	4.7222E-02
5	65.00	0.00332	5.0282E-07	33.00	9.167E-02	8	80.00	0.0031	4.6396E-07	19.00	5.2778E-02	9	55.00	0.0028	4.2529E-07	23.00	6.3889E-02	10	50.00	0.0026	3.8663E-07	68.00	1.8333E-01
6	70.00	0.00357	5.4128E-07	35.00	9.722E-02	10	50.00	0.0026	3.8663E-07	68.00	1.8333E-01	11	47.00	0.0024	3.6343E-07	66.00	1.8167E-01	12	0.00	0.0000	0.0000E+00	0.00	0.0000E+00
7	65.00	0.00332	5.0282E-07	45.00	1.250E-01	13	0.00	0.0000	0.0000E+00	0.00	0.0000E+00	13	0.00	0.0000	0.0000E+00	0.00	0.0000E+00	14	0.00	0.0000	0.0000E+00	0.00	0.0000E+00
8	60.00	0.00308	4.6396E-07	55.00	1.528E-01	14	0.00	0.0000	0.0000E+00	0.00	0.0000E+00	14	0.00	0.0000	0.0000E+00	0.00	0.0000E+00	15	0.00	0.0000	0.0000E+00	0.00	0.0000E+00
9	55.00	0.00281	4.2529E-07	65.00	1.806E-01	15	0.00	0.0000	0.0000E+00	0.00	0.0000E+00	15	0.00	0.0000	0.0000E+00	0.00	0.0000E+00	16	0.00	0.0000	0.0000E+00	0.00	0.0000E+00
10	50.00	0.00255	3.8663E-07	75.00	2.083E-01	16	0.00	0.0000	0.0000E+00	0.00	0.0000E+00	16	0.00	0.0000	0.0000E+00	0.00	0.0000E+00	17	0.00	0.0000	0.0000E+00	0.00	0.0000E+00
11	49.00	0.00250	3.7890E-07	81.00	2.250E-01	17	0.00	0.0000	0.0000E+00	0.00	0.0000E+00	17	0.00	0.0000	0.0000E+00	0.00	0.0000E+00	18	0.00	0.0000	0.0000E+00	0.00	0.0000E+00
12	0.00	0.00000	0.0000E+00	0.00	0.000E+00	18	0.00	0.0000	0.0000E+00	0.00	0.0000E+00	18	0.00	0.0000	0.0000E+00	0.00	0.0000E+00	19	0.00	0.0000	0.0000E+00	0.00	0.0000E+00
13	0.00	0.00000	0.0000E+00	0.00	0.000E+00	19	0.00	0.0000	0.0000E+00	0.00	0.0000E+00	19	0.00	0.0000	0.0000E+00	0.00	0.0000E+00	20	0.00	0.0000	0.0000E+00	0.00	0.0000E+00
14	0.00	0.00000	0.0000E+00	0.00	0.000E+00	20	0.00	0.0000	0.0000E+00	0.00	0.0000E+00	20	0.00	0.0000	0.0000E+00	0.00	0.0000E+00	21	0.00	0.0000	0.0000E+00	0.00	0.0000E+00
15	0.00	0.00000	0.0000E+00	0.00	0.000E+00	21	0.00	0.0000	0.0000E+00	0.00	0.0000E+00	21	0.00	0.0000	0.0000E+00	0.00	0.0000E+00	22	0.00	0.0000	0.0000E+00	0.00	0.0000E+00
16	0.00	0.00000	0.0000E+00	0.00	0.000E+00	22	0.00	0.0000	0.0000E+00	0.00	0.0000E+00	22	0.00	0.0000	0.0000E+00	0.00	0.0000E+00	23	0.00	0.0000	0.0000E+00	0.00	0.0000E+00
17	0.00	0.00000	0.0000E+00	0.00	0.000E+00	23	0.00	0.0000	0.0000E+00	0.00	0.0000E+00	23	0.00	0.0000	0.0000E+00	0.00	0.0000E+00	24	0.00	0.0000	0.0000E+00	0.00	0.0000E+00
18	0.00	0.00000	0.0000E+00	0.00	0.000E+00	24	0.00	0.0000	0.0000E+00	0.00	0.0000E+00	24	0.00	0.0000	0.0000E+00	0.00	0.0000E+00	25	0.00	0.0000	0.0000E+00	0.00	0.0000E+00
19	0.00	0.00000	0.0000E+00	0.00	0.000E+00	25	0.00	0.0000	0.0000E+00	0.00	0.0000E+00	25	0.00	0.0000	0.0000E+00	0.00	0.0000E+00	1	49.00			82.00	
20	0.00	0.00000	0.0000E+00	0.00	0.000E+00	1	49.00			82.00		2	51.00			295.00		1	49.00			69.00	
21	0.00	0.00000	0.0000E+00	0.00	0.000E+00	2	51.00			295.00		2	47.00			234.00		2	47.00			234.00	
22	0.00	0.00000	0.0000E+00	0.00	0.000E+00																		
23	0.00	0.00000	0.0000E+00	0.00	0.000E+00																		
24	0.00	0.00000	0.0000E+00	0.00	0.000E+00																		
25	0.00	0.00000	0.0000E+00	0.00	0.000E+00																		



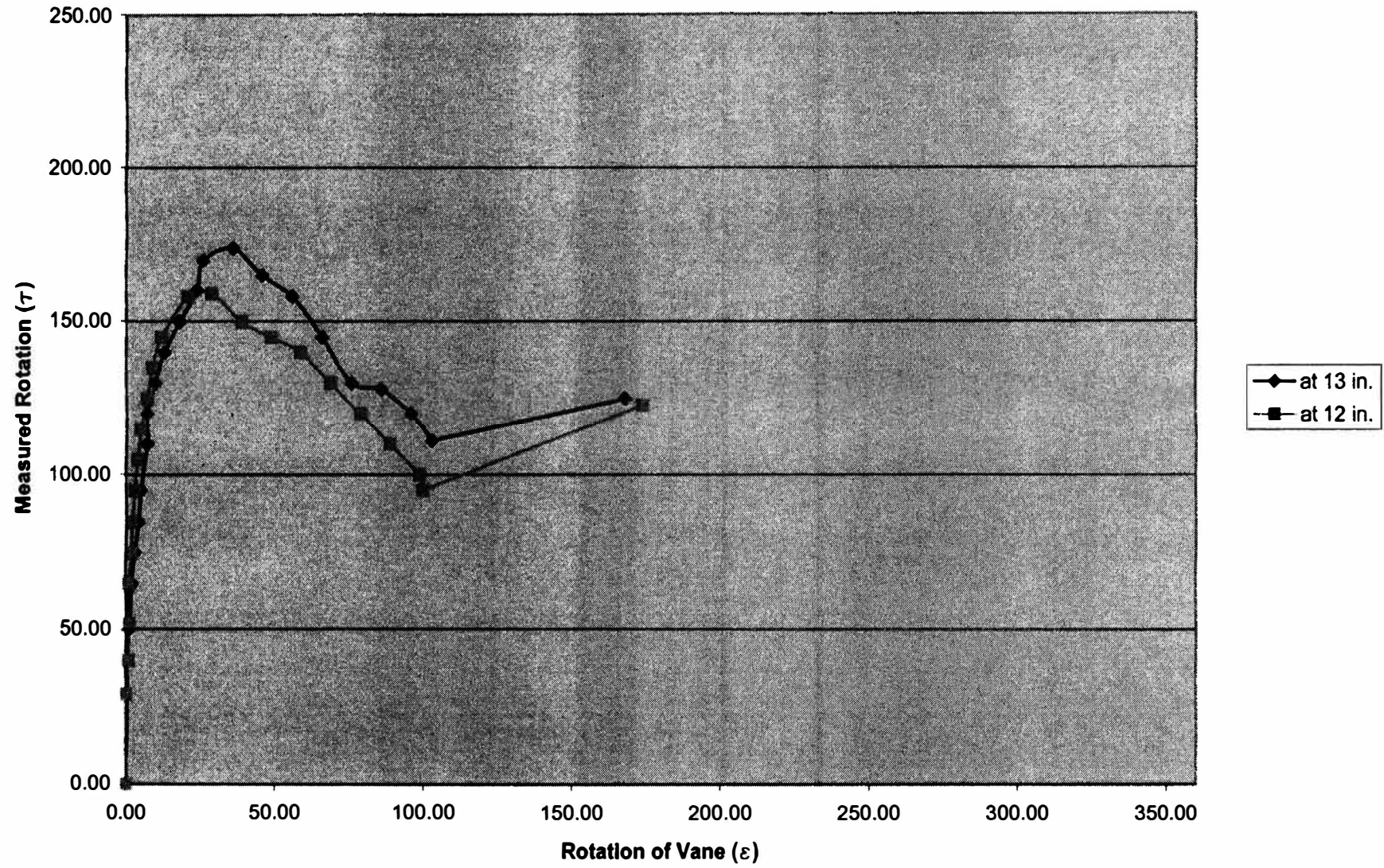
Appendices B

Laboratory Data Graphs

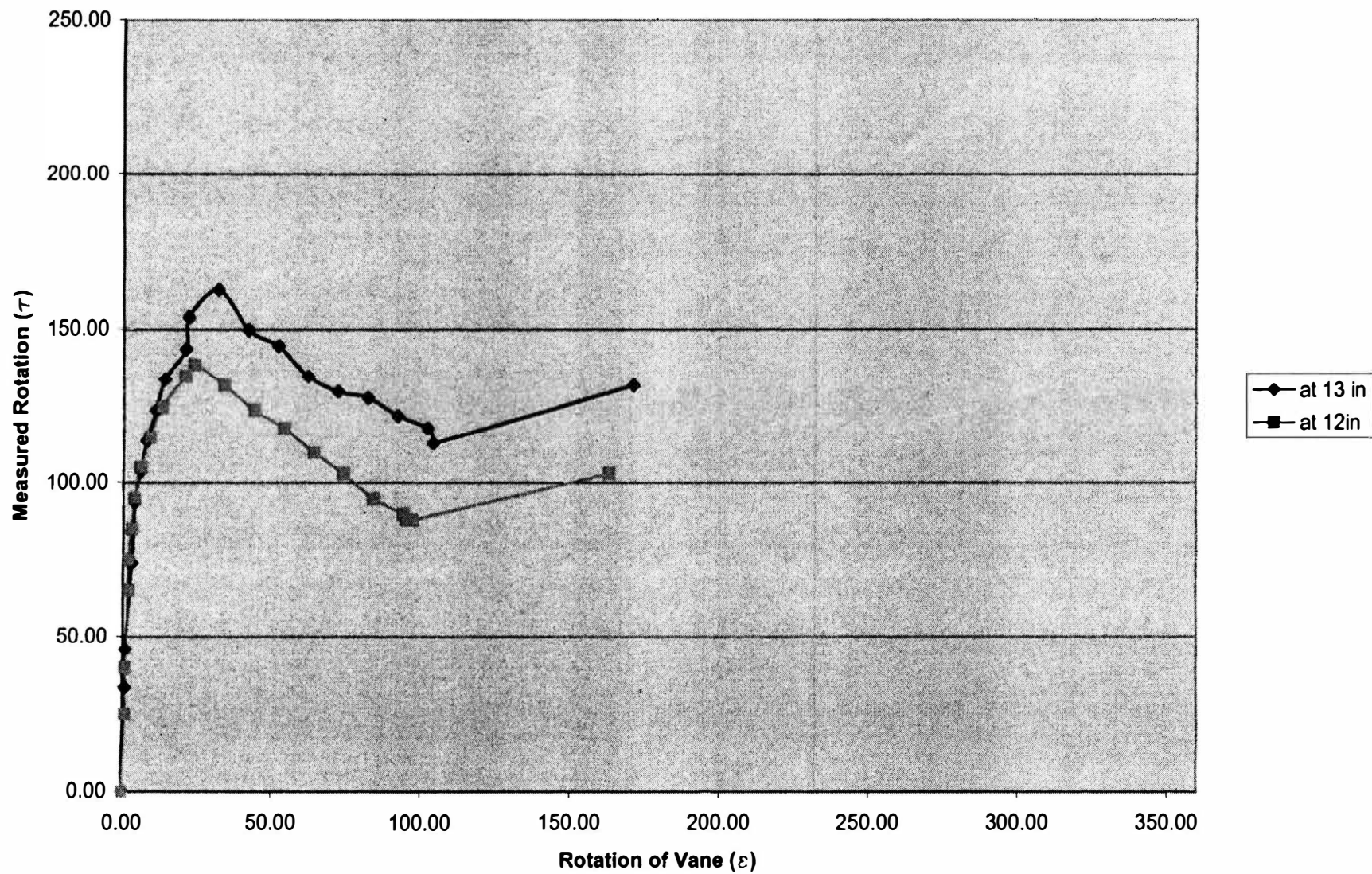
Strength of Soil for a wc of 18.5%



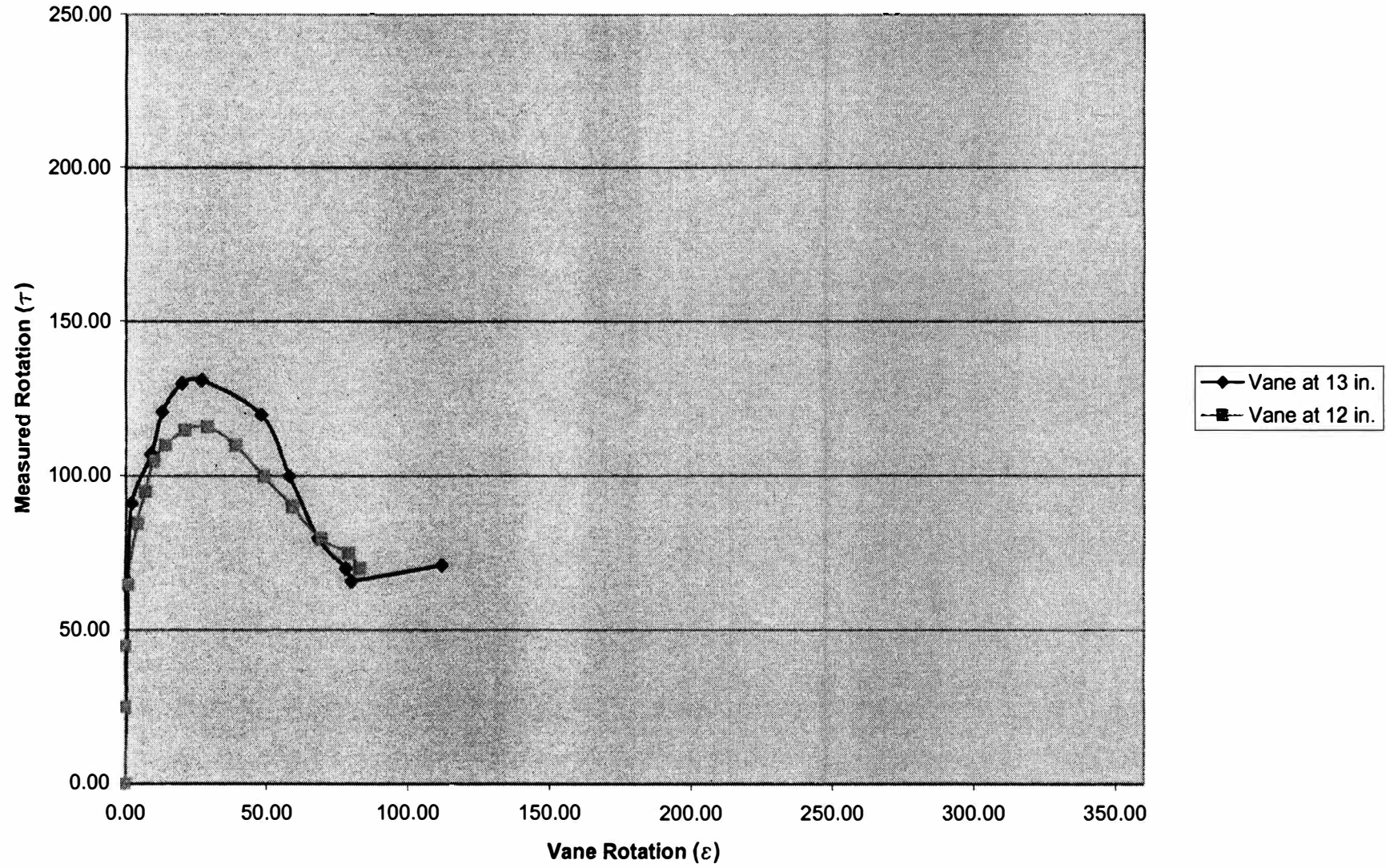
Strength of Soil at a wc of 19%



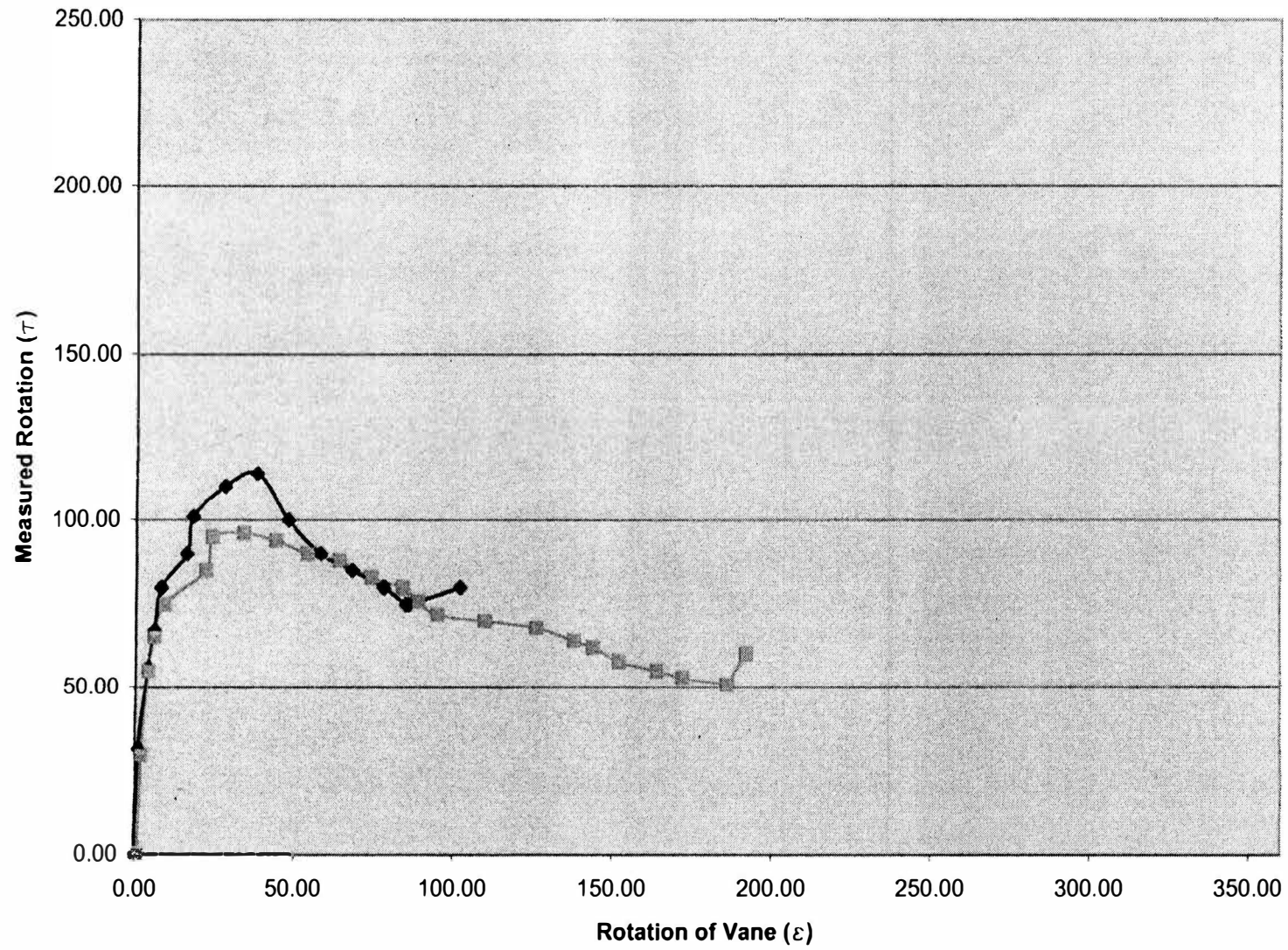
Strength of Soil at a wc of 19.5%



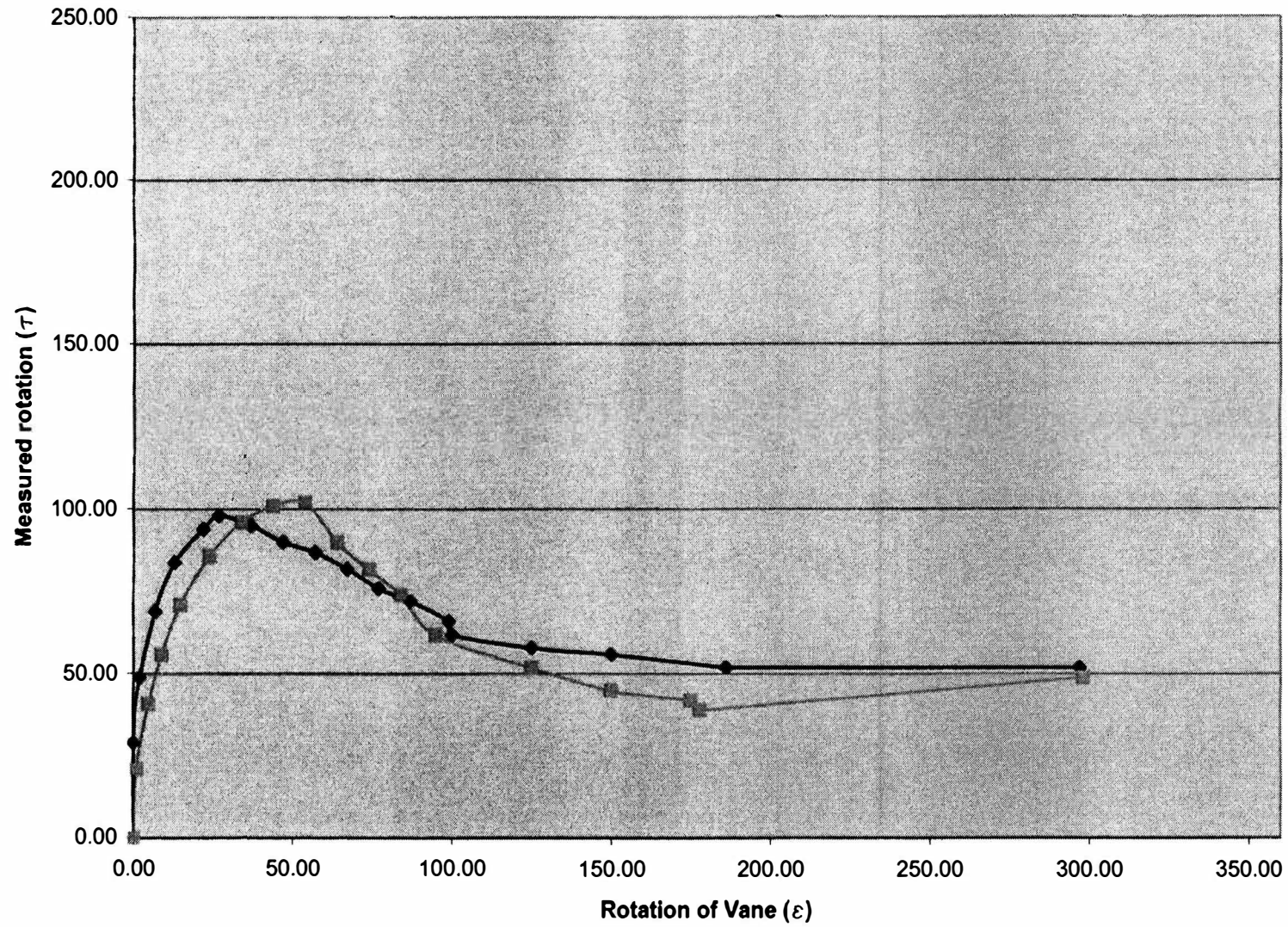
Strength of Soil for a wc of 20%



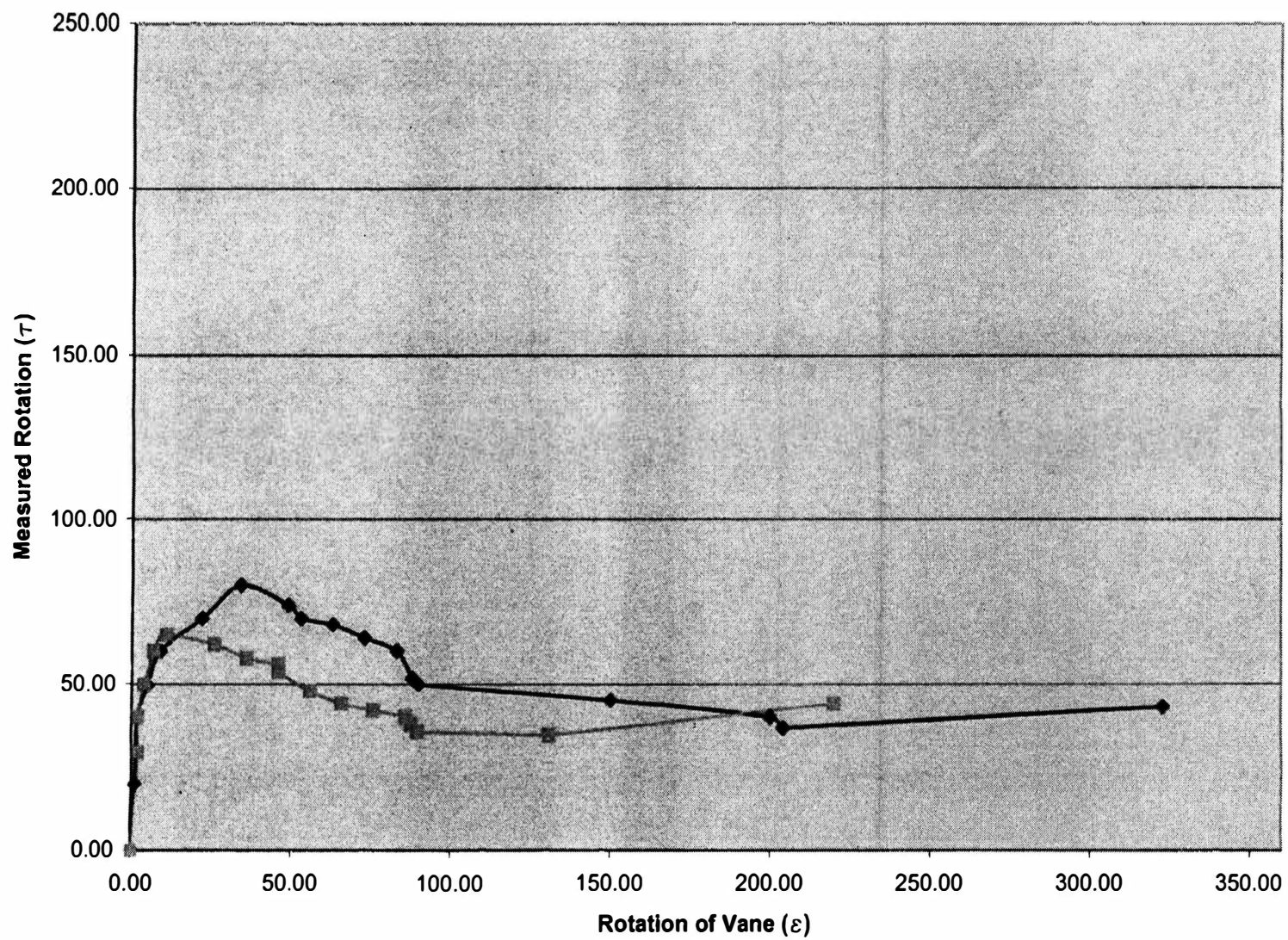
Strength of Soil for a wc of 20.5%



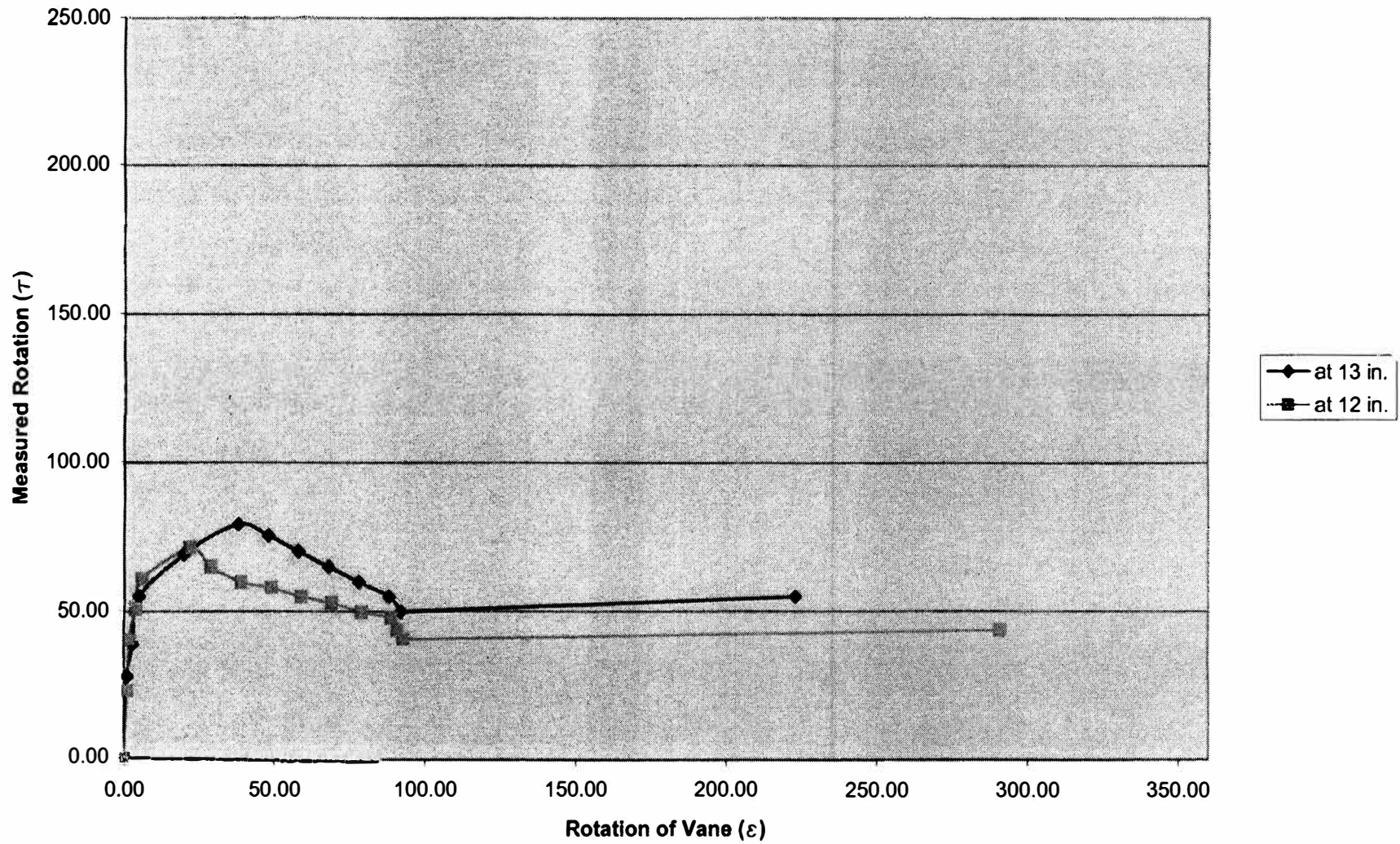
Strength of Soil for wc of 21%



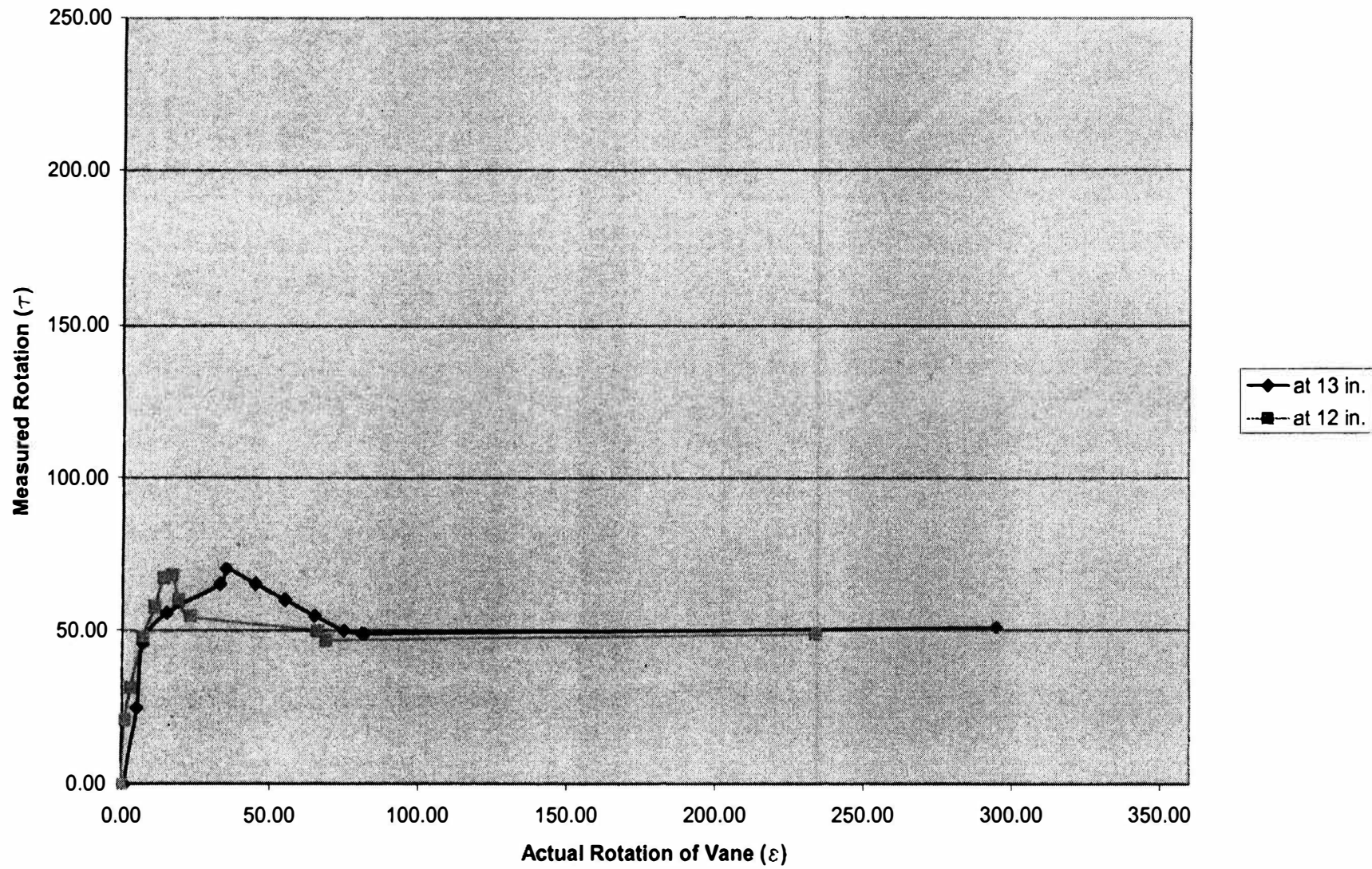
Strength of soil for a wc of 21.5%



Strength of Soil for a wc of 22%



Soil Strength for a wc of 22.5%



**Development of Spring Flow Rating Curve
For Ha Ha Tonka Spring**

March 2005

**Vanessa L. Eckhoff
University of Missouri – Rolla
Opportunities for Undergraduate Research Experience
Participant**

Abstract

The objective of this project was to develop a rating curve for the Ha Ha Tonka spring, located in Ha Ha Tonka State Park. The rating curve is an empirical relationship between spring discharge and the water level at the stream observation point. An additional goal of the project was to develop an interpretative display to communicate current spring discharge to park visitors. Spring discharge and water level were measured periodically between April 2004 and March 2005. A rating curve was plotted using the collected data. Two possible types of interpretative displays were presented to park visitors. The option preferred by most visitors has been submitted to park staff for approval and implementation.

Introduction

Ha Ha Tonka is an excellent example of karst landform complexes in Missouri. It is thought to be a single cave system in various stages of maturity. The major karst features located at Ha Ha Tonka include a cavern-collapse chasm, a karst spring, a natural bridge, sinkholes, and several sizable caves.

The Ha Ha Tonka chasm, or gorge, is a canyon formed by the collapse of a karst cavern. The strata above the cavern walls were thinned by erosion, leading to roof failure and collapse. The resulting gorge, with its 250 foot high walls, contains the flow from the spring. The spring emerges from Eminence Dolomite at the head of the gorge.¹

The large sinkholes in the vicinity are thought to be the points of recharge for the spring. Whispering Dell sinkhole is 150 feet deep, and the Coliseum sinkhole measures 500 feet long and 300 feet wide. An underground stream that flows through nearby River Cave is also a likely point of recharge for the spring. An upland area to the south and east of the spring is the source of recharge waters. Average spring flow is 50 million gallons per day (MGD).¹

The geology that exists at Ha Ha Tonka is quite diverse. A stratigraphic column of the area is shown in Figure 1. The uppermost formation is the Roubidoux formation, which consists of dolomites and sandstones with a variety of cherts. The Gasconade formation lies approximately 70 feet below the Roubidoux. It is vuggy and supports numerous algal structures. The basal member of this formation is the Gunter member, and dolomitic-cemented sandstone. The Eminence formation, from which the spring emerges, is crystalline dolomite that contains small amounts of chert.¹

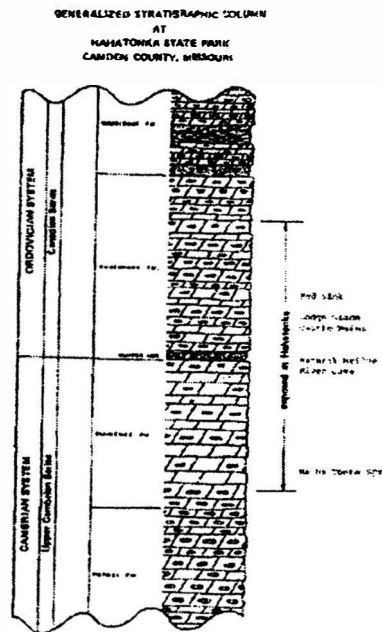


Figure 1. Geological formations present at Ha Ha Tonka State Park.

The average daily spring flow cited in Ha Ha Tonka State Park literature is 48 MGD.² Measurements made by the United States Geological Survey between June 1994 and August 1996 show an average flow of 78 MGD (Table 1.) The USGS measurements do not include data for stream water levels, and therefore a rating curve is not available for the spring.³

Table 1. USGS data, Ha Ha Tonka Spring flow.

Date of Measurement	Volumetric Flow Rate, MGD
June 1994	193.97
August 1994	62.716
November 1994	114.44
April 1995	109.92
June 1995	161.64
August 1995	67.242
December 1995	51.078
April 1996	161.64
June 1996	80.173
August 1996	81.033
Average Flow Rate	77.802

Larry Webb, an Interpretative Resource Specialist at Ha Ha Tonka State Park, expressed interest in a display that would allow park guests to determine the amount of water flowing from the spring at the time of their visit. He relates that visitors commonly pose questions about daily flow. He asserts that a method conveying daily flow data as well as information about seasonal changes in flow would be a welcome at the park.

The goals of this project were to develop a rating curve for Ha Ha Tonka Spring, and to use the curve to develop an interpretive display to be erected at the spring observation point. The project resulted in new geological data that may be used by scientists and others. The project was also an opportunity to inform the public of engineering practices and procedures. Public interest was ongoing throughout the project, culminating with a survey of park visitors to determine a preferred format for the display signage.

Experimental Design Considerations

The first issue that was addressed was the selection of a spring measurement location. The area immediately adjacent to the emerging spring is characterized by a steeply sloping gravel bank that disappears under the bluff, and water depths greater than 10 feet. The stream leaving the spring then progresses to a shallower depth, but the width at this area is greater than 75 feet. The excessive width would require extensive depth and velocity measurements, increasing the possibility for error in the calculated flow rate. Approximately 30 feet downstream from the spring, a gravel bar on one side of the stream causes the channel to narrow to roughly 50 feet. The depth at this location varies from a few inches to approximately 3 feet, so that researchers can safely enter the stream and collect data. A large Sycamore tree growing on the bank near the trail to the spring served as a marker, enabling measurements to be taken at the same location each time.

The selection of a reference position was another important concern. Water level had to be measured at a point that would be stable throughout the year-long course of the study. Natural features such as trees or rocks were at risk of displacement by storms or floods. Therefore, a portion of the boardwalk trail was chosen as a reference point. The section chosen protrudes over the stream approximately 25 feet downstream from the flow measuring location. A 4 inch by 4 inch post, which supports the railing for the boardwalk, was the chosen as the exact point of reference.

Problems with data collection procedures were discovered during early expeditions to collect spring flow information. Conditions were often characterized by rainy weather and swift water in the stream. In an attempt to make measurement more accurate and easier to complete, site-specific equipment was developed. A non-stretch rope was purchased, and was carefully measured. Brightly colored waterproof tape was applied at 2 foot intervals along the length of the rope. This tool greatly increased the speed and accuracy of stream width measurement, with only a small pocket measuring tape needed to determine the distance between the last mark over the

stream and the bank. The 2 foot intervals were also useful for collecting the depth readings, which are taken every 2 feet across the channel's width. Precise measurement of the depth of the water was another challenge. The swift water caused many lightweight measuring devices to bow or bend in the deeper water. A 5 foot length of 1 inch diameter galvanized pipe was purchased, and a flange normally used to attach the pipe to a flat surface was threaded onto one end. A measuring tape was secured to the entire length of pipe with clear waterproof tape, with an allowance made for the flange. The pipe remained straight and visible in even the swiftest of water. The flange prevented the device from sinking into the gravel streambed, improving the accuracy of the depth measurements.

Public involvement was also considered during the planning period. Several methods of including the public in the project were investigated. These included a survey of park visitors to determine their interest in a display detailing spring flow information, and a survey of Missouri state park personnel to collect similar information. A questionnaire posted on the Ha Ha Tonka State Park website was also discussed. The method of public involvement chosen was a survey of park visitors requesting information about their preferred type of interpretative display.

Experimental Procedure

Measurements were made to determine the volumetric flow rate (Q) of the spring, in MGD. Volumetric flow rate is a function of the cross-sectional area of the stream and the average velocity of the stream. Water elevation and depth at a reference point was also recorded, to facilitate accurate placement of a gauging device to accompany the interpretative display.

The first measurement taken during each data collection expedition was the width of the stream in feet. Next, the depth of the water was measured at 2 foot intervals across the width of the stream. These measurements were taken in inches, to the nearest 1/8 of an inch. This data was used to calculate the cross-sectional area of the stream.

The float method was used to determine the average stream velocity. A floating device was attached to a string 10 feet in length. The device was placed in the water, and a stopwatch was used to gauge the time for the device to float the 10 foot distance. Several measurements were taken across the width of the stream. Care was taken to include measurements of both very swift and very slow moving portions of the stream. This data was used to compute the average velocity of the water.

The last data to be collected during each trip was water elevation and depth at the reference position. The designated boardwalk railing post was used as a reference point. The distance from bottom of the post to the surface of the water was recorded, establishing a reliable elevation for the water level. The depth of the water directly beneath the post was also recorded.

The expeditions always included an informal interaction with park visitors about the research and engineering procedures. As guests passed by on the boardwalk and trail, they frequently questioned the researchers about the measurement activities. These opportunities were

used to discuss scientific procedures and experimental design with the visitors. The reactions of the inquisitive guests were overwhelmingly favorable. Many expressed intent to return to the park to view the interpretative display and associated study results

The data collected at the spring was used to determine the volumetric flow rate (Q) in millions of gallons per day (MGD.) The volumetric flow rate data and the water level data were plotted to obtain a rating curve. The equations used for calculation are as follows:

- 1) Average stream depth (feet) = Sum of all depths (feet) ÷ Number of measurements
- 2) Stream cross sectional area (feet²) = Average depth (feet) x Stream width (feet)
- 3) Average float time (seconds) = Sum of all float times (seconds) ÷ Number of trials
- 4) Average surface velocity (feet per second) = Distance floated (feet) ÷ Average float time (seconds)
- 5) Corrected average stream velocity (feet per second) = Average surface velocity (feet per second) x Correction factor (0.8 for streambed composed of loose rocks and coarse gravel)
- 6) Volumetric flow rate (Q, feet³ per second) = Cross sectional area (feet²) x Corrected average stream velocity (feet per second)
- 7) Q (million gallons per day) = Q (feet³ per second) x 0.64656 (conversion factor)

Interpretative Display Development

The first for display option considered involved the placement of a staff gauge in the stream near the spring, in a location easily seen from the trail. A staff gauge is a post or rod that is marked in increments visible to users. The position of the water surface on the staff gauge relates information about water level in the stream. A sign including a representation of the rating curve would be posted on the trail. The sign would include instructions for reading the gauge and determining daily flow from the curve. Alternatively, a table could be used in place of the graph to simplify the display. An environmental product catalog and local sign companies were consulted in order to obtain a rough estimate of the cost of implementing this option. Cost of this option, including staff gauge and signage, is approximately \$500.00.

The alternate option for the display uses an electronic float gauge placed in the stream. The float gauge determines water level by sensing the relative position of floating device. The method is similar to that used to monitor the level of gas in a car's tank. The float gauge would relay water level information to a display site on the trail. The data would be

processed by a device at the display, and an LED readout of spring flow would be seen by visitors. The readout would be part of a sign including the rating curve and an explanation of the method of determining the flow information. This option requires the float gauge, a device to process data, an LED or similar display, and signage. A power source, either battery or solar, will also be necessary. Estimated cost for implementing this option is \$2,000.00.

Small samples of both displays were prepared. The samples were produced with Microsoft PowerPoint software, and were printed on standard letter size paper. The options were presented to park visitors in March 2005. Visitors were asked to indicate which option they would rather view when visiting the spring. The sample signs are shown in Figure 2.

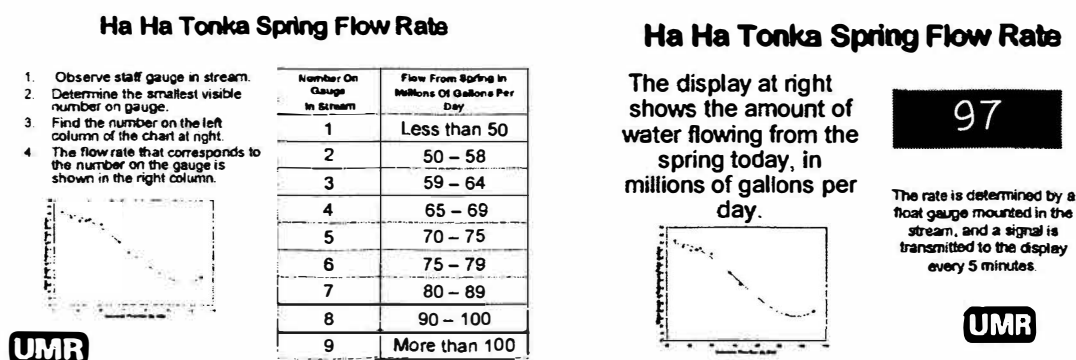


Figure 2. Sample signs shown to park visitors.

Results and Conclusions

Data collected during the ten trips spring is summarized in Table 2. The rating curve that was plotted from the information is shown in Figure 3. Water elevation was plotted instead of water depth because this measurement was thought to be more accurate over time. The points do not all lie perfectly on the curve. This may be attributed to minor changes in channel shape and streambed composition over time. However, most of the points have good fit to the curve. Overall, the data collected and the resulting curve do a good job of characterizing spring flow and water levels over a wide range of discharge rates. In the event that water level is greater than or less than levels measured during the study, the display will relate that flow is less than 43 MGD or greater than 104 MGD.

The results of the survey of park visitors are outlined in Table 3. An overwhelming majority of those questioned preferred the digital display and float gauge option. The most common reason given for this choice was ease of viewing and interpretation. Some older guests expressed concern for their ability to read a staff gauge located in the stream. Those who chose the staff gauge option noted its reliability over time. They frequently voiced concern about the ability of an electronic display to remain operational under harsh conditions. A small number of participants had no opinion.

The completed rating curve and the associated data have been sent to Ha Ha Tonka State Park staff. Representations of both display options were also forwarded, as well as the results of the survey. The final decision as to what type of display will be erected and the exact content of the signage will be made by park officials. The researchers involved in this study plan to participate in the installation of the chosen display.

Table 2. Spring flow and water level data collected during study.

Date	Flow Rate (Q), MGD	Elevation of Water
April 2004	43.5	48.25
May 2004	47.1	47.5
July 2004	50.6	47
August 5, 2004	53.2	47
August 20, 2004	54.9	47.25
September 2004	59.7	46.5
October 2004	67.8	44
November 2004	72.3	42.5
March 2005	104.6	39

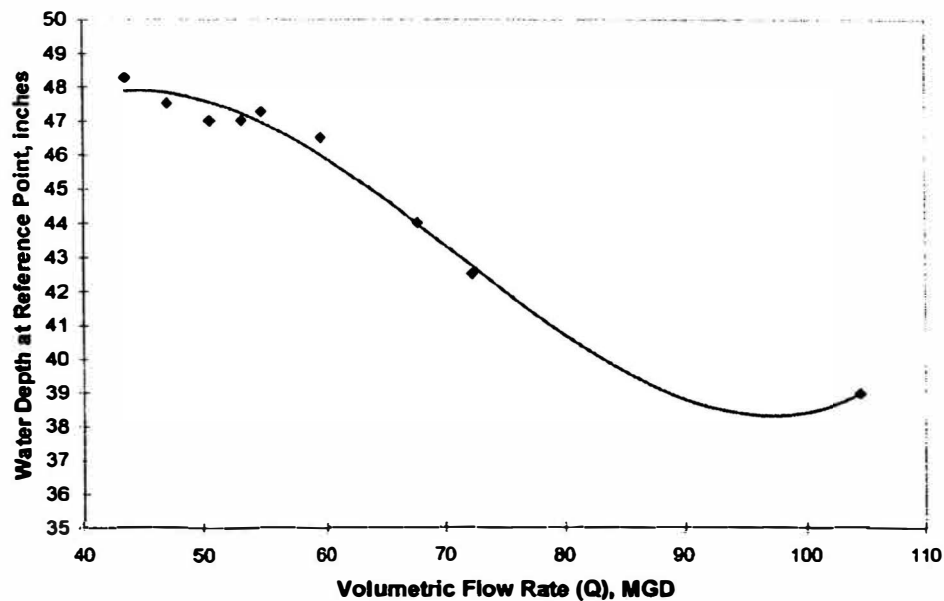


Figure 3. Rating curve for Ha Ha Tonka Spring, showing flow rates (Q) and water elevation at reference point.

Table 3. Data collected during survey of park visitors

Display Option	Number of Votes
Staff Gauge	43
Float Gauge	6
No Opinion	3

Acknowledgements

Elmore, Curt. P.E., Ph.D. Professor of Geological Engineering and Project Advisor, University of Missouri – Rolla

Martin, James. Ph. D. Professor of Psychology, University of Missouri – Rolla

Webb, Larry. Interpretative Resource Specialist, Ha Ha Tonka State Park.

References

1. Beveridge, Thomas R. 1990. Geologic Wonders and Curiosities of Missouri. Missouri Department of Natural Resources: Division of Geology and Land Survey, 280-282.
2. Missouri State Parks. Ha Ha Tonka State Park –Missouri's Karst Showcase. Missouri Department of Natural Resources.
3. United States Geological Survey, Historical Discharge Data.

OURE FINAL REPORT

Jacob James Elmer

4/11/05

Effect of Phosphodiesterase Inhibitors and Dibutyryl cGMP on Gravitropism in *Arabidopsis thaliana*

Jacob Elmer, Jen Jacobi, Kristin Russell

University of Missouri – Rolla, Biological Sciences Department, Rolla, MO

Abstract

Plant roots always orient themselves in the direction of the force of gravity. When reoriented 90 degrees, seedling roots were observed to respond by reorienting their root tips in the same fashion and then growing in that direction. The mechanism for this response, as suggested by Pagnussat et al.(2003)¹, is initiated by nitric oxide and results in cGMP production. When we exposed *A. thaliana* seedling roots to cGMP, those roots reoriented quicker than control roots. The roots were also exposed to phosphodiesterase inhibitors(drugs that prevent the natural degradation of cGMP), which sensitized the roots to the NO- signal and gave an earlier response to reorientation. These results indicate that cGMP and the PDE inhibitors encourage the differential growth in root reorientation.

Introduction

Following germination, plant roots always orient themselves in line with the force of gravity. It has also been observed that roots will reorient themselves when the force of gravity changes direction, as in the rotation of the growth medium. The reorientation is caused by differential growth of the root tip. The existing root maintains its original orientation, but the top of the root tip region grows more than the bottom of the root tip region, resulting in a bending action of the root tip. What causes this differential growth? A mechanism for differential root growth was suggested by Pagnussat et al(2003)¹ in which auxin initiates a reaction that begins with nitric oxide(NO-) and results in the production of cGMP(Figure 1). That experiment tested the effect of NO- on root formation. In our experiment we tested the existence of such a cycle in *A. thaliana* root growth during the reorientation response, beginning with the signal molecule NO-. NO- occurs naturally in *A.*

thaliana, as in other plants, where it is produced by a species-specific nitric oxide synthase(NOS) complex. NO- then activates guanylate cyclase, which converts GTP into cGMP. The effects of NO- donors and inhibitors of the NOS complex and guanylate cyclase were documented in two other reports by Jacobi and Russell. This report primarily focuses on the effects of accumulation of cGMP. Dibutyryl cGMP, a membrane permeable analogue of cGMP, was used to test the effect of cGMP on the growth response. Results showed that plants exposed to this exogenous cGMP had a quicker reorientation response than control plants. Then two PDE inhibitors(Viagra and IBMX) were applied to seedling roots to test the effect of inhibiting the degradation of naturally occurring cGMP, resulting in an accumulation of cGMP. These roots also showed a quicker reorientation response than control plants. These results indicate that cGMP does indeed encourage growth.

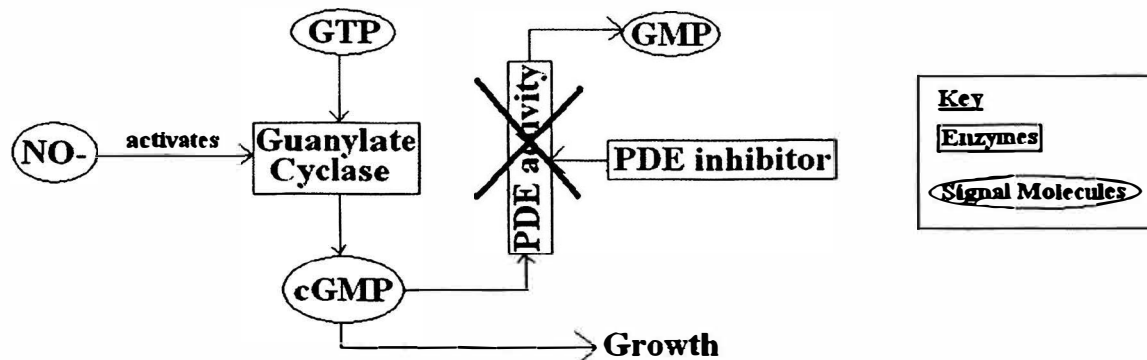


Figure 1. Nitric oxide(NO^-) activates guanylate cyclase, which then converts GTP to cGMP. Normally, the cGMP produced will be degraded by the cell's own phosphodiesterases. However, in the presence of PDE inhibitors like Viagra and IBMX, cGMP remains. cGMP then somehow initiates growth.

Results

Effects of cGMP (Figure 2)

Four week-old seedlings were transferred into agar plates each containing 100uM concentrations of dibutyryl cGMP. There was much variation in the reorientation rates of each plant, but three out of four of the plants showed a response within 2 hours. The control plants, however, didn't initiate reorientation until after 2 hours. At the end of 4 hours, the cGMP exposed roots showed a wide range of reorientation, from 8.75 to 60.95 degrees while the control plants finished from 22.75 to 48.01 degrees.

Effects of Viagra (Figure 3)

Four week-old seedlings were transferred into agar plates each containing 100uM concentrations of Viagra. These Viagra-exposed seedlings showed a much more uniform response than the cGMP seedlings, with every plant showing a clear response within two hours. Once again, this response was quicker than the control seedlings. The graphs of each seedling's reorientation response were very similar, indicating a good trial. Interestingly, even though the Viagra seedlings had an earlier

response, they ended up with approximately the same reorientation as the control plants after four hours.

Effects of IBMX (Figure 4)

Four week-old seedlings were transferred into agar plates, each containing 100uM concentrations of IBMX. Like cGMP and Viagra, the IBMX seedlings showed a good reorientation response within two hours. However, the reorientation rates of the IBMX-treated seedlings were much more sporadic than with the other two drugs, with periods of quick rates of reorientation followed by slower rates. After four hours, reorientation angles were similar to control seedlings.

Comments on Control Plates (Figure 5)

Two different controls were used, a 90-degree rotated control and a clinostat control(eliminates the effect of gravity by continuously rotating the seedlings). The 90 degree control roots showed no reorientation response until two hours had passed. The clinostat plants showed no curvature, they simply grew in the same direction as before they were transplanted.

Figure 2. cGMP Plants

Each line represents a different seedling. A and B refer to the first and second plants while X and Y refer to the first and second plates. Note how each graph has shown some response within two hours, with the exception of cGMPYA. cGMPXB, which had a reorientation angle of 60.95 after four hours, turned out to be the maximum reorientation angle.

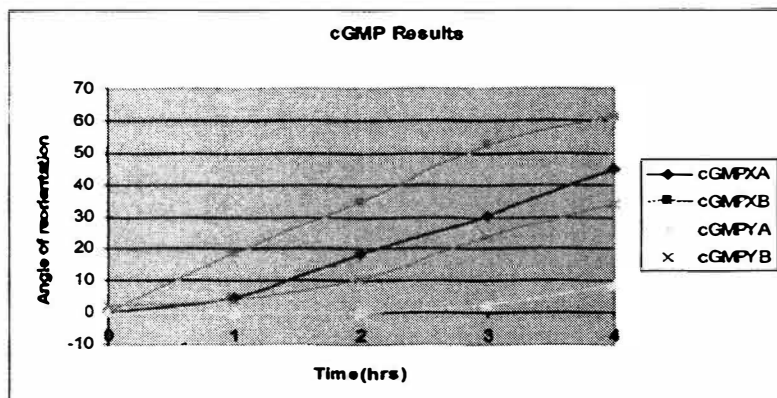


Figure 3. Viagra Plants

Each line represents a different seedling. A and B refer to the first and second plants while X and Y refer to the first and second plates. Note how each graph has shown some response within two hours. Note how the rates of reorientation of each seedling is similar. The roots on plate Y were shorter, possibly explaining the lesser response in that plate.

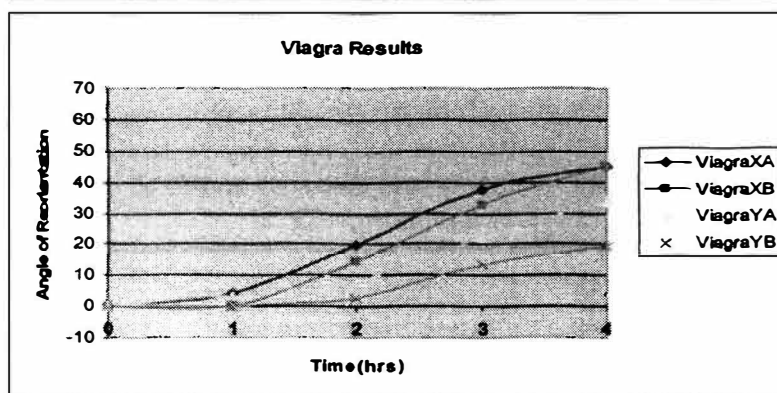


Figure 4. IBMX Plants

Each line represents a different seedling. A and B refer to the first and second plants while X and Y refer to the first and second plates. Note how each graph has shown some response within two hours. Note the sporadic behavior of the graphs; this is probably due to the non-specific nature of IBMX as compared to Viagra.

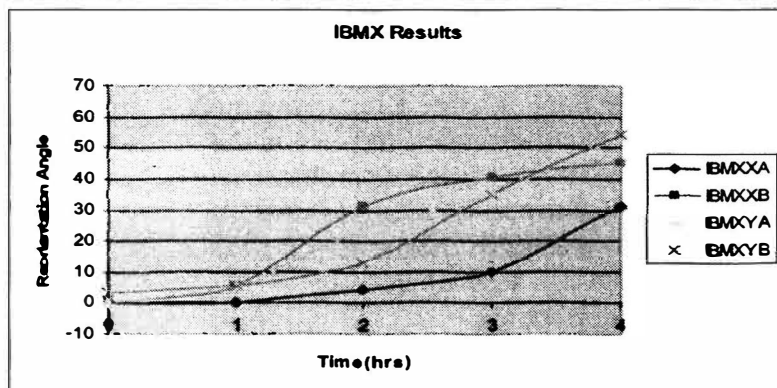
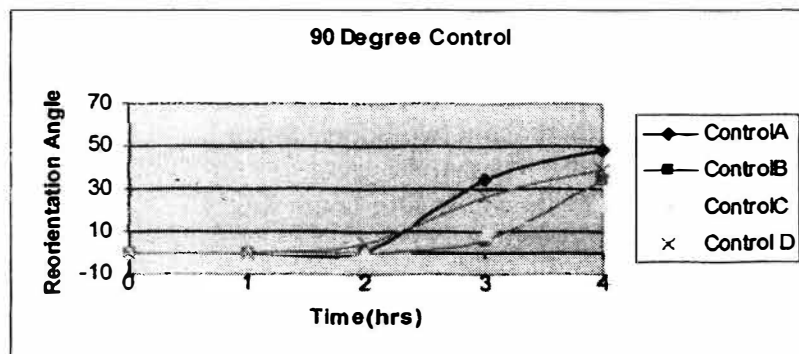


Figure 5. Control Plants

Each line represents a different seedling. Controls C & D were measured on a different day than controls A & B. Note how each root showed no response until after 2 hours. The response was later than the drug plates, but the reorientation rate of each control root was much quicker than any of the drug exposed roots.



Discussion

Overall, the results we obtained were close to what we expected to get. All of the drugs had at least some sensitizing effect on the plant roots – they all showed a response earlier than the control plants. This is what we expected for Viagra and IBMX. As phosphodiesterase inhibitors, their main effect in the Pagnussat's pathway is to magnify the NO- signal by maintaining the levels of cGMP. Therefore, if the NO- starts accumulating immediately after orientation, then these results are to be expected. The PDE inhibitor plants built up cGMP to a response level earlier than the control plants because there was no natural degradation of the cGMP, as there were in the control plants. As a result, any plants exposed to Viagra or IBMX should become sensitized to any NO- signal from reorientation and show an earlier response than normal control plants. This is exactly what was observed. The uniform response from Viagra was the best set of results of the experiment. IBMX on the other hand, showed a lot of variation, not only in the final angles, but also in the rates for each plant. This was probably a result of the nonspecific nature of IBMX's PDE inhibitor activity. Nonetheless, all the IBMX plants still showed an early reorientation response.

The results for cGMP were acceptable. The levels of cGMP should have been higher in the plants than in the controls, so they should logically show a response right away. Most plants did show this effect, but one plant lagged until about two hours. What was encouraging was that the greatest reorientation angle within four hours was obtained with cGMP.

The control results worked out to our expectations. We did trials for different drugs on different days, and each day we had a similar control plate with no drugs on

it. These results were pretty much the same, as can be seen in Figure 5. This is a good sign of reproducibility in the results.

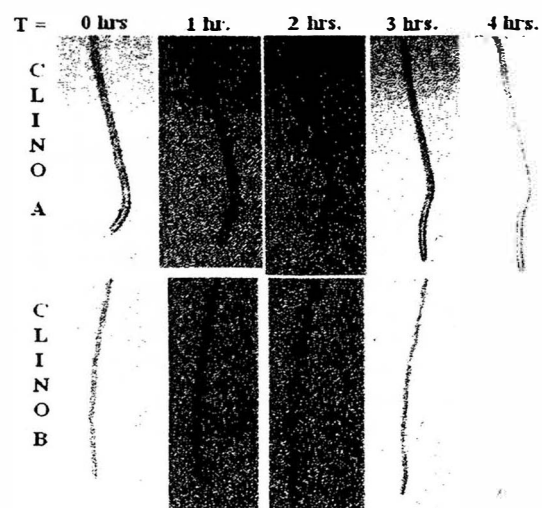
However, we expected the roots to reorient immediately after being turned 90 degrees. This indicates to us that perhaps there is a minimum level of cGMP necessary before a response can be initiated.

The clinostat controls were decent (Figure 6). Without the effects of gravity, the root should have no bearing on which way to grow, and therefore go off at all angles. This was shown in both clinostat roots, as the two roots turned in opposite directions of one another. No drugs were applied to the clinostat plates.

There is still much work to be done in this area. More trials need to be done with each drug in order to get some more solid results and ensure reproducibility. The photo session also needs to be extended to a time in which full reorientation can be achieved by the roots. There are also some NOS mutants of *A. thaliana* that can be used to test this pathway.

Figure 6. Clinostat Control

Two seedlings were placed on the clinostat machine. As you can see, the first seedling reorients downward, while the second seedling slightly reorients in an upward direction to the left.



Material and Methods

Seed Preparation

All seeds were obtained from the Columbia Seed Company. Prior to planting, seeds were sterilized in a 50% bleach, 45% dH₂O, 5% Tween20(a detergent) mixture for 10 minutes. They were also rinsed in ethanol for one minute, followed by rinsing again in dH₂O.

Planting Process

Seedlings were all grown on agar medium. Agar was prepared by mixing 1.1g MS+gamborg vitamins, .25g MeS, 2.5g sucrose, and 2g phytigel per 500mL of water and then stirring for 10 minutes. The liquid agar solution was then brought to a pH of 5.75. The agar was autoclaved for 30 minutes and allowed to cool to 50°C before pouring into plates. Once the agar had solidified, seeds were put on the surface with a syringe modified with a micropipetter tip. Seeds were then placed in a growth chamber at 24°C for 6 days.

Drug Plate Preparation

All drug plates were made two hours prior to the trial. The process for making the agar was the same as mentioned earlier. However, the cGMP, Viagra, and IBMX were added to the liquid agar after autoclaving but before the agar had solidified. All drugs were prepared in 100uM concentrations in the 50 mL plates. After solidifying, the plates were allowed to cool for another hour before the seedlings were applied.

Transplantation

Seedlings were transferred from their original growth plates to freshly made drug plates on hour before the beginning of the trial. Tweezers were sufficient to grab the plants and transfer them to the new plates. The seedlings were laid down close to the

bottom of the plate and then pulled up until the top of the plant was within a centimeter of the top of the plate. This process ensured the root was laid out straight. The plants were then given an hour to adjust to the new plate before they were ready for reorientation.

Pictures

All pictures were taken with Dr. Anne Maglia's digital camera microscope, which she was kind enough to let us use. During the four hour photography session, plants were not in the growth chamber, but laid out in the camera lab. Plants were turned 90 degrees at the beginning of the session and pictures taken at hour intervals thereafter. The microscope was set on 2.1 X magnification. Adobe Photoshop was the program used to capture the pictures on the computer. The images obtained from the trials were then measured for reorientation angles using the ImageJ software. Graphs in Figures 2-5 were prepared using Excel, while the pictures in Figures 1 & 6 were prepared using Paint.

Acknowledgements

Many thanks are due to Dr. Marshall Porterfield and Kacey Morris, whose advising help was indispensable. We would also like to thank Dr. Anne Maglia and Barb Banbury, who showed us how to use their camera to obtain our images.

I would like to thank my partners, Jen Jacobi and Kristin Russell, for their help in this long process.

References

1. Pagnussat GC, Lanteri ML, Lamattina L (2003) Nitric oxide and cyclic GMP are messengers in the indole acetic acid-induced adventitious rooting process. *Plant Physiol* 132: 1241–1248

Exploration of Various Techniques for Quantitative Detection of Antibodies in Solution

**Researcher: Tom Fennewald
Of the Yinfa Ma group
In the Chemistry Department**

Research done and report prepared under the OURE program

27 March 2005

ABSTRACT

We have continued our development of a biosensor and are developing new methods of antigen detection. A fluorometer was previously constructed and was shown to have the ability of quantitatively detecting the amount of fluorescence of fluorescent beads purchased from Molecular Probes. This ability thus corresponds to an ability to quantitate the amount of fluorescent beads which are in solution. Difficulties arose in attaching protein to these beads by the method given by molecular probes and this problem was examined using UV-Vis spectroscopy. Amongst other proposed approaches to antigen detection, one most attachment of antibody to gold so that antigen could be detected by bridging the gold and antibody covered beads. An alternative to this which is planned to be examined is to use polymer trays with wells from ELISA kits instead of gold substrate.

INTRODUCTION

Uses for bio-sensor technology as well as a pressing need to develop reliable detection methods for antigens and viruses is growing in the current ages of Biotechnology, Bio-terrorism, and quickly spread virus outbreaks. In addition to these "threat orientated" reasons for wishing to develop biosensors, there are other reasons as well. Techniques that could quickly and specify what bacteria and viruses were in an ill, or even healthy, patient's blood would be of particular use. In response to these needs, the researchers at UM-Rolla have begun developing a bio-sensor to test for the presence of an antigen, with the intent of further development and application in detection of potentially harmful biological agents and viruses.

The work utilizes 4 μ m diameter, yellow-green, Sulfate-modified FluoSphere beads (Molecular Probes product F-8859). These beads, made of polystyrene and are listed by the manufacture as having a 505/515 excitation/emission. The beads are covered with sulfate functionality groups, allowing them to be coated by way of a chemical synthesis to protein.

This property makes it possible to use the beads as a platform upon which an antibody, (a type of protein), can be placed. That antibody, in this case Monoclonal Anti-Human IgG unconjugated from mouse (Sigma product I 5885), will theoretically readily bind to a corresponding antigen. The antigen chosen was IgG from human serum (Sigma product I 8640). Also available for use are OvA and anti-Ova as less costly alternatives.

When excited by 505 nm light the yellow-green FluoSpheres fluoresce as this report shows we have quantitated, emitting light of a higher wavelength. Since this amount of light fluorescence is measurable using a photosensitive detector, differences in the amount of fluorescence between beads that have been coated with antibody (Anti-Human IgG) and those with out can then be quantitatively measured. A silicon photo detector was used to quantitatively measure the amount of fluorescence emitted from the microsphere beads under a variety of conditions.

Due to considerations of cost and the "proof of concept" nature of the experiment, it is not necessary to use IgG. Rather, Oval albumin (OvA) from chicken and anti-OvA may be used. This allows for increased amounts of protein and lowered cost during the initial experimentation.

EXPERIMENTAL

Metal Substrates

Toward the development of gold (or other metal substrate surface) glass slides were covered with each of the following metals: gold, silver, and copper. Subsequently solution containing OvA was applied to the Au plated substrates in the form of concentrated 500 μ l drops and left in open air to dry. What was then planned was to rise the remaining OvA off of these substrates, but after 12 hrs in a fume hood drying, the Au plating had shriveled and peeled away from the glass.

A test to ascertain the source of the shriveling was conducted as both the OvA and the solvent evaporation from the surface were suspected sources. Buffer with no OvA and even cold ice which was applied and tested since the OvA was applied cold, fresh from the refrigerator, had no shriveling affect on the substrate. As with Au, similar results were noted with Ag substrates, but with Cu substrates only loss of color was noted.

Dilution of the OvA applied was able to reduce the shriveling effect and let a layer of Au remain on the surface.

Coating of Fluorescent Beads with Proteins

To make sure that the beads are indeed being coated by the OvA a procedure supplied by Ed Leber of Molecular Probes was used. The technique is simple in principle: add beads to a solution in a UV cuvette cell with a quantitatively known amount of protein and monitor the adsorption of OvA; if the beads are centrifuged or allowed to settle after having opportunity to react with the protein in solution, then they would precipitate with the OvA attached and a subsequent reading should theoretically have a lower absorbance.

To best determine what wavelengths would be best for quantitative detection of the protein in solution, a scan of the OvA protein was run from 200 - 400 nm. A subtle peak was noticed at 273 nm (0.2246 abs) and a series of major peaks at 205, 215, 217, and 221 nm. The tallest, 217 nm experienced an absorbance of 2.3522. These peaks however were due to the plastic material of the disposable cuvette cells absorbing, so the peak at 273 nm was referred to in making a standard curve.

The standard curve thus came from the following data:

All samples were prepared in 50 mM PBS pH 7.40, 0.9 NaCl Buffer.

Sample	Abs	Wavelength of greatest Abs
Blank (Buffer only)	0.0000	---
0.328 M OvA	0.2451	278
0.655 M OvA	0.4999	279
1.31 M OvA	1.03	278

This data is very quantitative and shows that the 0.5 M to 1.0 M range is close to ideal for working with UV detection of OvA presence.

To have greater sensitivity may require referencing a lower absorbance value, however as many tests were conducted at the lower range of absorbencies, except quartz cells were used to eliminate the effect of the plastic cell absorbance. Use of these cells allowed for quantitative absorbencies down as low as 205 nm, and perhaps 200 nm, but for our purposes the slightly weaker Abs signals achieved at 205 nm were enough to reach conclusions while avoiding the noise in the signal experienced at 200 nm and below. All measurements after this will refer to 205 nm readings unless otherwise stated.

Further, the cells used were half cells. It was found that they needed only 400 μ l of solution to attain a consistent reading with the Beckman DU-600 UV-Vis spectrometer (this reduced the volume of material which had to be used during tests).

Additionally, the beads were known to show a absorbance in this range, so this necessitated that the amount of absorbance due to the beads for each sample be accounted for.

Determination of the concentration of OvA to use was done by dilution of OvA to various concentrations. 28 μ g / ml was found to have an absorbance near 0.6, which is in the ideal range for quantitative measurements of absorbance.

To test for the bonding of OvA to the beads the following procedure was used. Disposable centrifuge cells were filled with a volume of 500 μ l each under the following procedure:

Sample A: pH 6.5 Phosphate buffer (Blank)
Sample B: 25 μ g / ml OvA in pH 6.5 Phosphate buffer
Sample C: 0.05% solids Sulfate modified fluorescent beads (Blank also used for D, to eliminate the effect of the beads)
Sample D: 25 μ g / ml OvA in pH 6.5 Phosphate buffer and 0.05% solids Sulfate modified fluorescent beads

Each of the samples was shaken for several minutes by vortex during which time the protein should attach itself to the beads according to the claims made by molecular probes [attachment would be rapid lasting only a few seconds]. Molecular Probes did note that conformational changes of the protein might last several hours, but this was not of concern to us.

After this initial binding period the samples were centrifuged to separated the supernatant (which unless interaction with beads had occurred should still contain OvA protein at a close to 0.6 Abs or slightly less since these samples are 25 mg/ml rather than 28 μ g/ml). A micropipette was then used to decant the top 400 μ l to Quartz half cells and UV scans of the range 195 to 220 nm were taken, for which the values at 205 nm are reported below:

	Run 1	Run 2	Blank Used
Sample B:	0.52 Abs	0.55 Abs	(if blanked to A)
Sample C:	0.08 Abs	0.08 Abs	(if blanked to A)
Sample D:	0.68 Abs	0.64 Abs	(if blanked to A)
Sample D:	0.58 Abs	0.57 Abs	(if blanked to C)

These data seemed to indicate that there was little or no interaction between the beads and the OvA protein. Surprisingly the absorbance actually increased in the samples which contained beads as though there must be some residual material in the liquid the beads are supplied in which has absorbance similar to the protein under study. Sample D's absorbance of 0.58 (once the effect of the bead "residue" which sample C measures is subtracted) is still more than the OvA protein alone! So even with the residual effect of the beads removed the effect seems to be opposite of the intended and expected result. It should be noted that without centrifuging the absorbance of this concentration of beads is extremely high and noticeable. Due to this fact and used of an LED light which can be used to activate the beads so they are individually visible to the naked eye, we can be certain that the supernatant contained no whole beads and only residuals from the solution or the surface modifiers on the beads which came off during degradation.

It was thought that perhaps a high enough concentration of beads was not used as Molecular Probes recommended that 0.5 to 1.0 % solids be used. Suspected was that the protein had simply be centrifuged out, but this was not a major issue as given that the absorbance read in sample B was close to what would have been expected at the starting absorbance of ~0.6 Abs at 0.28 µg/ml.

In case the concentration of the beads was not great enough relative to the concentraion of the protein to achieve the desired effect of the beads adsorbing all or most of the protein in solution, a similar test with a much higher concentration of beads as in the following preparation procedure:

Samples prepared in 500 µl centrifuge tubes.

Sample A: 200 µl of pH 6.5 Phosphate buffer
Sample B: 100 µl of buffer, 100 µl of 28 micrograms / ml OvA
Sample C: 100 µl of buffer, 100 µl of 2% Sulfate-modified beads (Note: 2% is the undiluted stock concentration)
Sample D: 100 µl of 28 micrograms / ml OvA, 100 µl of 2% Sulfate-modified beads

All samples subjected to the following treatment: 3 min vortex, 3 min centrifugation, dilution by adding 300 ml buffer to the side of the centrifuge tube, 3 min centrifugation, the upper 400 µl decanted to new centrifuge tubes by use of pipette, centrifuge the new set of centrifuge tubes (A', B', C', D') for 3 min, decant the upper 380 ml to quartz UV half cells, and take UV readings in the 195 - 220 nm range.

The results were as follows for the 205 nm readings:

Sample B' (protein):	0.21 Abs	(blanked to A)
Sample C' (beads):	0.74 Abs	(blanked to A)
Sample D' (beads and protein):	1.00 Abs	(blanked to A)
Sample D' (beads and protein):	0.25 Abs	(blanked to C)

Despite the added precautions to remove beads, the effect of the "bead residual" is still very apparent from these measurements. In theory the sample which contains the beads should only have zero absorbance. That it does not is not a problem as the residual from the beads can be blanked out as has been done, but what is very clear is that with the bead residual blanked out the amount of fluorescence left would be expected to be due to protein left in solution. This amount of absorbance left, 0.25 Abs, is very similar to the standard, solution B, which contained no beads and had an even lower absorbance of 0.21! So the effect of the beads in all tests conducted was to increase the absorbance rather than reduce it, which implies that there was no interaction between the beads and the protein.

NOTES

As a side note for application in future research: a complication was experienced when plastic cuvettes made of materials that absorbed under 280 nm were erroneously used. If disposable cuvettes are used, the type which does not absorb until 220 nm should be used.

Another error experience was the incomplete dissolving of the OvA. Even after vigorous shaking and dilutions this was always a problem with the OvA as stringy pieces of material remained in solution.

If concentrations of protein are too high (for which many beads, perhaps even a costly amount, may be needed to have a substantial effect to absorb a measurable amount of) what could also be done to reduce the amount of beads needed to be used in each run in addition to use of half cells is use of Bradford dye reagent. This dye could be applied to protein and make small quantities of protein much more easily visible, so less protein would be needed, and hence less beads as well. Of course the main advantage of this would be that the concentration of protein / concentration of beads ratio would be substantially lowered. In fact this was an idea visited with little success in a preliminary experiment, but it could be revisited as the use of centrifugation prior to addition of the dye would be a very helpful revision on the old procedure.

CONCLUSIONS

All of the data produced was indicative of there being no attachment of protein to the beads, which contradicts claims made by molecular probes. It is possible that the beads were expired and no longer able to attach to protein. This is the only logical explanation outside of failure of the protein, the OvA, itself to attach or an unseen error in experimental design (which would have likely been detected from the over 10 attempts and trials of the Molecular Probes procedure).

The first recommendation for future research is thus to purchase more beads from Molecular Probes (or another set of beads from a comparable company). It would still be highly recommended that Sulfate modified beads be used as these beads provide the simplest method for attachment of protein to the beads, however a different size - perhaps smaller - might prove better for the experiment. In fact, in retrospect it has been realized that for the original plan which incorporated the beads in solution to have antigen detection by way of changing the fluorophore environment would have been difficult to achieve since the beads were large and the fluorescent dye was well inside the beads. If such a method were to have a good chance at working, this method should be attempted with the absolute smallest beads possible. With extremely tiny beads, detection could be more feasible, perhaps even by measuring the diffraction using instrumentation that could detect the change in the overall diameter of the beads as they were coated.

A more practical approach, however, would be to focus on the use of these antibody coated beads (large or small) incorporated into the position in an ELISA in the position traditionally occupied by fluorescent dyes or radioactive labels. Here the beads are at their maximum potential for used in detection of small assays - possibly even on the order of one molecule. Such a technique if developed would have great potential for "lab on chip" techniques and could possibly even replace conventional ELISA techniques as an individual bead contains the same fluorescence experienced by numerous dye labeled antibodies; if a single antibody was able to attach link a fluorescent polystyrene bead to a polymer or gold surface, this would provide a means of quantitative single molecule detection.

It might be possible to monitor the degradation of the beads by centrifugation: by examining the supernatant over time to see if there was any 205 nm absorbance, which is known to be present after a year (as revealed in the above experimentation) could possibly explain why the protein does not attach to the beads, particularly in the unlikely, however theoretically possible, case that the modifiers on the surface of the beads which are meant to attach proteins have somehow come off the bead surfaces and remain floating in solution, thus explaining why there would be an increase in absorbance even after the beads have been centrifuged and explaining why the beads no longer are active in the manner Molecular Probes claimed they would be. I originally suspected that this effect was due to the fluorescent dye leaching from the interior of the beads, but this is very unlikely. What is probable is that the sulfate modifiers are leaching from the surface as the beads pass expiration. This could be easily monitored using the centrifugation technique described, but an IR analysis might be more sensitive and definitive as to what groups and chemicals were leaching / present and not. If fluorescent dye was leaching from the interior this could be seen best with a fluorometer, such as the one constructed for this project, or a conventional scanning fluorometer.

Also examination of the beads at 280 nm (or 273 nm), even though this would require increased amounts of protein and potentially beads as well to be used, would be a highly recommended next step. Such an examination should provided better results with fewer side effects due to the "bead residue" phenomena.

As speculation I might suggest that interaction between the residual chemicals from the beads (speculated to exist) and the protein which would be speculated to bind to these chemicals in solution explains the reason why the absorbance could consistently slightly increase; these chemicals are interacting, just not on the bead surface. If there is

interaction between the OvA protein and the sulfate modified groups which it might be presumed are no longer on the bead surface and now suspended in solution, this interaction might be monitorable using IR to look for the formation of new functional groups.

Future work will need to establish a way to attach protein to Sulfate-modified or perhaps another type of bead before proceeding to ELISA technique tests and development.

ACKNOWLEDGEMENTS

I extend my thanks to Dr. Yinfa Ma, for his inspiration and support to which this project owes its origin, Dr. Zhou of MRC who has kindly prepared the substrates for our future work, group members who have assisted me in my frustrations, and my other friends and family who have likewise provided motivation and encouragement. I would also like to thank Wei and Suman of the Ercal group for supply of Bradford dye and their suggestions on how to best use it.

SCOUR ON BRIDGE PIERS DUE TO FLOOD WAVES

Gaston E. Ferrari, UMR Undergraduate Student

ABSTRACT

A mathematical solution is presented for approximating the time-dependent scour response to flood waves. This solution is in the form of a convolution integral involving a time-varying scour-forcing function and an exponential scour-response function. In this report, an idealized triangular hydrograph is considered from which an analytic solution is obtained, and also an analytical hydrograph is used from which an analytical solution is also obtained for scour associated with flood waves.

Because of the exponential scour rate, the response obtained from the convolution method is found to lag the scour forcing in time, and is damped relative to the maximum scour potential such that only a fraction of the equilibrium response actually occurs.

INTRODUCTION

Many empirical methods of estimating scour have been developed, but there is still need for analytical methods of analyzing scour on bridge piers due to flood waves.

In this report, an analytical method suitable for preliminary calculations of the time-dependent scour due to severe flood waves is presented.

The development of this method is described based on the observation that piers subjected to steady-state scour-forcing conditions respond toward a stable or equilibrium form in approximately an exponential manner. This exponential scour response is convolved with a time-dependent scour-forcing function to obtain the time-dependent scour response. The forcing mechanisms considered here are flood waves, and the present report assumes triangular flood waves as well as an analytical hydrograph which analytic results are obtained for the resulting scour. The magnitude of the scour response is then shown to be determined by two parameters: (1) The equilibrium or maximum potential response, R_{∞} ; and (2) the characteristic erosion time scale, T_s , that governs the exponential rate at which the profile responds toward this new equilibrium.

MAIN BODY - THEORETICAL DEVELOPMENT

The basis for the convolution method is the observation that scour response to steady-state forcing conditions is approximately exponential in time.

The response as a function of time, $R(t)$, may be approximated by the form

$$R(t) = R_{\infty}(1 - e^{-t/T_s}) \quad (1)$$

where: R_{∞} = maximum scour reached,

T_s = the characteristic time scale of the exponential response

The response suggested by (1) has been observed in many laboratory experiments as reported by Swart (1974), and in large-scale wave-tank experiments as reported by Dette and Uliczka (1987), Sunamura and Maruyama (1987), and Larson and Kraus (1989). According to (1), the rate of response must then be proportional to the difference between the instantaneous and final or equilibrium scours. As a result, the differential equation governing the exponential response to steady-state forcing conditions must be of the form:

$$\frac{dR(t)}{dt} = \frac{1}{T_s} [R_\infty - R(t)] \quad (2)$$

As noted, R_∞ , is generally defined as the maximum potential scour.

A more general form of the differential equation governing the macroscale response may be obtained by assuming a time-varying erosion-forcing function on the right-hand side of (2). It is assumed that for a time-varying flood wave, the maximum potential response may be determined for the peak water level while the scour-forcing function may then be expressed as R_∞ times an amplitude function of time, $f(t)$. Thus, a linear differential equation governing the response to variations in water level is assumed to have the form:

$$\frac{dR(t)}{dt} = \frac{1}{T_s} [R_\infty f(t) - R(t)] \quad (3)$$

or

$$\frac{dR(t)}{dt} + \alpha R(t) = \alpha R_\infty f(t) \quad (4)$$

where α = the characteristic rate parameter of the system, defined as:

$$\alpha = \frac{1}{T_s} \quad (5)$$

The general solution to (3) or (4) may be obtained formally by the method of Laplace transforms. However, it is well known that the solution to differential equations of this kind may be given by the convolution of the time-dependent forcing and the characteristic solution for steady forcing, in this case an exponential function. As a result, the time-dependent solution for macroscale profile response may be expressed in the form of a convolution integral as:

$$R(t) = \frac{R_\infty}{T_s} \int_0^t f(\tau) e^{-(t-\tau)/T_s} d\tau \quad (6)$$

or

$$R(t) = \alpha R_\infty \int_0^t f(\tau) e^{-\alpha(t-\tau)} d\tau \quad (7)$$

where: τ = a time lag

This response is typical of many linear dynamical systems and has other analogies in civil engineering, for example in the unit hydrograph methods applied to the prediction of streamflow. In the present case, the system output (time-dependent response) is governed by the input (time-dependent scour-forcing function) and by the basic filtering characteristics (exponential response) of the system to any step-type forcing. As a result, (6) suggests two important and general characteristics of response: that the response will *lag* behind the scour forcing, and that it will be *damped* relative to the maximum scour potential of the system.

Scour Response due to Triangular and Symmetrical Flood-Waves:

The convolution method may now be applied to any time-varying forcing function. In this first case, we consider an idealized triangular and symmetrical flood-wave hydrograph in order to obtain closed-form solutions for scour response. In this first case, the flood-wave function is:

$$(a) f(t) = Q = \frac{2Qp}{Td} t \quad (8)$$

$$(b) f(t) = Q = 2Qp - \frac{2Qp}{Td} t \quad (9)$$

where T_D = the total flood-wave duration defined as the time from the beginning to the end of the water-level rise.

Substituting the time-dependent forcing in (8) and (9) into the convolution integral in (6), gives the following time-dependent erosion response:

$$R(t) = \alpha R_x \int_0^{t/2} \left(\frac{2Qp}{Td} \tau \right) e^{-\alpha(t-\tau)} d\tau + \int_{t/2}^T \left(2Qp - \frac{2Qp}{Td} \tau \right) e^{-\alpha(t-\tau)} d\tau \quad (10)$$

This may be integrated directly to obtain a solution for the time-dependent scour response:

$$\frac{R(t)}{R_x} = \frac{e^{-\frac{\alpha t}{2}} Qp \left[-2 + e^{\frac{\alpha t}{2}} (2 + 2\alpha(Td - t)) + \alpha(-2Td + t) \right]}{\alpha.Td} + \frac{e^{-\alpha t} Qp \left[2 + e^{\frac{\alpha t}{2}} (-2 + \alpha t) \right]}{\alpha.Td} \quad (11)$$

The predicted time-dependent scour response from the convolution method in (11) is shown in Fig. 1. This figure depicts the predicted scour response for a given condition.

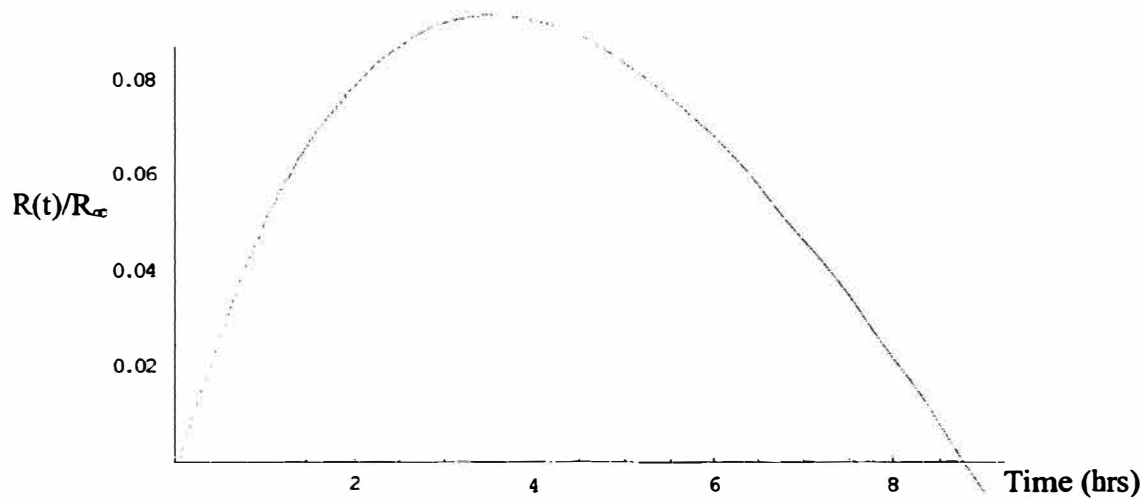


Figure 1

If the profile responded instantly to the water-level change, the response would follow the triangular flood-wave curve. Because of the relatively slow morphologic response however, the predicted response based on the convolution integral lags the flood-wave hydrograph and only a fraction of the maximum potential scour is realized.

Scour Response due to Triangular and Symmetrical Flood-Waves:

The convolution method may now be applied to any time-varying forcing function. In this second case, we consider an analytical flood-wave hydrograph, which represents much more accurately the reality, in order to obtain a closer solution for scour response. In this second case, the flood-wave function is:

$$Q = Qb + (Qp - Qb)\left(\frac{t}{tp}\right)^m e^{[(tp-t)/(tg-tp)]} \quad (12)$$

where: Q = Flow rate
 Qb = baseflow
 Qp = peak flow
 tp = time to peak
 tg = time-to-centroid
 t = time
 m = tp / (tg - tp)

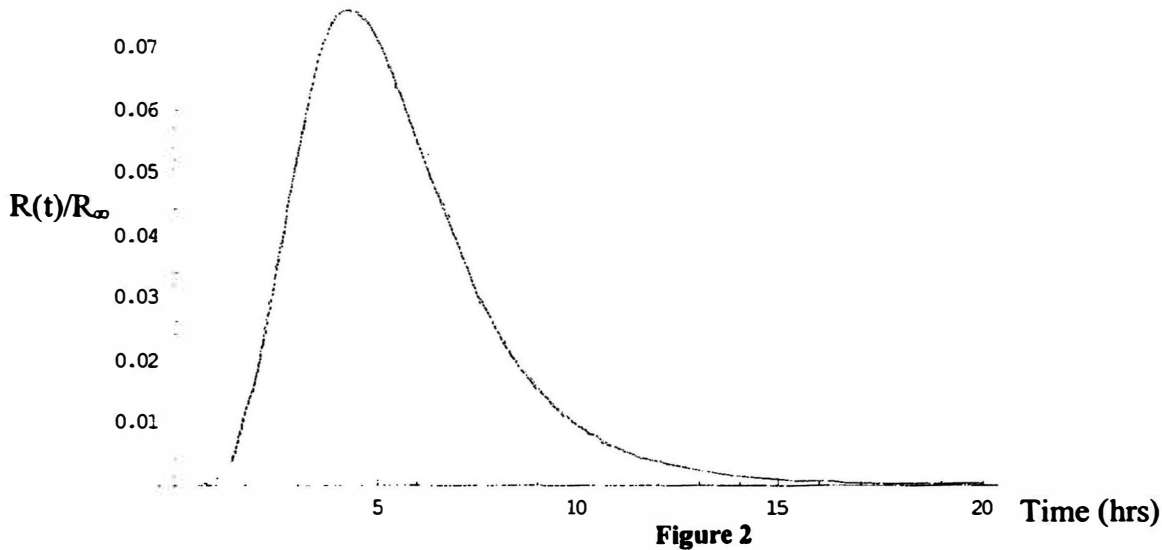
Substituting the time-dependent forcing in (12) into the convolution integral in (6), gives the following time-dependent erosion response:

$$R(t) = \alpha R_{\infty} \int_0^t [Qb + (Qp - Qb)\left(\frac{\tau}{tp}\right)^m e^{[(tp-\tau)/(tg-tp)]}] e^{-\alpha(t-\tau)} d\tau \quad (13)$$

This may be integrated directly to obtain a solution for the time-dependent scour response:

$$\begin{aligned} \frac{R(t)}{R_{\infty}} = e^{-\alpha t} & \left[Qb(-1 + e^{\alpha t}) - \alpha \cdot Qb \cdot e^{-\frac{1}{tp+tg}} \left(\frac{1}{tp} \right)^m \left(-\alpha + \frac{1}{-tp+tg} \right)^{-1-m} \left(\Gamma(1+m) - \Gamma \left[1+m, \left(-\alpha + \frac{1}{-tp+tg} \right) t \right] \right) \right] \\ & + \alpha \cdot e^{-\frac{tp}{-tp+tg}} \left(\frac{1}{tp} \right)^m Qp \left(-\alpha + \frac{1}{-tp+tg} \right)^{-1-m} \left[\Gamma(1+m) - \Gamma \left[(1+m), \left(-\alpha + \frac{1}{-tp+tg} \right) t \right] \right] \end{aligned} \quad (14)$$

The predicted time-dependent scour response from the convolution method in (14) is shown in Fig. 2. This figure depicts the predicted scour response for the same conditions given for the previous case of triangular flood-wave condition.



If the profile responded instantly to the water-level change, the response would follow the analytical flood-wave curve. Because of the relatively slow morphologic response however, the predicted response based on the convolution integral lags the flood-wave hydrograph and only a fraction of the maximum potential scour is realized.

Both figures approximate to the same value for peak scour. It is also noted that according to this graph there would be a period of recuperation after peak scour is reached, but this is not real; in reality this does not happen; therefore, the function after peak scour is not valid and is due to the mathematical integration.

Future work is needed on calibrating these equations using experimental results for scour on bridge piers due to flood waves. Also a method for obtaining R_{∞} needs to be adopted in order to obtain the final $R(t)$ function.

ACKNOWLEDGMENTS

- Dr. Cesar Mendoza; my research advisor; for the help, support and confidence given to me during the whole process of my research.

REFERENCES

- Simons, D. and Senturk, F. (1977). "Sediment Transport Technology." Water Resources Publications, Fort Collins, Colorado.
- Kriebel, D. and Dean, R. "Convolution Method for Time-Dependent Beach-Profile Response." ASCE.
- Chang, W.; Lai, J. and Yen, C. (2004). "Evolution of Scour Depth at Circular Bridge Piers." ASCE, Journal of Hydraulic Engineering, September 2004.
- Latta, G. "Handbook of Applied Mathematics." Ch. 11, Transform Method, p. 571-601.

Opportunity for Undergraduate Research

Due April 1, 2005

Nicole Golden

Advisor: Dr. Frank, Biological Sciences

Abstract

There is possibly more than one PAL gene in soybeans. The PAL gene encodes part of the phenyl propanoid pathway. BLAST searches were done to find sequences that are similar to the already determined PAL gene. From there everything above .03% accuracy was kept for further study. Those sequences were placed in Batch Entrez then consensus sequences were formed in Sequencher. This was done in order to try and produce primers for other possible PAL genes so that they can be seen when running a gel.

Introduction

The phenylpropanoid pathway is important in legumes and PAL is the first enzyme in the pathway which makes it really important. The pathway leads to many secondary metabolites in legumes as well as isoflavonoids. The genes that encode this pathway are useful for defense against pathogens, protection from cold, extended UV light and a lack of nutrients. Since PAL is a key enzyme in the pathway it is important to research.

Materials and Methods

A BLAST search was done on the NCBI website on the genetic code of the PAL gene that was already determined. From the results of the BLAST search everything above .03% accuracy was placed in Microsoft Excel and put them through a Batch Entrez search from the NCBI website. The results of this search were then put into Sequencher. Once they were in Sequencher, contigs were found by running the program and lining up the sequences based on genetic similarity. Then the EST's in each contig were recorded in Microsoft Excel and transferred to Gene Tool for sequence alignment and evaluation. Once the consensus sequences were determined they the steps were repeated starting with the BLAST search. This allowed for new contigs to be made based on the new search results. The Excel files were then evaluated for repeated EST's so that the over lap between the first set of sequences and the second set of sequences wasn't based on repeated sequences instead of genetic similarity. Lastly, 4 micoL of 5X Green Go Taq Buffer, 4 micoL of 1:100 dilution dNTP, 2.5 microL of 1:20 dilution 010 Primer, 2.5 microL of 043 Primer 1 microL of 1:10 dilution of pP1053.3 and 5 microL of nuclease free water were put in a tube and PCR was run to amplify the DNA. Then a gel was run with 0.6g NuSieve 3:1 Agarose, 3 mL of 10X TBE, and 27 mL of dH₂O. The stain used for the gel was 1:100 mL of ethidium bromide; the gel was stained for 10 minutes then destained for 10 minutes in distilled water.

Results and Discussion

The results of the first BLAST search followed by the Batch Entrez search produced five contigs in Sequencher. Each contig was then put into a BLAST search and

Batch Entrez search again by it's self to produce a varying number of contigs from the original ones. The contigs produced are still being evaluated for possible primers for other PAL related genes. The results from the gel showed a band of DNA in the appropriate place for the sequence we were looking for.

Nomenclature

A PCR is a polymerase chain reaction that amplifies specific sequences of DNA. Sequencher and Gene Tool are computer programs used to put together similar sequences. EST's are expressed sequence tags which is how each sequence is labeled.

Acknowledgements

Dr. Ronald Frank of the Biological Science Department over saw and guided the project

Soures

Genetic Analysis, 8th Edition, Griffiths et al.

Carbon-14: Basics of the system and its use in dating secondary mineralizations on degraded concrete

Sara Grondin

sig@umr.edu

Advisor: Dr. Eliot Atekwana

**Department of Geological Sciences and Engineering
125 McNutt Hall, Univ. of MO – Rolla, Rolla, MO, 65409**

Abstract:

Carbon 14, the radioactive isotope of carbon, provides an isotopic dating system that is very useful in determining ages for fairly recent, organic, fossilized materials. Paleoclimatic studies benefit from the use of the carbon system, because carbon 14 can provide an age for a structure and stable carbon isotope variations provide indications about past climate trends. The system can also be used to calculate ages for inorganic materials, specifically building materials partially composed of lime. The creation of the building materials involves burning fossil limestone, and allows the capture of atmospheric carbon dioxide, as the material hardens after construction. Often through degradation of such structures, secondary carbonate mineralization takes place in the form of speleothem-like formations underneath bridges. Isotopic analysis of the carbonate in such structures can provide information on sources of carbon in the structure as well as past ambient temperatures.

Introduction:

The purpose of this study is to investigate speleothem-type formations found under man-made concrete bridges, and to conduct an isotopic analysis of the formations. These speleothems are secondary deposits, forming as the concrete forming the bridge begins to degrade and minerals such as calcite and calcium carbonate dissolve from the material comprising the bridge and re-precipitate in crystalline form. Concrete degrades either physically, through mechanisms such as freeze thawing, stress cracks or salt wedging, or through chemical processes like the formation of secondary minerals. Similar to the speleothem formations found in caves, these speleothems also form in growing layers. This project is attempting to ascertain information about changes in atmospheric carbon 14 from chemical analysis of samples collected from all over the country. These changes can help determine paleoclimates and more recent climate trends, and can aid with predicting climate changes in the future.

Because dense speleothems and building materials can be considered closed systems after hardening, they can be dated using most isotopic systems. However, the most common method of dating inorganic carbonate materials is carbon dating. This is ideal because of the very recent age range of materials such as cement, mortar and plaster, and because all of these substances can be made with limestone. A summary of the carbon 14 method of dating inorganic carbonate formations, particularly building materials, is presented. The dating of ancient churches in the Aland Islands, Finland provides an example of the system's use in archaeology.

Isotope Systematics of Carbon-14 Dating:

The information in this section is summarized from the following sources; the NTD Resource Center, the University of Arizona AMS Laboratory webpage, and Wellington & Grottoli-Everett (1996). Carbon has three isotopes, ^{12}C , ^{13}C and ^{14}C . ^{14}C is formed as neutrons from cosmic radiation enter the upper atmosphere and are captured by nitrogen nuclei (Figure 1).

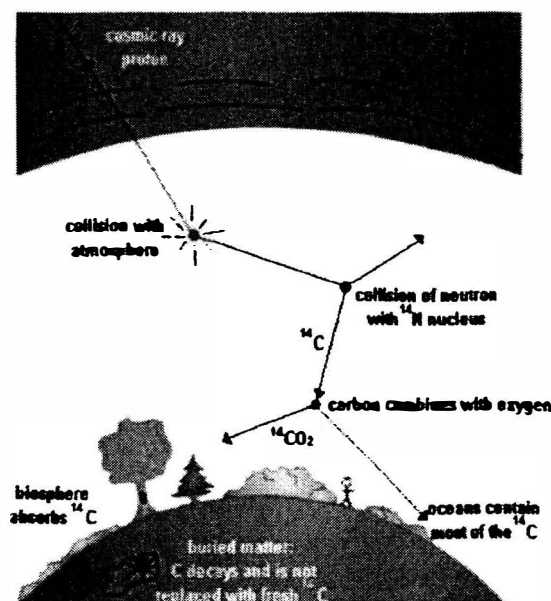
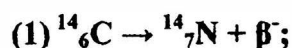


Figure 1: Formation of ^{14}C and the Carbon Cycle (NTD Resource Center)

^{12}C and ^{13}C are stable, while ^{14}C decays via weak beta decay to ^{14}N as shown by the following equation:



and has a half-life of approximately 5,730 years. Once the ^{14}C is formed, it can bond with O_2 to form $^{14}\text{CO}_2$ which then enters the Earth's carbon cycle. This carbon cycle and its properties provide the basis for the carbon isotope dating system.

Plants absorb carbon in the form of CO_2 during photosynthesis. Herbivores then receive the carbon as they eat plants, and the cycle continues. Through the basic processes of breathing and eating, an organism's carbon supply is constantly replenished. All terrestrial plants and animals will maintain approximately the same level of ^{14}C due to metabolic processes and constant levels in the atmosphere. Oceanic organisms display the same tendency, but with a slightly different ^{14}C level than terrestrial organisms.

When an organism eventually dies and becomes a fossil, its ^{14}C decays along with its body, and is not replaced. Thus, the fossil is no longer at equilibrium with the carbon cycle, and the loss of ^{14}C can be used to attain a date for it. This is done by burning a sample to convert the carbon to CO_2 gas, and then using some type of radiation counter to measure the number of electrons given off as ^{14}C decays to ^{14}N . Older types of radiation counters allow measurements of up to approximately 50,000 years, while a newer method, accelerator mass spectrometry (AMS) (Figure 2) extends that to approximately 100,000 years. The advantage of this method is not only that it doubles the age range ^{14}C dating is useful for it also requires a much smaller sample than the traditional measurement.

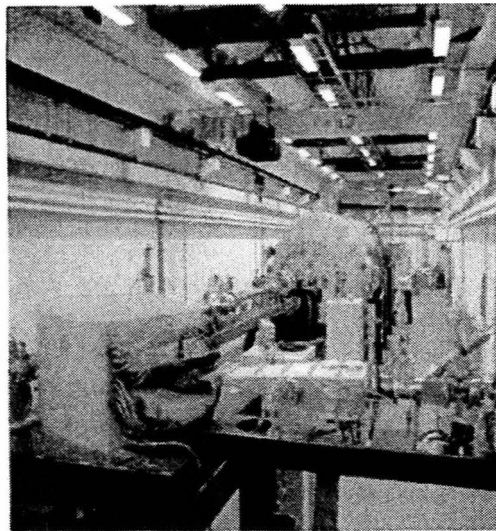


Figure 2: Proton Accelerator - Particle accelerators such as this one at a laboratory in Aarhus, Denmark, can be used to separate carbon-14 from the more abundant isotopes of carbon (carbon-12 and carbon-13), a technique called accelerator mass spectrometry (AMS). The major advantage of AMS over conventional radiocarbon measurement (counting electrons emitted by the radioactive decay of carbon-14) is that much smaller samples are required. Whereas conventional measurement typically requires several grams of carbon, AMS demands only a milligram. (Photograph courtesy of Jan Heinemeier.) (Hale et al)

The equation for radioactive decay of carbon from an organism that died t years ago is:

$$(2) A = A_0(e^{-\lambda t})$$

Where

- A is the measured activity due to ^{14}C in units of disintegrations per minute per gram of carbon
- A_0 is the activity of ^{14}C in the same specimen when the organism was alive
- λ is the decay constant, and
- t is time. (NTD Resource Center)

Carbon 14 dating has been most often used to date organic materials such as fossilized bone, shells, wood or peat, or carbonate deposits such as speleothems. In the 1960's, however, French scientists were able to extend the usefulness of the system to include man-made, inorganic materials such as mortar or concrete. This was possible because these building materials contain lime, from fossil limestone, and maintain a concentration of carbon that was fixed when the material hardened.

Inorganic Carbonates – Dating Mortar:

A study was conducted on ancient churches and stone towers in the Aland Islands, Finland, and in the United States by a team consisting of two archaeologists, an art historian, a geologist and a nuclear physicist (Hale et. al, 2003). The team created and refined a method for dating building materials such as mortar, cement and plaster that all have a common ingredient; lime.

Mortar is made from limestone (CaCO_3), which is heated to 900°C (Figure 3). During the heating process, CO_2 is released and CaO is formed. The mortar then hardens by reabsorbing CO_2 and becomes CaCO_3 again. This means the ^{14}C ratio is fixed in the

newly formed CaCO_3 at the exact time of construction. The material can then be considered a closed system, and radioactive decay of ^{14}C proceeds as usual. The parent and daughter isotopes are measured and used to create an isochron to determine ages.

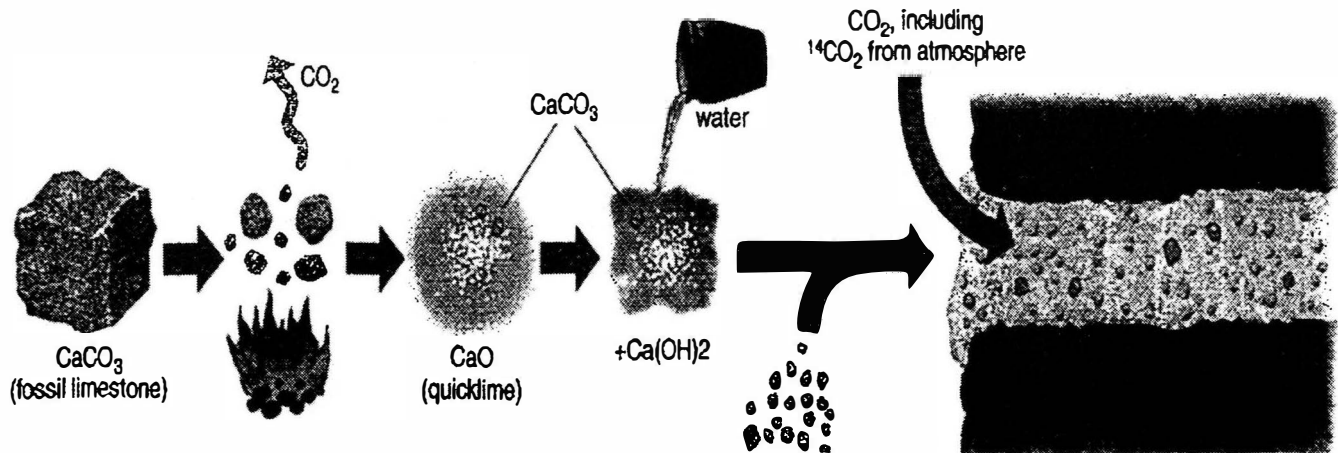


Figure 3: Creating Mortar from Fossil Limestone – Entrapment of Atmospheric CO_2 - Mortar is made using limestone, which is primarily composed of calcium carbonate. The limestone is crushed and heated to at least 900 degrees Celsius, causing the release of carbon dioxide and the formation of calcium oxide (“quicklime”). Adding water and sand (the “aggregate”) then creates mortar, a substance that hardens by absorbing carbon dioxide from the atmosphere, transforming the quicklime back into calcium carbonate. Ancient mortar thus contains a sample of atmospheric carbon, which can be subjected to radiocarbon dating. The presence of fossil carbon, however, complicates the endeavor. Particles of unburned limestone (calcium carbonate that survived the heating) constitute one source of contamination (tan). The aggregate used can also prove problematic, particularly if the sand employed to form the mortar contains shells, which are made of calcium carbonate (red). Various chemical and mechanical treatments help to identify and reduce the effects of such troublesome components. (Hale et al)

Several sources of contamination led to problems when this type of dating was first introduced. Impurities can be introduced if the original limestone is not fully burned or if the sand added in the mortar creation process contains fossils or other carbonate material. These impurities make the method quite complicated and unreliable, because different sources of ^{14}C will give different age results. Fortunately Hale et al. found ways to minimize the sources of error. Fine meshes and dry and wet sieving help to mechanically separate the pure lime from various contaminants, and cathodoluminescence can display impurities that were missed. Using these techniques, impurities can be identified and removed to make the dating process much more reliable. Hale et al. used standard procedures to process the mortar for dating. Samples were crushed, sieved and combined with acid to yield CO_2 . The CO_2 was dated via accelerator mass spectrometry (AMS).

Current Study:

The sample analyzed for this project was a flowstone obtained from the Meridian St. Bridge over Fall Creek in Indianapolis, Indiana (Figures 4, 5).

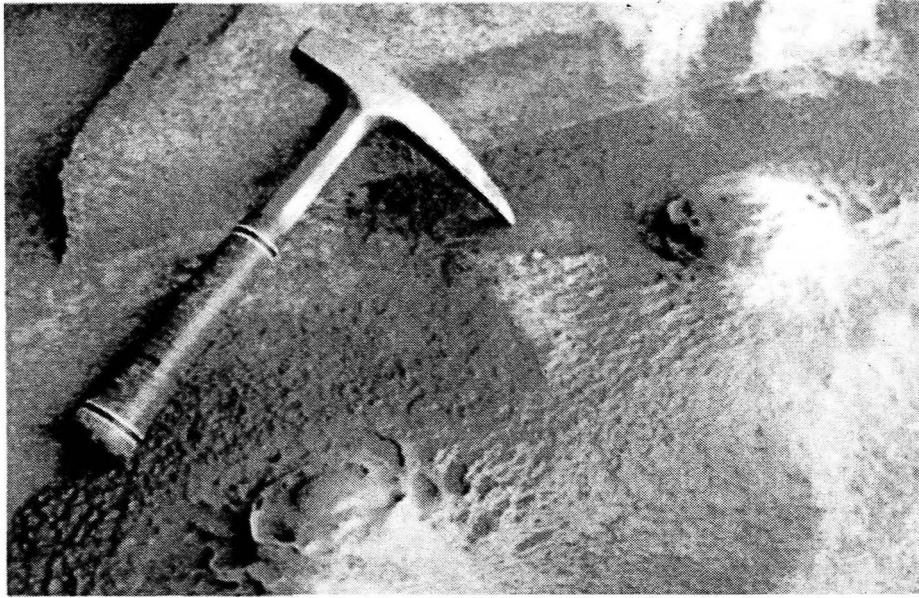


Figure 4: Flowstones under the bridge before they were removed for sampling (*Atekwana*)

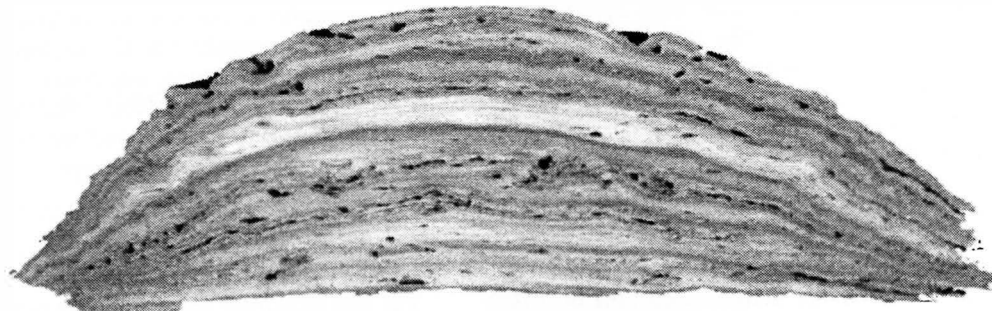


Figure 5: Cross section of a sample flowstone measuring 3.5 cm by 13 cm – note growth layers are visible. (*Atekwana*)

The sample was divided into seventeen layers for analysis, with layer one, the oldest, at the bottom and layer seventeen, the youngest, at the top. These divisions were made in an attempt to represent different growth layers of the sample. It was analyzed isotopically by reacting CaCO_3 with 100% phosphoric acid (Krishnamurthy et al., 1997). This provided data on the $\delta^{13}\text{C}$ CaCO_3 and $\delta^{18}\text{O}$ CaCO_3 (Figure 6) levels present.

youngest



oldest

Cross-section of Flowstone

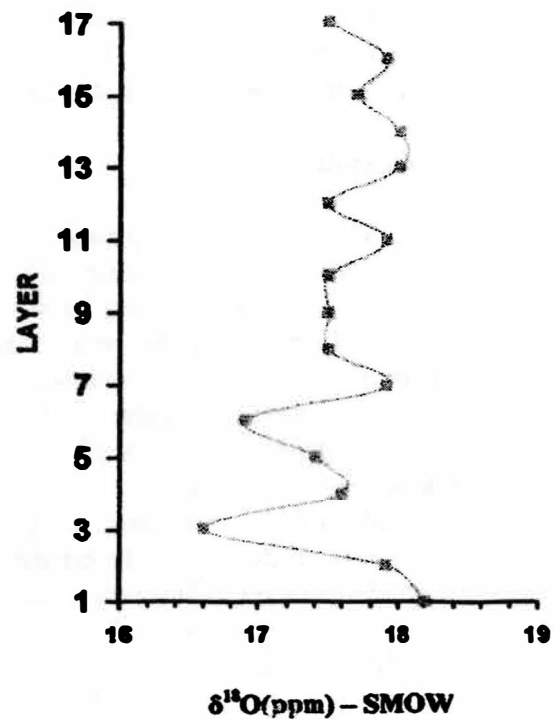
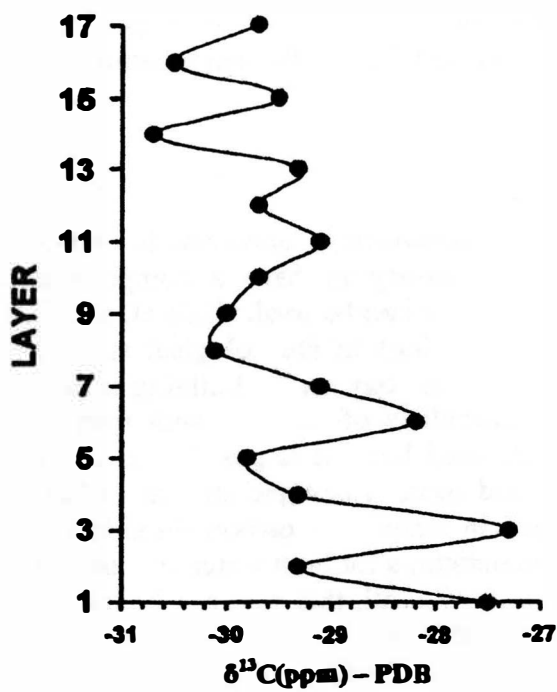
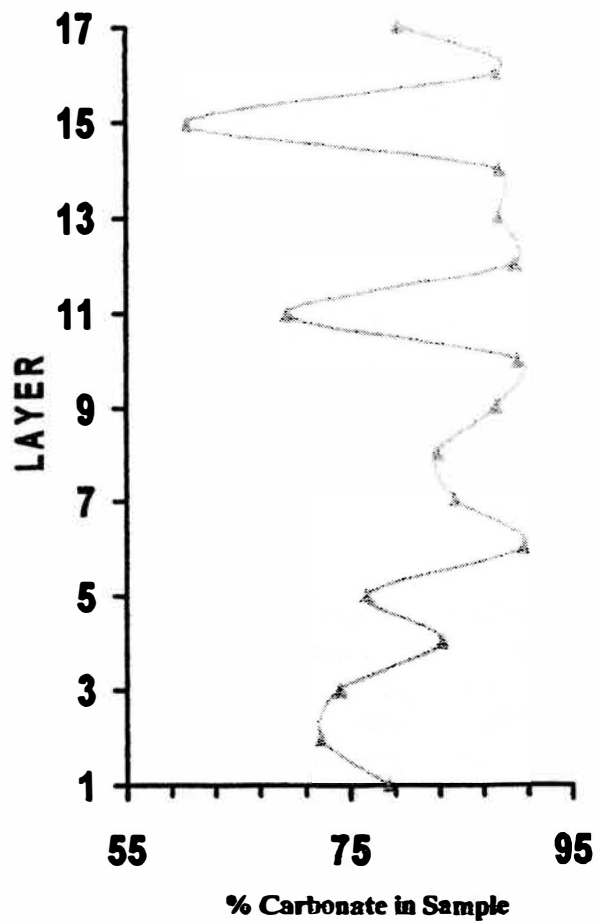


Figure 6: A cross-section of sample against % carbonate, $\delta^{13}\text{C}(\text{ppm})$ and $\delta^{18}\text{O}(\text{ppm})$ (Atekwana, 2005)

This isotope abundances found in this sample are reported here as compared to the international standards, i.e. Pee Dee Belemnite for the carbon isotopes and Standard Mean Ocean Water (SMOW) for the oxygen isotopes (Atekwana, 2005).

Isotope Analysis Data:

As can be seen from the graph, the amount of carbonate found in the sample fluctuates quite a bit, and the range of fluctuation increases with time. The carbon isotopes range from -27 to -31 parts per million (ppm) and show a negative trend over time. The oxygen isotopes do not noticeable trend negatively or positively, but begin to have a smaller range of variation over time.

Implications/Discussion:

The fluctuations found in the percentage of carbonate found in the sample could be due to several different occurrences. A change in climate or weather patterns such as a large storm event or pollution changes could cause changes in the amount of carbonate precipitated. The negative trend of the carbon isotope data is consistent with the addition of light CO² (-7 ppm) or fossil fuel CO² (-25 to -35 ppm) to the atmospheric reservoir. The addition of either of these two types of CO² increases the negativity of the $\delta^{13}\text{C}_{\text{PDB}}$ measured. The oxygen isotope data, under equilibrium conditions, is related to water temperature via the following equation:

$$(3) 1000 \ln \left\{ (1000 + \delta^{18}\text{O}_{\text{carbonate}}) / (1000 + \delta^{18}\text{O}_{\text{water}}) \right\} = 2.78 * 10^6 / T^2 - 2.89$$

where T is in degrees Kelvin (Atekwana). This equation can be used to estimate the temperature of the water the carbonate formed in and hence the temperature of the ambient air at the time of formation.

Conclusion:

The goal of this project was to look at the variations of atmospheric carbon in recent carbonate formations. To do that, it is necessary to have a comprehensive understanding of the carbon 14 dating system and how it can be used. Hale et. al (2003) successfully clarified the role of historical stone buildings in archeological studies by determining the date of construction using ¹⁴C geochronology on the building materials. Their study provided valuable insight into the difficulties of working with man-made carbonate materials. In working with the sample used here, it is possible to come to several conclusions about the nature of carbon and oxygen isotopic studies. Changes observed in $\delta^{13}\text{C}$ over time may reflect changes in where the carbon dioxide in the atmosphere comes from. Information on paleotemperatures for both water and air can be obtained using the $\delta^{18}\text{O}$ data obtained in this study. Overall, this data can be used as a proxy to obtain environmental information about the very recent past that may be difficult to obtain otherwise. The importance of this study is that it explores the processes governing degradation of concrete, and their environmental implications.

Acknowledgements:

Dr. Eliot Atekwana, OURE Advisor and Assistant Professor, Geological Sciences and Engineering Department

Dr. John Hogan, Associate Professor, Geological Sciences and Engineering Department

References:

Druffel, E. M. and Linick, T. W., Radiocarbon in Annual Coral Rings of Florida, *Geophysical Research Letters*. 5. 913 – 916, 1978.

Geyh, M. A. and Hennig G.J., Multiple Dating of a Long Flowstone Profile, *Radiocarbon*. 28. 503-509, 1986.

Hale, J. et al., Dating Ancient Mortar, *American Scientist*. 1. 130-137, 2003.

Krishnamurthy, R.V., Atekwana, E.A. and Guha, H., A Simple, Inexpensive Carbonate-Phosphoric Acid Reaction Method for the Analysis of Carbon and Oxygen Isotopes of Carbonates, *Analytical Chemistry*. 69. 4256-4258, 1997.

NTD Resource Center, Carbon-14 Dating, Retrieved December 1, 2004 from <http://www.ndt-ed.org/EducationResources/CommunityCollege/Radiography/Physics/carbondating.htm>.

Shopov, Y.Y., Ford, D.C., and Swarcz, H.P., Luminescent microbanding in speleothems: High-resolution chronology and paleoclimate, *Geology*. 22. 407-410, 1994.

University of Arizona AMS Laboratory, Basic Principles of Radiocarbon Dating, Retrieved December 1, 2004 from <http://www.physics.arizona.edu/ams/education/theory.htm>.

Wellington, G. & Grottoli-Everett, A., 1996, Paleoclimate Reconstruction in Reef Coral Skeletons: Interpretation of Stable Carbon Isotopes: Environmental Institute of Houston, Retrieved December 1, 2004 from <http://www.eih.uh.edu/publications/96annrep/well1.html>

Mapping the Gamma Flux Level Around the UMR Reactor Core for Irradiation Applications

**Jason Hall
University of Missouri – Rolla
Nuclear Engineering Department
Fulton Hall
Rolla, MO 65409
jahznb@umr.edu**

OURE Report

Submitted to:
Office of Undergraduate & Graduate Studies
207 Parker Hall
1870 Miner Circle
Rolla, MO 65409

April 1, 2005

Abstract

This experiment uses the UMR Nuclear Reactor research facility after a high power run to map out the gamma flux at the different positions on the grid plate. Measuring the gamma flux is done by using a gamma-photon sensor to detect the level of radiation that is present at precise point near the core of the reactor. Measurements of the gamma flux are taken in rad/hr with respect to time. A range of values of rad/hr is 480 rad/hr at C7 to 1.8 rad/hr that were taken. A graph is formed and along with a formula. Once there are enough measurements to produce a correlation, a mathematical formula can be obtained. These values have variables that depend on how long and how much the reactor has been ran. This is in kW-hr.

Table of Contents

	Page
Abstract.....	i
1. Table of Contents.....	1
2. Introduction.....	2
3. Experiment.....	2
4. Results.....	3
5. Discussion.....	9
6. Conclusions.....	9
7. References.....	10
8. Nomenclature.....	10
9. Acknowledgements.....	10

Introduction

It is important to know the amount of gamma ray photons that an experiment receives for a variety of research especially material science and engineering. Over the past few years, UMRR has increasingly provided gamma-irradiation services for novel material R&D and to characterize the vulnerability of commercial-off-the-shelf (COTS) electronic parts. In order to provide gamma-irradiation in a precise manner, we need to quantify the radiation level in time at locations where we are likely to place samples. The gamma radiation field that is used results after shutdown from a high-power reactor run. Therefore the radiation level decays in time to some steady level. Since the reactor fuel is not distributed symmetrically, there is likely to be spatial dependence of the gamma flux level as well. The proposed measurements will quantify in location and time the gamma radiation level in strategic grid positions of the UMR reactor. The radiation level will be measured using a gamma-photon sensor that is available at UMRR. With this information, UMRR will be able to precisely irradiate samples.

Experiment

The objective of the experiment was to know the amount of gamma rays at a certain position on the grid plate by using a correlation from research. This information is given in rad/hr. Since the intensity is time, distance, and core power dependant, the amount of intensity changes with these variables. The detector that was used is the Technical Associates DMU-1 Ion Chamber, which is used with CP-MU Electronics. It measures medium to high gamma energies for underwater use. The ion chamber is taped to an aluminum I-beam at the center that has an insertion to be placed in the grid hole. After a high power run for about two and half hours (most used at the reactor), the data would be taken. There would be about one hour after shut down that the probe could not be placed in a measuring position. This is from the neutrons that are still being produced that would cause neutron activation on the probe. Therefore the data would not be useful. The orientation of the probe is critical. It must be concise with every measurement. To keep this the same, I kept the orientation of the probe facing away from the core with relation to the pool wall. Data would be then taken and the probe could be moved to

another location to gather more data. The data that was taken is the gamma intensity (rad/hr), time after shutdown (min), and the core power before the measurements (kW-hr). The gamma intensity and time was plotted to produce a handy graph for each location. An equation was produced from this also. The experiment was to be used for UMRR to be able to know what amounts of gamma an experiment is going to receive. To do this, a correlation was to be known. First I needed to get a relationship of one of the positions to the power the core has before the measurements with a formula by using a few equations that were gathered from the graphs. Then this would show the difference in the gamma intensity with the change of the power of the core (which is denoted b). Now the change of position in relation to this initial spot can be taken. This is done by a multiple factor (m) to the gamma intensity of the initial location with the know power of the core. This will produce a correlation to know the gamma intensity. Some data was taken on the with the gamma probe taped to the bottom of the I-beam. For more information on axial measurements would require another experiment with a new probe that could move in the axial direction easily. The log counter in the control room is shown to have proportionality to the amount of gamma flux. I have shown this correlation with C8 by taking data from this location and the log counter with respect to time. I have made an approximation to show how to find the gamma flux at a position just by using the correlation and multiple factor.

Results

To produce the gamma flux at a certain location by using the procedure above, the measurements have been taken for each location and are shown in table 1 for C7. I have only shown one location due to the amount of space that is taken for each location. Then this information is then plotted to produce a rad/hr vs. time. The time is taken after shutdown in minutes.

Time (min)	Gamma(rad/hr)	Time (min)	Gamma(rad/hr)
65	480	69	400
70	440	76	380
77	420	79	360
96	350	81	360
113	300	84	340
		87	340
		90	340
		92	320
		96	310
		100	300
		103	300
		105	300
		107	290
		108	280
		109	280
		112	280
		115	270
		119	270
		123	260

Table 1

The left group on the table show the data taken on 9/10/2004 with a power run at 180 kW for 2.5 hours before the measurements was taken.

The right group shows data taken on 9/17/2004 with a power run at 180 kW for 3 hours before the measurements were taken.

This is then plotted to produce the following graph:

C7

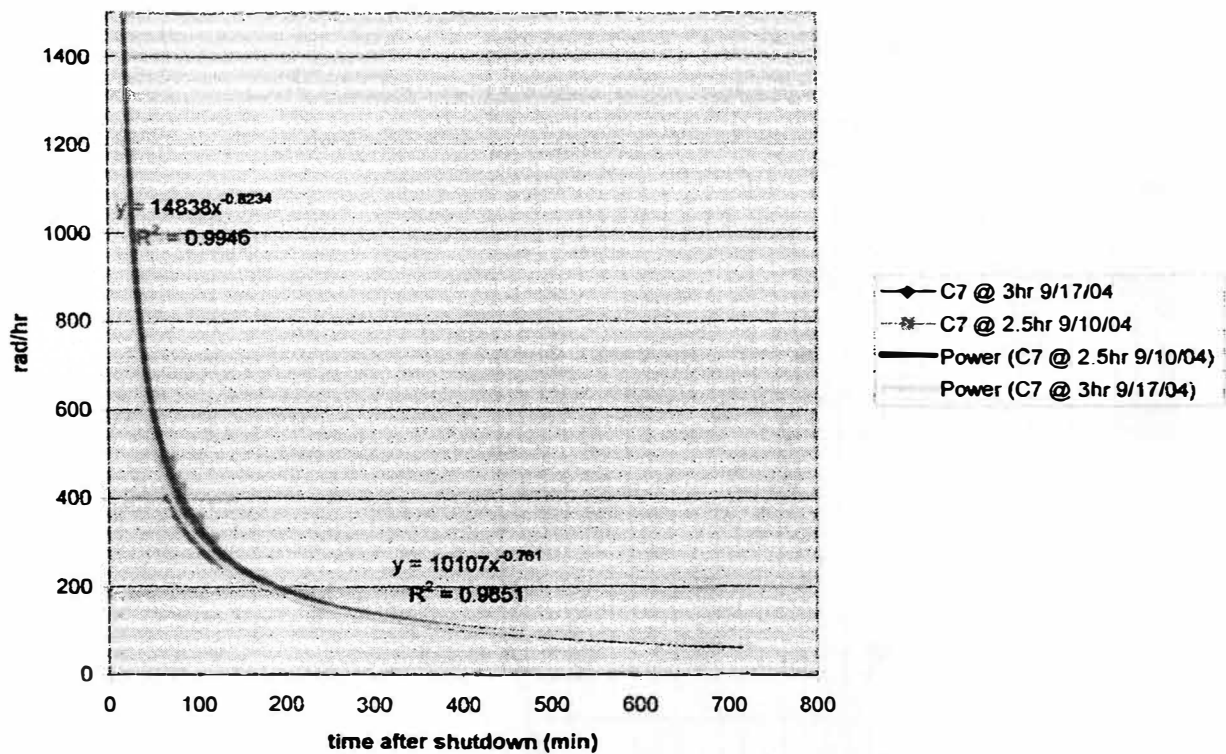


Figure 1

The graph shows the two different runs with in the same position.

It was found out after a high power run on a Friday, that the exponential was not the best choice for the graph. This is from taking measurements on the following Monday that the exponential dropped off to quickly and the data was not as accurate. The better choice for graphing the data came to be using a power function. This is used in figure 1 above.

This is done at all the locations that are possible on the core grid plate. All the equations were developed and put on figure 2.

	192 200	2236 000	534 240	480 253	728 050	453 680	497 000	1704 800	multiple factor for A9 (m)
(kW-hr) of week before	---	2236 000	534 240	480 253	728 050	453 680	497 000	1704 800	
(kW-hr) directly before measuring (b)	410 94	540 00	450 00	450 00	441 00	270 67	453 67	301 67	
where 450 kW-hr = 2.5 hr 180 kW (90% full power)									
A1					$y = 1655.2x - 0.8217$				$43851x - 1188$ A1
A2						$y = 3014.7x - 0.8658$			$79868x - 0755$ A2
A3						$y = 6520.8x - 0.9583$			$1.7275x - 0.17$ A3
A4						$y = 13517x - 1.0577$			$3.581x - 1.184$ A4
A5			$y = 6772.8x - 0.8814$						$1.7943x - 0.0599$ A5
A6				$y = 5605.4x - 0.859$					$1.485x - 0.023$ A6
A7				$y = 6333.4x - 0.9249$					$1.6779x - 0.164$ A7
A8				$y = 3446.8x - 0.8553$					$91316x - 086$ A8
A9		$y = 810.14x - 0.5729$	$y = 3774.6x - 0.9413$			$y = 1206x - 0.8749$			1 A9
B1					$y = 3077.8x - 0.8719$				$8154x - 0.094$ B1
B2						$y = 11612x - 1.0475$			$3.0784x - 1.062$ B2
B3						$y = 16813x - 1.0299$			$4.4542x - 0.886$ B3
B4						$y = 22602x - 1.0195$			$5.9879x - 0.782$ B4
B5			$y = 9208.5x - 0.8167$			$y = 7948.8x - 0.9668$			$2.4391x - 1.246$ B5
B7			$y = 8842.6x - 0.8603$						$2.3427x - 0.81$ B7
B8			$y = 8443.3x - 0.9172$						$2.2369x - 0.241$ B8
B9		$y = 4371.7x - 0.8771$							$1.1582x - 0.642$ B9
C1					$y = 4551.3x - 0.8859$				$1.2058x - 0.554$ C1
C2						$y = 12752x - 0.976$			$3.3784x - 0.347$ C2
C3						$y = 19037x - 0.9381$			$5.0434x - 0.032$ C3
C7	$y = 14838x - 0.8234$	$y = 10107x - 0.781$							$3.931x - 0.1179$ C7
C8	$y = 9102.2x - 0.8015$	$y = 4850.4x - 0.8775$							$2.4114x - 1.398$ C8
C9	$y = 4942.1x - 0.7811$	$y = 6668.5x - 0.8755$				$y = 5562.4x - 1.0214$			$1.3093x - 1.809$ C9
D1					$y = 5984.8x - 0.9036$				$1.5855x - 0.377$ D1
D2						$y = 7095.8x - 0.7935$			$1.8799x - 1.478$ D2
D9				$y = 4571.9x - 0.7428$					$1.2112x - 1.985$ D9
E1	Table 2				$y = 8103.5x - 0.9024$				$1.617x - 0.389$ E1

To produce a formula that would link the power before the measurements took place, I took A9 and with the different power changes and made a formula:

Equation 1

The gamma flux at A9 = $y = 3774.6x^{-0.9413} + n$

$$n = \frac{1206(x^{0.0664} - 3.13)}{x^{0.9413}} \left(\frac{450 - b}{180} \right), \text{ b is in kW-hr,}$$

where $630 > b > 270$

b = power of the run before the measurements.

This can be used by a multiple factor to know what each position's gamma intensity is. Using the research data that I have gathered with the equations, I set the equations equally to A9 and found a multiple factor that made this equation true. This multiple factor (m) is shown in Table 2. To find the gamma intensity, you must first find A9 then multiply it by the multiple factor.

Equation 2

$$y = 3774.6x^{-0.9413} + \frac{1206(x^{0.0664} - 3.13)}{x^{0.9413}} \left(\frac{450 - b}{180} \right) (m)$$

Putting the probe on the bottom of the I-beam has produced some information about the bottom measurements.

	2/18/2005
(kW-hr) of week before	687.580
(kW-hr) directly before measuring	450.00
where 450 kW-hr = 2.5 hr 180 kW (90% full power)	
A1	$y = 582.73x - 0.6854$
A3	$y = 527.75x - 0.5548$
C1	$y = 2882.9x - 0.9172$
C3	$y = 99658x - 1.4761$

Table 3

More information would be required for a complete analysis of the axial measurements.

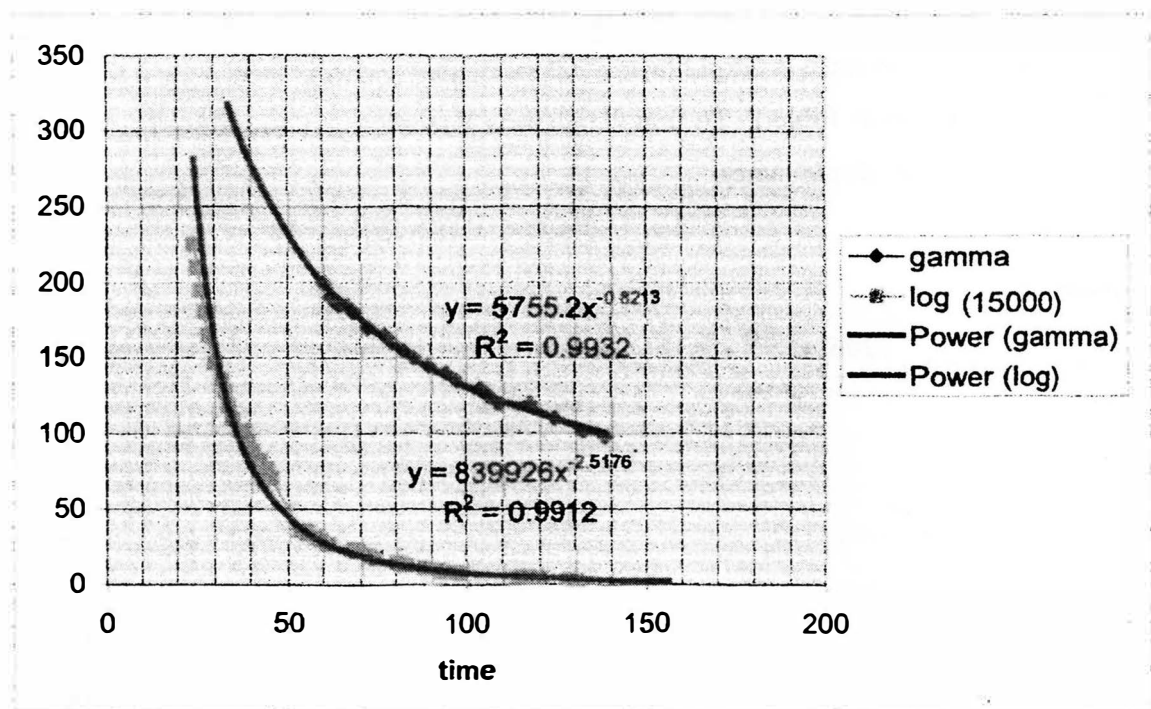


Figure 2

Measurements were taken for a run after a high power run and compared to the log level in the control room to that of C8 (figure 2). The log level was multiplied by 15000 to produce a closer look to the gamma function. Setting the two equations equal to each other produced a multiple factor of:

Equation 3

$$\nu = 102.75x^{1.6963}$$

Basically you need to know the time after shutdown and the log level and equation 2 multiplied by log level will tell you what the gamma flux in C8 is.

Discussion

Due to the continuous changes of the core with fission fragments, samples, and moving of the core, the ability to find the exact measurement would be almost impossible. These measurements are just an approximation. Positioning the gamma probe is also a factor that cannot be precise every time. To produce the axial measurements would require another probe that would be not fix. It would have to be able to move up and down to get the measurement quickly time wise. Knowing that the ion detector only picks up medium and high gamma rays might have an influence on the what is actually be irradiated. The Log level may not be as accurate since this has only been done once and has not been tested again.

Conclusion

Overall the correlation that has been made gives the UMRR enough information to be able to irradiate samples precisely. This is done at all possible locations on the UMRR core's grid. This will tell UMRR where to place samples that need a certain dose of gamma intensity.

References

<http://www.tech-associates.com/dept/sales/beta-gammapicker.html>

Nomenclature

Throughout the paper:

$y = \text{rad/hr}$

$x = \text{time after shutdown (minutes)}$

equation 1:

$b = (\text{kW-hr}) = \text{power of the core before the measurements were made}$

$n = \text{the factor for A9 compared to different (b)}$

equation 2:

$m = \text{multiple factor from Table 2}$

Table 2:

The equations that are shown in Table 2 are shown in $y = _x_,$ where the number after the x is raised to that power.

Equation 3:

$V = \text{multiple factor for log level}$

Acknowledgements

Thanks to all the help,

Akira Tokuhira

Brian Porter

Bill Bonzer

Maureen Henry

Dan Estel

I could not have done it without them.

Extent and Distribution of Individual Proterozoic Orogenic Belts in Southern Africa from Gravity and Magnetic Data

David Heeszel
University of Missouri-Rolla
Department of Geological Sciences and Engineering
dshcm4@umr.edu

Abstract

Newly compiled gravity and magnetic datasets, in conjunction with existing geochemical/geochronological data have been able to provide a unique view into the structural evolution of individual Proterozoic mobile belts of southern Africa. Currently there is little actual evidence to support the proposed boundaries for many of the Proterozoic belts that surround the Kaapvaal and Zimbabwe Cratons except for very limited geochemical data and even more limited structural mapping. These newly compiled gravity and magnetic datasets have been able to significantly improve our understanding of the structural geology of these belts and better constrain their evolution and the tectonic interrelationships that control that evolution.

Introduction

Archean cratons comprise only small portions of the modern day continents. However, these portions of the earth's crust represent the oldest cores of the modern day continents and some of the most fertile regions in terms of mineral wealth. One such region is in Southern Africa where the Kaapvaal craton and the Zimbabwe craton collided during the latest Archean (1) and were subsequently surrounded by younger orogenic belts when the rest of Africa accreted to this 'core'. As a natural result of this incredible age, the structural geology of Southern Africa is very complex. Surrounding the Archean cratons that began stabilizing at approximately 3,080 Ma (million years) (2) are several orogenic belts of Proterozoic age. Previously these belts have been poorly constrained due to the fact that they are typically buried under thick blankets of younger sediments (3). The flat topographic profile over much of southern Africa illustrates this fact well, and many of the areas with significant topographic relief still have recent cover that obscures the basement geologies of these areas. Fortunately, geophysics, particularly gravity and magnetic data analysis, provides a unique view into these deeply buried terrains (4). These methods are able to effectively image the deep crustal features that have no surface expression.

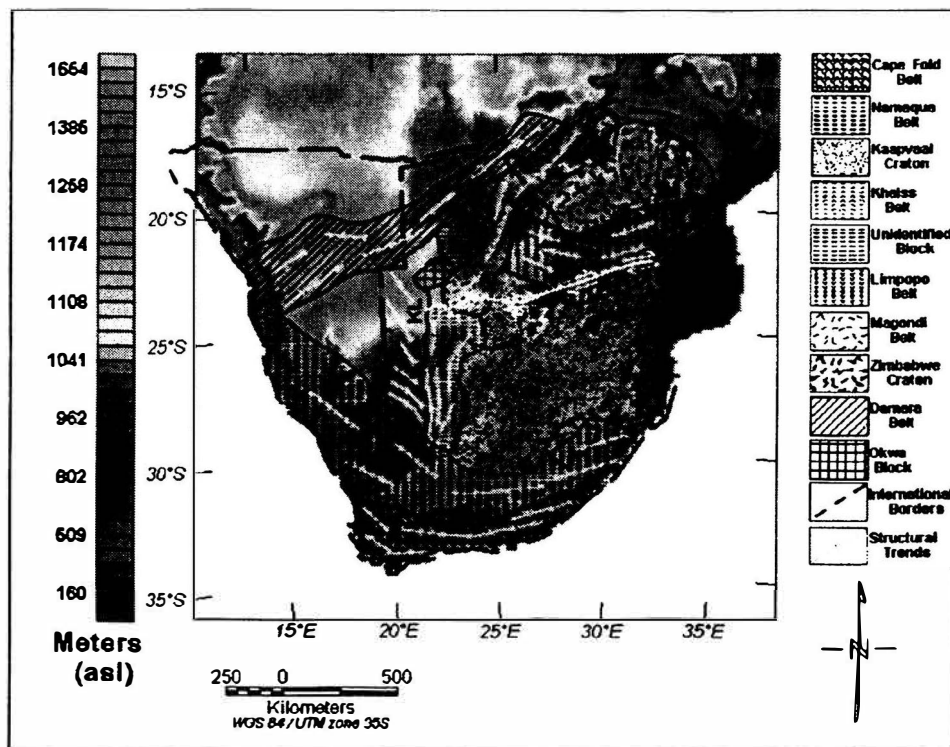


Figure 1: A topographic map of southern Africa with the major tectonic boundaries lay on top. Note that many of these features have very little topographic relief. This has made delineation of these belts very difficult in the past. KL=Kalahari Line; PLZ=Palala-Zoetfontein Shear Zone (Data courtesy of Geosoft)

Gravity and magnetic data on the cratonic and continental scales are typically collected by airplanes or helicopters. These aircraft are fitted with specialized equipment that is able to measure the acceleration due to gravity and the intensity of the total magnetic field to a high degree of accuracy (5). The databases with this information can then be compiled to generate regional gravity or magnetic databases for interpretation. One such database of recently compiled data, provided by the South African Council for Geoscience, was the source of the geophysical data used in this study.

With the aid of geochemical analysis from boreholes in several of these Proterozoic belts it is possible to constrain the tectonic history of one of the oldest regions of the earth. In addition, it is possible, with the aid of gravity and magnetic data from this region, to create two-dimensional profiles of the subsurface structures that define these Proterozoic belts. This combination of structural analysis from geophysical data, geochronological dating, and modeling provide a unique view of the structure and evolution of the crust in Southern Africa.

Methods

The data provided by the South African Council for Geoscience was processed using Geosoft's Oasis Montaj suite for the analysis of potential field data. The data, comprised of thousands of individual data points, was displayed on a two-dimensional grid and color contoured. By using a local datum transform it was possible to geo-reference the data and project in on a lat-long map. Various mathematical filters were applied using processing algorithms built into Oasis Montaj, namely a Fast Fourier Transform algorithm to convert the data from the space into the frequency domain. The data was then manipulated mathematically primarily by

taking the first vertical derivative to heighten vertically controlled changes in the data and by removing the higher frequency components a process known as upward continuation. The data is then converted back into the space domain to be displayed for interpretation (6). These processes make deeper features more pronounced and easier to interpret. In addition, it is possible to better delineate structural trends within the basement geology. This was done by carefully comparing the newly available gravity, magnetic and the previously published geochemical/geochronological data.

A profile was extracted from the data using GM-SYS, a two-dimensional (vertical and one horizontal direction) modeling package, which allowed me to model the structure of a Late Archean orogenic belt, the Limpopo Belt, from the surface to the crust-mantle boundary. This is done by matching a calculated model to the data extracted from the dataset. GM-SYS and Oasis Montaj are integrated in such a way as to make the extraction process very simple. In addition constraints were placed on the crust-mantle depths by seismic data from the Kaapvaal Seismic Project (7). The basic crustal structure was assumed to be that proposed by Kampunzu and Rangani (8).

Data and Discussion

A basic tectonic reconstruction as defined by geophysics and geochemistry is shown in figure 2. The oldest structures, the Kaapvaal and Zimbabwe cratons, collided at the very end of the Archean in a Himalayan type orogenic event creating the Limpopo Belt. Throughout the Proterozoic there were several orogenic events on the western and southern margins of the assembled block that can be easily discerned in the geophysical data. There may have also been belts on the eastern margin of the Zimbabwe and Kaapvaal cratons, but they were destroyed by the breakup of Gondwanaland during the Mesozoic, and there was poor data coverage to the north of the Zimbabwe craton. The age of the Proterozoic belts decreases with distance from the Archean cratons.

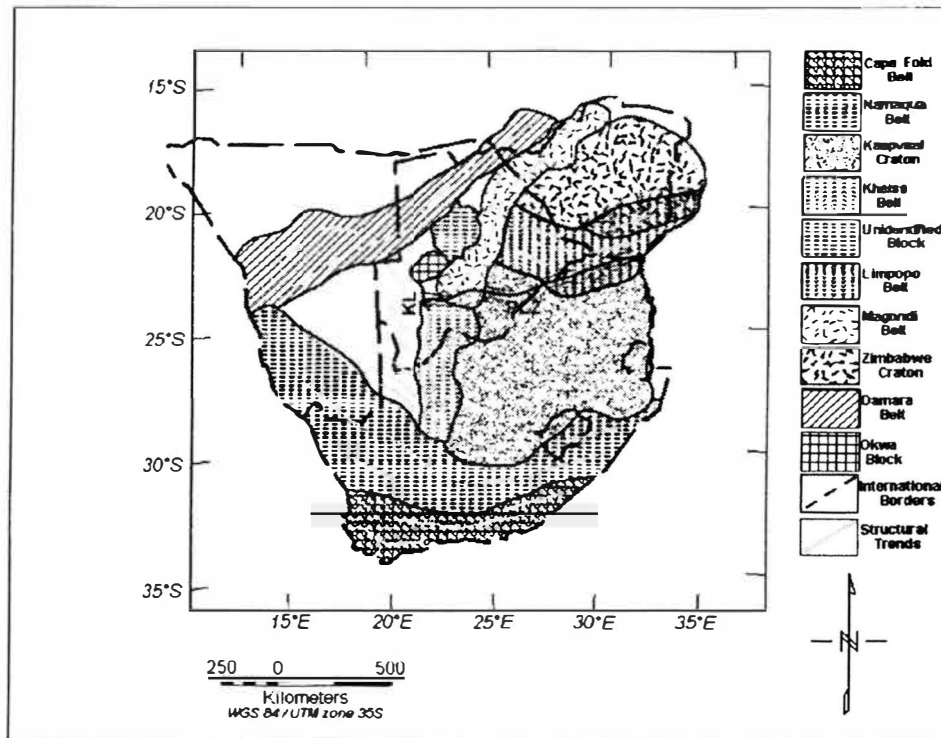


Figure 2: Tectonic interpretation of the basement geology in southern Africa. PLZ=Palala-Zeitfontein Shear Zone; KL=Kalahari Line

The Limpopo Belt

The Limpopo Belt is one of the first major Himalayan type orogenic belts in the world (1). It occurred at the end of the Archean Eon as a result of collision between the Zimbabwe and the Kaapvaal craton and has been dated to at approximately 2595 Ma (9). This collision created a mountain belt that, according to seismic data has a crustal thickness slightly greater than that of the cratons themselves (7). It is defined by not only a thickening of the crust, but also appears to override portions of the cratons. The southern marginal zone marks a location where the Limpopo Belt covers the Kaapvaal craton at shallow crustal level, and the northern marginal zone represents the same phenomena in the Zimbabwe craton (3). It is possible to extract a gravity profile across the Limpopo Belt using the GM-SYS modeling package and generate a model for the subsurface structure of the Limpopo Belt. Figure 3 shows the location of the extracted profile, and figure 4 displays the model that was generated using constraints provided by geochemistry and seismology (7,9).

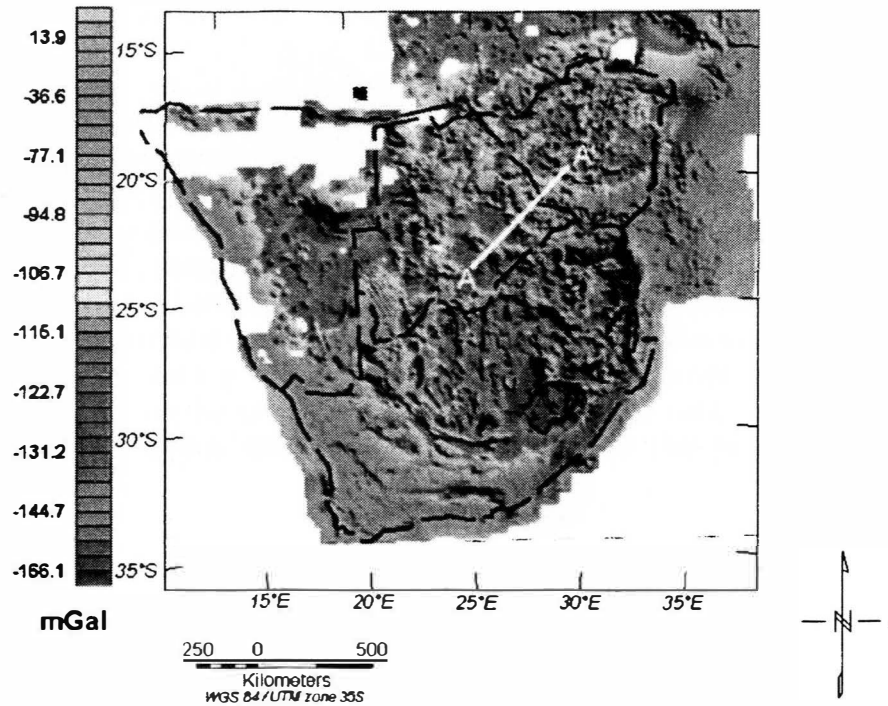


Figure 3: Color shaded relief of gravity data showing the location of the extracted gravity profile, A-A', from southwest to northeast. Dashed lines represent national borders

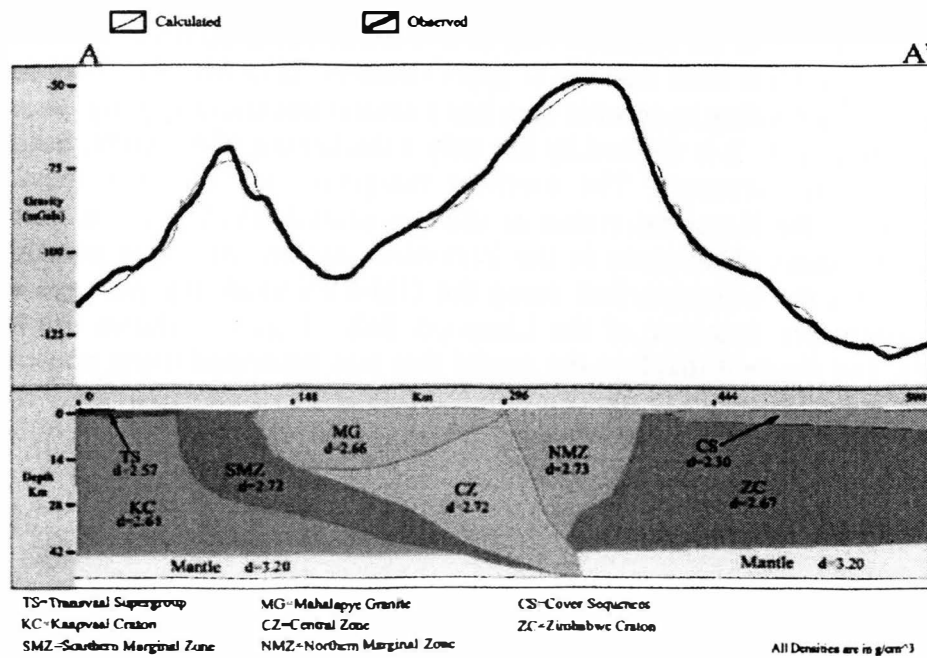


Figure 4: Gravity model of the Limpopo Belt in southern Africa. Note that densities are in g/cm³.

The model of the gravity anomaly over the Limpopo belt displays three unique shear zones sandwiched between the Archean cratons. The densities used represent averages for the rock-types that comprise each unique tectonic unit (5). The Southern Marginal Zone (SMZ) represents a thrust front is exposed at the surface. It is bounded in the northeast by the Mahalapye Granite (MG) that overlies the Central Zone (CZ) of the Limpopo Belt in this area. This granite is a post tectonic event that is bounded by the Northern Marginal Zone and completely covers central zone (4). The general shapes of the cratonic blocks indicate the SMZ and the CZ were thrust onto Kaapvaal craton and the NMZ was thrust backward on to the Zimbabwe craton. This is consistent with the pop-up structures seen in the Himalayan Mountains today (1).

The Kheiss and Magondi Belts

The region directly to the west of the assembled cratonic cores is comprised of two Proterozoic orogenic belts; the Kheiss Belt and the Magondi Belt. Argument has raged over whether these belts were of a contemporaneous age, but recent geochronological evidence suggests that the Magondi Belt predates the Kheiss. Dating of the Kheiss and Magondi Belts is difficult due to the lack of exposed bedrock. As a result, little geochemical and geochronological work has been done on the Kheiss Belt. More has been done on the Magondi Belt therefore its age and evolution is better understood. The conclusion that the Magondi Belt predates the Kheiss is supported by the interpretations drawn in this report as the Kheiss Belt butts up against the Magondi Belt and the structural trends in both belts are non-parallel.

The southern belt, the Kheiss Belt, defines the western margin of the Kaapvaal craton and is defined by a north-south structural trend, indicating an east west stress direction, and a large magnetic and gravity high on the east and west edge. It represents an orogenic event in the Early Proterozoic that is loosely constrained between 1928 Ma and 1750Ma (10). The north-south trend that defines the belt is truncated in the south by the Namaqua-Natal belt and on the north by the Palala-Zeitfontein Shear Zone (PLZ). But the Kalahari Line which defines the western extent of the Kheiss Belt extends north to the Okwa Block, a small crustal block of uncertain origin, suggesting that the Kheiss belt may extend further north and connect directly to the Okwa Block and simply be obscured due to reactivation along the PLZ. It is also interesting to note that the structural trends within the Kheiss Belt closely mirror that of deeper mantle structures as defined by shear wave anisotropy (11). This may be another line of evidence supporting the idea that the Kheiss Belt extends north of the PLZ as the seismic anisotropy along the PLZ is dominantly east-west and it would be difficult for a crustal feature to eradicate such a deep seated structural lineation.

The new datasets provided for this survey also help to constrain the westward extent of the Kheiss Belt. Previously it was thought that the extreme southwestern section of the belt extended to the west of the location mapped in figures 5 and 6 (12). However, the structural trends mapped within both the gravity and magnetic datasets support the conclusion that the Kalahari Line extends further south than previously thought and that it defines the western boundary of the Kheiss Belt along its entire length.

The structural trends indicated along the southwestern margin of the Kheiss Belt are drawn from both the gravity and the magnetic data. The gravity data shows several parallel to sub-parallel structures further north of this area that closely mirrors this dominant trend. However, there is no evidence for this in the magnetic data and without geochemical or other structural data from the area it is impossible to comment on what the structure may be.

The Magondi Belt is an Early Proterozoic orogenic belt that is curved around the northwest boundary of the Zimbabwe craton and has been dated to between 2000 Ma and 1900 Ma (13). It is bordered on the northwest by the Damara Belt and on the south by the Okwa Block (figures 5 and 6). In addition, there is a newly defined round structure that is as yet unidentified directly to the west of the Magondi belt. This block appears on both the gravity and the magnetic datasets, and yet is ill-defined in terms of geochemistry and geochronology. It may be an anomalous crustal block similar in origin to the Okwa Block on its southwestern boundary. The dominant structural trends within this belt are southwest-northeast and indicate a primary stress direction of northwest-southeast. Much like the Kheiss Belt to the south the edges of the Magondi Belt are defined by the large positive gravity and magnetic gravity anomalies. Based on recently published geochronological data (14) and the structural analysis within this paper it is reasonable to conclude that the Magondi Belt predates the Kheiss Belt and defines the extreme northeast corner of the Kheiss Belt.

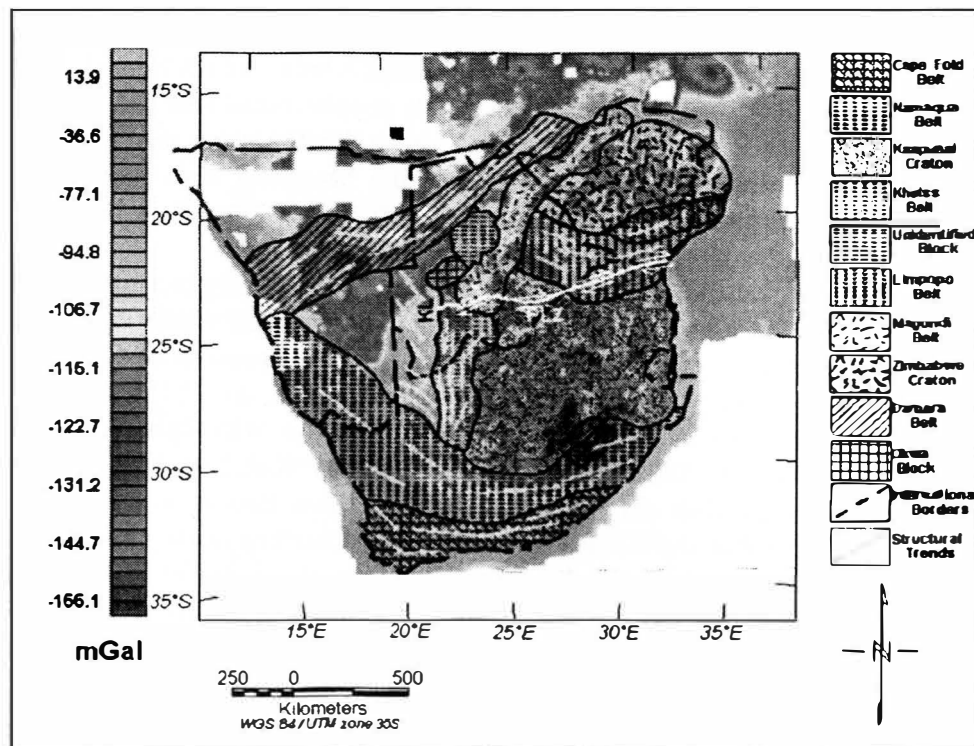


Figure 5: Raw gravity data with tectonic boundaries lay on top. PLZ=Palala-Zoetfontein Shear Zone; KL=Kalahari Line

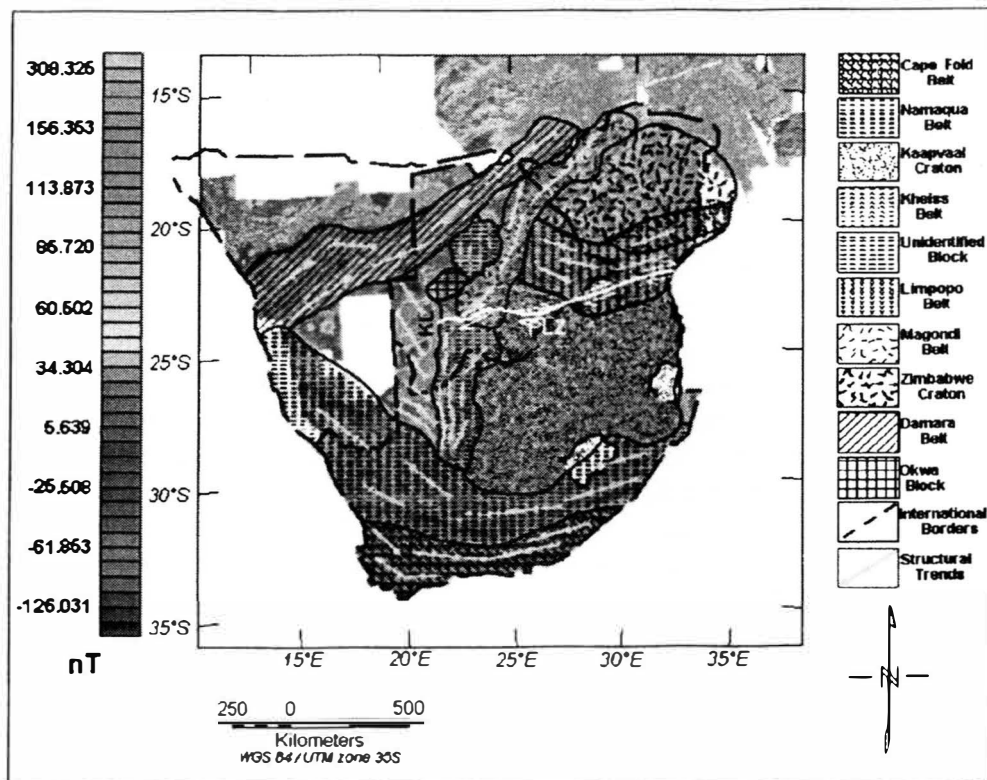


Figure 6: Raw magnetic data with tectonic boundaries lay on top. PLZ=Palala-Zoetfontein Shear Zone; KL=Kalahari Line

The Namaqua-Natal and Damaran Belt

The Namaqua-Natal Belt is a Middle Proterozoic orogenic belt that defines the southern boundary of both the Kaapvaal craton and the Kheiss Belt. It is defined by a structural lineament that is curved sympathetically with the southern boundary of the older structures. It has been dated to between approximately 1200 Ma and 1000 Ma (15). This belt is defined once again by high gravity and magnetic values on its edges and structural trends that are perpendicular to the primary stress directions. The crust that composes the Namaqua-Natal Belt is composed of many dissimilar crustal blocks that were all deformed at approximately the same time. Many of these blocks are believed to be crustal terrains that developed elsewhere and accreted to the edge of the growing continent (10). The structural strength of these terrains was low so they curved to accommodate the shape defined by the much older, well constructed crust of the Archean craton (16) (see figures 5 and 6).

The Damara Belt is a Middle Proterozoic belt that corresponds to the northwestern border of the Magondi belt. It is essentially coeval with the Namaqua-Natal Belt and shows many of the same characteristics as its southern counterpart. The Damaran and the Namaqua-Natal Belts combine in the western portion of Namibia. Unfortunately the gravity and magnetic data coverage for this area is rather poor, but it does appear that the Namaqua-Natal Belt serves as a structural stop for the Damaran Belt. This suggests that the Namaqua-Natal Belt is the older of the two, at least in the limited area in which there is data coverage (15,16).

The Cape Fold and Thrust Belt

The Cape Fold and Thrust Belt of South Africa is an orogenic belt of Late Proterozoic age that is linked to the creation of Gondwanaland. It has a low gravity and magnetic structure and is primarily defined by a minor high that defines the boundary between it and the Namaqua-Natal Belt to the north. It has been dated to approximately 578 Ma (10) and is composed mostly of folded and thrust sedimentary units and a minor granite component in the Cape of Good Hope region.

Conclusions

Existing geochemical/geochronological data, when compiled with the structural insights gained from the analysis of the newly compiled gravity and magnetic datasets is able to give unique insights into the structure of the crust in southern Africa. This is important in that many of the rocks that may be dated in boreholes or from small samples at irregular outcrops may now be correlated to the larger crustal structure of which they are a part. This allows for the large scale mapping of individual orogenic events even though they may lie under large columns of cover sediments and have little or no surface expression. In addition, it is now possible to better constrain the evolution of these individual orogenic belts. Whereas previously our understanding of the evolution of these large belts with complex interrelationships was restricted to our limited knowledge of their upper and lower age dates, we are now able to bring to bear the tools of structural geology such as cross cutting relationships and preferential structural trends to better define their evolution.

Acknowledgements

I would like to thank Dr. Estella Atekwana for all of her help in putting this project together, the South African Council for Geoscience for providing the data-sets, and Dr. R. Mapeo and the late Dr. A. Kampunzu for pointing me in the right direction.

References

1. Holzer, L., Barton, J.M., Paya, B.K., and Kramers, J.D., 1999. Tectonothermal history of the western part of the Limpopo Belt: tectonic models and new perspectives, *Journal of African Earth Sciences*, **28**, 383-402.
2. Moser, D.E., Flowers, R.M., and Hart, R.J., 2001. Birth of the Kaapvaal Tectosphere 3.08 Billion Years Ago, *Science*, **291**, 465-468
3. Atekwana, E.A., 2004, *Personal Communication*.
4. Ranganai, R.T., Kampunzu, A.B., Atekwana, E.A., Paya, B.K., King, J.G., Koosimile, D.I., and Stettler, E.H., 2002. Gravity Evidence for a largher Limpopo Belt in southern Africa and geodynamic implications, *Geophysical Journal International*, **149**, F1-F6.
5. Telford, W.M., Geldart, L.P., and Sheriff, R.E., 1990, *Applied Geophysics*, 2nd ed., Cambridge UP.
6. Geosoft, 2004, *Users Manual for Oasis Monta.j*
7. Nguuri, T.K., Gore, J., James, D.E., Webb, S.J., Wright, C., Zengeni, T.G., Gwavava, O., Snoke, J.A., and Kaapvaal Seismic Group, 2001. Crustal structure beneath southern Africa and its implications for the formation and evolution of the Kaapvaal and Zimbabwe cratons, *Geophysical Research Letters*, **28**, 2501-2504
8. Kampunzu, A.B. and Ranganai, R.T., 2002. *Personal Communication*.
9. McCourt, S. and Armstrong, R.A., 1998. SHRIMP U-Pb zircon geochronology of granites from the Central Zone, Limpopo Belt, southern Africa: Implications for the Age of the Limpopo Orogeny, *South African Journal of Geology*, **101**, 329-338.
10. Hanson, R.E., Proterozoic geochronology and tectonic evolution of southern Africa, in Yoshida, M., Windley, B.F., and Dasgupta, S. (eds), 2003. *Proterozoic East Gondwana: Supercontinent Assembly and Breakup*, Geological Society, London, Special Publication, **206**, 427-463.
11. Silver, P.G., Fouch, M.J., Gao, S.S., Schmitz, M., and Kaapvaal Seismic Group, 2004. Seismic anisotropy, mantle fabric, and the magmatic evolution of Precambrian southern Africa, *South African Journal of Geology*, **107**, 45-58.
12. Mapeo, R.B.M., Ramokate, L.V., Armstrong, R.A., and Kampunzu, A.B., 2004. U-PB zircon age of the upper Palapye group (Botswana) and regional implications, *Journal of African Earth Sciences*, **40**, 1-16.
13. McCourt, S., Hilliard, P., Armstrong, R.A., and Nunyanyiwa, H., 2001. SHRIMP U-Pb zircon geochronology of the Hurungwe granite northwest Zimbabwe: Age constraints on the timing of the Magondi orogeny and implications for the correlation between the Kheiss and Magondi Belts, *South African Journal of Geology*, **104**, 39-46.
14. Mapeo, R.B.M., Armstrong, R.A., and Kampunzu, A.B., 2001. SHRIMP U-Pb zircon geochronology of gneisses from the Gweta borehole, northeast Botswana: implications for the Palaeoproterozoic Magondi Belt in southern Africa, *Geological Magazine*, **138**, 299-308.
15. Kampunzu, A.B., Akanyang, P., Mapeo, R.B.M., Modie, B.N., and Wendorff, M., 1998. Geochemistry and tectonic significance of the Mesoproterozoic Kgwebe metavolcanic rocks in northwest Botswana: implications for the evolution of the Kibaran Namaqua-Natal Belt, *Geological Magazine*, **135**, 669-683.
16. Van der Voo, R., 2004. Paleomagnetism, oroclinal, and growth of the continental crust, *GSA Today*, **14**, 4-9.

**Application of Slovic's Risk Perception Research to
Next Generation Advance Reactors**

OURE 2004-2005

Final OURE Report 2005

University of Missouri-Rolla

Nuclear Engineering

Research done by

Ms. Reanea Hunter

In collaboration with

Dr. Akira Tokuhiko

Submitted to Office of Undergraduate and Graduate Studies

On

April 1, 2005


Reanea Hunter

Abstract

Over the past few years the United States has seen a dramatic increase in energy demand and consumption. With this increase there is a great need for a cheap, clean, energy source. In order to meet future energy needs the United States will have to build Generation (III+) and Generation (IV) power reactors, which have increased capabilities and passive safety features. One major challenge for this new exciting technology is public acceptance. In the past, the nuclear industry has had grim luck with public perception of any nuclear technology. However, there is hope for a solution to this problem; a problem that stems only from the lack of knowledge about nuclear energy. The American public knows a great deal about the risks involved with nuclear technology, but very little about the benefits it also brings. If most people were aware of all the diverse benefits associated with nuclear energy then the nuclear industry would gain public acceptance on a large scale. To achieve this, the nuclear industry and all stakeholders must familiarize the public through some massive means, inserting a constructive image into the nation's mind. People will then realize nuclear energy as a part of their everyday lives, and will open the country to new sustainable social, economic, and environmental possibilities.

Introduction

The nuclear industry plays an important role in the everyday lives of all Americans, even though most are completely unaware of it. There are so many examples of the important products and services provided by nuclear technology that improve both present and future generations. For instance, about twenty percent of the nation's power comes from nuclear power plants, and without it, the already struggling energy situation would be a disaster. Deaths and serious injuries are prevented every day thanks to gamma-radiography, which finds cracks and defects in the materials used in common structures and machines, such as commercial aircrafts. Dangerous criminals are caught based on neutron activation, which allows police to detect weapons, drugs, and explosives. Even nuclear technology is behind the customary smoke detector, which saves lives all over the world. Finally, the medical uses seem to be endless, from simple x-rays to PET Scans; people everywhere are enjoying the benefits of this modern technology.

Imagine what the nuclear industry would be like if the majority of U.S. citizens were aware of all the aforementioned benefits. Unfortunately, very few Americans have any idea about all of the positive impacts nuclear technologies have on themselves and their loved ones; and if they did, it is certain that the average perception associated with the word *nuclear* would be much brighter.

The largest problem the nuclear industry faces is negative public perception. Paul Slovic is a psychologist who has done extensive research on risk perception of the nuclear industry. His work has helped explain some of the industry's public perception setbacks. Perception is a key issue because in a democracy the people control policy,

whether directly or indirectly. It has been seen that without supporting government policy, nuclear progress is almost impossible. It has also been seen that the converse is true in countries such as France and Japan. If public perception is positive then government support will materialize and progress will prevail.

Risk, Media and Stigma and Paul Slovic

The main source of research in this paper is the book Risk, Media and Stigma: Understanding Public Challenges to Modern Science and Technology edited by James Flynn, Paul Slovic, and Howard Kunreuther. This book is particularly relevant to the nuclear industry and explores its case in depth. Before going into detail about Slovic's works it is necessary to first define the terms *risk* and *stigma*.

Risk is nothing but a probability, a probability of something bad or dangerous happening. Very often a person's perception of a risk is quite far off from the true statistical risk value. Several explanations of this will be examined later.

According to Erving Goffman, the word *stigma* was created by the ancient Greeks, referring to signs imposed on one's body to show something bad, immoral, or strange about the bearing person.¹

For the current situation, the term *technological stigma* is used. It is very similar to the stigma used by the Greeks, except that technological stigma is placed on a certain technology or industry, and so is viewed as being spoiled or hazardous by a substantial number of people. Also, the process of a something receiving stigma is called *stigmatization*.

Risk Perception

Risk-perception is often stemmed from stigma – if a stigma is placed on a technology then it will be perceived as in one way or another as risky. There are six characteristics of this which have been classified through empirical research (Jones et al., 1984, p. 24).²

1. *Concealability*. Is the condition hidden or obvious? To what extent is its visibility?
2. *Course*. What pattern of change over time is usually shown by the condition? What is its ultimate outcome?
3. *Disruptiveness*. Does it block or hamper interaction and communication?
4. *Aesthetic qualities*. To what extent does the mark make the possessor repellent, ugly, or upsetting?
5. *Origin*. Under what circumstances did the condition originate? Was anyone responsible for it and what was he or she trying to do?
6. *Peril*. What kind of danger is posed by the mark and how imminent and serious is it?

These six characteristics of stigma induce risk-perception; sadly the nuclear industry has had a serious history with all of the characteristics because of accidents like Three Mile Island, Chernobyl, and the Fermi I Breeder Reactor. More recently, issues like nuclear waste storage, transportation, and proliferation have further complicated the evolution of risk-perception. It is easy to conclude that as a result of these incidences and policy issues the nuclear industry is perceived with high risk. Surprising to some, the difference between the perceived risk and the actual risk is very large. Statistically, the risk associated with the nuclear industry compared with other industries is exceedingly low, as opposed to what the average person believes.

Media

Media plays an important role in public perception of all technology and industry. The media is the means through which most people gather facts about technology,

especially if they have no *human* resources about that technology. It has been experimentally proven by psychologists John Farquhar and Nathan Maccoby (1977; Maccoby & Alexander, 1980; Maccoby, 1980) that face-to-face communication is far more effective than media.³ However, in the case of the nuclear industry, very few direct human sources of information are available due to the relatively small number of experts in the field. This means that almost all of the information accumulated by the public is obtained through the media. Because so few human resources are available, the media has a tremendous responsibility to report accurately on the subject of nuclear technology.

The media is a money making business like any other. It will grab viewers in any way it can, even if that means reporting on nuclear related topics in a dramatic way. The media has perhaps inadvertently caused a stigma to be placed on the nuclear industry by way of its vivid reporting.

As mentioned before, accidents like those at Chernobyl and Three Mile Island have been devastating to the industry, greatly as a result of the style of the reporting. The coverage of the Three Mile Island accident was particularly intense and frightening. Words used to describe the accident included “horror,” “catastrophe,” and “the first step of a nuclear nightmare.”⁴ These reports caused the first major downturn in America for the industry.

Since the Three Mile Island accident almost all reporting on nuclear related topics have been of the same nature. More recently Yucca Mountain has received a fair amount of media attention. Similar types of words have been used to describe it such as “radioactive grave,” “dump or a tomb or a shaft full of gunk,” “atomic garbage”, and “big

R.I.P.”⁵ Because of these kinds of expressions used by the media, the public has an overall fear and disgust for nuclear energy.

Another current topic in media focus is that of nuclear weapons of mass destruction. This media subject has been ongoing since nuclear weapons were created or obtained by other countries around the world, especially Russia. After 9-11 the threat of these weapons falling into the hands of terrorists became very real. In the following months the United States even attacked Iraq based on the possibility that they might have nuclear weapons. Nuclear weapons in the media are here to stay simply because they are so important and are received with so much dread.

Another interesting story that seems to frequently show up in the news is the report about a catastrophic nuclear accident that has not happened but could happen soon. It is a very strange story because most news is about something that did happen or it is at least about an event that is probable to happen. The chances of this kind of nuclear accident to happen in the U.S. are slim to none. But this type of story is really scary to the public because it is easy for people to imagine this scenario and all the awful images that go along with it.

It seems still that any media publicity of the word nuclear is always grim and frightening. With all the wonderful means of technology today, the mass media extends far beyond the news; sources such as internet sites, movies, television shows, books, and radio are all contained in the long spectrum of media. Again, through all of those sources the nuclear industry is often made to look sensationally terrifying and ugly. One perfect example is the hit movie The China Syndrome, which came out in 1979, just 12 days before the Three Mile Island accident. It was made with specific anti-nuclear intentions,

and the timing could not have been worse. The title comes from the scenario of a core meltdown that melts right through the world all the way to china. Furthermore, about 25 years later, today, if a curious individual decides to use an internet search engine to look up the word “nuclear,” he or she is shown several negative sites or images, most of which are about nuclear arms or are very scientifically incorrect, but sound really eloquent. On a positive note, more pro-nuclear websites are showing up, which are quite informative and accurate.

Public Perception

Public perception of nuclear technology has evolved greatly over the decades. The Department of Energy’s “Nuclear Age Timeline” gives a detailed description of nuclear technology’s history.⁶ In the 1930’s and 1940’s the first nuclear activities began to take place. The United States was entering and fighting World War Two at the time, and people viewed nuclear energy as a technology that could help win the war; that was about all that was on most people’s minds in that period in history. When President Truman decided to drop the bombs on Japan, it was then the public first realized the power and terror of nuclear radiation, even though it was not fully understood. Right as World War Two ended, the Cold War began with the Soviet Union weapons race. Then the 1950’s was the decade of the famous “Atoms for Peace” speech given by Eisenhower, promoting the peaceful applications of nuclear energy for power generation. According to the U.S. Department of Energy Office of Environmental Management’s Nuclear Age Timeline, ‘He (Eisenhower) pledged the United States’ determination “to help solve the fearful atomic dilemma—to devote its entire heart and mind to find the way by which the miraculous inventiveness of man shall not be dedicated to his death, but consecrated to

his life.””⁷ In 1957 the first major nuclear power plant began operations in Shippingport, Pennsylvania, literally kicking-off the Atom’s for peace movement. The 1950’s was a very promising time for nuclear energy. In the 1960’s Americans were encouraged to build fall-out shelters in case of a nuclear attack, and the threat of nuclear radiation became very real. Also, the Non-proliferation Treaty and the Limited Test Ban Treaty was being signed by the United States and other nations. Even still, a massive amount of commercial nuclear power reactors were built in those years. The most notable events in the 70’s were, of course, the Three Mile Island accident and Carter’s banning of nuclear fuel reprocessing. As mentioned before, Three Mile Island was the point at which public confidence in nuclear technology took a turn for the worse. The Anti-nuclear mind-set became prominent across the nation, and since then no new nuclear power plants have been built. The eighties were equally dim with the accident at Chernobyl, which caused extreme fear and discomfort with nuclear power. People continued to perceive nuclear energy with dread on through the 90’s.

In 2005 it is difficult to gauge the level of public acceptance of nuclear energy. Based on the history, one would conclude that the perception is still rather negative, and the industry is still stigmatized. Clearly, public perception is too low for the nuclear industry to make any bold moves.

Several attempts have been made to measure the amount of public acceptance of nuclear energy through different national surveys. Each study has a slightly different finding. According to a 2005 study conducted by Bisconti Research Inc., 67% of Americans favor nuclear energy.⁸ However, according to the Gallup Poll, only 44% of Americans approve of “expanding the use of nuclear energy,” while 51% disapprove.⁹

Even though that poll was conducted in 2001, the overall public opinion is certainly not going to jump from 44% approval to 67% approval in only four years. The Associated Press also conducted a poll in 2001 and found that 50% of Americans support the use of nuclear power to generate electricity, with 30% opposing the use of nuclear power.¹⁰ If one conclusion can be drawn from all the surveys conducted; it is that between about 45% and 65% of Americans approve of nuclear power. This neighborhood of approval is not high enough for the nuclear industry to make any major expansions in the current political environment.

With the generation (III+) and generation (IV) initiative in mind, the American public will not lend enough support to the building of a new nuclear reactor. Many of the people who do accept nuclear power do not want it in their own back yard because they are uneasy about nuclear reactors. Massachusetts Institute of Technology has done extensive research on public attitudes toward nuclear power and has found discouraging results. The Future of Nuclear Power: An Interdisciplinary MIT Study reports that “.....the U.S. public is unlikely to support nuclear power expansion without substantial improvements in costs and technology. Second, the carbon-free character of nuclear power, the major motivation for our study, does not appear to motivate the U.S. general public to prefer the expansion of the nuclear option.”¹¹ People do not seem to realize that carbon-free nuclear power will help with the fight against global warming. This is an example of Americans not being at all conscious of the benefits of the technology, but instead they seem to be focused on the risks. A shift in focus would lead to a shift in confidence.

Industry Stigma

The nuclear industry is a perfect example of a stigmatized industry. It is easy to see how the industry became stigmatized just by looking back on the history, which is only about a century old. Any new technology is going to be initially feared if it is unfamiliar and not understood, as nuclear technology certainly is. Going back to the definition of stigma, it is a term having to do with signs, meaning that stigma is all about imagery. It is simple to prove that the nuclear industry is stigmatized by researching the imagery associated with the industry. Paul Slovic researched this subject thoroughly and reported his findings in Risk, Media, and Stigma. He looked specifically into the nuclear images linked with the potential Yucca Mountain nuclear waste repository in Nevada. Slovic found a round about way to obtain images associated with the nuclear industry by surveying individuals about their personal images of Nevada. The survey was taken by Phoenix, Arizona residents in 1988. Nevada was chosen for this survey because it has a lot of nuclear images associated with it and it is the home of Yucca Mountain and the weapons test site. Slovic constructed the following table to illustrate the types of nuclear images people had.

Images Associated with an “Underground Nuclear Waste Storage Facility”¹²

Category	Frequency	Images included in category
1. Dangerous	179	Dangerous, danger, hazardous, toxic, unsafe, harmful, disaster
2. Death/sickness	107	Death, dying, sickness, cancer
3. Negative	99	Negative, wrong, bad, unpleasant, terrible, gross, undesirable, awful, dislike, ugly, horrible
4. Pollution	97	Pollution, contamination, leakage, spills, Love Canal
5. War	62	Warm, bombs, nuclear war, holocaust
6. Radiation	59	Radiation, nuclear, radioactive glowing
7. Scary	55	Scary, Frightening, concern, worried, fear, horror

8. Somewhere else	49	Wouldn't want to live near one, not where I live, far away as possible
9. Unnecessary	44	Unnecessary, bad idea, waste of land
10. Problems	39	Problems, trouble
11. Desert	37	Desert, barren, desolate
12. Non-Nevada locations	35	Utah, Arizona, Denver
13. Nevada/Las Vegas	34	Nevada (25), Las Vegas (9)
14. Storage location	32	Caverns, underground salt mine
15. Government/industry	23	Government, politics, big business

Many of the images the Phoenix residents had corresponding with nuclear waste storage are the same images shared by most Americans when thinking about any nuclear technology that they are not familiar with. These images are the ones that define nuclear stigma.

The nuclear industry is not the only industry that has been stigmatized. Technological stigma is a growing concern in today's business world and is a problem that many companies have faced. Usually stigmatization occurs when a scary or dramatic event happens with a particular product or industry, and most of the time the event is very improbable. For example, in 1982 fewer than ten people were killed from cyanide poisoned Tylenol®. These poisonings led to around 125,000 printed news stories and cost the company millions of dollars.¹³ People were very afraid to buy the brand for a long time after that even though it was extremely unlikely that an individual would buy a tainted bottle. Tylenol® made an incredible comeback and is still a very popular product today, proving that it is possible for an industry overcome a massive stigmatization. Other stigmatized industries or industries that have been stigmatized in the past include: fertilizer companies, pesticide companies, beef, eggs, video game makers, chemical manufacturers, cigarette companies, and the oil industry. Each of these industries have experienced stigma in a different way; arguably, some were deserved and some were not.

An interesting scenario should also be considered, that is when an industry should be stigmatized but is not. It can be a fairly dangerous situation if the risks are severe enough. Risk, Media, and Stigma examines the case of automobile airbags. Statistically, airbags are actually really dangerous, especially for smaller people like the elderly, women and children. By 1999 over 100 deaths of drivers and small children, and thousands of injuries had been caused by airbags.¹⁴ Although airbags could be made a lot safer, there is no public outcry or demand for it. Airbags have been known to inflate at crash impact speeds as low as 8 miles per hour and on average airbags are designed to detonate at impact speeds between 13 and 18 miles per hour, and when the average airbag detonates, it does so with a force of 2000 pounds and a rate of 200 miles per hour.¹⁵

One would wonder why airbags are not seriously stigmatized. Slovic found three possible answers to this question. The first explanation for this absence of stigma is public ignorance. If the public is unaware of the risky facts, then clearly they cannot be outraged over them. Various surveys have been conducted to find out whether people know about the risks associated with airbags and the results show that people are relatively ignorant of these risks.¹⁶ Secondly, personal optimism was proposed to explain the lack of airbag stigma. Personal optimism is when people think “it won’t happen to me.” Also, most Americans believe that they are great drivers for some reason. Even if this justification is correct, society should be infuriated by the amount of children’s lives airbags have claimed. However, a more logical and complicated explanation is provided. It is that most people trust that the benefits outweigh the risks. In Risk, Media, and Stigma it is noted that “Howard Margolis of the University of Chicago has argued that the public reaction to many technological dangers can be best understood as following a

danger-opportunity calculus. If a technology's danger is 'on-screen' but its benefits are 'off-screen,' there will be public demands for a 'better safe than sorry' approach to government policy. This is in fact the public response to nuclear power and agricultural pesticides, technologies that have imaginable dangers yet benefits that are difficult for ordinary people to fathom. If a technology's benefits and dangers are both 'on-screen,' then Margolis' prediction is that people will approach the issue with an attitude of 'fungibility' (Margolis, 1996). This attitude is far more tolerant of danger than the 'better safe than sorry' attitude."¹⁷ In the case of airbags, the benefits are definitely "on-screen," and that could mean that the industry will never be sufficiently stigmatized.

As stated by Margolis, the nuclear industry's benefits are "off-screen" and unknown by the common person. Nuclear technology could really profit from Margolis' analysis, in knowing that if more people were aware of the benefits and the risks then they would be willing to accept the industry's risk-benefit balance. The nuclear industry needs to find an efficient way of getting the advantages of the technology "on-screen." American Nuclear Society has made some great progress in this area, but the facts just need to be presented to an even larger audience. With this strategy in mind, next generation advanced reactors along with the nuclear industry as a whole have some encouraging possibilities.

Reversing Negative Public Perception Today

Currently, the nuclear industry is taking a few steps to improve public relations. For example, almost all the nuclear power plants across the nation have a nice visitor's center and offer free tours and information about the technology. This is a great way to increase public support especially on a local level, which is very important. The

American Nuclear Society (ANS) has also made tremendous efforts to educate the public on nuclear topics with the official American Nuclear Society website and a new website called "About Nuclear." ANS has also set out to educate the public through the "grass roots method," which is quite effective because it involves the human factor. The hope of this method is that it will take the domino effect; that is that one person will become educated and then educate his or her friends and family and the process will continue. ANS and other organizations also offer resources to teachers of all age levels. One of the most important audiences to reach is the children because they will be the next generation of law makers. The Department of Energy and some of the national laboratories also partake in similar forms of public outreach offering educational programs, extracurricular activities, and tours. All of these methods used have been very vastly effective in helping individuals make informed decisions and opinions about nuclear energy.

A Possible Ad-campaign for the Nuclear Industry

The nuclear industry has a great deal of potential to introduce an ad-campaign to inform the public of all the benefits offered by its technology. Doing this would improve public acceptance substantially. It is shameful that an industry does so much for a society which is completely unaware of it. Even though the nuclear industry is very broad, it can still launch an ad-campaign as many other generic or broad industries have. Milk, beef, cotton, and eggs are all generic products that have had impressive advertising accomplishments. Generic stigmatized industries have also introduced successful ad-campaigns, such as the "Plastics make it Possible" promotion. The plastic industry presented those commercials because plastics were beginning to become stigmatized due to their petroleum derivatives. Most people seemed to then realize how important

plastics are to society, and all the negative plastic publicity began to dwindle. Something of a similar nature could take place for the nuclear industry, even with its rocky past.

Instead of “Plastics make it Possible,” the nuclear industry might introduce an advertising phrase like “Nuclear Technology: Saving Lives, Enriching Life” because nuclear technology is responsible for making life safer and better with its various applications to materials, agriculture, cleanliness of instruments and food, power, public safety, military, and medicine. Plus, there is no doubt that many more applications will be invented in the future, especially since the technology is less than a century old. If America understood these things, then there would certainly be an abundance of enthusiastic support behind the industry.

The introduction of a nuclear ad-campaign is tempting to criticize, particularly when recalling the American Nuclear Energy Council’s (ANEC) 1991 advertising campaign for the Yucca Mountain repository site in Nevada. The advertising goal was to help the public understand that the transportation of high-level nuclear waste was safe. The methods used by the campaign designers looked good on paper, but backfired swiftly. One television commercial showed a truck with a waste container being smashed into by a large train. The spokesman proclaims that the container is fully intact after parts and machinery fly everywhere during the collision. Department of Energy scientists appeared in other ads, assuring the public that high-level nuclear waste cannot explode and that living near a nuclear power plant does not cause cancer. Another commercial showed that nuclear waste is solid, not liquid or gaseous as usually expected.¹⁸

Despite the valiant effort of ANEC, the campaign failed miserably. A later survey concluded that people responded to the ads with feelings of disbelief and insult. Many people disagreed with the ads or were indifferent, but some were also positive. Less than 15% of respondents felt more supportive after the ads, 32% felt less supportive, and 52% said that their opinion was unchanged.¹⁹ To make matters worse, the campaign became an issue of media criticism and satire. The American Nuclear Energy Council went about their attempts all wrong. They simply defended the case for nuclear waste transportation, thereby emphasizing the perceived risks. Defending a product will never make people realize its advantages.

The Nuclear Energy Institute (NEI) has also recently run into some problems with its ads. The NEI was reported to the Better Business Bureau for claiming that nuclear power is environmentally clean.²⁰ This problem has received ample media coverage about the industry's alleged "greenwashing" citizens into supporting nuclear power by making them believe that it produces no waste. This has offended the public and added to the distrust of nuclear business. Dishonest claims or even claims that are generally accepted as false do not make for acceptable advertising, especially for the nuclear industry. Advertisements for nuclear technology must be designed very carefully with human psychology in mind.

A psychological aspect that makes people uneasy about nuclear energy is the fact that they are not familiar with it. Most people have received little or no education on atomic energy. An ad-campaign showing how nuclear technology is an everyday part of life would familiarize the public enough that they would feel more comfortable with it. An example of how this works is given by Psychiatrist Dr. Robert DuPont, who said, "It's

like when I have a fearful flyer. Get him on an airplane. I want him to meet the pilot. I want him to tell the flight attendants that he's a fearful flyer. What they do is they humanize that scary environment. I don't want him in 17A, cowering like this. I want him talking to people. Well, that's exactly what you would do with nuclear power. You'd want him to talk to the engineers. You want to talk to the laborers in there. You want to talk to everybody in there, so they know they're just neighbors doing their work. And that's very reassuring to see that.”²¹ According to DuPont, familiarity reduces fear. A reduction of fear is exactly what the industry needs.

Imagery and visualization also play a key role in how people perceive a technology. If people could associate positive images with the nuclear industry they would be more likely to support it. Presently, the images associated with the nuclear industry include *mushroom clouds, death, sickness, radiation, glowing, cancer*, and so on. The table on page 11 shows some of the current nuclear imagery of Yucca Mountain, which applies to all the nuclear industry. People have these images because they appear on the television, in newspapers and articles, and even in history books. These are not images that are going to cause any public support. Adding nuclear associated images such as *life, wellness, safety, future generations, environmentally friendly, health, prosperity, and beauty* to the public's mind would also make people more likely to support the technology. Pictures truly are worth a thousand words. Advertisements about nuclear technology with these images presented clearly and sensibly will cause people to be less one-sided when thinking about nuclear energy because there will be new positive images along with the former negative images.

If the nuclear industry did decide to launch an ad-campaign, it would have to make sure it did so truthfully, politically correctly, and non-defensively. It would have to be able to make the public feel comfortable with nuclear energy, and do so using constructive imagery. Advertising just may be the answer to the nuclear public acceptance problem if done correctly.

Conclusion

Today, more than ever, it is important to reawaken the nuclear industry with the generation (IV) reactor initiative in order to meet the world's energy needs. The nuclear industry has experienced major difficulties and low points with the media and public opinion, but is still slowly recovering. America is ready for an attitude change because there has not been an accident for more than two decades and public confidence seems to be on the rise. All the industry needs to use is a little psychology to minimize the people's fear and maximize the people's knowledge of common beneficial nuclear technology. After more than fifty years of nuclear technology, there are finally helpful applications with which all people can relate and can appreciate. The idea of public acceptance of next generation advanced reactors should not be an *if* or a *when*, but instead a *how*. Gaining public support and consequently political support is not impossible; it just must be done in the right way. It is time for the nuclear industry to take action to enhance life for the present and for the future.

Endnotes

- ¹ Goffman, Erving. Stigma. Simon & Schuster, Inc.: New York, 1963.
- ² James Flynn, Paul Slovic, and Howard Kunreuther, eds. Risk, Media, and Stigma: Understanding Public Challenges to Modern Science and Technology. Sterling, VA: Earthscan Publications Ltd, 2001. p. 15
- ³ Meyers, David G. Social Psychology. 5th ed. McGraw Hill Companies, Inc.: 1996. p. 289-291
- ⁴ Lankester, Joanna. "The Effect of Public Perception on the Nuclear Power Industry." Mar. 2002. 3 Mar. 2005. < <http://userfs.cec.wustl.edu/~jall/nuclear/nuclearpowerpaper.html> >
- ⁵ James Flynn, Paul Slovic, and Howard Kunreuther, eds. Risk, Media, and Stigma: Understanding Public Challenges to Modern Science and Technology. Sterling, VA: Earthscan Publications Ltd, 2001. p. 22-23
- ⁶ U.S. Department of Energy Office of Environmental Management. Nuclear Age Timeline. 15 Nov. 1999. 5 Mar. 2005 <<http://web.em.doe.gov/timeline/>>
- ⁷ U.S. Department of Energy Office of Environmental Management. Nuclear Age Timeline. 15 Nov. 1999. 5 Mar. 2005 <<http://web.em.doe.gov/timeline/>>
- ⁸ Bisconti, Ann Stouffer. "Public Sees Nuclear Energy as Fuel of the Future; Favorability/Support Reach New High" Perspective on Public Opinion. Feb. 2005. Nuclear Energy Institute. 24 Feb. 2005 <http://www.nei.org/documents/PublicOpinion_05-02.pdf>.
- ⁹ Reiner, David M. The Gallup Poll. March 5-7, 2001. 24 Mar. 2005 <www.climnet.org/ctap/workshop2004/unicambridge>.
- ¹⁰ Associated Press Poll Apr. 18-23. 2001 "Nuclear Energy Poll Results." Online Posting. 25 Apr. 2001. HighRAD. Administrator Number 2. 7 Mar. 2005 <http://64.226.100.129/cgi-bin/ultimatebb.cgi?ubb=get_topic;f=8;t=000008>
- ¹¹ Massachusetts Institute of Technology. The Future of Nuclear Power: An Interdisciplinary MIT Study. MIT. 2003 p. 6
- ¹² James Flynn, Paul Slovic, and Howard Kunreuther, eds. Risk, Media, and Stigma: Understanding Public Challenges to Modern Science and Technology. Sterling, VA: Earthscan Publications Ltd, 2001. p. 95
- ¹³ James Flynn, Paul Slovic, and Howard Kunreuther, eds. Risk, Media, and Stigma: Understanding Public Challenges to Modern Science and Technology. Sterling, VA: Earthscan Publications Ltd, 2001 p. 203-217
- ¹⁴ James Flynn, Paul Slovic, and Howard Kunreuther, eds. Risk, Media, and Stigma: Understanding Public Challenges to Modern Science and Technology. Sterling, VA: Earthscan Publications Ltd, 2001 p. 241
- ¹⁵ Sensible Solutions, LLC Airbag Safety-It's up to You. 26 Feb. 2005 <<http://www.airbagonoff.com/index.htm>>
- ¹⁶ James Flynn, Paul Slovic, and Howard Kunreuther, eds. Risk, Media, and Stigma: Understanding Public Challenges to Modern Science and Technology. Sterling, VA: Earthscan Publications Ltd, 2001 p. 248-250
- ¹⁷ James Flynn, Paul Slovic, and Howard Kunreuther, eds. Risk, Media, and Stigma: Understanding Public Challenges to Modern Science and Technology. Sterling, VA: Earthscan Publications Ltd, 2001 p. 251-252
- ¹⁸ James Flynn, Paul Slovic, and Howard Kunreuther, eds. Risk, Media, and Stigma: Understanding Public Challenges to Modern Science and Technology. Sterling, VA: Earthscan Publications Ltd, 2001 p. 301-302
- ¹⁹ James Flynn, Paul Slovic, and Howard Kunreuther, eds. Risk, Media, and Stigma: Understanding Public Challenges to Modern Science and Technology. Sterling, VA: Earthscan Publications Ltd, 2001 p. 302-303
- ²⁰ Nuclear Energy Information Service. 31 Aug. 2004. Better Business Bureau Criticizes Nuclear Industry Advertising. 12 Mar. 2005 <<http://www.neis.org/press/bbb-pr.htm>>
- ²¹ "Nuclear Reaction: Why do Americans Fear Nuclear Power." PBS Report, April 22, 1997.

Preparation of Acrylic Emulsions for Use in Waterborne Coatings

Kylee Hyzer
University of Missouri at Rolla
Chemistry Department
Rolla, Missouri

April 1, 2005

Prepared in fulfillment of the requirements for Opportunities for Undergraduate Research Experience (OURE), for the University of Missouri Rolla under the direction of Harvest Collier, Ph.D.

Participant: 
signature

Research Advisor: 
signature

Table of Contents:

Abstract	1
Introduction	2
Results and Discussion	3-7
Acknowledgements	8
References	9
Attachments	10-13
Reflections on Learning Experience	14-15

Abstract:

Acrylic emulsions are formed by co-polymerizing diol amide derived from methyl soyate with maleic anhydride and phthalic anhydride through an emulsion polymerization reaction. The anionic surfactants used are sodium dodecyl sulfate and sodium lauryl sulfate. Two different initiators can be used: potassium persulfate and sodium bisulfite. Molecular weight of the polymer can be increased by using the initiator in smaller quantities. The anionic surfactant is used in excess to ensure the maximum amounts of micelles to be present, in which polymerization takes place. The emulsion polymerization reaction is conducted between 50⁰C and 85⁰C in distilled water. The acrylic emulsions are then stabilized with ammonium hydroxide to a pH range of 8-12.

Introduction:

The goal of this project is to design a coatings system for traffic paint while abiding by several factors. While synthesizing this coatings system, cost was kept to a minimum, renewable resources were used, and an environmentally friendly process was utilized.

In order to keep cost at a minimum, two strategies were employed. The first strategy was to design a “one pot” synthesis. In this sort of synthesis, all of the reagents that are initially used are present in the final product. This means that no waste is created which can be costly to dispose of. It also means that the process is simple and does not require transferring chemicals between many stages of the synthesis. Another strategy to keep cost at a minimum was to use water as the solvent. Water is inexpensive and easily attainable.

Perhaps the biggest goal of this project was to incorporate methyl soyate, which is a soy bean oil derivative, into a coatings system. It is beneficial to use methyl soyate as a binding component, because it is derived from soy beans, which is a renewable resource. Once the synthesis of this paint is perfected, it can be reproduced without any concern of running out of materials.

The United Soybean Board recently published an initiative to increase soy bean usage in America. In this initiative, they claim that the need for paints and coating systems are expanding with the growing economy. Once this coatings system is produced, the demand will be fulfilled. [1]

Results and Discussion:

Emulsion Polymerizations:

An emulsion polymerization was chosen for this process, as it is a common way to make coatings in the paint industry. The main ingredients of an emulsion are the solvent, stabilizer, initiator, monomer, comonomer, and surfactant. [2]

The solvent that was always used was water. Water was chosen as it is readily available, inexpensive, and not harmful to the environment. The amount of water used was varied from about 25 ml to 100ml.

The stabilizer works to keep the emulsion in a homogeneous state. The stabilizer that was used in all of the experiments was sodium dodecyl sulfate (SDS). It is readily available and inexpensive, which are two important attributes for the goals of this coating. [2]

The initiator starts the reaction. It works to produce a free radical which then reacts with other molecules in order to produce a polymer. The amount of initiator used had a direct impact on the percent solids produced in the reaction; if more initiator was used, more polymer chains started, producing a polymer with lower percent solids. If less initiator was used, fewer polymer chains were formed, which allowed the polymer chains to grow longer and created a product with greater percent solids. In the reactions, the initiator was varied between potassium persulfate ($K_2S_2O_8$) and sodium bisulfite ($NaHSO_3$). These are both common initiators used in coatings applications. [3]

The monomer used in all of the reactions was diol amide (the detailed synthesis of diol amide is described on p 5). This is made from methyl soyate, which comes from soybeans. Once this monomer is incorporated into a coatings system, the demand for soybeans will increase. The use of soybean oil derivatives in paints is beneficial because soybeans are a renewable resource and are not harmful to the environment. [1]

The comonomers used were varied in this reaction. The role of the comonomer is to act as a binding agent for the monomer in the polymer chains. The comonomer can be varied in order to change the properties of the polymer chain. Some experiments were done in which a mixture of equal parts of phthalic anhydride and maleic anhydride were used. Other reactions were performed in which only phthalic anhydride was used, and some in which only maleic anhydride was used.

The surfactant was used in some experiments and not used in others. Its role is to provide micelles, or reactive sites for the polymer to form. The surfactant that was used in some experiments was fatty acid soap (Ivory© brand). [3]

Main experimental setup:

In all of the experiments conducted, a 100 ml flask was filled with a varying amount of distilled water. The prescribed amount of comonomer and selected amount of SDS was added. The solution was allowed to heat to approximately 70°C and stir until all components were dissolved. Then, the selected amount of diol amide was added via pipet and shortly after that several grains of initiator were added. The reactions were then all allowed to heat and stir for approximately an hour. If the reaction proved to be unstable, a small amount of base was added to stabilize the emulsion. They were then allowed to cool and a cold-roll steel test substrate (Q-Panel) was cast from the product. If the Q-panel had desirable qualities, it was put through a series of tests such as the flexibility test in which the plate is bent in both inwards and outwards in order to test for film adhesion and cracking/crazing properties of the coating. The product was then tested for percent solids by drying a small measured volume of the product and comparing the initial weight to the dried weight. Also, the product was kept in a beaker and observed frequently to determine if the emulsion remained stable.

Variance in Surfactant:

Simple dishwashing soap (Ivory® brand), was used as the surfactant in this experiment. Each time it was used as a surfactant, it produced emulsions that contained air bubbles. With no way to remove these bubbles, the reaction was continued without use of the surfactant. It was clear after several reactions were conducted without the use of surfactant, that reaction sites were still forming and polymers were being produced. The sodium lauryl sulfate (SDS) that was always added as the stabilizer is known to act as a surfactant as well. The SDS most likely formed the micelles in the absence of the dishwashing soap and created a film with fewer bubbles. Eliminating the soap might have caused the reaction to continue at a slower rate. [4]

Variance in Initiator:

The initiator most commonly used in the reactions was potassium persulfate ($K_2S_2O_8$). It was found that the best emulsion was produced when only a few crystals of potassium persulfate were added to the reaction. When films with potassium persulfate as an initiator were cast on metal Q-panel, the film became a golden color and it appeared that the Q-panel rusted. When the same film were cast on plastic sheets, they did not turn the same golden color. This feature is unacceptable because when the paint is used for traffic coatings, it should not rust the metal machines used to apply it or the cars that will drive on it. The initiator was then changed to sodium bisulfite ($NaHSO_3$). This produced an emulsion that was not uniform and created crystals in the bottom of the beaker. When the reaction with sodium bisulfite was reproduced with more stabilizer, the emulsion was still not uniform and contained chunky, waxy components in the bottom of the beaker.

Variance in amount of solvent:

The amount of water used varied from 25-100 ml. This was found to have a direct effect on the percent solids formed. When more water was used in the emulsion, the percent solids decreased, and when less was used, the percent solids increased as would be expected. The percent solids are very important when producing coatings applications for traffic paints, because the paint industry has strict guidelines concerning the percent solids needed to make a useable traffic paint.

Variance in proportions of monomer and comonomer:

It was found that the ratio between the monomer and comonomer directly affected the properties of the polymers that were produced. The reaction that seemed to produce the best results was made from 67 percent comonomer and 33 percent monomer. The only problem with this reaction was that the film cast from it had a waxy component to it.

In order to eliminate the waxy component, a reaction with less diol amide was performed. When 5% diol amide and 95% comonomer were used, after the reaction was complete, a white powdery substance remained at the bottom of the flask. The film that was cast from this reaction was not desirable. The white powdery substance is assumed to be unreacted comonomer.

Stabilizing the emulsion:

Many emulsions formed were only stable for about 24 hours. After this time, waxy chunks settled to the bottom of the flask. It was found that the unstable emulsions were all very acidic (pH of about 2-3). This problem was combated by adding a strong base to the emulsion after it was cooled. The base was added until the pH was changed to about a 9, and this made the reaction much more stable and created emulsions that remained homogeneous for months. It is important to have a stable emulsion as the emulsions used for coatings applications may need to sit for months before being put to use and need to still be homogeneous when they are used.

Synthesis of diol amide:

Equimolar amounts of methyl soyate (9.72 mmol, 14.514 g) and diethanolamide (9.72 mmol, 5.365 g) as well as a stir bar were added to a 100ml 3-neck flask. 5 mol percent of NaOH (0.486 mol, 0.038 g) was then added. The 3 neck flask was heated using a heating mantle and was allowed to heat at approximately 70°C and stir for 23 hours. A viscous golden yellow product was produced.

Changes in diol amide:

The diol amide that was used in the experiments had an unsaturated component. This came from the part of the methyl soyate that is unsaturated. It is believed that this unsaturated portion caused many of the coatings to be waxy in nature. This waxy property is undesirable for a coating. There was an attempt to remove

the unsaturated component through a "winterization" process as described below. A similar process is used in the food industry to separate oils for salad dressings. [5]

The winterization process of the methyl soyate was conducted as follows: the methyl soyate was frozen for several days. It was then removed from the freezer and centrifuged. The frozen and unfrozen portions were separated from each other. The unfrozen portion was disposed of and the remaining portion, the saturated portion, was again frozen and the entire process was repeated to ensure all of the saturated component was discarded. This "winterized" methyl soyate was then used in place of regular methyl soyate to produce diol amide. An IR was run on both the winterized and unwinterized components of the methyl soyate. The comparison of these IRs was not very useful, because it was expected that the IR of each of these samples would be similar. There was not enough difference in either IR to draw any conclusions. These IRs can be found on pages 10 and 11.

The new diol amide was employed in reactions that had been run with "unwinterized" diol amide. The coatings that were created still contained a waxy property.

It is thought that the winterization process failed because the methyl soyate was frozen very quickly. Most winterization procedures call for the oil to be frozen slowly while being lightly shaken so that the saturated and unsaturated components can separate from each other. [5] The methyl soyate was frozen at one temperature, which most likely froze it in a homogeneous state inhibiting separation of the saturated and unsaturated components.

Concern with production of Crystals:

Many of the procedures led to a production of white crystals which settled at the end of the reaction to the bottom of the container. It is thought that in the cases where these crystals were formed, the crystals did not polymerize, but were simply recrystallized and settled to the bottom of the container. This hypothesis is supported by the fact that the comonomers used (maleic anhydride and phthalic anhydride) are both white crystals. An IR was run on a sample of crystals from the bottom of one of these beakers and compared to an IR run on a mixture of maleic anhydride and phthalic anhydride. It was clear from this comparison, that the white powdery substance was not simply a mixture of recrystallized maleic anhydride and phthalic anhydride, because the IRs were very different. The results of these IRs can be found on pages 12 and 13.

Specific Reactions with Results:

- The reaction that produced the crystals which were analyzed by IR (page 12) was performed in the following manner: 50 ml water and 0.730g SDS were heated and stirred to 60°C. 0.5g maleic anhydride and 0.5g phthalic

anhydride were added and then heated until they dissolved. Then, 0.5 g diol amide was added followed by a few flakes of sodium bisulfite. This heated at 78°C for one hour. It was then allowed to cool. The crystals that formed had a melting point of 182-187°C

- The reaction that seemed to work best was performed in the following manner: 50 ml water was added to a 100ml round bottom flask. 1.0g SDS and a stir bar were added and the reaction was allowed to heat at 60°C for about 5 minutes. Then, 0.5g maleic anhydride and 0.5g phthalic anhydride were added to the reaction flask. After these two substances were dissolved, 2.637 g diol amide was added via pipet. The reaction turned a dark yellow color after about ten minutes. A few grains of potassium persulfate were then added which caused the solution to become dark orange. Upon further heating and stirring, the reaction evolved into a cream color. At this point, the heat was removed. Ammonium hydroxide was added drop-wise to the mixture until it reached a pH of 9. The only undesirable property of this film was that it rusted the Q-panel.
- A reaction without diol amide: 50 ml water and 1.0g SDS was heated to 60°C. 0.5g maleic anhydride and 0.5g phthalic anhydride were added to the mixture. After they were dissolved, a small amount of potassium persulfate was added and the mixture was stirred and heated for 90 minutes. The solution changed from pink to creamy peach and back to pink in this time. After the coating cooled, a few drops were placed in an aluminum pan. It was clear that the coating was not waxy, but it was very sticky. This property shows that polymer was likely not formed. From this reaction it was concluded that, diol amide plays an integral role in the formation of polymer.

Acknowledgements:

I would like to thank the Office of Undergraduate Research for providing me with such an interesting and rewarding research opportunity. I would like to extend a special thank you to all of the people who helped me on this project: my supervisor, Dr. Harvest Collier, for his continuous attention and general concern about my understanding of the science being conducted; and Kyle Anderson and Eric Weidner for their patience and willingness to answer all of my questions.

References:

- [1] The United Soybean Board. [online:web]. October 2003. URL:
http://www.unitedsoybean.org/tsmos_pdf/mos5.pdf
- [2] Flory; Williams. [online: web]. Updated 2 Sept. 1995. URL:
<http://web.umn.edu/~wlf/Synthesis/emulsion.html>
- [3] University of Southern Mississippi: Department of Polymer Science.
[online: web]. Cited 10 Sept. 2004. URL:
<HTTP://www.pslc.ws/macrog/index.htm>
- [4] Harkins, William. (1947, June). A General Theory of the Mechanism of Emulsion Polymerization. *Journal of the American Chemical Society*. 79 (6), pp.1428-1444.
- [5] National Cottonseed Products Association. Updated: 2002. [online: web]
URL: <http://www.cottonseed.com/default.asp>

Reflection on the Learning Experience:**1. Describe your foundational understanding of how research is conducted in your discipline.**

Research in chemistry is conducted in a several step process. The first step is to figure out the problem and then to find all information of related science that has been conducted. The next step consists of finding information from this data that is relevant to the experiment that will be conducted. This is followed by planning an experimental design and then conducting the experiment based on that design. Once the experiment is analyzed, the researcher must attempt to interpret the chemistry that occurred and then create more experiments that will alter this chemistry to produce a desirable effect.

2. How have you expanded your understanding of the informational resources available and how to best use these resources?

I have greatly developed my knowledge of the uses of SciFinder. This program was very useful to me when I first started with my project so that I could understand ways in which scientists addressed similar problems to mine. I also learned how to use certain internet sites to my advantage and was able to find information in polymer text books that benefited me.

Perhaps the greatest resource that I was able to use was other scientists. I was able to talk with both professors and students to increase my understanding of the science being conducted in my research project.

3. Describe the knowledge you have gained regarding the fundamentals of experimental design

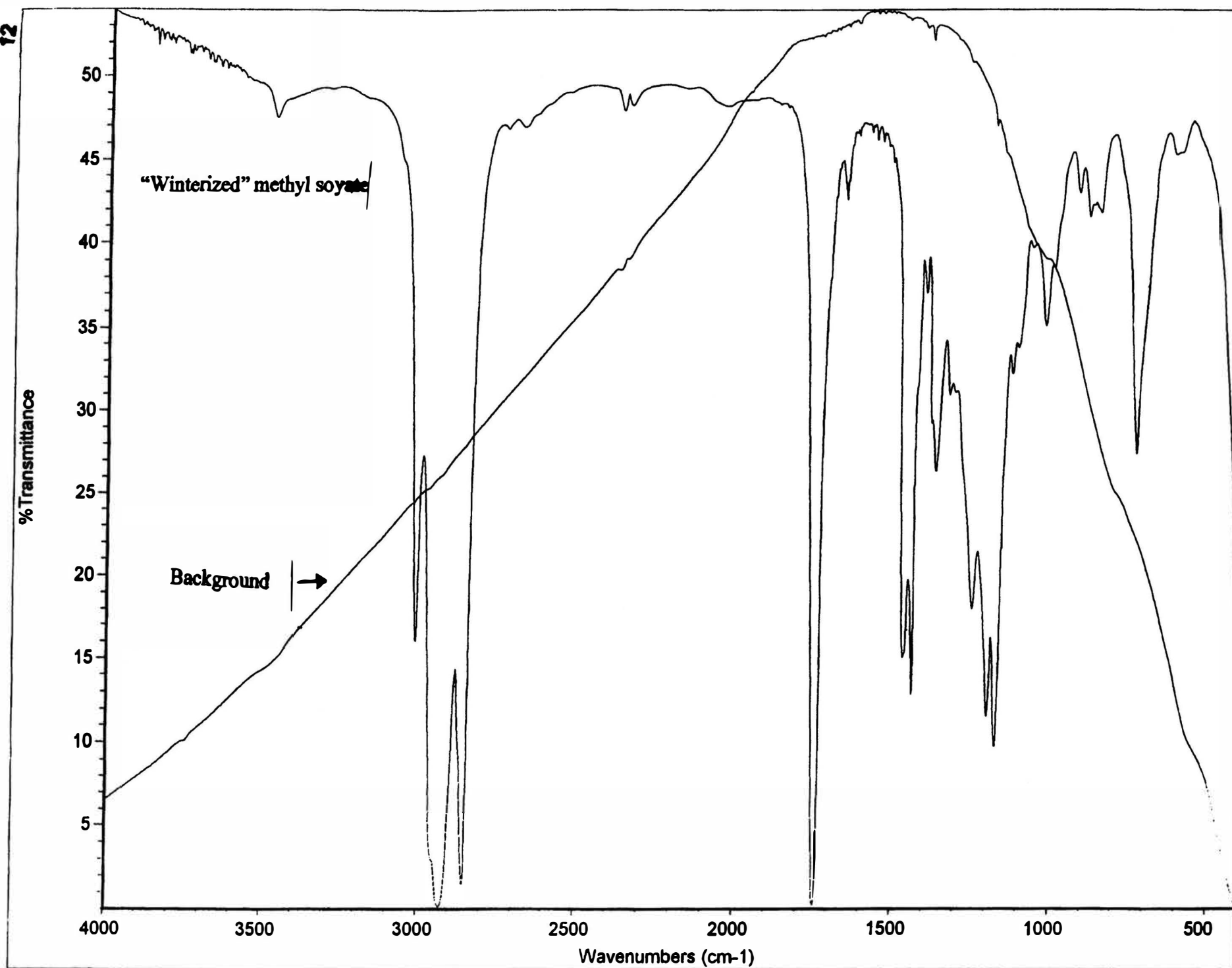
I now believe more in the scientific approach as it was taught in school. Through my experiments, I learned that changing one variable at a time is extremely important in order to isolate the variable that is causing a change.

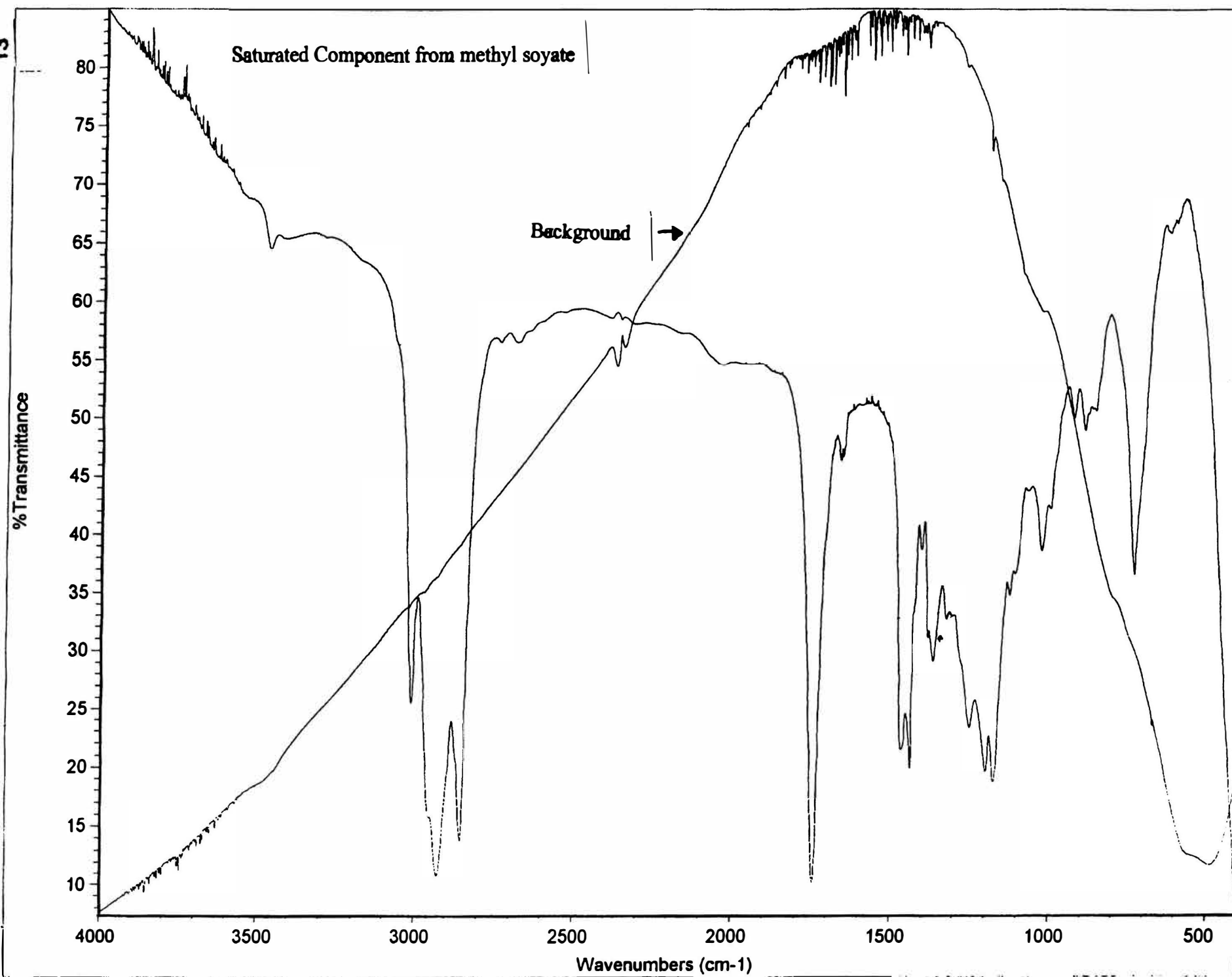
4. Describe how you have learned to interpret the results of your research project.

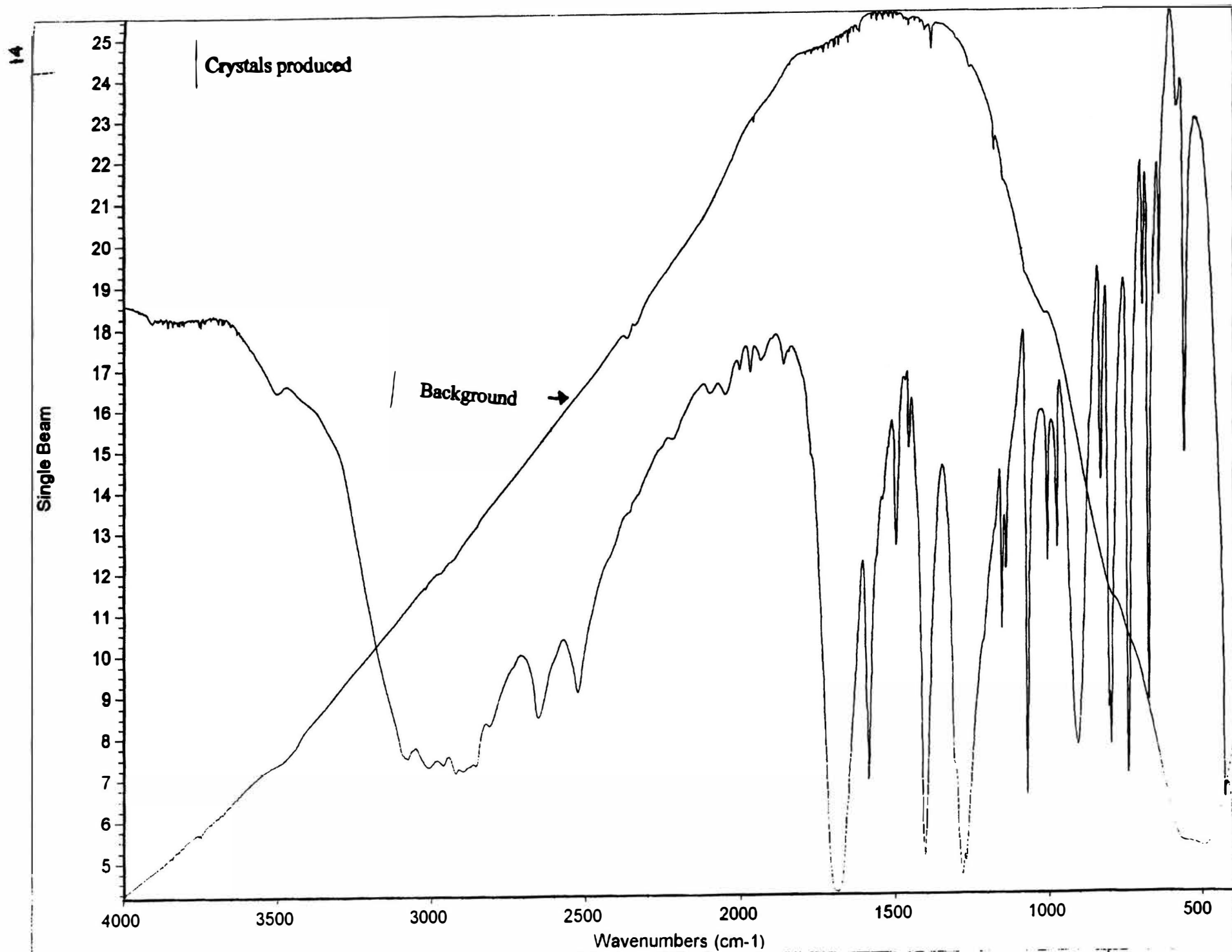
By making one change at a time on my experiments, I was able to determine the roles of the various chemicals used in my experiments. Isolating each of these changes allowed me to interpret the exact effect of each factor in my experiment.

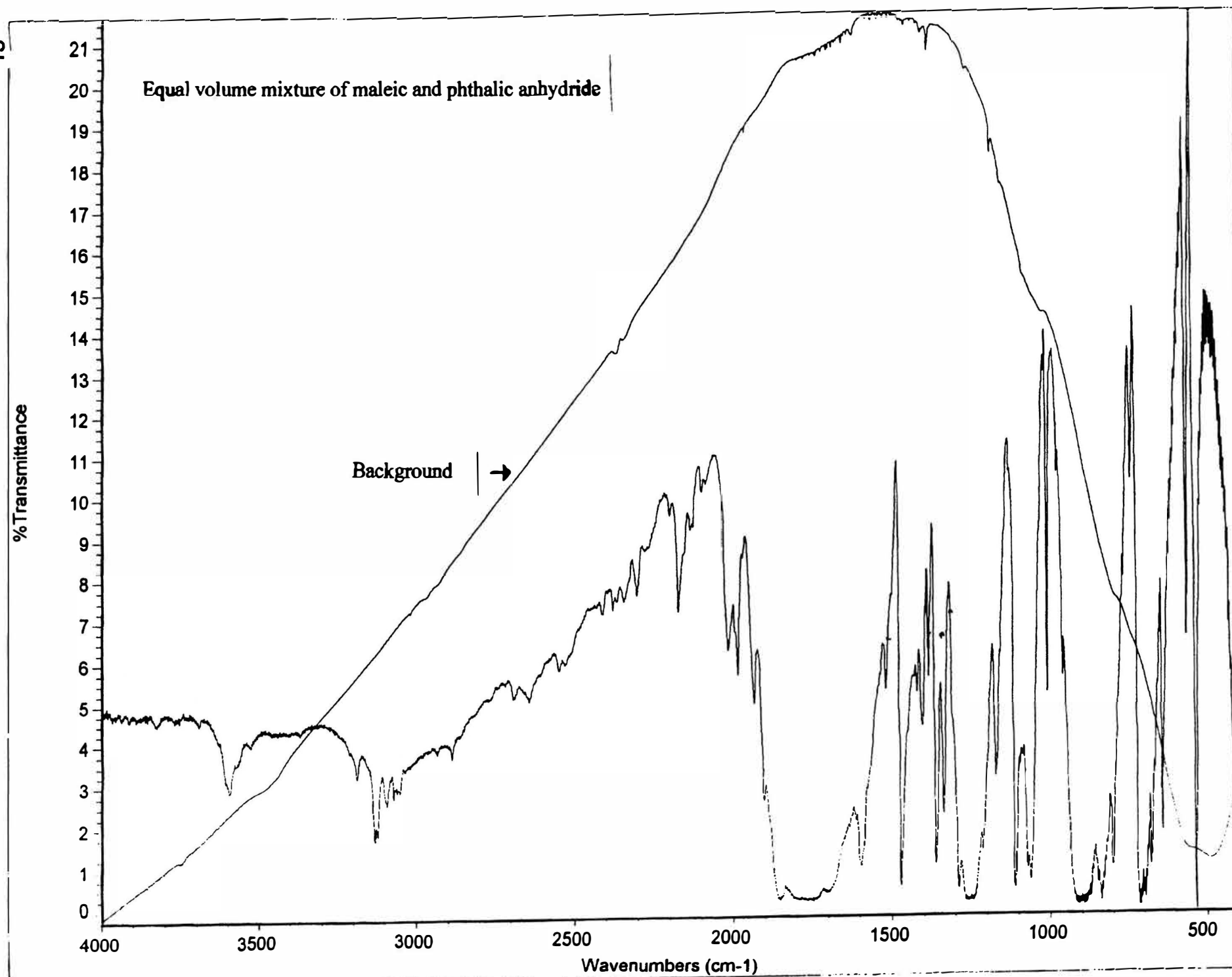
I was upset at first that nothing seemed to work that would benefit companies, but then realized that even though the things we produced

were not useful to industry; we still gained valuable information on chemicals such as methyl soyate, which may be used in future applications.

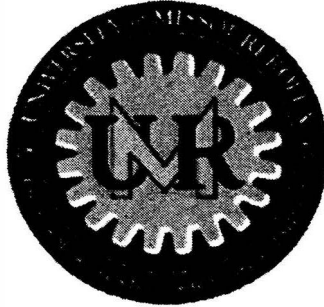








University of Missouri-Rolla
Department of Civil, Architectural, and Environmental Engineering



**Opportunities for Undergraduate Research Education (OURE)
Report**

**GCTS Servo-Controlled Direct Shear Testing of Soils
(Peak & Residual Strengths)**

Fall Semester 04 – Winter Semester 05

**Submitted By:
John Keeven**

**Submitted to:
Office of Undergraduate & Graduate Studies**

**Submitted on:
March 24th, 2005**

TABLE OF CONTENTS

Abstract.....	Page 1
Acknowledgements.....	Page 2
Introduction.....	Page 3
Historical Development.....	Page 4
Basic Forces Involved in the Direct Shear Test.....	Pages 4 - 5
Advantages of the Direct Shear Test.....	Pages 5 - 6
Disadvantages of the Direct Shear Test.....	Page 6
GCTS Servo-Controlled Direct Shear Testing of Soils (Peak & Residual Strengths).....	Pages 6 - 15
Objective of Testing.....	Page 6
Soils Tested and Relation to Other Research.....	Pages 6 - 7
Equipment Used.....	Page 8
Procedure of the Collinsville Silt Test.....	Pages 8 - 10
Description of the Stages of Testing Collinsville Silt.....	Page 10
Results of the Research.....	Pages 10 - 15
Conclusions.....	Page 15
Reflection on the Learning Experience.....	Page 16
References.....	Page 17
Appendix A – Collinsville Silt Consolidation Plots	
Appendix B – Collinsville Silt Shear Stress Plots	
Appendix C – GCTS Servo-Controlled Direct Shear Test User’s Manual	
Appendix D – Pneumatic Direct Shear Test Brief Overview	
Appendix E – Pneumatic Direct Shear Test User’s Manual	

Abstract

Using a Direct Shear Machine, various soils can be tested to figure out their strength properties. This research used an older pneumatic Direct Shear Machine and a newly purchased hydraulic Direct Shear Machine (Gcts Servo-Controlled Direct Shear Machine). The pneumatic machine was used to learn the basics of a how a direct shear machine works. The majority of the research was done on the hydraulic Direct Shear Machine. The Gcts Servo-Controlled Direct Shear Machine can perform conventional direct shear tests as well as consolidation and much more advanced tests. Since, no one had ever used this new machine; a simple user's manual was completed so that others will be able to use this machine. A Collinsville Silt was tested using the Gcts machine. The strength parameters found and other results of the tests on the Collinsville Silt will aid the graduate students in their research.

Acknowledgements

I would like to give a big thanks to my research adviser Dr. Luna. Without him this research wouldn't have been possible. He has taught me so much and I am very grateful to have worked with him. I would also like to thank Rachael Mudd. She is a graduate student who has helped with many aspects in the Geotechnical Labs. Lastly, I would like to thank anyone else who has helped me in any way during this whole research.

Introduction

One of the most important engineering properties of soil is the shearing strength. Shearing strength is the ability of the soil to resist sliding along internal surfaces. The shear strength of a soil helps maintain equilibrium on a sliding surface. Some examples of sliding surfaces are natural hillsides, back slopes of highway cuts, levees, or earth dams. The shear strength of a soil ultimately shows what the bearing capacity of it will be. The bearing capacity failure occurs when the shear stresses induced by a footing exceed the shear strength of the soil. Almost every problem in soil engineering involves the shearing properties of the soil. (Kazdi)

There are many different tests available both in the lab and in-situ that will give shearing properties of soils. Most choices as to what test should be run depend on the cost, time available, and the desired results. The Direct Shear Test is one of the most popular tests available in the lab. It is the simplest and easiest of the plane shear tests. It is very useful in gaining the shearing properties of soil. The Direct Shear Test is the basis for this report.

This project came about because I had an interest in some type of research. I knew I would be graduating in May 2005 and I figured this would be a great way to learn about how to conduct independent research. Dr. Luna had contacted me about possibly doing some research for him. I was immediately interested. He explained to me that I would be working with the new Direct Shear Machine that was purchased for the Geotechnical Labs. This interested me very much, since I would be the first person to work with this new equipment. I would have to figure out how the equipment and software worked and my overall results of testing would aid the graduate students in their research. The main objective of the research was to run some Direct Shear Tests on a Collinsville Silt. I would be measuring the peak and residual strengths and be getting the strength parameters of that soil. These results would be given to the graduate students.

A new and improved testing device has been purchased for the Geotechnical Engineering Laboratories. This system features electro-hydraulic closed-loop digital servo control of the shear and normal loads for test automation. Loads or deformations for both the shear and normal actuators can be prescribed to automatically perform conventional direct shear tests as well as more advanced tests. This system can be programmed to perform tests such as the constant normal stiffness test where the normal load is a function of a prescribed stiffness to simulate actual compressibility of a ground shear plane (e.g. soil-pile interaction) at failure.

The project consisted of first using the older pneumatic Direct Shear Machine to run some tests and then create a user's manual for it. The next part of the project consisted of learning all the software and hardware that form the hydraulic servo-controlled direct shear testing system. A simple user's manual has been completed with many graphics, for others to be able to run laboratory tests on this testing device. Preliminary trial tests were run on standard sand specimens (Ottawa Sand 20/30) and a demonstration was delivered to the CE 215 (Fundamentals of Geotechnical Engineering) class in the fall semester of 2004. Tests were run on a Collinsville Silt to aid the graduate students in their research.

Historical Development

The origins of the Direct Shear Test date back to 1846, when the French engineer Alexandre Collin was the first person to attempt to measure the shear strength of a soil. Collin first experimented with a split box. The split box that he used was 350 mm long which held a 40 x 40 mm section of clay. This section of clay was subjected to double shear under a load applied by hanging weights. In 1915, a Briton named A. L. Bell, was the first to record data of a Direct Shear Test. Bell constructed a device that would be a model for future shear box designs. He became the first person to run shear tests of various types of soils and have them published.

In 1934, a new advancement in the shear box came about. This new apparatus provided a single plane of shear. In this device the load was applied in increments (the 'stress control' principle) by progressively adding weights to a pan. The operator of this device needed to pay close attention to determine the load at which failure of the sample occurred.

The next advancement in the test came in 1936 when Gilboy, at MIT, developed a constant rate of displacement machine (the 'strain control' principle). This device used a fixed speed drive motor. Throughout the years, improvements to this device came about.

Shear box machines are still widely based on the displacement control principle. They provide a vast range of displacement speeds. Some machines can provide displacement from a few millimeters per minute to about 10,000 times slower. The stress-control method isn't as widely used anymore. It is mainly used to study the effect of 'creep' under constant shear stress. (Head)

Following the basic ideas of the first devices, Direct Shear Tests have become much more advanced. Some Direct Shear Tests use pneumatic power with dial gauges. Perhaps the most advanced Direct Shear Tests are the hydraulic controlled tests which can be hooked up to a computer and obtain all kinds of data about the shearing properties of the soil sample. The pneumatic and hydraulic controlled tests are the ones used in this report.

The Direct Shear Test doesn't have the ability for large shear displacements to reach some residual strengths. Residual strengths can be reached by shearing the sample back and forth. This can be done on the new GCTS hydraulic direct shear machine, but not on the pneumatic machine. Another way is to use a ring shear test. This test uses an annular-shaped soil sample that is subjected to a known normal load and is rotated. This test has an unlimited strain capacity and can be used to find residual strengths that need larger displacement.

Basic Forces Involved in the Direct Shear Test

In order to understand what is happening in the Direct Shear Test, basic forces must be explained. A force is defined as the influence which causes a change of state of motion of a body. Normal stress, shear stress, friction, and shear strain are involved in this test. (Head)

Normal Stress:

Stress is a force acting on a certain area. An external force is applied to a body which sets up an internal force that is an equal and opposite reaction. Normal forces are perpendicular to the plane where the force is being applied. Stress is defined as:

$$\sigma = \frac{P}{A} \quad \text{where: } \sigma - \text{symbol for direct stress}$$

P – downward force (lbs or newtons)

A – cross-sectional area

Shear Stress:

A shear stress acts parallel to the plane and the applied force causes layers of the plane to slide over each other. Shear stress resists an angular change of the shape. Shear stress is defined as:

$$\tau = \frac{F}{A} \quad \text{where: } \tau - \text{symbol for shear stress}$$

F – horizontal force

A – cross-sectional area

Friction:

Consider an object at rest on a level table top. If that object is pushed by a small horizontal force, less than required to move it, then an equal and opposite force will act on the object at the surface of contact. The force is due to friction between the object and the table top. In the case of soil, internal friction between the soil grains is desired.

Shear Strain:

Shear strain is the deformation in a body due to a force. Shear strain is related to the amount of shear stress on an object. Shear strain is defined as:

$$\gamma = \frac{\Delta L}{L} \quad \text{where: } \gamma - \text{symbol for shear strain}$$

ΔL - the change in length of the original length

L – the original length

Advantages of the Direct Shear Test

1. The Direct Shear Test is simple and inexpensive. Unlike an Unconfined Compression Test, the Direct Shear Test is not as complicated to set up and run.
2. The basic idea behind the Direct Shear Test is easily understood. Basically, a normal load is applied, and while that load is applied, a shearing force is applied.
3. There is rapid consolidation due to the small thickness of the soil sample. This results in less time waiting for the sample to reach its consolidation under the normal load.
4. The Direct Shear Test allows a wide range of soils samples to be tested, that could cost more by other tests. For instance, soils samples with large particles are more expensive using a different test, other than the Direct Shear Test.

5. In addition to the shearing properties, friction between the particles of the soil sample can be measured. This gives the internal angle of friction.

6. Both the peak strength and residual strength can be measured. The peak strength is determined when the sample fails. The residual strength can be determined by a multi-reversal process. This is when the same sample is used over and over again to see where the stress starts to become constant resulting in its residual strength.

Disadvantages of the Direct Shear Test

1. The Direct Shear Test limits the soil sample to fail along a predetermined plane of shear. Since the apparatus always shears at the same height, the shearing of the soil will always take place in the same plane. This means that the sample may not be shearing along the weakest plane.

2. Stresses along the soil sample may not be uniform. A stress may vary on one side of sample than the other.

3. The directions of the planes of principal stresses rotate as the shear strain is increased.

4. There is no way of controlling the drainage of a soil sample. The Direct Shear Test doesn't have a way of controlling the rate of drainage, except for controlling the rate of the shear displacement.

5. The pore water pressure that develops in the soil sample cannot be measured.

6. The shearing of the soil is only limited by the maximum length of travel of the apparatus.

7. The area of contact between the soil in the two halves of the shear box decreases as the test proceeds. This affects the shear and normal stress equally, and the effect on the Coulomb envelope is usually negligible, which is usually ignored.

Gcts Servo-Controlled Direct Shear Testing Of Soils (Peak & Residual Strengths)

Objective of Testing

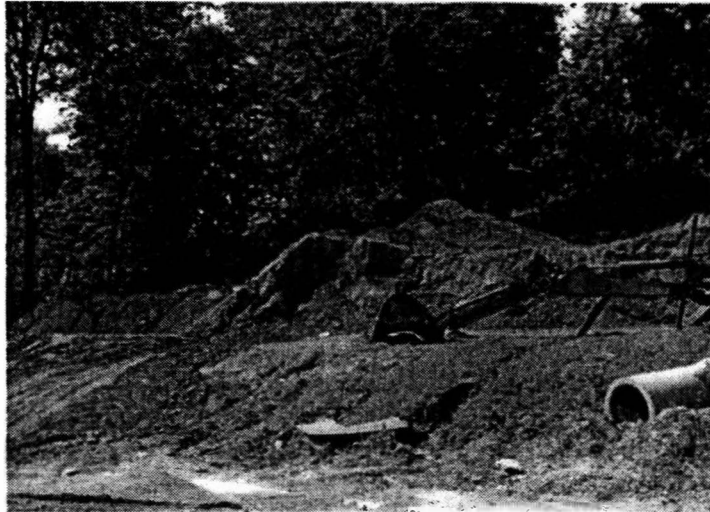
The objective of this research was to run a direct shear test on Collinsville Silt. The purpose of a direct shear test is to measure the shear strength of a soil along a predetermined failure surface. The properties measured in this test are the shear strength, cohesion (c) and the friction angle (Φ) of the soil.

Soils Tested and Relation to Other Research

The first soil tested was a well-graded sand. This was used to learn how the machine would work. The next soil tested was an Ottawa Sand (20/30). This soil was mainly used for the demonstration to the CE 215 class.

The soil tested to aid the graduate students was taken from a sub-division in Collinsville, IL. It is a light brown silt with a small natural clay content (about 16%). Its natural moisture content is around 10%. Its USCS classification is a ML silt. The silt has a plastic limit of 22 and a liquid limit of 28.5. The specific gravity of this test was run and found to be 2.72.

A picture of the silt in the field is shown below:



Picture 1 – Collinsville Silt in the Field

This soil is being researched by the graduate students. The research they are doing is for the US Bureau of Reclamation. They are consolidating silt slurry to simulate field conditions. It is very difficult to sample silt in the field without disturbing it, so they are consolidating it in the laboratory to get as close as they can to actual field conditions and still get a testable sample. The graduate students are then testing these samples in the triaxial machine to determine the critical state of the soil. They are using the triaxial testing machines because they can simulate the three dimensional stresses that the soil feels in its natural state in-situ. Once the graduate students have reestablished these stresses they are able to strain the soil to failure and determine how the soil reacts under the load. From this data they are able to get the effective internal angle of friction (ϕ') as well as the shear strength of the soil. Eventually, their intention is to also test this soil dynamically and determine at what dynamic stresses the soil liquefies, if it liquefies at all. They will then compare this to the amount of over consolidation the soil felt before the dynamic loading. They are attempting to predict liquefaction given the soil properties of the silt. The graduate students will then take this data and compare it to other silts with added clay to determine how much clay can be added before liquefaction no longer occurs.

My data can help them to know at what stress critical state occurred in my testing. I will give them the unit weight and void ratio of my soil during testing. Once they know critical state stress at several void ratios, they can plot this line on an $e - \log p'$ curve and they will have an estimate of the "Critical State Line." These results are not included in this report.

The soil used in the Direct Shear Test was a paste that was mixed to a water content just below the liquid limit. The liquid limit is a plastic state of the soil. This means it deforms without cracking. Its consistency is that of a soft butter to stiff putty.

Equipment Used

The research started off by working with the older pneumatic Direct Shear Machine. This equipment uses compressed air to control the loads and all the gauges must be read by hand. This equipment was used to learn how the Direct Shear Machine works and get some experience before I focused on the new hydraulic Direct Shear Machine. The pneumatic Direct Shear Test Brief Overview can be found in appendix D and the pneumatic Direct Shear Test User's Manual can be found in appendix E.

The main part of the research dealt with the GCTS Servo-Controlled Direct Shear Test. This equipment is hydraulically controlled and can be hooked up to computer which will receive the data. The GCTS Servo-Controlled Direct Shear Test User's Manual can be found in appendix C.

Procedure of the Collinsville Silt Tests

The procedure of the testing is divided into setting up the software program that controls and acquires the data of the testing device (C.A.T.S.), preparing the sample, running the test, removing the sample.

Setting Up C.A.T.S. (Computer Aided Testing Software)

A program had to be set up in order to test the samples. This is done in the C.A.T.S. software. There are two stages to this test. The first stage was a consolidation stage. The consolidation stage is a constant normal stress that acts on the sample for an amount of time. The consolidation stress squeezes out the voids of the sample, which are full of water and ultimately reduces the sample height. The first part to setting up the consolidation stage was to enter in the constant normal stress. Stresses of 100 kPa, 150 kPa, and 200kPa were used. These stresses simulate depths in the ground of approximately 9, 13, and 18 meters respectively. The next step was to enter in the duration for the consolidation stage. Preliminary tests suggested that the sample's height leveled off around 24 hours. So, the consolidation stage was entered in to be 1440 minutes (24 hours). The next part was set up the program to have data acquisition at timed increments of 0.500 seconds. After the consolidation stage was set up, the next stage was shearing. This stage is where the strength parameters will come from. The first part of the stage was to enter in the rate of shear displacement. The rate was set to be 0.05 mm/minute, so that the build up of pore pressure would not be likely, according to ASTM D 3080. The next part of the stage was to enter in an initial start value of 0 mm and a final displacement value of 15 mm. This means that the sample will shear until the displacement reaches 15mm. After that, the control input for the normal actuator was set to normal stress with a constant value of 100 kPa, 150kPa, or 200 kPa, depending of what test was run. The last part of this stage was to set the data acquisition to timed increments of 2 seconds.

Table 1 below shows how the tests were set up:

Test #	Displacement Rate (mm/min)	Consolidation Stage (hours)	Constant Stress (kPa)	Total Shear Displacement (mm)	Moisture Content (%)
1	0.05	24	100	15	27
2	0.05	24	150	15	27
3	0.05	24	200	15	27

Table 1 – Test Parameters

Preparing the Sample

After the tests were set up, the sample had to be prepared. The first part of this was to find out what the target moisture content needed to be. The sample was wanted to have moisture content just under the liquid limit. The liquid limit for the Collinsville Silt was determined from the graduate students to be 28.5. The moisture content used for the sample was 27%. The 27% moisture content made the silt a paste like substance. To find the 27%, the dry sample was weighed out to see how much would fit into the 63.50 mm ring. Then it was calculated to see how much water was needed to obtain the desired moisture content. After, the desired moisture content was obtained; a wet paper towel was placed over the sample. It then sat overnight. This would ensure that all of the silt grains would be wet.

The next day the sample was placed into the direct shear mold with the porous stone on bottom. Then the mold was placed into the loading yoke on the direct shear machine. All eight screws were tightened down to hold the ring in place. The top porous stone was placed on top of the silt sample. Then water was added into the loading yoke, up to a level just under the top edge of the top ring. This represents an undrained condition for this test. Next, the loading yoke was slid under the normal actuator. The shear actuator coupler was connected to the loading yoke and the sample was ready to be tested after it sat there for 15 minutes so the sample could saturate.

Running the Test

After the direct shear machine had been plugged in, turned on, and connected to the computer, a file was created for the sample about to be run. Next the hydraulic pumps were turned on in the C.A.T.S. software. The test was executed. The normal actuator moved down and started to apply a stress to the sample. It increased its stress until it reached the normal stress that was specified in the program (either 100 kPa, 150 kPa, or 200 kPa). After the stress leveled off it applied the stress for the whole duration of 24 hours. It was noted that air bubbles could be seen coming up to the surface of the water from the air be squeezed out of the soil. The sample height was changing, over time, as was seen from the normal displacement getting larger. After the consolidation stage ended, the shear stage began. The same stress was held constant during this stage. The shear stress being read in C.A.T.S. could be seen. The shearing stage continued until it reached the 15 mm displacement.

Removing the Sample

After the test was over, the file of data was exported to the computer. The normal actuator was raised up off the sample. The shear actuator was moved be to the initial starting position. The coupler that attached the loading yoke to the shear actuator was

taken off. The loading yoke was slid out and the valve to the loading yoke was opened. This allowed the water in the loading yoke to drain out into a bowl below. The eight screws were taken out and the shear ring was removed. The silt was taken out and disposed of. The loading yoke and shear rings were washed up and ready for the next test to begin.

Description of the Stages of Testing Collinsville Silt

The first stage of the test was a consolidation stage. This stage was to apply a constant normal stress of either 100 kPa, 150 kPa, or 200 kPa to the sample for 24 hours. This represents the settlement of the sample and it squeezes out the voids and pore water pressure. *The next stage was the shearing stage.* This stage started after the 24 hours of the consolidation stage. It had the same constant normal stress as the consolidation stage. The shearing stage is where the strength parameters will ultimately come from. The sample was sheared at a rate of 0.05 mm/min and sheared to a displacement of 15 mm. The load cell on the shear actuator read the shear stress that was present.

Results of the Research

Four main results were obtained from this research. The older pneumatic Direct Shear Machine was used to test well graded sand and a user's manual was completed for it. A simple user's manual was created for the Gcts Servo-Controlled Direct Shear Machine, a demonstration was given to the CE 215 (Fundamentals of Geotechnical Engineering) class, and strength parameters from the testing of the Collinsville Silt were obtained to aid the graduate students.

Pneumatic Direct Shear Machine

The pneumatic machine was used to test a well-graded sand at loose and dense compactions to see what would happen. Also a user's manual was completed for the Pneumatic Direct Shear Machine. Doing work on this machine helped prepare for the new hydraulic machine that most of the research time was spent on. The results of this portion of the research can be found in Appendix D and E.

The same stress of 100 kPa was tested on the well-graded sand at loose conditions for the pneumatic and hydraulic machines. This was done to see if the results were comparable to each other. The results were very close to each other. The hydraulic machine had a peak stress of 87.84 kPa, while the pneumatic machine had a peak stress of 87.11 kPa. These are very close numbers. When looking at the plots of shear stress vs. shear displacement, the same shape is noted on both. Both machines peaked out around a displacement of 1.5 mm and went to a residual stress around 80 kPa. This is good that both machines are reading fairly close to the same numbers. The only difference is that the hydraulic machine is constantly reading data points; therefore it had a lot more points on the plot.

The plots are shown below in figures 1 and 2:

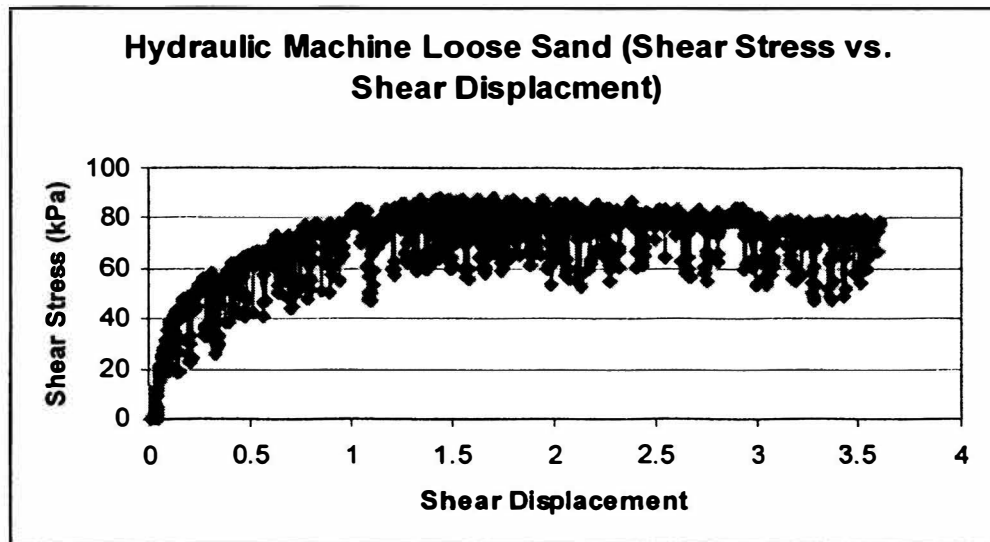


Figure 1 – Hydraulic Machine Loose Sand

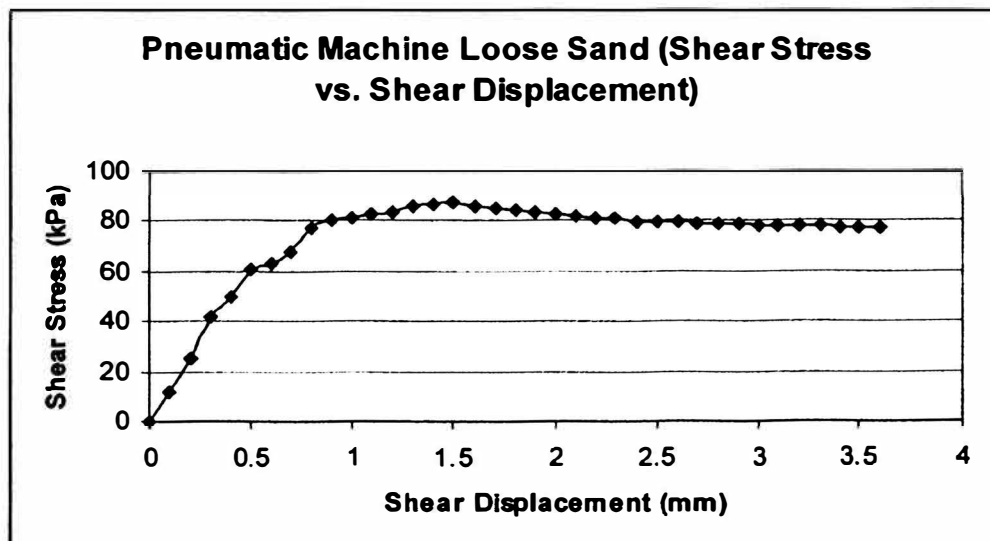


Figure 2 – Pneumatic Machine Loose Sand

GCTS Servo-Controlled Simple User's Manual

In preparing the user's manual a lot of time was put in to learn how the software and hardware worked. The software was worked on first. After a few weeks of learning how the software worked, program was went through step-by-step and screen shots were captured. The manual goes through a step in the software then displays a screen shot to help. After the software was learned, the actual physical parts of the machine were looked at. The machine had to be figured out and how it worked. After learning how it all went together, the hardware part of the user's manual was created. This part consisted of digital photographs to aid the description of the step. The result of this work can be in Appendix C - GCTS Servo-Controlled Direct Shear Test User's Manual.

Demonstration to the CE 215 (Fundamentals of Geotechnical Engineering) class

On November 15, 2004 I gave a demonstration to the CE 215 class. There were a total of four groups which received the demonstration. The first part of the demonstration was telling them how this machine worked. I went through the major aspects of this machine and how it was hydraulically controlled. I then took a sample of Ottawa Sand 20/30 and showed them how to load it in the machine. I asked for a volunteer to help with the loading, so they would get a little hands on experience with the device. I had my screen on the computer projected, so I could show them how the software worked. I went through how to set up a test and what each button did on the software. I described how different tests could be set up depending on what was wanted. Next, I got the sand sample ready and started a test. I got an active plot of shear stress vs. displacement and projected it on the wall. This way they could actually see what was happening to the sample. As the sample was shearing, I described what was happening. After the test was over, I showed all the results that were obtained and what could be done with them. I then summarized what happened and asked if there were any questions. The demonstration went very well and it seemed that they got a good understanding of how the direct shear test works.

Results of the Collinsville Silt

The void ratio that was calculated for all samples was 0.7344. The unit weight with the desired moisture content of 27% was found to be 21.1 kN/m^3 .

The consolidation tests results showed that all three samples' heights leveled off after 24 hours. Figure 3 below shows a sample consolidation plot:

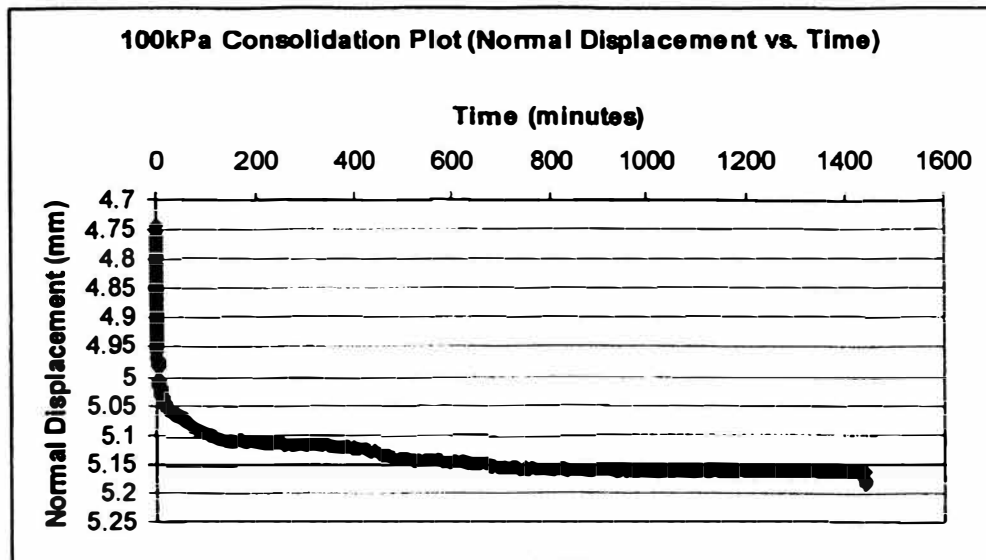


Figure 3 – Sample Consolidation Plot

The consolidation plot shows the normal displacement (mm) vs. time (minutes). It reads the initial displacement, and then it keeps that constant normal stress that was defined in the test. Over time, the air voids and pore water pressure are being squeezed

out of the sample, which decreases the sample height. Within the first couple minutes there was rapid consolidation, as can be seen by the big drop in normal displacement. Eventually the sample leveled off to a constant height, which meant all the voids were mostly squeezed out. Consolidation represents the settlement of the sample. All of the consolidation plots from the Collinsville Silt can be found in Appendix A. Table 2 shows the change in height of the sample:

Test #	Normal Stress (kPa)	Initial Normal Displacement Reading (mm)	Final Normal Displacement Reading (mm)	Total Change in Height (mm)
1	100	4.74259	5.17904	0.43645
2	150	4.27111	4.64205	0.37094
3	200	7.60806	7.93178	0.32372

Table 2 – Consolidation Results

As can be seen the changes in height ranged from 0.32 mm to around 0.44 mm. This means that there may have been more air voids in some of the samples, resulting in larger consolidation.

After the consolidation stage was over the shearing stage of the sample began. Figure 4 below shows a sample Shear Stress plot:

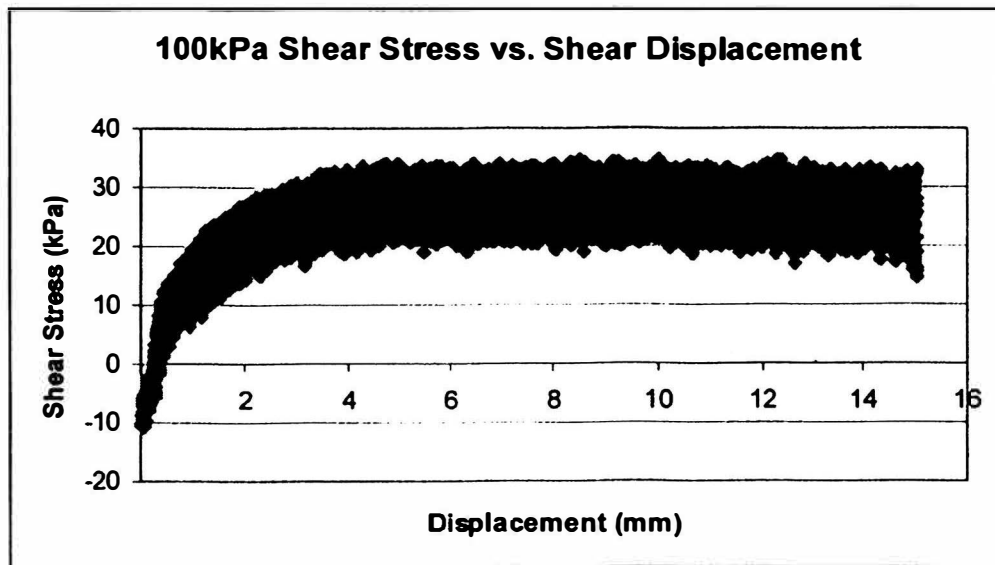


Figure 4 – Shear Stress Plot

The Shear Stress plot shows the peak and residual strengths of the soil sample. The peak strength is the highest point on the curve. The residual strength is where the curve drops and levels off. The residual strength usually occurs at a much larger shear strain. This particular curve shows a peak strength around 5 mm and it then drops from there to a residual strength. There is not a real definite peak stress on the plot. Most

plots show an obvious peak stress and then a residual stress from there. All the Shear Stress Plots from the Collinsville Silt tests can be found in Appendix B.

After running all shearing tests a Mohr-Coulomb Failure Line could be drawn. The Mohr-Coulomb Failure Line will allow engineers to project the test data back into the analyses of existing field conditions. To get the Mohr-Coulomb Failure Line, the peak stresses had to be found from each test. These stresses were found from the shearing stage of the test run. These stresses are located in Table 3 below.

Test #	Normal Stress (kPa)	Maximum Shear Stress (kPa)
1	100	34.81
2	150	49.4364
3	200	71.4221

Table 3 – Maximum Shear Stresses

The maximum shear stresses were then plotted up on the exact same scale as the normal stresses to create a Mohr-Coulomb Failure Line. This will give the strength parameters. A best fit line was drawn between the points. This line represents a line connecting the tops of all the Mohr circles for this soil (the highest shear strengths of all possible loading conditions). The Mohr-Coulomb Failure Line for total stresses can be found below:

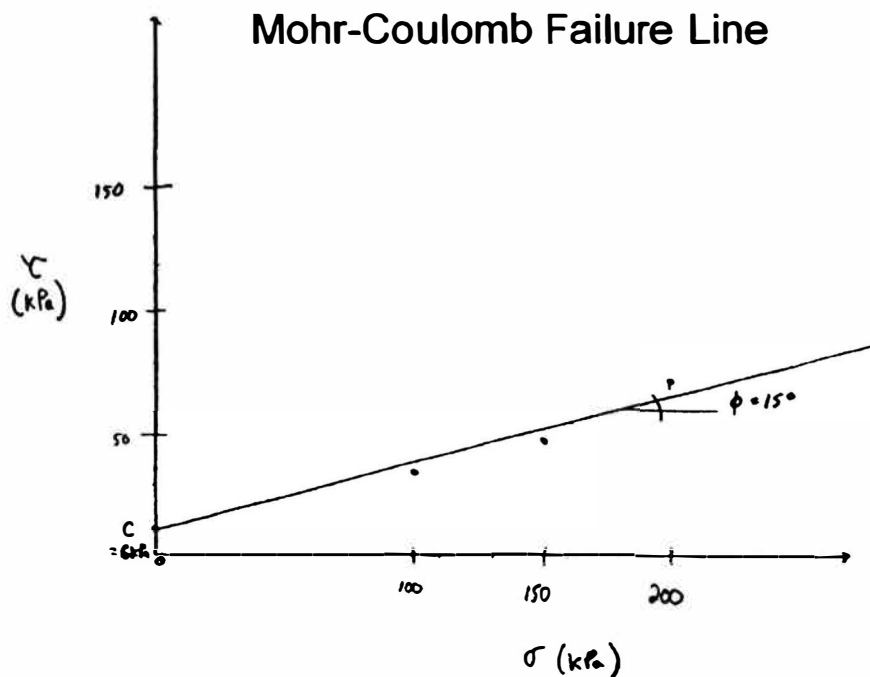


Figure 3 – Mohr Coulomb Failure Line

The failure plane was parallel to the direction of movement, so it makes sense that the peak stress would be at 90 degrees in the Mohr's circle, according to the laws of Mohr's circle. Therefore, these peaks are plotted and a best fit line drawn. The equation of that line is:

$$\tau = c + \sigma \tan (\Phi)$$

From the equation of the best fit line, c and Φ can be determined. The results of c and Φ can be found in the Table 4 below:

c	Φ
6 kPa	15 degrees

Table 4 – Strength Parameters

All of the results were given to the graduate students to aid in their research.

Conclusions

The research started off by looking at the background information of Direct Shear Tests. This showed how significant Direct Shear Tests are to Geotechnical Engineering. The historical development and how the direct shear tests came to be today were learned about. Next, work was done with the pneumatic Direct Shear Machine and showed the basics of how a direct shear machine works. Tests were done on that machine and a user's manual was created for it. Working on the pneumatic machine helped prepare for the major part of the research; working with the hydraulic Gcts Direct Shear Machine.

The simple user's manual that was created for the Gcts Direct Shear Machine will be very helpful so that others will be able to run the tests. It has all the steps needed to get the basics of the machine down and to run a test. The demonstration that was given was very successful. The students learned how the test is run and got to see exactly what was going on during the test. This gave good practice in giving demonstrations.

The results from the direct shear testing of the Collinsville Silt will be given to the graduate students. This will aid in their research by giving them the strength parameters found and the void ratio and unit weights of the tests. This will help them develop the stress where critical state occurred and the $e - \log p'$ curve.

Much was learned from all of the aspects of the research. This research gave a good understanding of how important research is and what all goes into it. It was a very good experience.

OURE Reflection on the Learning Experience *(written in first person)*

1. Describe your foundational understanding of how research is conducted in your discipline.

I have found out that there is a lot of background information that needs to be looked at before testing can begin. Then the machine that is going to be used for testing needs to be learned to the best of someone's ability. After that the testing begins and every detail has to be noted. The procedure for setting up the samples to be tested is very delicate and requires careful and precise preparation. After the results are obtained the data analysis is an important part of the research. This requires extensive knowledge of what happened during the testing and what results are needed to satisfy the objective.

2. How have you expanded your understanding of the informational resources available and how to best use these resources?

I have expanded my understanding of the use of books and specifications. I have read in depth about how the tests were run in books. I used specifications to model my test off of. A good resource that I have found is talking with professors and graduate students who have some experience in that particular area. I've learned a lot about how to conduct research from them.

3. Describe the knowledge you have gained regarding the fundamentals of experimental design.

I have gained a good understanding of how to design experiments. I realize now how much work goes into designing an experiment. It takes a great deal of time and effort to go through every aspect of research. From learning the equipment to be used, to setting up the test, to getting the results, every one of these is very important.

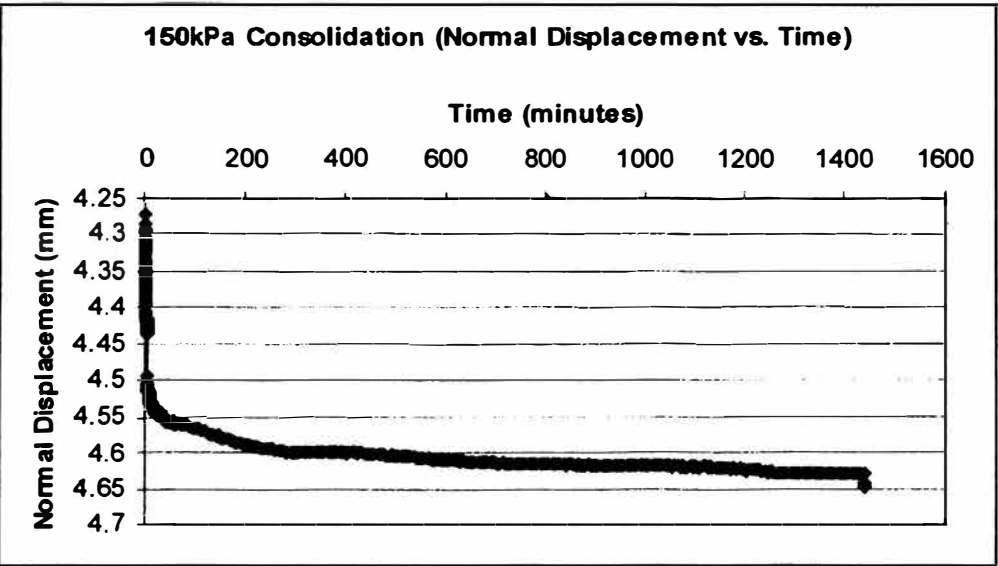
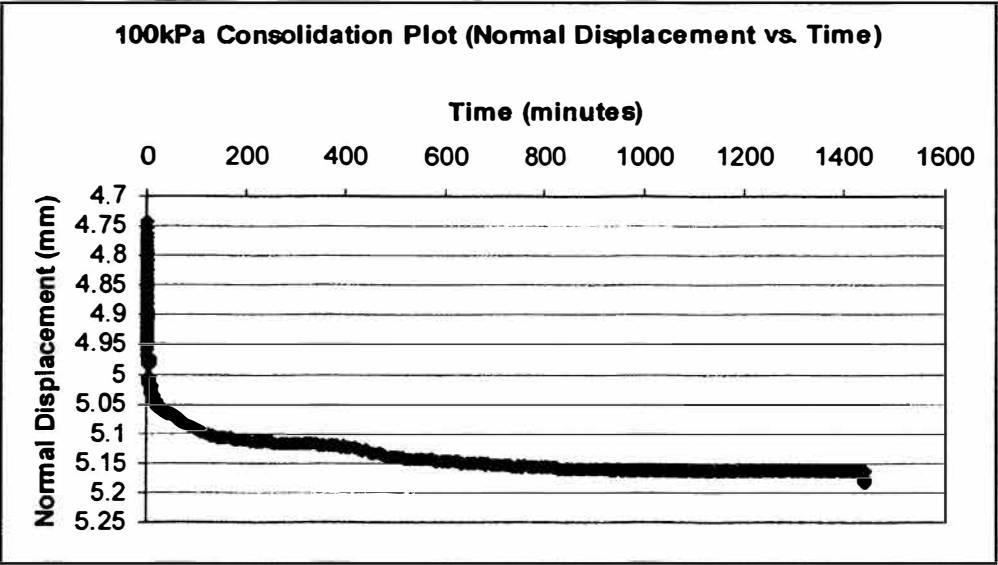
4. Describe how you have learned to interpret the results of your research project.

I have learned a great deal of how to interpret my results. I found out what results I would be getting from the machine I was using. I then made the graphs necessary to get the points I needed off them. I then ultimately made a graph that would give the strength parameters that I needed. I've learned how there are different results of between soils. I've used different books to help me interpret the results I was seeing, as well as professors. I learned a great deal about the results of this research.

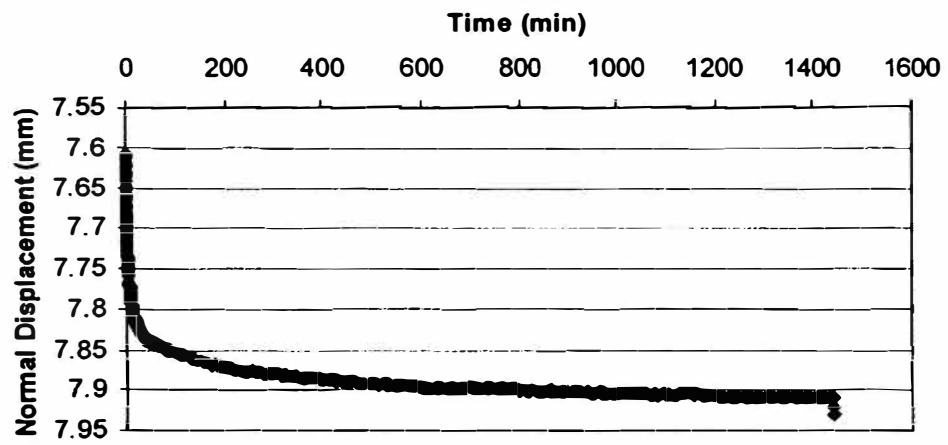
References

- ASTM D 3080 Standard Test Method for Direct Shear Test of Soils Under Consolidated Drained Conditions
- Coduto, Donald P. (1999), *Geotechnical Engineering Principles and Practices*, Prentice Hall, Upper Saddle River, NJ, pp
- Head, K.H., (1994), *Manual of Soil Laboratory Testing*, Vol. 2 Second edition, Pentech Press Limited, London, pp.
- Kezdi, Arpad (1980), *Handbook of Soil Mechanics*, Vol. 2 Soil Testing, Elsevier Scientific Publishing Company, Amsterdam, The Netherlands
- Mandal, J.H. and Divshikar D.G. (1995), *Soil Testing in Civil Engineering*, A.A. Balkema Publishers, Brookfield, VT, pp

APPENDIX A – COLLINSVILLE SILT CONSOLIDATION PLOTS

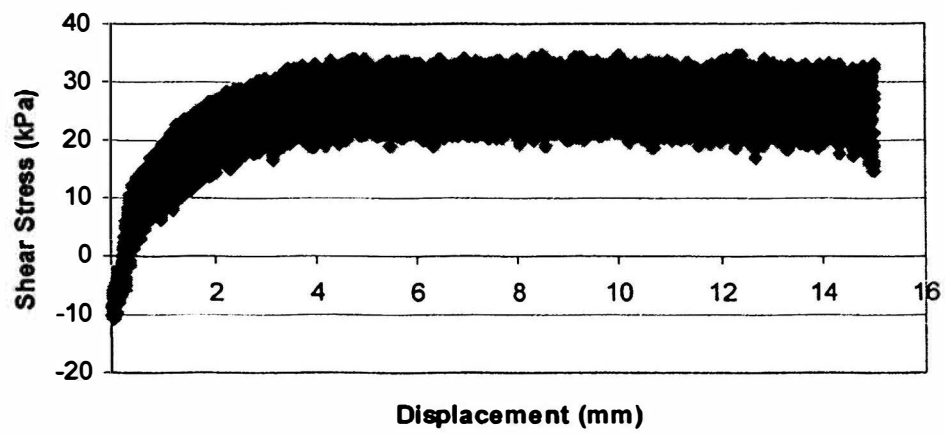


200kPa Consolidation (Normal Displacement vs. Time)

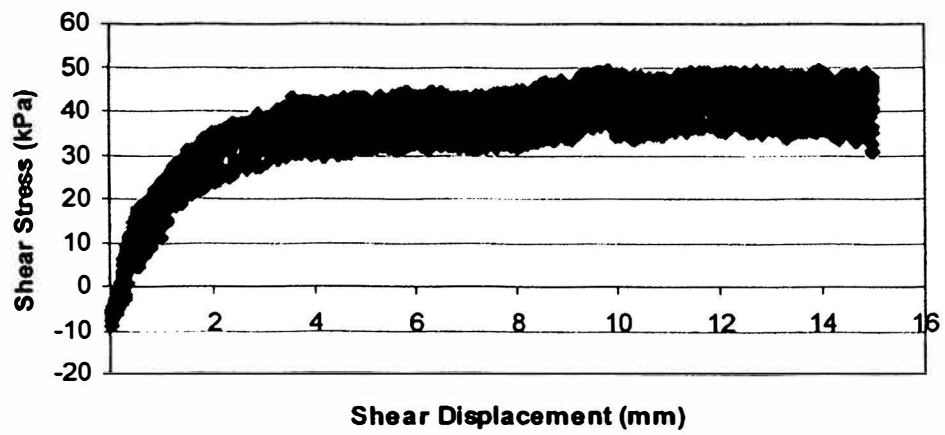


APPENDIX B – COLLINSVILLE SILT SHEAR STRESS PLOTS

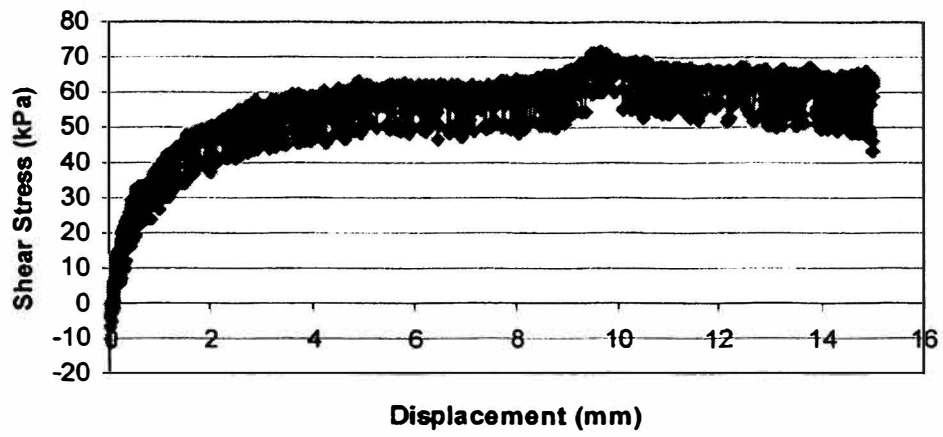
100kPa Shear Stress vs. Shear Displacement



150kPa Shear Stress vs. Shear Displacement



200kPa Shear Stress vs. Shear Displacement



**APPENDIX C – GCTS SERVO-CONTROLLED
DIRECT SHEAR TEST USER'S MANUAL**

GCTS Servo-Controlled Direct Shear Test User's Manual **Procedure**

Machine Set-up

1. Wheel the Direct Shear Testing Machine next to the computer to be used. Plug the machine into the wall outlet and then plug the serial communication cord into the back of the computer. (See Figures 1 and 2)

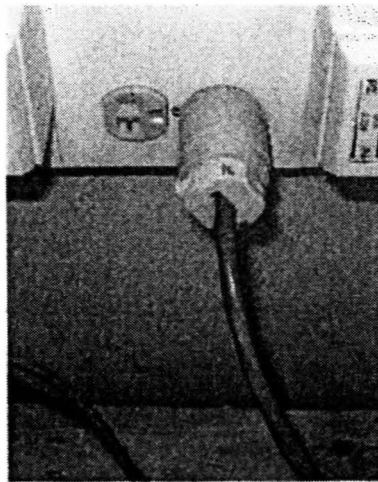


Figure 1 – Yellow Plug from Direct Shear Machine



Figure 2 – Serial Communication Cord plugged into back of computer

2. Log onto the computer as: username – geotech.
3. Flip Switch to turn on Direct Shear Machine. There should be green lights next to control, 24V power, and 5V power. (See Figure 3)

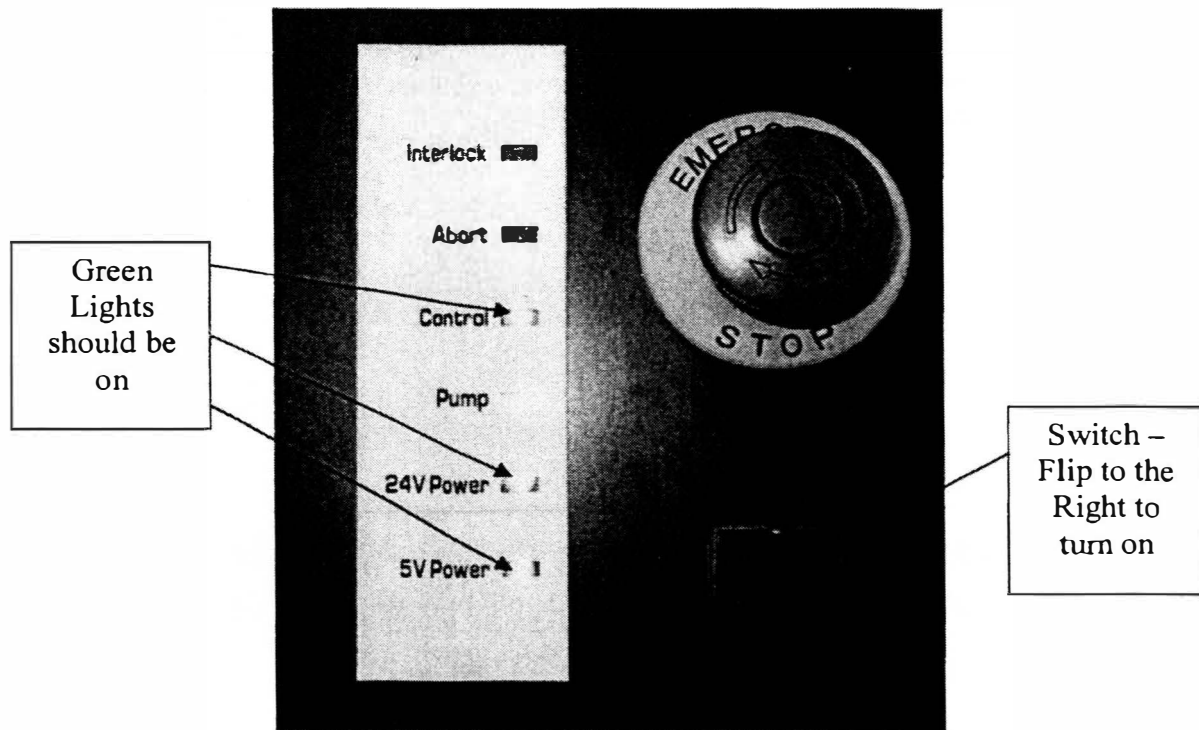
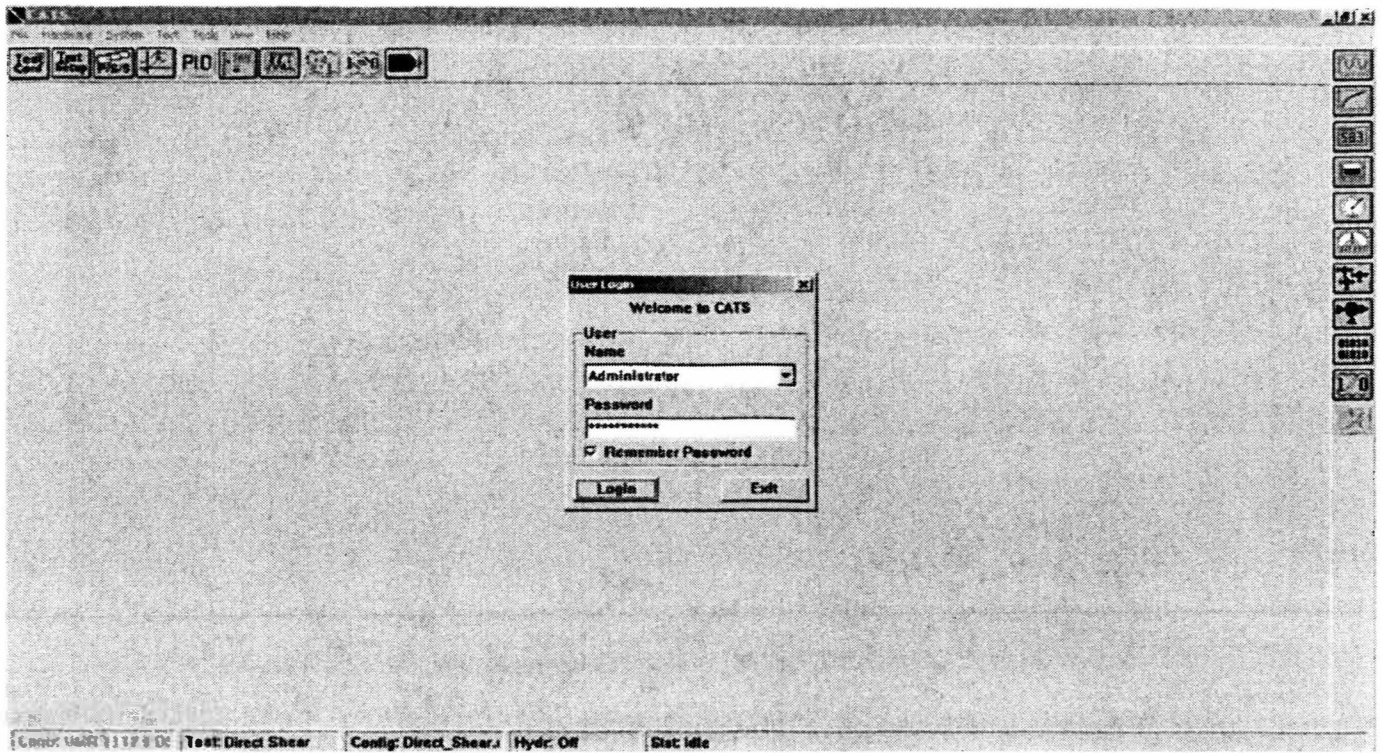


Figure 3 – Switch on Direct Shear Machine

C.A.T.S. Program Setup for the Direct Shear Test

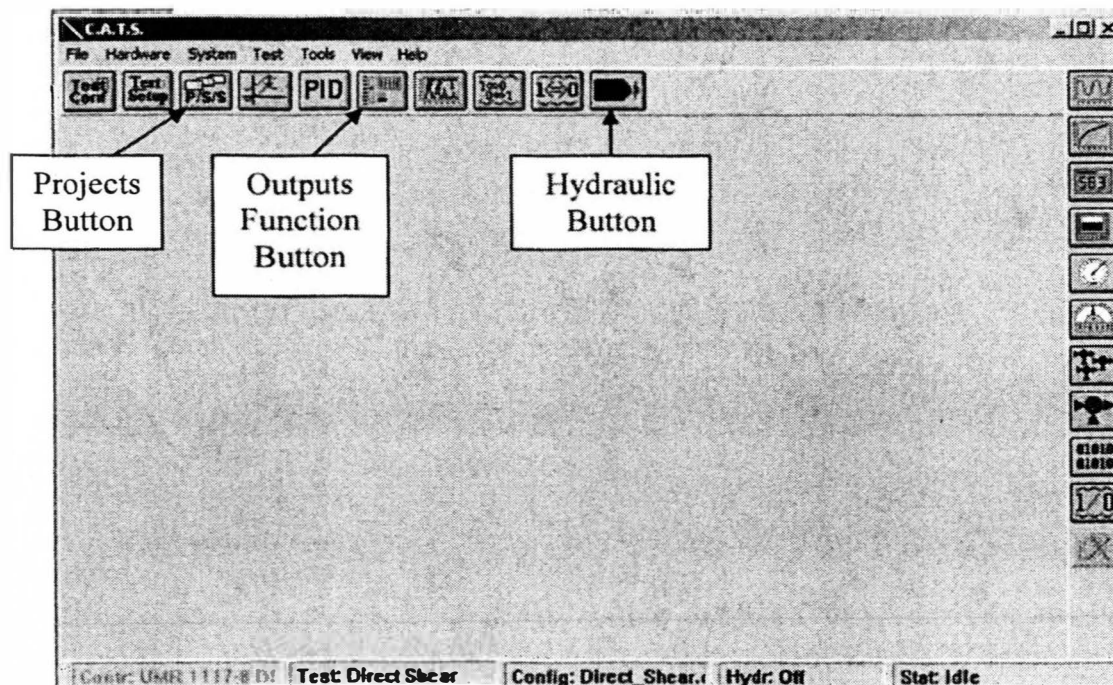
4. Load up the C.A.T.S. Software. Go to start – programs – C.A.T.S. – C.A.T.S. The C.A.T.S. software should start up.

5. The screen should look like this:



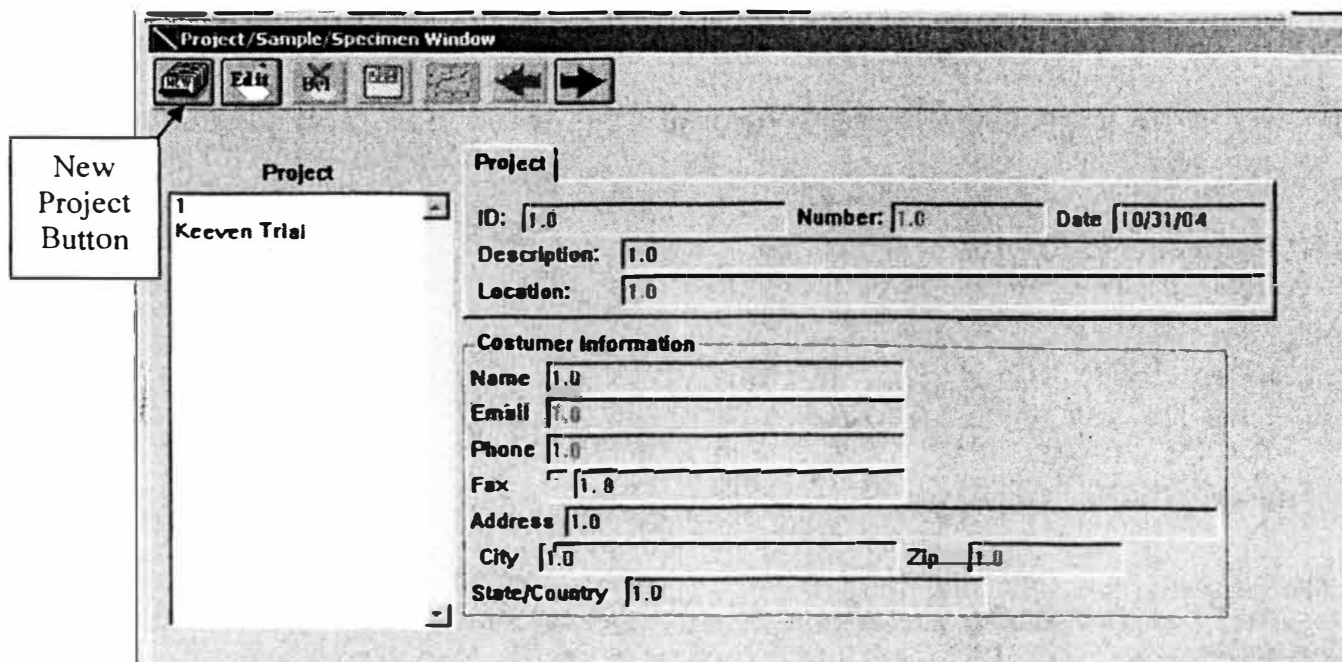
Click Login in the User Login Box. At the bottom of the screen it should say Test: Direct Shear, Config: Direct_Shear., Hydr: Off, and Stat: Idle.

6. At the top are the options to control the Direct Shear Testing machine.



7. A test needs to be set up in order for it to be run.

Click on the Projects button at the top (third from the left). This will open another window. This window gives the option to start a new project or to edit a project. To start a new project, click on the new project button.



8. The new project window is opened. Enter an ID for the new project and any other information that is desired. Then click OK.

The screenshot shows the 'Project/Sample/Specimen Window' with the 'Project' tab selected. On the left, a list box contains '1 Keeven Trial'. The main form has the following fields:

- Project**
 - ID: 3
 - Number: 3
 - Date: 10/31/04
 - Description: 1.0
 - Location: 1.0
- Customer Information**
 - Name: 1.0
 - Email: 1.0
 - Phone: 1.0
 - Fax: 1.0
 - Address: 1.0
 - City: 1.0
 - Zip: 1.0
 - State/Country: 1.0

At the bottom are 'OK' and 'Cancel' buttons.

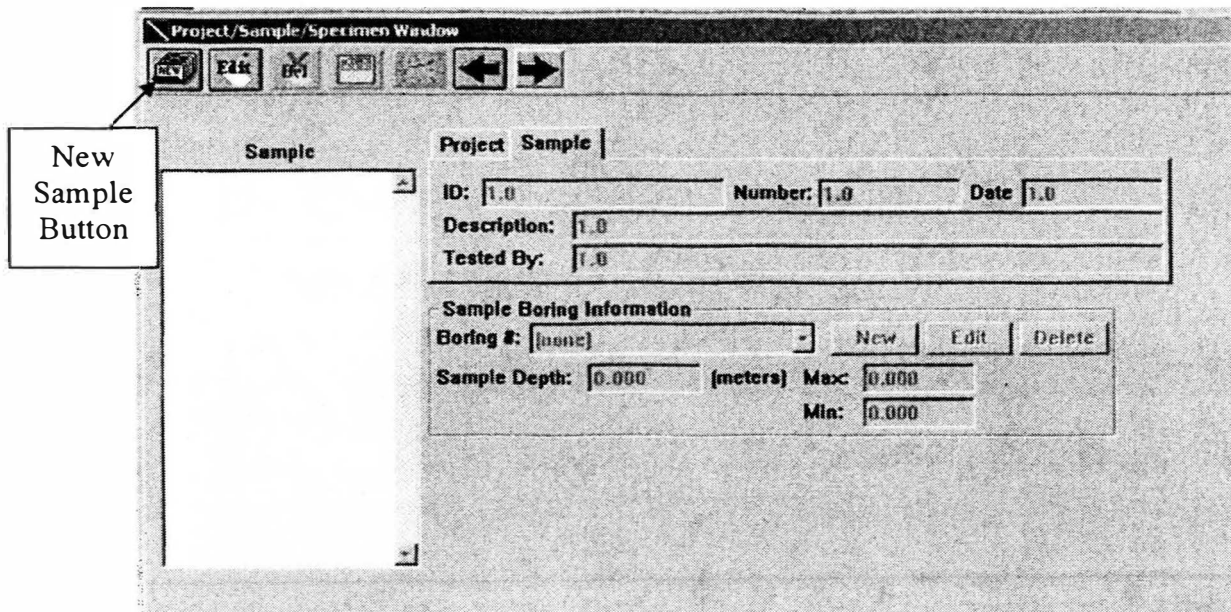
9. For this example, the ID entered was 3. After clicking OK, make sure that the Project desired is highlighted in the left and click on the blue arrow to go to Project Samples.

This screenshot is similar to the previous one, but with ID 3 highlighted in the left list box. A callout box points to the blue arrow button in the toolbar with the text: 'Blue Arrow – Used to go to next step'.

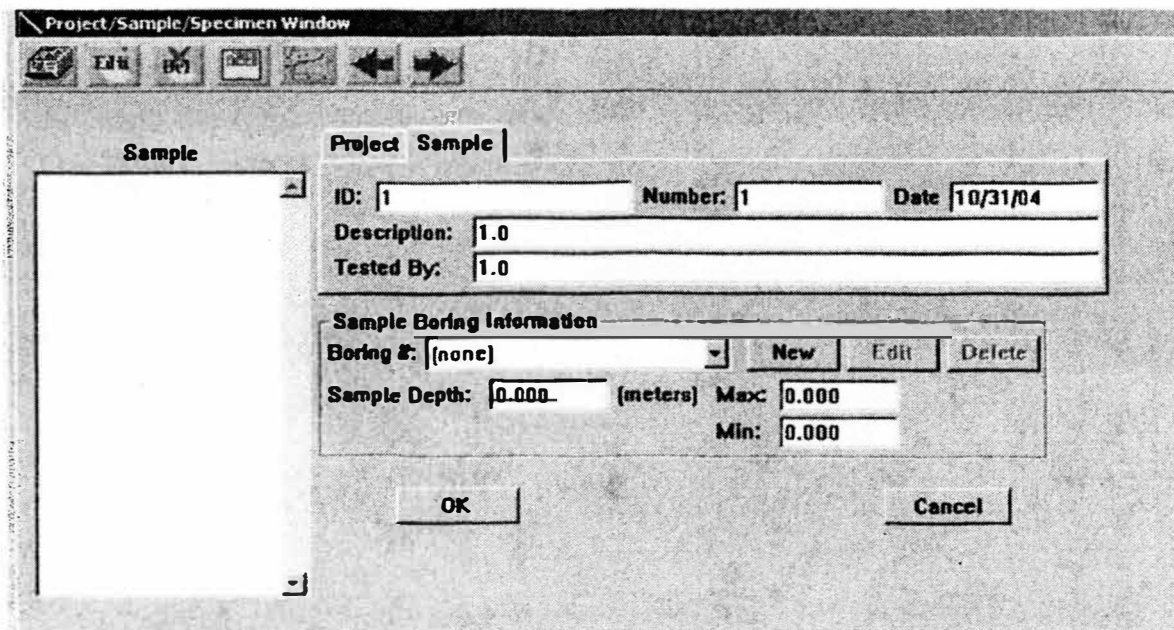
The form fields are the same as in the previous screenshot:

- Project**
 - ID: 3
 - Number: 3
 - Date: 10/31/04
 - Description: 1.0
 - Location: 1.0
- Customer Information**
 - Name: 1.0
 - Email: 1.0
 - Phone: 1.0
 - Fax: 1.0
 - Address: 1.0
 - City: 1.0
 - Zip: 1.0
 - State/Country: 1.0

10. A new tab appears called Sample. The next step is to define a project sample. Click on new sample (top left).



11. Enter an ID for the sample, and any other information needed, then click OK when done.



12. Now make sure that Sample is highlighted in the left hand window and click on the blue arrow to go to the project specimen. The next tab that will appear is the Specimen tab. It looks like the screen shot below. Now click on new specimen at the top left of this window.

The screenshot shows the 'Project/Sample/Specimen Window' with the 'Specimen' tab selected. A callout box labeled 'New Specimen Button' points to the first icon in the top toolbar. The window contains the following fields:

Project Sample Specimen		
ID: 1.0	Number: 1.0	Date: 1.0
Description: 1.0		
Container ID: 1.0		

Information Results	
Direct Shear Test Specimen Information	
Type: <input checked="" type="radio"/> Cylindrical <input type="radio"/> Square <input type="radio"/> Rectangular <input type="radio"/> Other	Height: 0 (mm) Diameter: 0 (mm) Shear Surface Area: Circular

13. Enter the ID and other information needed. The type will be cylindrical and the diameter of the small ring is 63.50 mm (2.5 inches) and the diameter of the large ring is 101.6 mm (4 inches). The height will depend on the sample used (usually about 25 mm). After everything is entered, click OK.

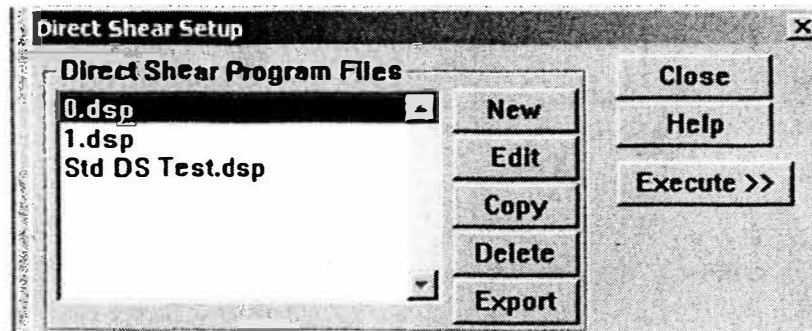
The screenshot shows the 'Project/Sample/Specimen Window' with the 'Specimen' tab selected. The following data has been entered:

Project Sample Specimen		
ID: 1	Number: 1	Date: 10/31/04
Description: 0		
Container ID: 0		

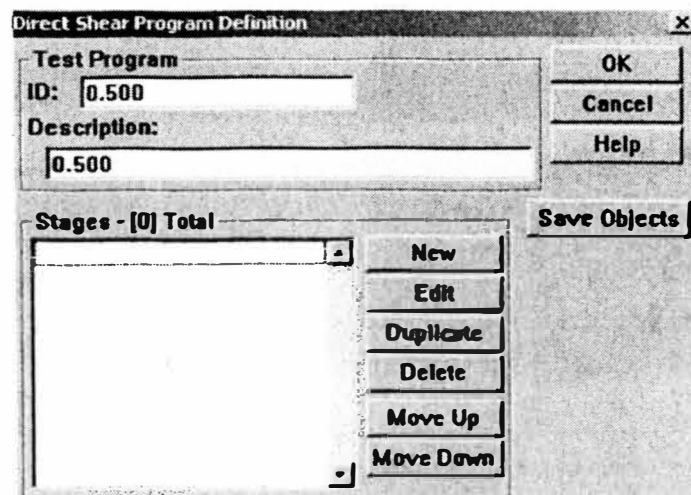
Information Results	
Direct Shear Test Specimen Information	
Type: <input checked="" type="radio"/> Cylindrical <input type="radio"/> Square <input type="radio"/> Rectangular <input type="radio"/> Other	Height: 25.00 (mm) Diameter: 63.50 (mm) Shear Surface Area: Rectangular
Loading Direction: <input checked="" type="radio"/> Long Axis <input type="radio"/> Short Axis	

Buttons: OK, Cancel

14. A new window pops up called Direct Shear Set up. This will give a choice to run any of the tests that have been previously established or to create a new test. If a previous test is established highlight the one desired and click Execute >> to run the test, or Edit to modify the test. To create a new test, click New (following steps are for New test).



15. A new window pops up called Direct Shear Program Definition. Enter an ID for it. This program allows different stages to be programmed (consolidation, shear loading, or universal). Click the New button. A new window pops up for the choice of either consolidation, shear loading, or universal (not shown). Typically a consolidation load is applied first then the shear loading begins. Make sure the bullet is highlighted next to consolidation and click OK.



16. This is what the Consolidation window looks like (below). Enter in the Normal Stress needed, how long to apply consolidation stress, and the duration for this first stage of the test. Next, click on the data acquisition tab.

The screenshot shows the 'Consolidation' tab of the 'Direct Shear Program Stage [1]: Consolidation' window. The 'ID' field is set to 'Normal Load'. The 'Consolidation Normal Stress' is 0 kPa. The 'Time to Apply Consolidation Stress' is 15.00 sec. The 'Duration Time for Consolidation Stage' is 0.00 Minute(s). Under 'Shear Deformation for Area Correction', 'Shear Actuator Defm.' is selected.

Direct Shear Program Stage [1]: Consolidation

Consolidation

ID: Normal Load

Consolidation | Data Acquisition

Consolidation Normal Stress: 0 (kPa)

Time to Apply Consolidation Stress: 15.00 (sec)

Duration Time for Consolidation Stage: 0.00 Minute(s)

Shear Deformation for Area Correction:

- ☐ Shear Box Deformation
- ☒ Shear Actuator Defm.
- ☐ None - No area correction

OK

Cancel

Data Acquisition tab:

Uncheck Level crossing and just leave timed increments at 0.5 sec.

The screenshot shows the 'Data Acquisition' tab of the 'Direct Shear Program Stage [1]: Consolidation' window. The 'ID' field is 'Normal Load'. The 'Timed Increments' are 0.500 sec. 'Level Crossing' is checked, and 'Peak/Valley' is unchecked. The 'Master Input' is 'Normal Displacement'. The 'Sensitivity' is 0.000 pfs. Under 'Shear Deformation for Area Correction', 'Shear Actuator Defm.' is selected.

Direct Shear Program Stage [1]: Consolidation

Consolidation

ID: Normal Load

Consolidation | Data Acquisition

☒ Timed Increments: 0.500 (sec)

☒ Level Crossing

☐ Peak/Valley

Master Input: Normal Displacement

Sensitivity: 0.000 pfs

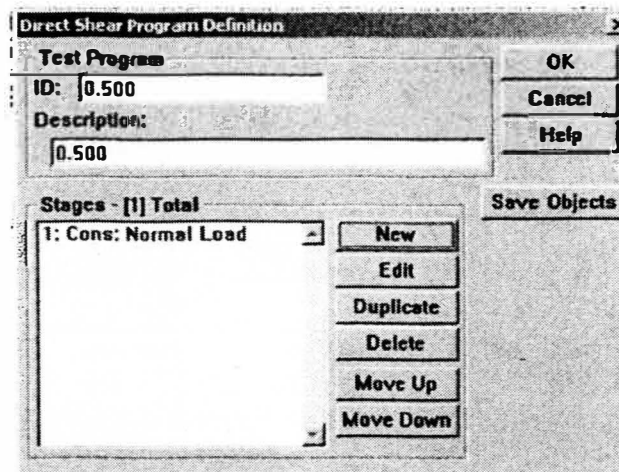
Shear Deformation for Area Correction:

- ☐ Shear Box Deformation
- ☒ Shear Actuator Defm.
- ☐ None - No area correction

OK

Cancel

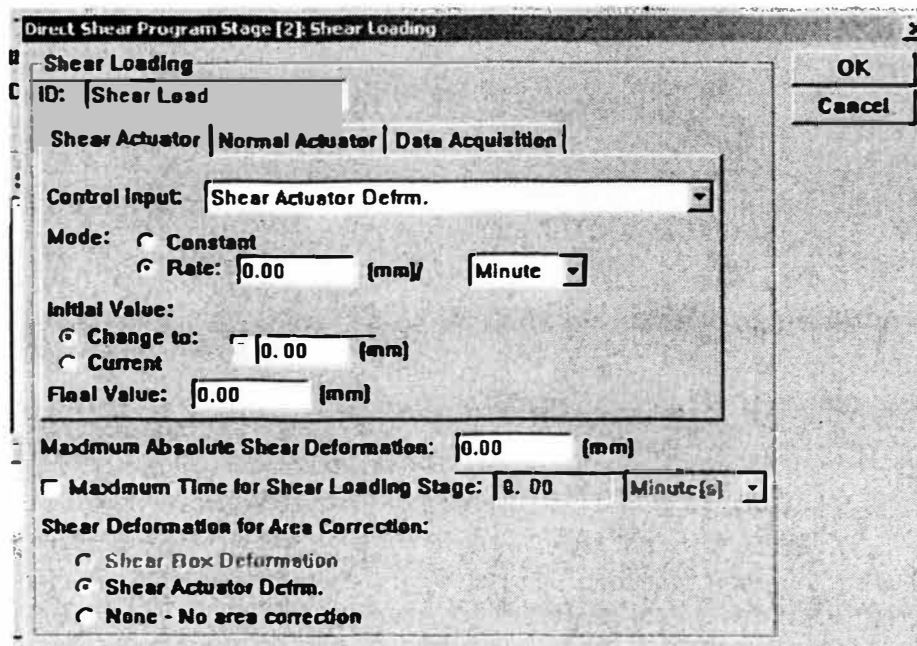
17. After the consolidation load has been set up the window of Direct Shear Program Definition should have the first stage listed like this:



18. To make the shear loading stage click on New, then click the bullet next to Shear Loading, then OK.

Shear loading windows:

Enter in the desired information for the test to be run. Click on rate and enter the rate at which shearing will take place (i.e. 1.00 mm/minute). Under Initial Value, click on current. Under Final Value, enter the maximum amount of deformation wanted (i.e. 10 mm – will shear until it reaches 10mm, can't be more than 18mm). Next click on the Normal Actuator tab.



Normal Actuator tab:

Enter in the control input that should be constant throughout the test. There are a bunch of different choices (normal load, normal stress, shear stress, shear load, etc.) If Normal Stress is picked, then the mode should be constant and the constant value should be current. It should say the number that was previously entered in the Shear Actuator tab next to the Maximum Absolute Shear Deformation (i.e. 10 mm). Next click on the Data Acquisition tab.

The screenshot shows a software window titled "Direct Shear Program Stage [2]: Shear Loading". It has three tabs: "Shear Actuator", "Normal Actuator" (which is selected), and "Data Acquisition".

Inside the "Normal Actuator" tab:

- There is a label "ID:" followed by a text box containing "Shear Load".
- Below the tabs, there is a "Control Input:" label followed by a dropdown menu showing "S - Normal Stress".
- Under "Mode:", there are two radio buttons: "Constant" (which is selected) and "Rate:". The "Rate:" option has a text box with "0.00", a unit label "(kPa)", and a dropdown menu showing "Minute".
- Under "Constant Value:", there are two radio buttons: "Change to:" and "Current" (which is selected).
- Below these, there is a label "Maximum Absolute Shear Deformation:" followed by a text box with "0.00" and a unit label "(mm)".
- Below that, there is a checkbox labeled "Maximum Time for Shear Loading Stage:" followed by a text box with "0.00" and a unit label "Minute(s)".
- At the bottom, there is a label "Shear Deformation for Area Correction:" followed by three radio buttons: "Shear Box Deformation", "Shear Actuator Defrm." (which is selected), and "None - No area correction".

On the right side of the window, there are "OK" and "Cancel" buttons.

Data Acquisition tab:

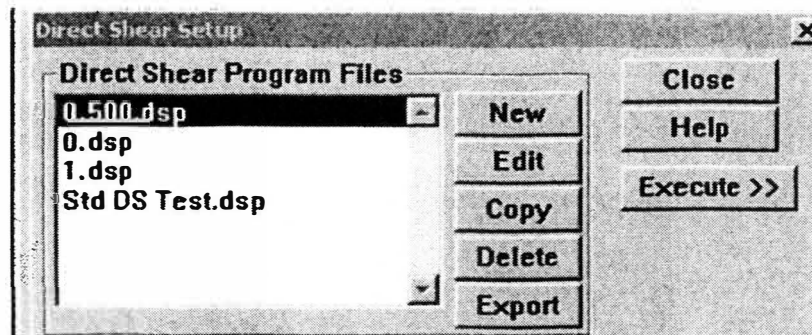
Uncheck Level Crossing and Peak/Valley. Leave Timed Increments checked and enter in the desired time (i.e. 2 sec). It should say the number that was previously entered in the Shear Actuator tab next to the Maximum Absolute Shear Deformation (i.e. 10 mm). After everything is entered click OK.

The screenshot shows the 'Direct Shear Program Stage [2]: Shear Loading' dialog box. It has three tabs: 'Shear Actuator', 'Normal Actuator', and 'Data Acquisition'. The 'Data Acquisition' tab is selected. The 'ID' field contains 'Shear Load'. The 'Timed Increments' checkbox is checked with a value of '2.000 (sec)'. The 'Level Crossing' and 'Peak/Valley' checkboxes are unchecked. The 'Master Input' dropdown is set to 'Shear Displacement'. The 'Sensitivity' is '0.100 pfs'. The 'Maximum Absolute Shear Deformation' is '0.00 (mm)'. The 'Maximum Time for Shear Loading Stage' is '0.00 Minute[s]'. Under 'Shear Deformation for Area Correction', the 'Shear Actuator Defrm.' radio button is selected. 'OK' and 'Cancel' buttons are on the right.

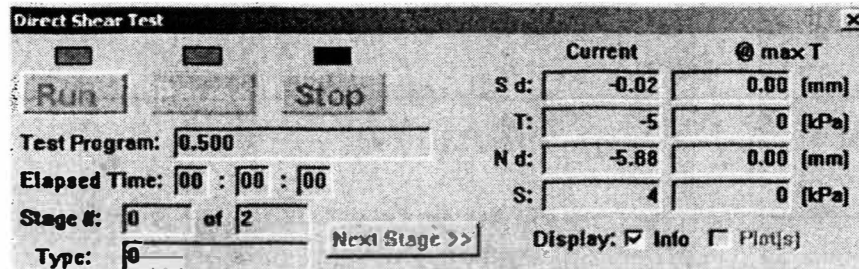
19. The Direct Shear Program Definition should have both stages that were determined on it. Click OK, if everything is correct.

The screenshot shows the 'Direct Shear Program Definition' dialog box. The 'Test Program' ID is '0.500' and the 'Description' is '0.500'. The 'Stages - [2] Total' list contains: '1: Cons: Normal Load' and '2: Shear: Shear Load'. To the right of the list are buttons: 'New', 'Edit', 'Duplicate', 'Delete', 'Move Up', and 'Move Down'. A 'Save Objects' button is at the bottom right. 'OK', 'Cancel', and 'Help' buttons are on the right side of the dialog.

20. Highlight which test to run and click Execute >>.



21. All those other windows will go away and a new window will appear. This will control the test. Before the test starts, the normal and shear actuator have to been in the correct place.



Preparing the Sample in the shear box

22. After the test has been set up the sample that will be tested needs to be prepared. This machine has a plate that slides up and down that allows the sample to be placed in the machine easily. Lift up the plate and while the plate is up, slide the loading yoke to the left. (See Figure 4)

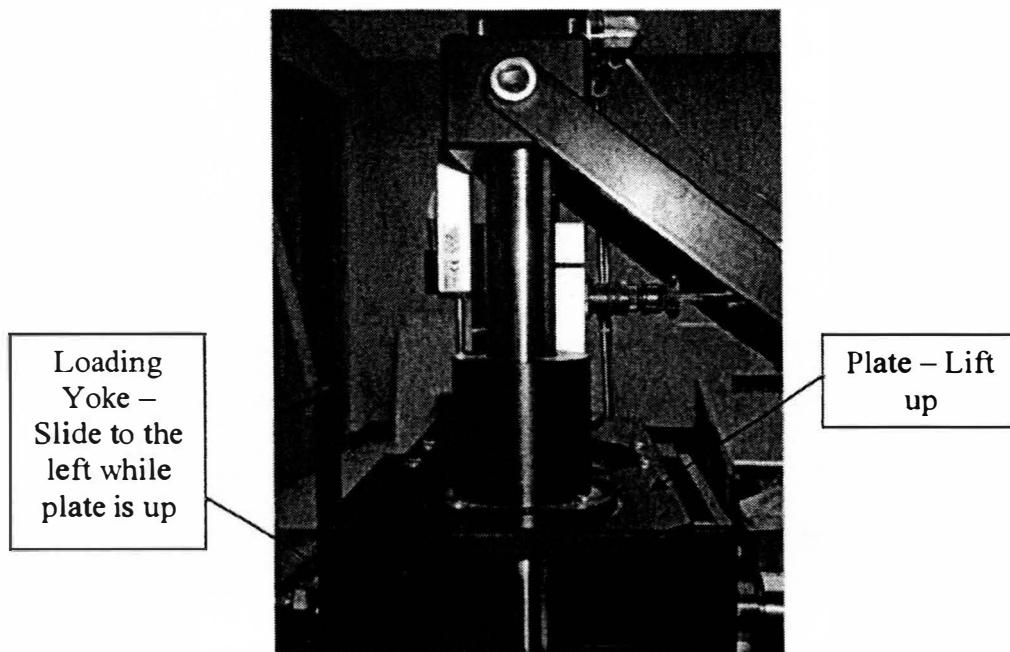


Figure 4 – Direct Shear Test

23. The loading yoke is now easily accessible. (See Figure 5)

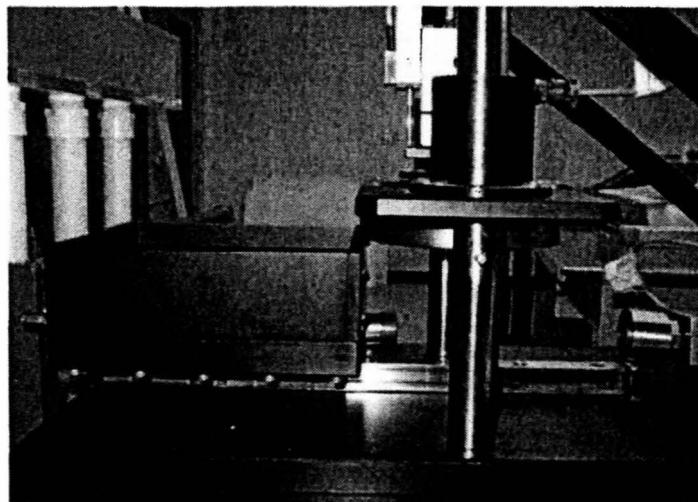


Figure 5 – Loading Yoke

24. The loading yoke is set up to hold a small and large circular ring. The holes shown in Figure 6 are where the rings are screwed down to the loading yoke.

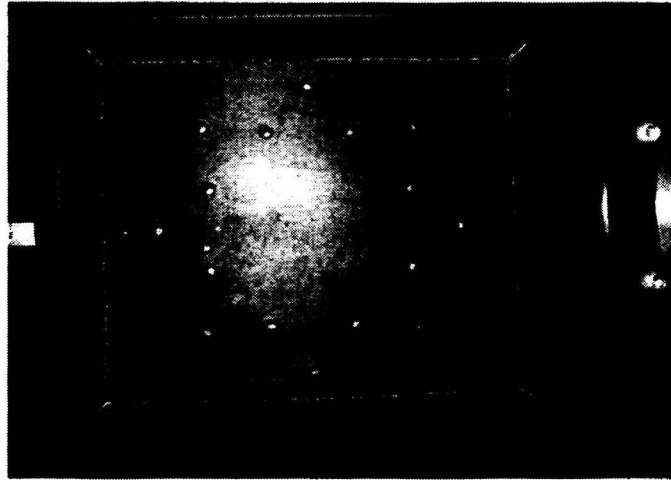


Figure 6 – Top View of Loading Yoke

25. Take a ring desired and make sure the holes are lined up in the ring. Then place the porous stone down at the bottom of the ring. Next, using an allen wrench, screw in tightly all eight screws. Then place the top ring on top. Note: The hole in the middle of the ring is used to pop out the porous stone from the underside. (See Figures 7 and 8)



Figure 7 – Small Ring without Screws

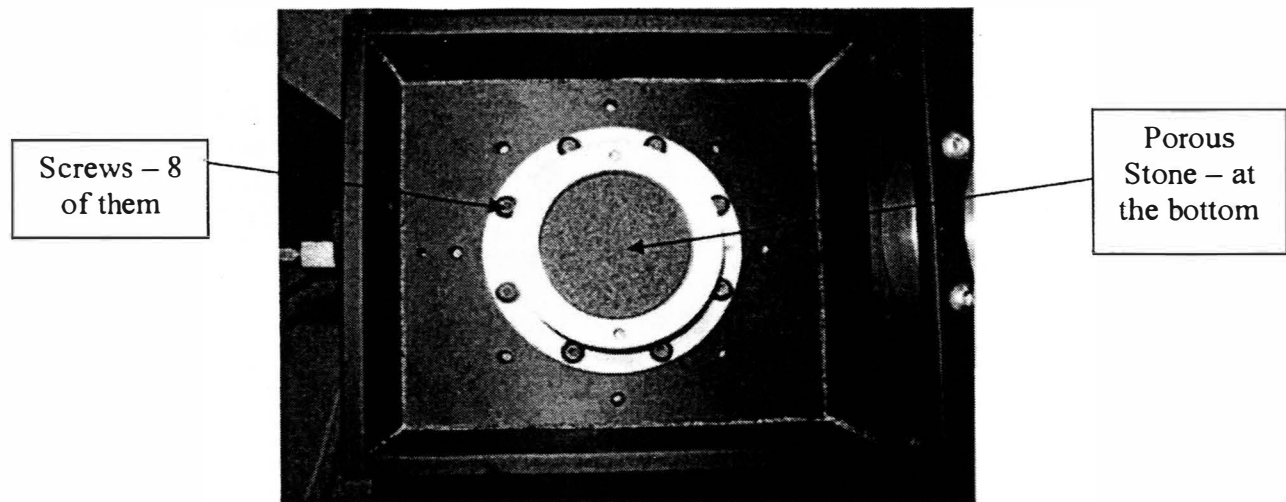


Figure 8 – Small Ring Screwed Down to the Loading Yoke with Porous Stone

26. Next place the two pins in the top ring to hold it in place. Then add the sample to the ring or the sample can be added first then the ring can be screwed in. After the sample is added place the porous stone on top. (See Figures 9 and 10)

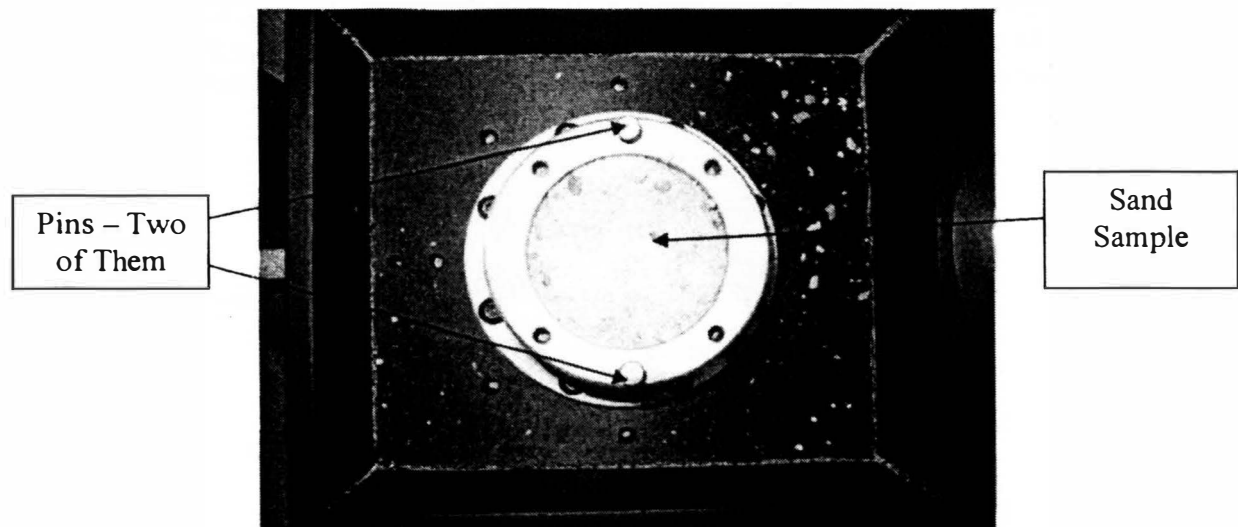


Figure 9 – Small Ring with Pins in Place and Sample Added

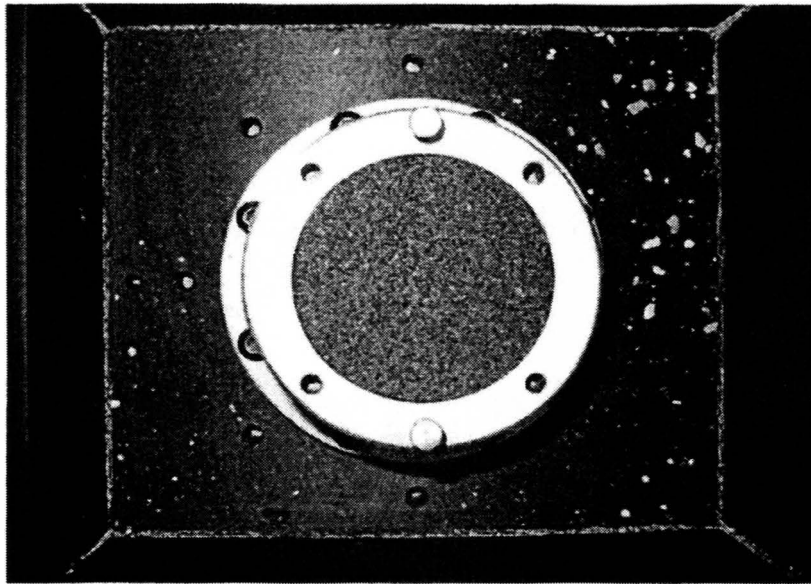


Figure 10 – Porous Stone Added to the Top

27. After the sample is added, pins are in place, and the porous stone is on top lift up the plate and slide the loading yoke back under the plate so that the normal actuator will line up to the sample. (See Figure 11)

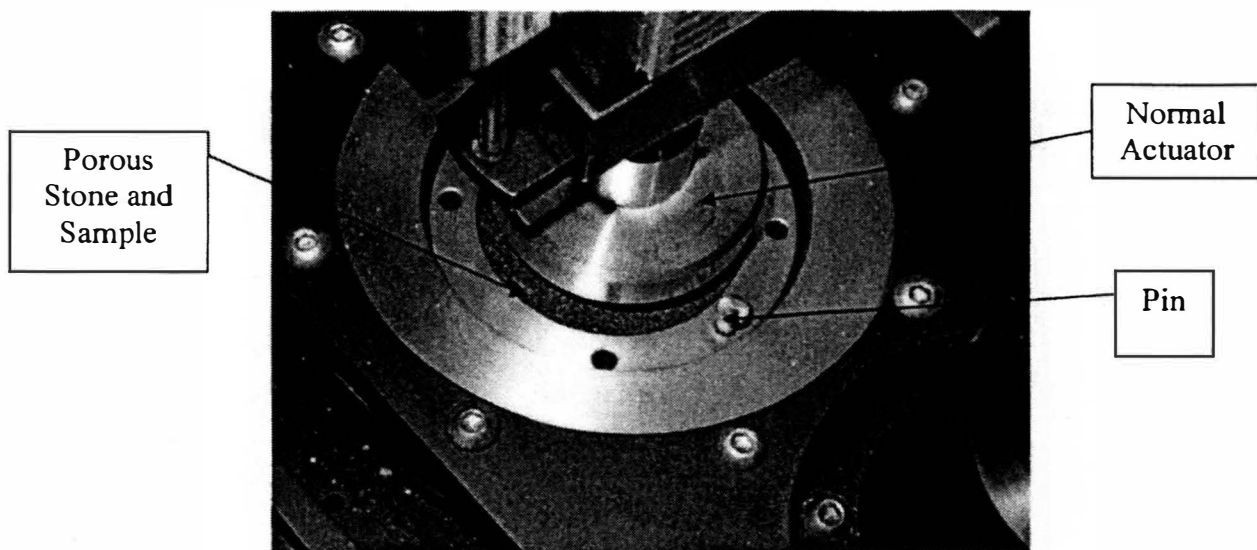


Figure 11 – Loading Yoke Under Normal Actuator

28. Next screw down the coupler on the shear actuator to the loading yoke (to the right of the loading yoke) (See Figure 12)

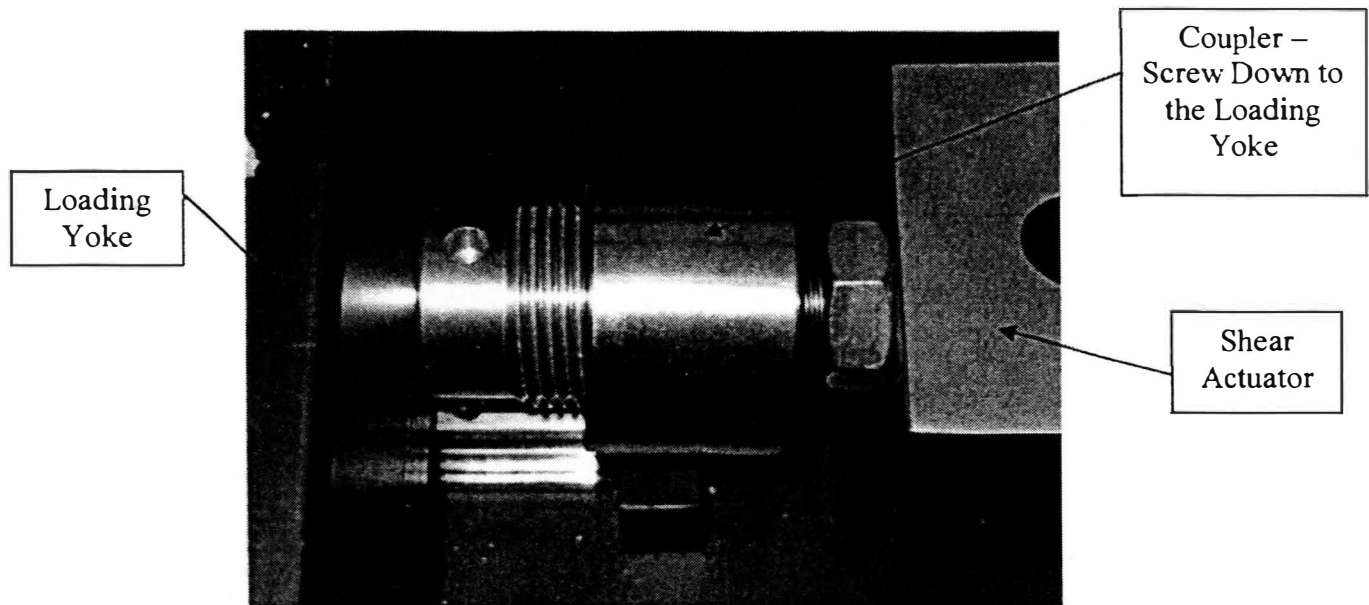


Figure 12 – Coupler Being Attached to the Loading Yoke

29. Finally take the pins out of the ring. And the sample is ready to be tested. (See Figure 13)

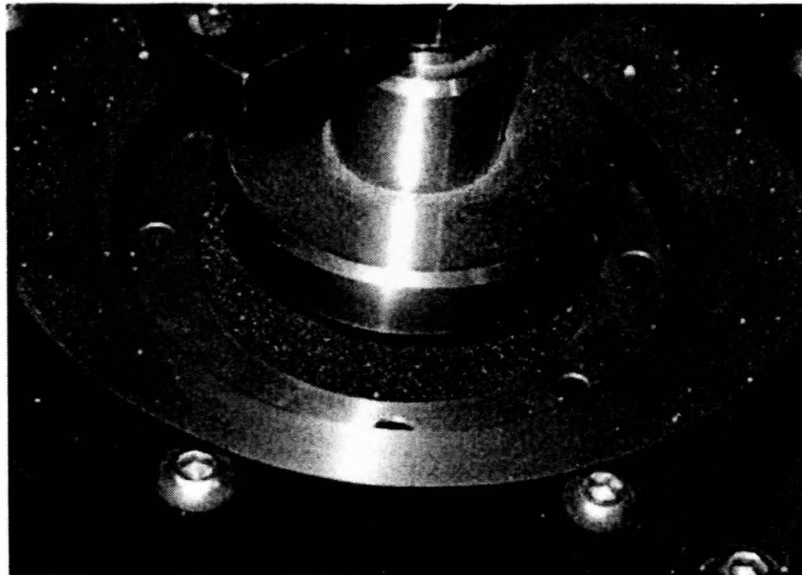
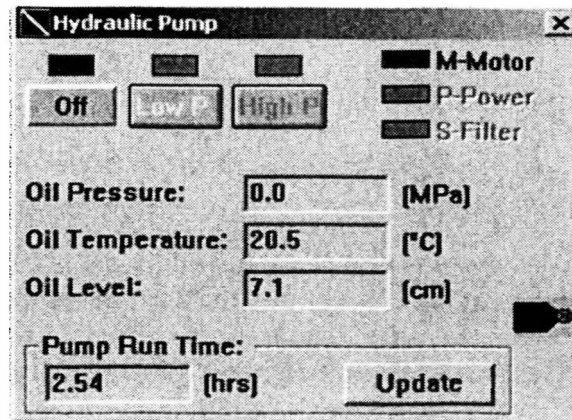


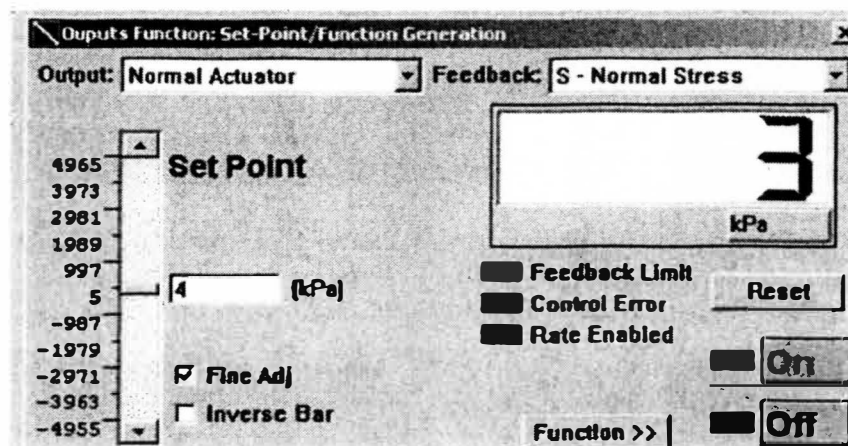
Figure 13 – Small Ring Under Normal Actuator Without Pins

Turning Pumps on and Adjusting Actuators

30. Before the test can be run the pumps have to be turned on. Click on the Hydraulic button (10th from the left at the top). A new window will pop up. To turn on the pumps first click on Low P and then click on High P. (Low P is mainly used to cool down the hydraulic oil, High P is needed to move the actuators and run the test).



31. After the pumps have been turned on, the normal actuator and shear actuator need to be positioned so that the test can be performed. To move the normal actuator and shear actuator click on Outputs Function (6th button from the left at the top). From this option you can move the normal and shear actuator. Under Output is the option for Normal Actuator or Shear Actuator. Under Feedback is the choices for that particular actuator. To move the Normal actuator up and down click on the arrow next to feedback, then scroll down to Normal Displacement. Then click On (green letters, this turns the actuator on). The point to where the Normal actuator will go can be entered or it can be moved by clicking on the arrows. This is also true for the shear actuator.

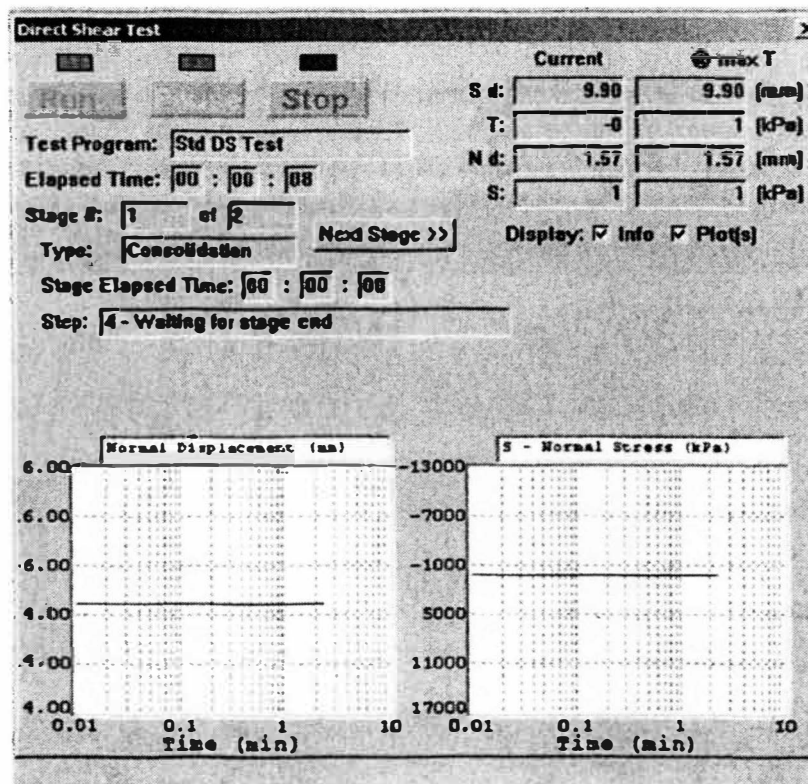


Starting the Test

32. When everything is in place and the test is ready to be run. Click Run.

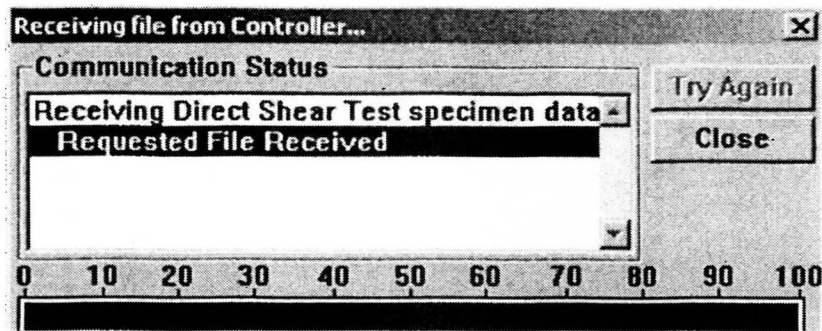
The screenshot shows the 'Direct Shear Test' window. At the top, there are buttons for 'Run', 'Stop', and 'Next Stage >>'. Below these, the 'Test Program' is set to '0.500'. The 'Elapsed Time' is '00 : 00 : 00'. The 'Stage #' is '0 of 2'. The 'Type' is '0'. On the right, there are two columns of data: 'Current' and '@ max T'. The 'Current' column shows 'S d: -0.02', 'T: -5', 'N d: -5.68', and 'S: 4'. The '@ max T' column shows 'S d: 0.00', 'T: 0', 'N d: 0.00', and 'S: 0'. The 'Display' section has checkboxes for 'Info' (checked) and 'Plot(s)' (unchecked).

A window will pop up that shows the test being run and what is currently happening. It will tell you what stage it is on, the elapsed time, the current results, and the maximum results. It will first do the consolidation stage until the time that was specified in the program setup, then it will go to the shearing stage. If the next stage of testing is desired before the desired time, click on Next Stage >>> button.

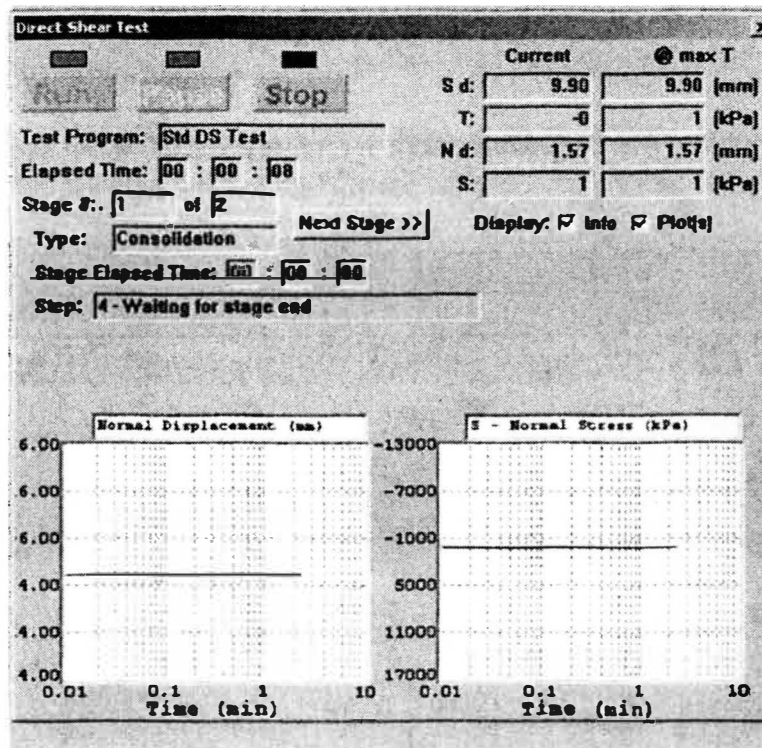


End of Test and Data Acquisition

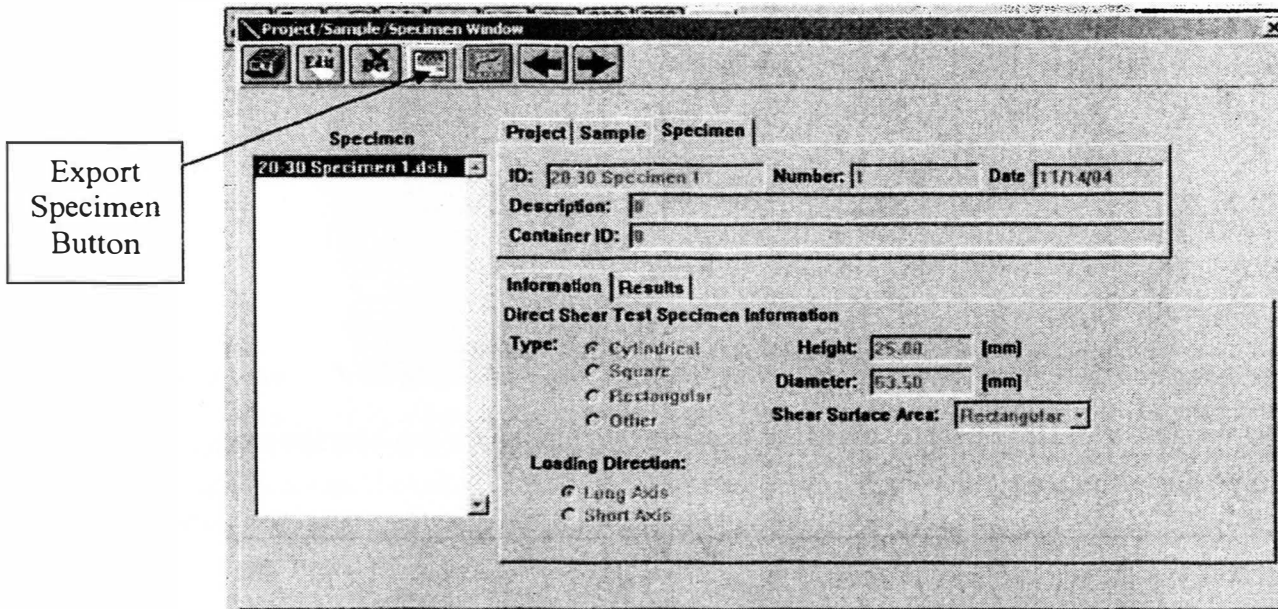
33. After the test is complete, a window will pop up that says Receiving file from Controller... After the blue bar is to 100, click Close.



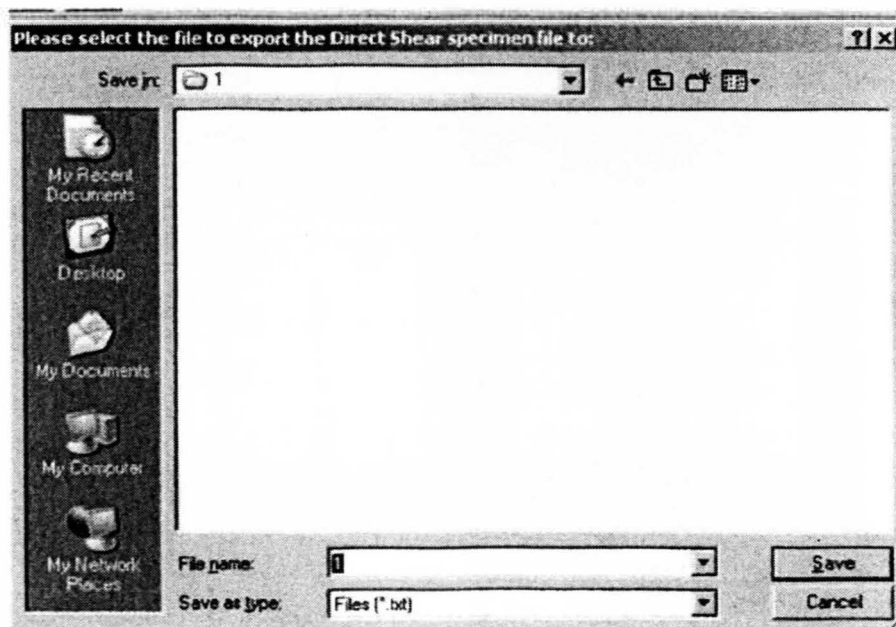
34. This window will still be there, close the window by clicking on the X in the top right.



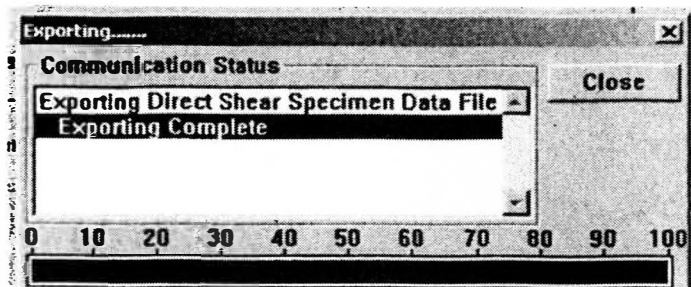
35. This window will pop up again. The data needs to be exported. Click on the Export Specimen Button (Fourth from the left). (Make sure the specimen that the test was just run on is highlighted).



36. A new window will pop up asking where to export the file. When the correct file name is entered and the location where the file will go is ready, click Save.



37. A new window will pop up that says it is Exporting..., when it is done, click Close. The file will be saved as a text file (.txt).

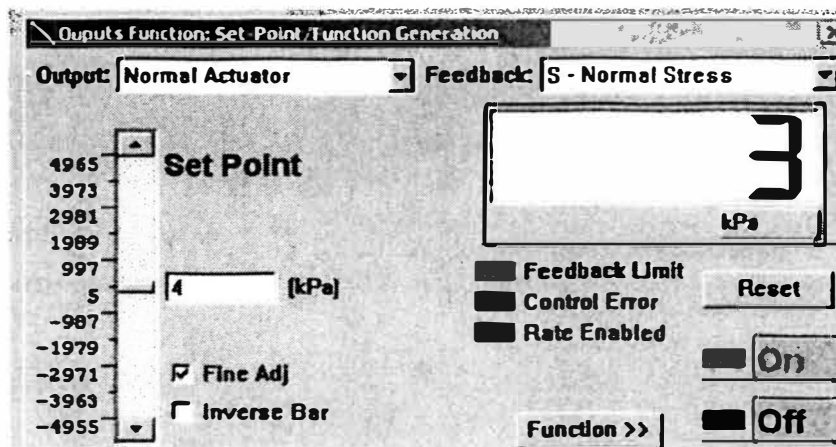


Now the data analysis can begin. It is best to put the data in Excel. This is done by opening Excel. Go to Data, then Import External Data, then Import Data. Find the file you want to open, then click Open. A new window will pop up that says step 1 of 3, click next. In step 2 of 3, under delimiters uncheck tab and put a check by commas. Then click finish.

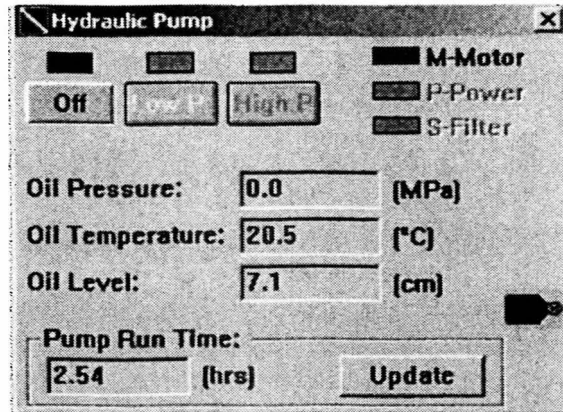
This will put all the data into an organized Excel file, where plots can be made.

Dismantling the Test

38. After the results are obtained, the test can be dismantled. First, click on the outputs button and bring it up (if it's not already up). Click on output: Normal Actuator and Feedback: Normal Displacement. Bring the displacement of the actuator up to the top. Next bring the shear actuator back to the zero position. This is done by clicking on Output: Shear Actuator, Feedback: Shear Displacement. Type the number 0 into the field. Both actuators should now be back in place. Click the X in the top right to close this window.



39. Turn off the hydraulic pumps, by clicking off. Click the X in the top right to close this window.



40. Unscrew the coupler that is attached to the loading yoke.
41. Lift up the plate and slide the loading yoke out to the left.
42. Using the allen wrench, unscrew all eight screws. Next take the shear rings out and dispose of the sample.
43. Clean up the shear rings. Clean up the loading yoke. This may have to be done with a vacuum. After everything is clean set the shear rings back into the loading yoke.
43. After all the cleaning up is done, close all the windows that may be open in the C.A.T.S. software. Close out the C.A.T.S. program.

44. Turn off the Direct Shear Machine

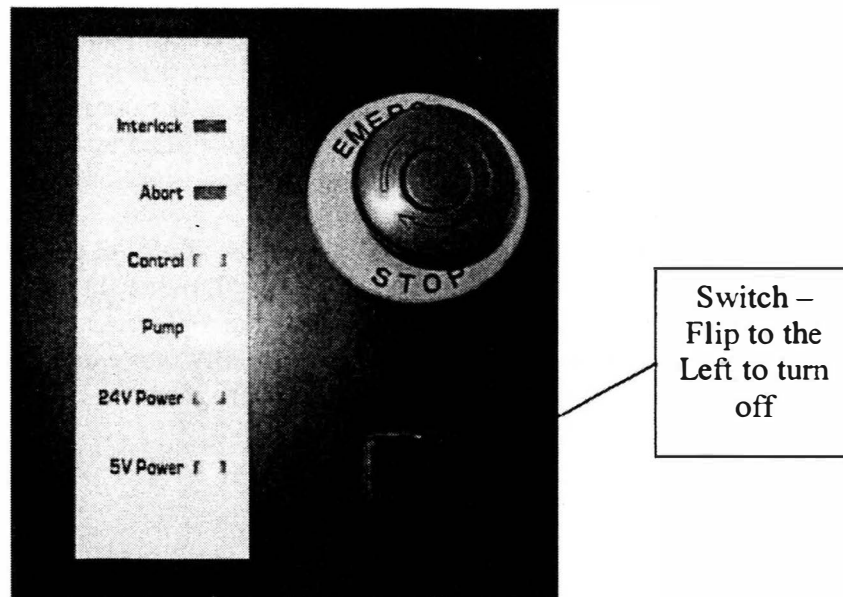


Figure 14 – Turing off the Direct Shear Machine

45. Unplug the machine from the wall outlet and then unplug the serial communication cord into the back of the computer.
46. Wheel the Direct Shear Machine back to where it was.
47. Log off the Computer.

Tips

Sometimes the normal stress will not read in the output function. This is a bug in the version of C.A.T.S. To fix this, a mock test program can be run. Without turning on the pumps, load up a test on a specimen and execute and run it. Then after a few seconds, stop the test. The controller will transfer the data to the computer. Then the stress should read. To make sure the stress is reading, press your hand upward on the normal load cell and notice that the stress is increasing on the output function.

The best way to run a test is get everything set up (about ready to click Run) and turn the pumps on. Using the normal displacement control, move the actuator just before it hits the porous stone. Then switch the feedback to normal stress then quickly click Run on the test window. The normal actuator will gradually move down until it reaches and maintains your normal stress desired in the test program.

APPENDIX D - PNEUMATIC DIRECT SHEAR TEST BRIEF OVERVIEW

Pneumatic Direct Shear Test

Brief Overview

Objective

The objective was to run a pneumatic Direct Shear Test on well-graded sand with one set loose and the other set dense. The results are to be compared between the two sets.

Soil Description

The Direct Shear Test was run on concrete sand taken from the Little Piney Creek, in Phelps County, Missouri. The sand was well-graded as can be seen from the Particle Size Analysis chart.

Procedures

First, loose sand was tested. A sample of 143.6 grams was taken and very loosely placed into the shear box to be tested. Each loose sand sample was taken with normal loads of 10, 15, and 20psi. The shear strain rate was constant for all tests at 0.25mm/min. After all loose sands were tested; a set of three dense sands was tested. A sample of 143.6 grams of dense sand was placed in the shear box, and then packed down with a tiny bit of moisture. The dense sand samples also had normal loads of 10, 15, and 20psi. (See appendix E for an in-depth look at the procedure for the pneumatic Direct Shear Test).

Results and Discussions (refer to Plots section)

The first plot is the Loose Sand Shear Stress vs. Horizontal Displacement. Looking at the plot shows most of the three tests went to a residual strength. The 0.4367kN load reached a residual strength with no evidence of a peak strength. The 0.3275kN load reached a little bit of a peak then started to come down and reach a residual strength. The last load of 0.21835kN didn't have a peak at all and just leveled out to a residual strength. Looking at this plot seems to show either something was wrong on the 0.21835kN load or the 0.3275kN load because they overlapped each other too much. The 0.4367kN load should have been larger than the 0.3275kN load the whole time. Both of these loads should be run again to see if better numbers could come about.

The next plot is the Loose Sand Mohr-Coulomb Failure for Peak Strength. The peak strengths of each load were plotted. From there the internal angle of friction was measured to be 53 degrees. According to the Manual of Soil Laboratory Testing by K.H. Head a typical value of a loose well graded angular sand is 39 degrees. For this particular sand, the internal angle of friction was higher.

The Dense Sand Shear Stress vs. Horizontal Displacement is plotted next. Looking at these plots shows that most of them reached a peak strength then went to a residual strength. The 0.21835kN load shows a definite peak and then going down to a residual strength. If the test was carried out longer it may have come down a little bit more. The

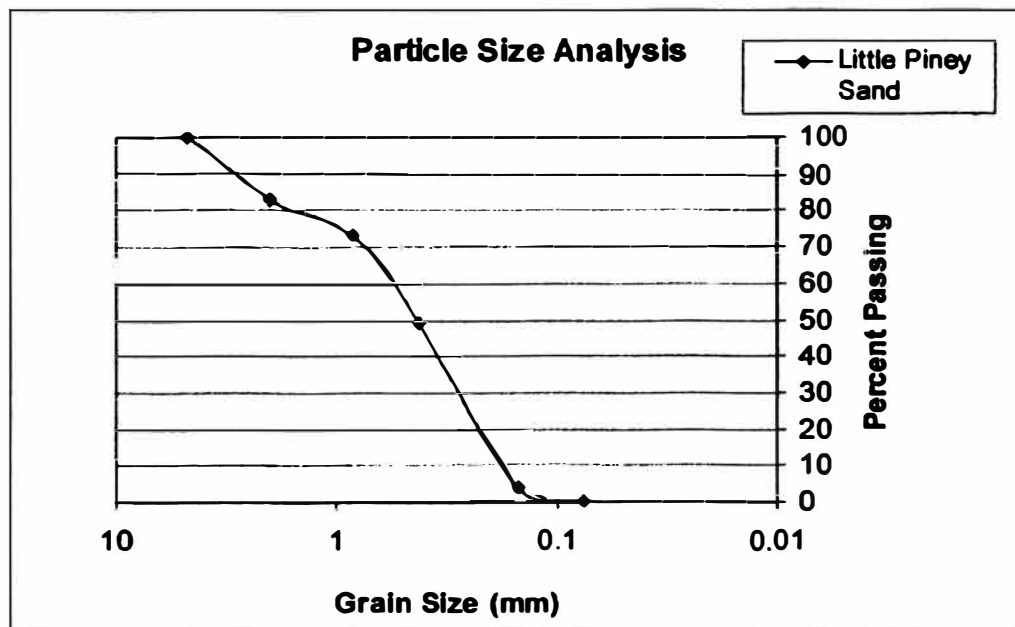
0.3275kN load reached a peak then had a few erroneous points before it came to a residual strength. The final load of 0.4367kN doesn't really show a peak strength. It may come down if the test had some more data points at the end.

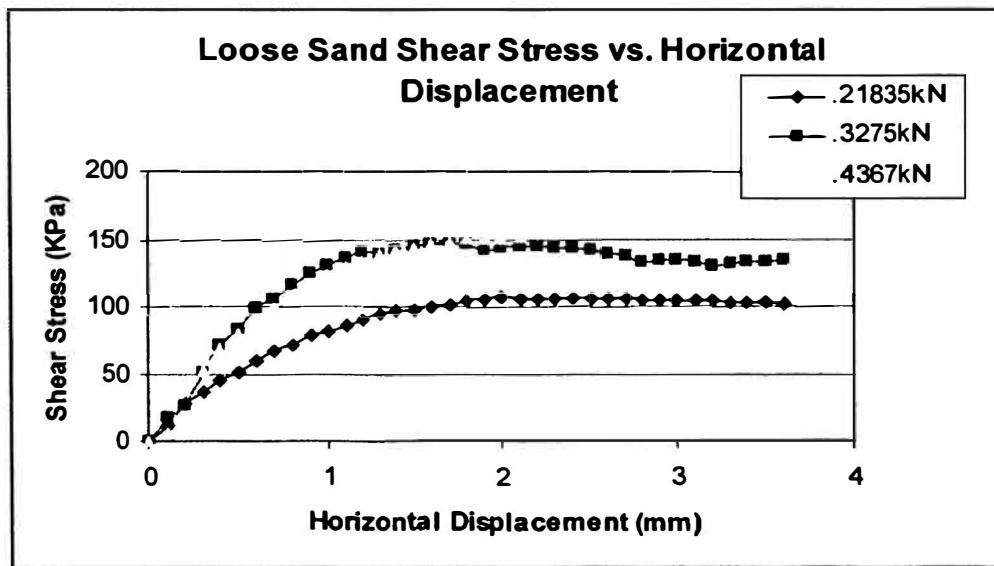
The final plot is the Dense Sand Mohr-Coulomb Failure for Peak Strength. The internal angle of friction is higher than the loose sand as was expected at 57 degrees. According to the Manual of Soil Laboratory Testing by K.H. Head a typical value of a dense well graded angular sand is 45 degrees. This too was higher than the typical values.

In comparing the loose sand maximum shear stresses with the dense sand maximum shear stresses the dense sand is about 1.15 times higher. This is because in dense sand the particles are packed closer together and the shear stress required for particles to override each other is higher. The effective angle of friction in dense sand is 4 degrees larger than the loose sands. This is expected since the voids are lower in dense sands, since the particles are closer together. Therefore, the dense sand would require more shear stress to reach a failure of the sand. As in all sands, there is no cohesion.

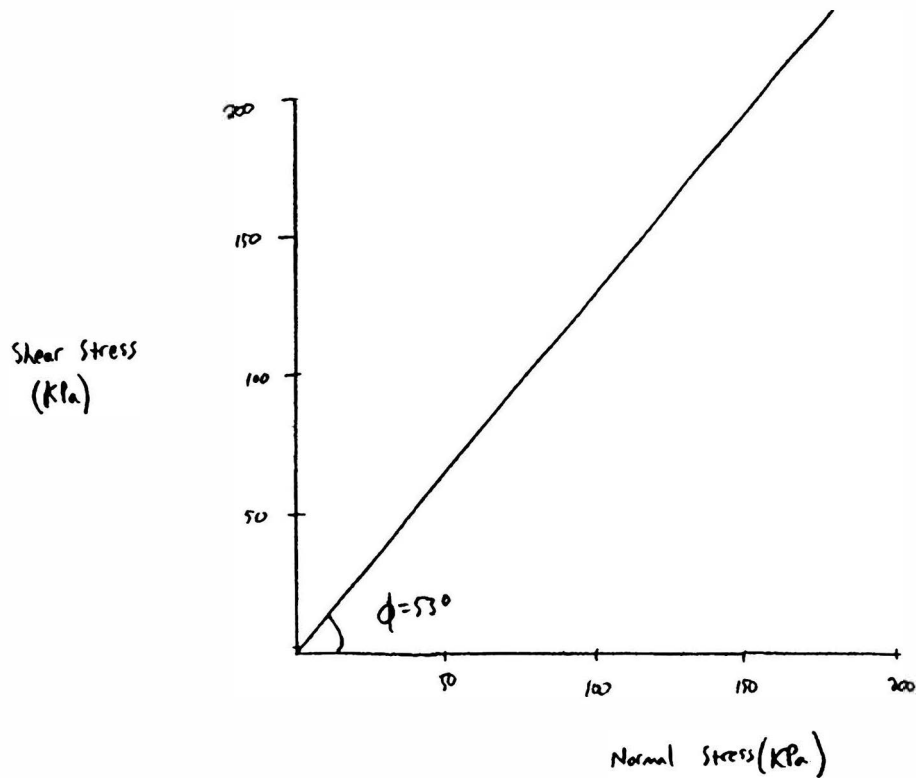
As can be seen in the graphs, the data is not perfect. This is because in the pneumatic Direct Shear Test, the area is constantly changing due to the shearing. This in turn causes the particles to override each other, thus constantly changing the normal load applied. So, sometimes the normal load was actually less or more than was specified. This could result in skewed results.

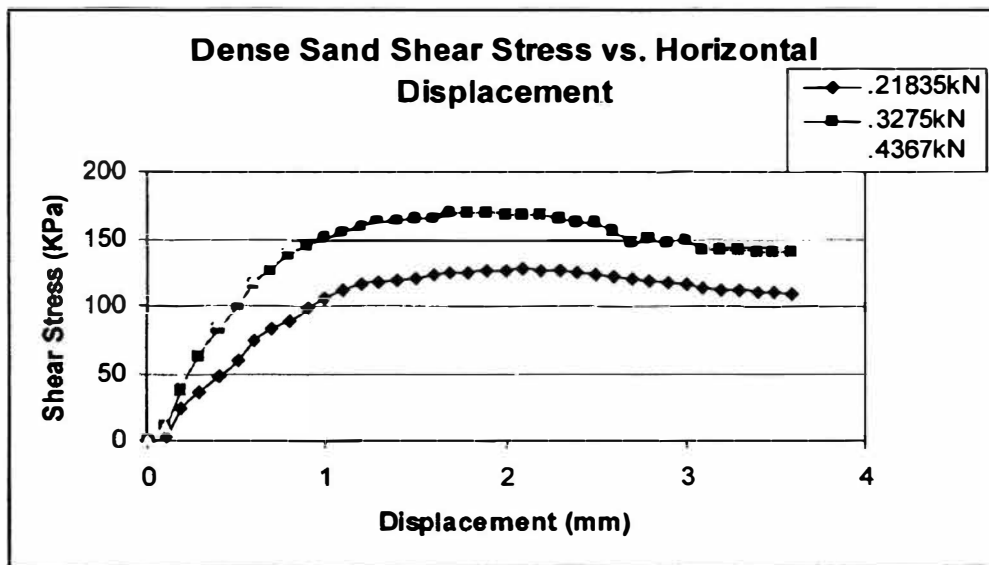
Plots



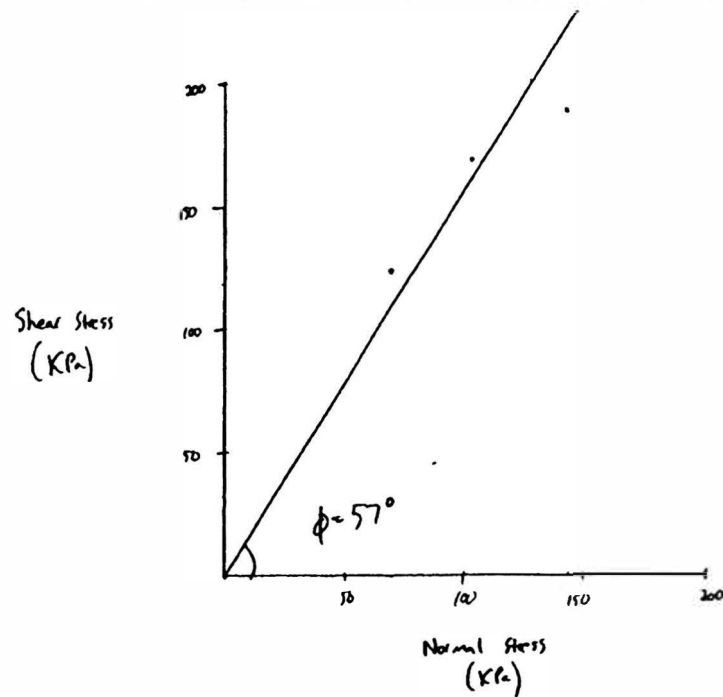


Loose Sand Mohr-Coulomb Failure Line





Dense Sand Mohr-Coulomb Failure Line



References

- ASTM D 3080 Standard Test Method for Direct Shear Test of Soils Under Consolidated Drained Conditions
- Head, K.H., (1994), *Manual of Soil Laboratory Testing*, Vol. 2 Second edition, Pentech Press Limited, London, pp. 220

APPENDIX E - PNEUMATIC DIRECT SHEAR TEST USER'S MANUAL

PNEUMATIC DIRECT SHEAR TEST

Procedure

Overview

The Direct Shear test is used to determine strength parameters of a particular soil sample. The test consists of placing a soil sample in a shear box that provides confinement on the vertical walls. Depending on the type of shear box, the sample has either a circular or square cross-sectional area. There are two porous stones located at the top and bottom of the sample which controls drainage. First, a normal load is applied to the soil sample. While that normal load is still applied, the soil is sheared at a constant rate. The magnitude of the normal load and the rate of the shear load are determined prior to the test. Once the test starts and the soil is sheared at a constant rate, the lateral displacement and lateral force are recorded. To find the shear stress, take the shear force and divide it by the nominal area of the sample. The normal stress on the failure plane is known since the direct shear device forces the failure plane to be horizontal.

The Direct Shear Test gives the shear strength of that soil sample. However during shearing, there is a rotation of the principle stress which may not be exactly like the field conditions. Mohr's circle can be drawn after the test. This will show the failure assuming that the failure surface is horizontal and the stress state is uniform.

Usually, a minimum of three samples of the same soil will be used. Each of the three samples will have a different normal load applied. This will give a relationship between shear strength and normal stress. After all three tests are completed at different normal stresses; a Mohr-Coulomb diagram can be drawn.

Set Up

1. Find mass of subject soil to be used.
2. Make sure that the shear box is clean and free of any particles.
3. Adjust box screws, so that they are flush on the bottom (uses an allen wrench). Place top of shear box on the bottom of the shear box. Screw in the white plastic bolts. Measure the diameter and height of the cylinder in the shear box. (See Figure 1)

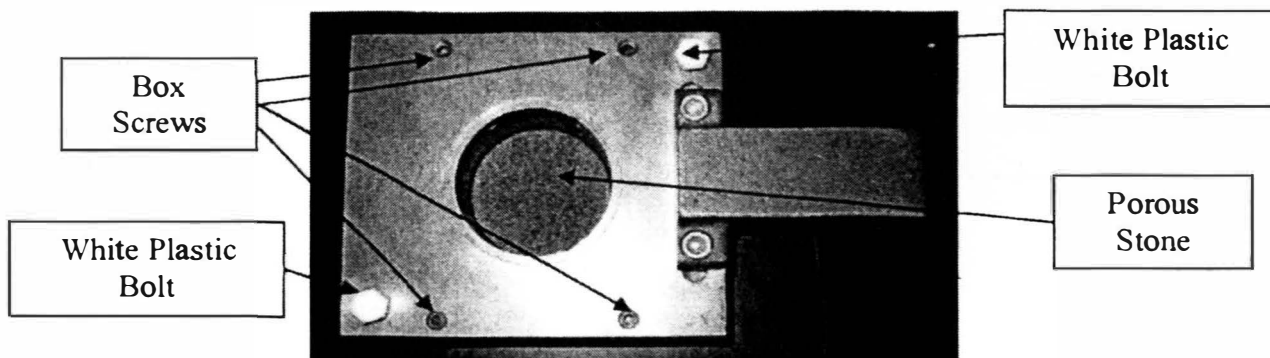


Figure 1 – Shear Box

4. Place the shear box in the loading yoke (on top of machine). Add the sample in the box. Place the porous stone and then the Loading cap on top. (See Figure 2)

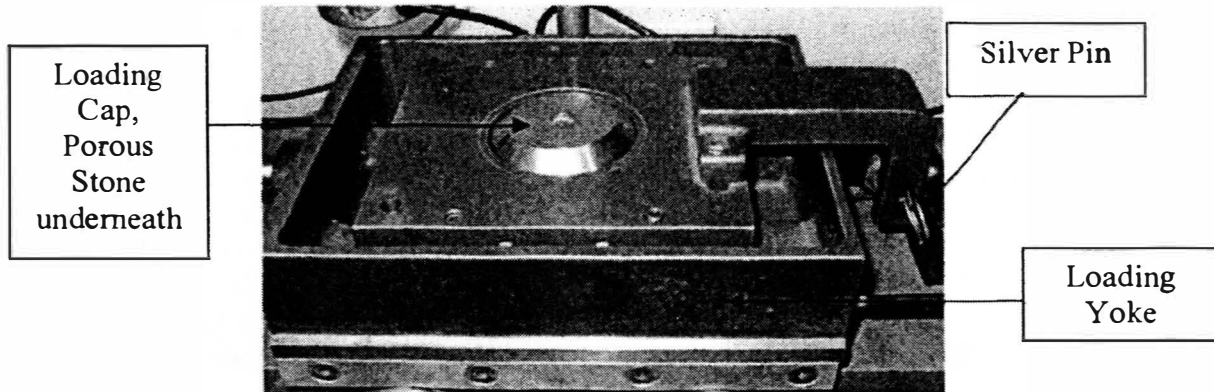


Figure 2 – Shear Box on Top of Machine

5. Center shear box housing by lifting out the anti-rotation pin on the gearbox assembly. Then rotate the wheel until the holes in the loading yoke line up with the holes in the load cell extension rod. (See Figures 3 & 4) After it is lined up, reinsert Anti-rotation pin.

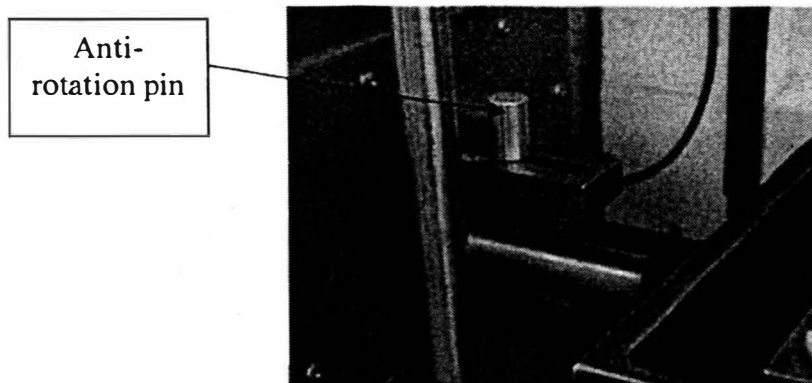


Figure 3 – Anti-rotation Pin

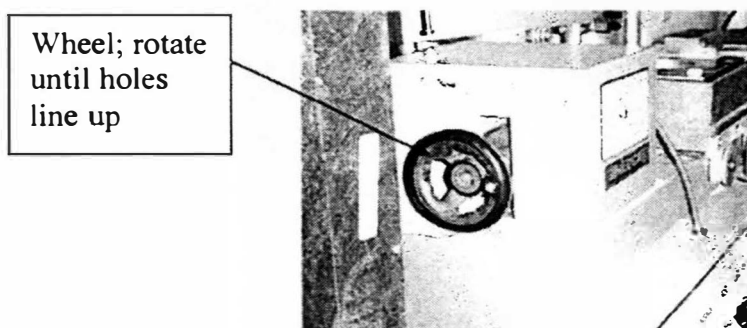


Figure 4 - Wheel

6. Fix the loading yoke with the silver pin (on the right side of the box). (See Figure 2)

Start of the Test (See Figure 6 for steps 1 - 9, unless otherwise specified)

1. All black knobs (Supply, Vent, and Load Applied) should be shut (clockwise).
2. Pressure Regulator (silver knob) should be all the way out (counter clockwise).
3. Open air valve into the machine. It is located to the left of the machine on the wall. (See Figure 5)

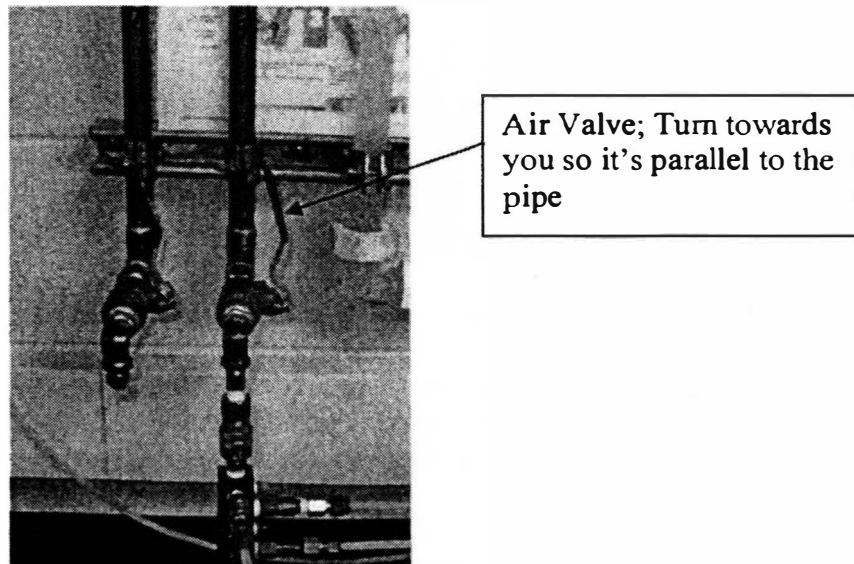


Figure 5 – Air Supply

4. Turn on the machine (flip switch to on). Open supply first (black knob, turn counter clockwise). This will allow the air to go into the machine. (The pressure gauge should show around 80 PSI, plus or minus)
5. Position Load on top over the cap. Then use the big bolt and screw it down to the apparatus. Move the dial gauge so it is over the load arm pressing down on it. Then open load applied valve (black knob, turn counter clockwise).

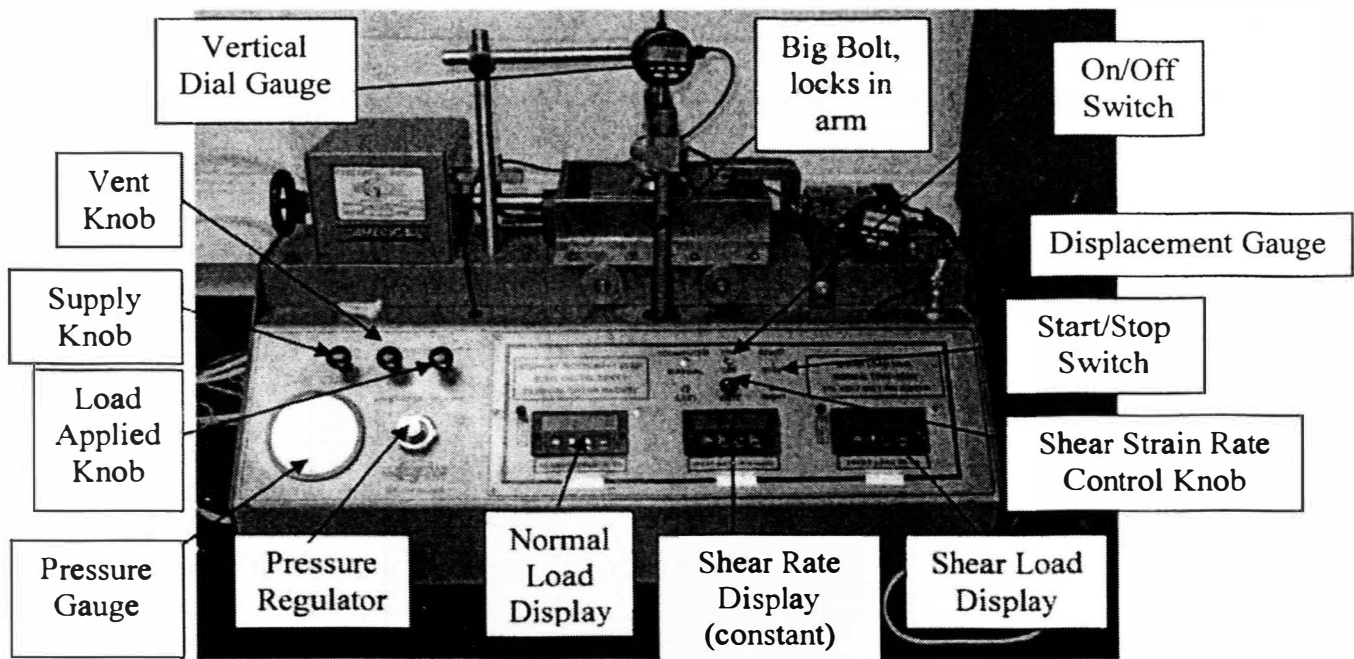


Figure 6 – Pneumatic Direct Shear Test Machine

6. Turn the Pressure Regulator knob, clockwise to open. This will apply the normal load. It will have to be constantly adjusted during the test to maintain the desired normal load (since during shearing, the particles are rearranged).
7. Using the allen wrench, screw all four box screws in a couple of turns (Clockwise). (This will help reduce the amount of friction between the plates.) Remove white plastic bolts from the shear box. Turn on both dial gauges (green on button).
8. Start the test by switching the start/stop switch to start. Adjust the shear strain rate to the constant that is desired with the shear strain rate control knob. Then turn the switch to stop. Adjust the load applied with the pressure regulator to what is needed.
9. After everything is adjusted and ready to begin, make sure the gauges are reading zero otherwise reset them, then turn the switch to start. After every 0.1mm or the desired amount (from the displacement gauge), take readings off of the vertical dial gauge and horizontal shear load display. *Remember that the pressure regulator will have to be adjusted to maintain the desired normal load.*

Data Collection / Acquisition:

During shearing the following gauges need to be read and recorded by hand. (A minimum of two persons are needed):

1. Shear Displacement (mm)
2. Shear Load (kn)
3. Vertical/Normal Load (kn) (Adjustable to keep constant)
4. Vertical Displacement (mm)

OURE RESEARCH REPORT

Rahul Kothari

**Department of Electrical & Computer Engineering
University of Missouri – Rolla
rkothari@umr.edu**

**Advisor: Dr. R. Moss
Advisor: Dr. W.V. Stoecker**

ABSTRACT

The dermvis research group at the University of Missouri-Rolla is seeking to identify melanoma automatically. They now have reported up to 90% diagnostic accuracy for malignant melanoma (1) and recently obtained about 93% correct melanoma identification, the highest obtained by research groups in North America. The goals of the OURE project described here were threefold:

1. Digitize images from existing photographic slides of dermoscopy images taken with the Heine Dermaphot unit.
2. Digitize images from patients with malignant melanoma or benign lesions in the infrared region using a new camera with hot mirror removed.
3. Determine microprocessor serial cable codes for the Nikon Coolpix 950 camera so serial images may be taken from the camera, both visible and infrared.

Results and sample images from the two kinds of image acquisition are presented along with the microprocessor serial cable codes.

BACKGROUND

Malignant melanomas cause the majority of deaths from skin cancer, approximately 7,000 per year in the United States in 2004. Image processing can yield information on structures within the lesions. There are two types of digital images used for malignancy detection. Clinical images were the usual images until the mid-1990s, with good quality images taken at approximately 1:1 magnification, sometimes using a dual flash system.

In the past decade, dermoscopy images have become the standard imaging system for pigmented lesions. Taken with a flash unit at 10:1 magnification with a liquid interface of alcohol or mineral oil, dermoscopy images provide more detail than the clinical images. In addition, the

interface and epiluminescent lamination can eliminate the contribution from the skin surface, making deeper structures more apparent.

Digitization of dermoscopy images is necessary for automatic processing of the images. Digital dermoscopy images may be acquired by either direct digitization in the clinic or by digitizing photographic slides. In this project, photographic slides were digitized by the Poaroid Sprintscan 35 Plus slide digitizer.

The second goal was to digitize images in the infrared region and obtain in vivo infrared spectra from patients using a new infrared camera developed by the group and a FieldSpec Pro infrared spectrometer. In this way, both detailed images within the infrared region and the spectrum itself could be obtained for further study. When enough spectra are acquired, they will be analyzed to determine the optimum wavelengths for melanoma discrimination. Groups in the UK and in New York (2,3) are obtaining infrared spectral images, but to our knowledge, no other groups are using an open, non-dedicated camera system, none are analyzing images for specific structures, and none are obtaining spectra.

METHODS

1. Sixty digital clinical and dermoscopy images were digitized using the Poaroid Sprintscan 35 Plus slide digitizer. Care was taken to use the appropriate resolution and remove casts when detected. In addition, the EDRA pigmented lesion disk, EDRA Medical Publishing, Milan, was the source of images for selection of specific white and blue areas.
2. Seven patients were studied using a Nikon 950 Coolpix camera modified by removing the hot mirror as shown in Figure 1. From each patient, spectra were obtained using the ASD FieldSpec Pro. A representative melanoma image from the visible and infrared regions are shown in Figures 2 and 3.

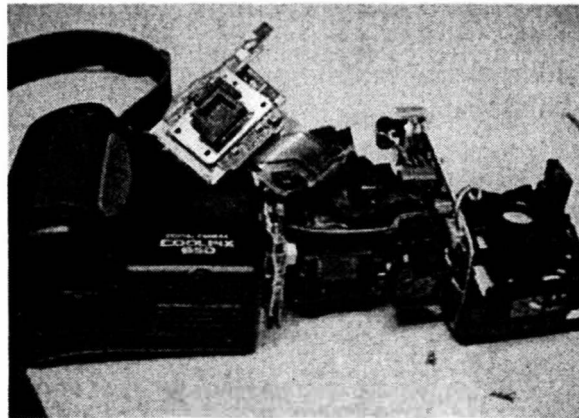


Fig. 1. Nikon 950 Coolpix disassembled, hot mirror removed.

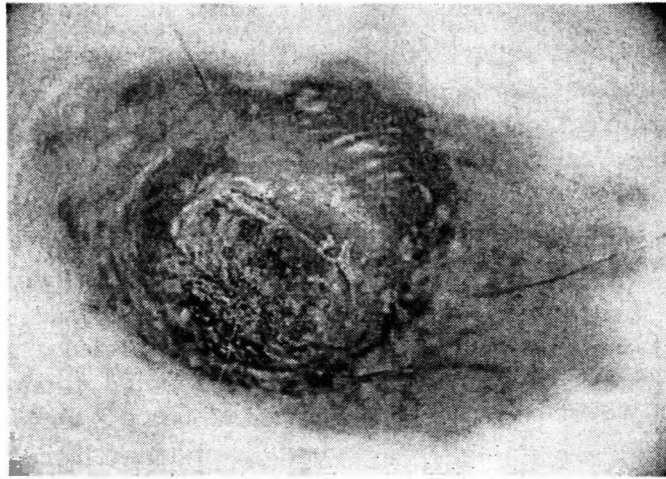


Fig. 2. Malignant melanoma visible-light image.



Fig. 3. Same patient, infrared image.

3. The method used to establish communication with the camera was a Simon Board. The Simon Board is a single board computer based on the P89LPC932 processor from Philips. The original purpose for this single board computer was to play the electronic game Simon. A Simon Board is shown in Figure 4.

In order to establish communication, open source software called “pcphoto” was found on the internet. This software was loaded on the computer and was then compiled. After compilation the software was ready to be used.

Once the software was installed a serial cable was connected from the computer to the camera and certain commands were given to the camera. These included, “take a picture”, “set the date and time” of each picture, “copy the picture” from the camera to the computer, “delete” the unwanted pictures etc. Once this was done, it was now time to somehow learn what sequence

of data was making the camera do the desired operations. In order to do that, a specially modified serial cable was made in the lab, with pin outs for the logic analyzer. The cable has serial pin connectors on each end and in the middle a special connector was added which was hooked up to the logic analyzer. This new serial cable was then connected to the camera and the logic analyzer and the command for taking a picture was given which generated a set of data. This data was captured by the logic analyzer. It was not clear what one was to expect but after constantly changing the settings on the logic analyzer like periods, time intervals, length of the data sequence etc. A set of data emerged which after some investigation looked right.

The next step was to take this data and write a program where instead of a PC, a Simon board could send this sequence of data and establish communication with the camera. This data sequence basically is a set of singly binary digits which are then converted to hexadecimal numbers for programming and these hexadecimal numbers are then sent to the camera. This data is by no means structured specifically for the Nikon Coolpix 950 camera but for any camera which uses the Fujitsu chipset.

The microcontroller was programmed using assembly language. Before programming the microcontroller a flow chart was made (see Figure 3) to better understand the logical progression of how the program should be written. The program sends a hexadecimal 00 to wake the camera up, and then wait till it receives a hexadecimal 15 at which time it lights the yellow LED on the board indicating that it has received a signal from the camera. The yellow LED is just one of four available LED's on the Simon board and it was chosen randomly. It is then ready to send the data sequence which is a long list of data to the camera, and once that is sent, it again waits for a reply from the camera which in this case is a hexadecimal 06. Once that is received it lights the Green LED indicating that the communication has been established and we are ready to go forward with next phase which is to take a picture. To make the Simon board take a picture was beyond the scope of this project. But what this project has done is to establish a way one can use the Simon board to accomplish the ultimate goal of creating a stand-alone system which can be used to control the camera and the Dermlite lens module which contains different sets of LED's.

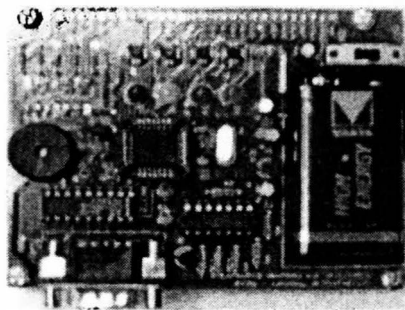


Figure 4: Simon Board

RESULTS

Images were made available to the group and analysis is pending. One promising feature was the combination of white and blue. Digital images were analyzed and white and blue areas were outlined using Paint Shop Pro. Filemaker was used in making the EDRA disk and store the images, but images with melanoma features and catalogued images had to be matched by hand because no direct image access method was possible.

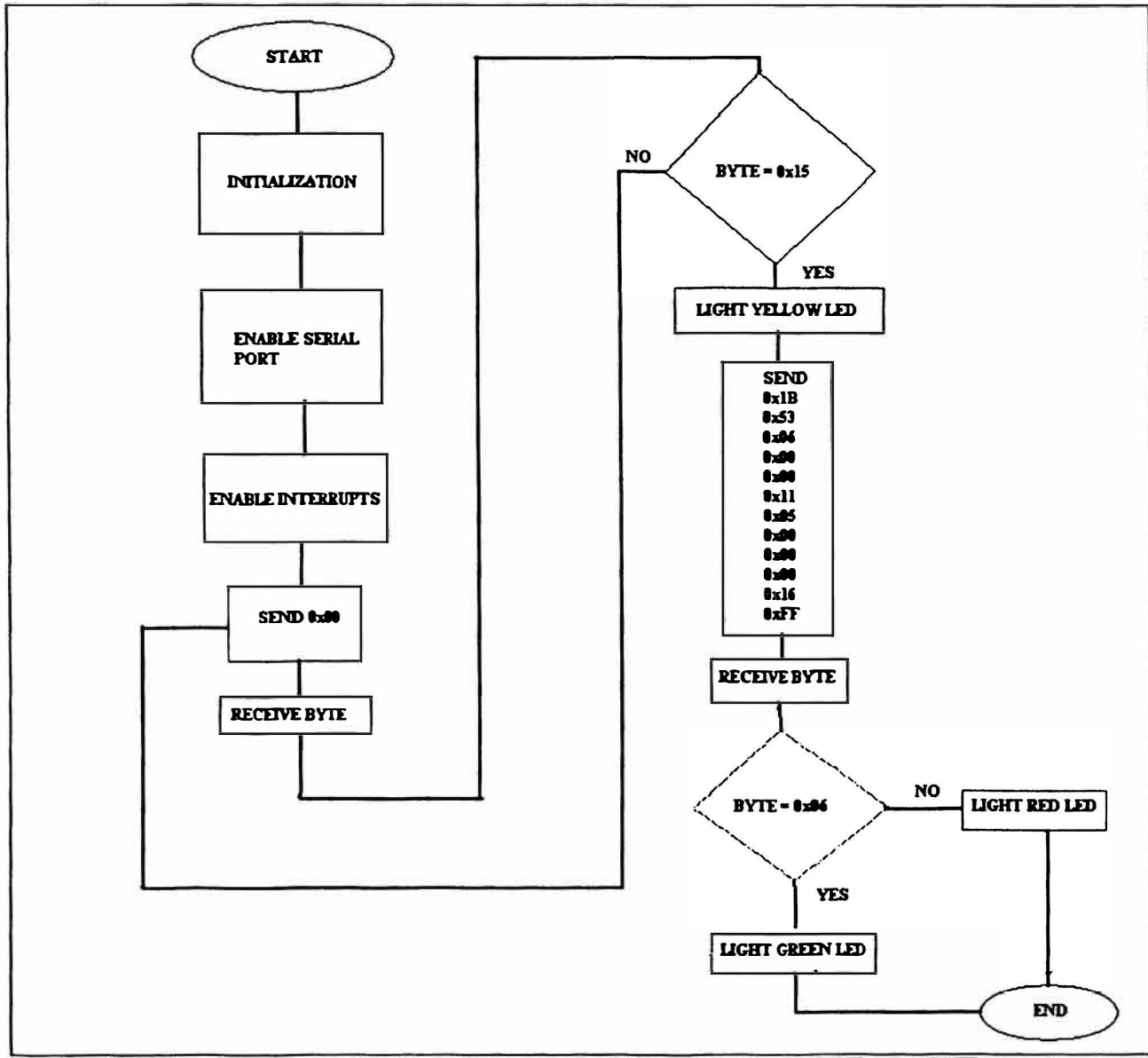


Figure 5. The flow chart utilized for programming the microcontroller is shown above. The hexadecimal commands were found using the logic analyzer and Simon Board.

ACKNOWLEDGEMENTS

I would like to thank Dr. Shrestha for giving me a chance to do undergraduate directed research. His faith in my abilities to perform the required task really helped me overcome a lot of

challenges I faced during the project. I was guided by his belief that if something is to be done, it be done with absolute perfection. His help and guidance has been a great source of inspiration.

I would also like to thank Dr. Moss and Dr. Stoecker for being so generous with his time to explain me about the different aspects of the skin cancer research. They helped me understand what was needed to further the research, and then helped me formulate a plan to finish the project.

I would like to offer a very special thanks to Mr. Roger Younger for taking time out from his busy work schedule to help me program the Simon Board. He helped me a great deal in understanding how a Simon Board works and how one needs to go about writing the assembly code for the microcontroller.

REFERENCES

1. Chen03 Chen J, Stanley R, Moss RH, Stoecker WV. Color analysis of skin lesion regions for melanoma discrimination in clinical images. *Skin Research and Technology* 9:94-104, 2003.
2. Elbaum M, Kopf A, Rabinovitz H, et al. Automatic differentiation of melanoma from melanocytic nevi with multispectral digital dermoscopy: A feasibility study, *J Amer Acad Dermatology* 44(2): 207-218, 2001.
3. Cotton99 Cotton SD, Claridge E, Hall P: A skin imaging method based on a colour formation model and its application to the diagnosis of pigmented skin lesions. *Proceedings Medical Image Analysis and Understanding 99*, Oxford: BMVA, 49-52, 1999.

The Effect of Soluble Salts on the Corrosion Process in Sandstone

Kuligowski, M and Wronkiewicz, D.J.

Abstract

Studies of failed engineering structures have found that soluble salts can cause extensive breakdown to sandstone and cement. The mechanism for this failure is postulated to result from crystal growth pressures as evaporate minerals crystallize in the pores. This postulated mechanism, however, is inconsistent with the thermodynamic theory as crystal precipitation and growth should occur in the most energetically favorable setting. We will test this hypothesis by examining the corrosion behavior of sandstone when it is constantly submerged in saline solutions (without crystal formation). A number of tests will be performed in order to observe the effect of saline solutions on sandstone matrix dissolution. The tests are performed on Jacobsville sandstone that was acquired from a construction site in Marquette, Michigan. A synthetic sea water, brine solution and deionized water will be used. Samples are placed in closed container containing one of the solutions. Samples are undergoing tests at room temperature, 90°C, and 200 °C. Degraded samples will be periodically examined in order to see the effects of salt corrosion and/or crystallization.

Introduction

Weathering of sandstone is a major problem that is slowly destroying many buildings around the world. Salt that crystallizes in the porous medium of sandstone will slowly break apart the sandstone. The crystallization process will exert pressure on the surrounding matrix and will force the sandstone to break apart (Goudie, 1995).

According to thermodynamic theory, the crystallization would occur in the most energetically favorable way. If the crystals are expanding in a confined space, they are exerting a large amount of force and this requires a lot of work. While such a process may commonly occur during solid-state phase transformations (e.g., hydrating clay grains), a crystal precipitating from an aqueous solution should not grow in a manner that requires such a high amount of energy. Salt solution in a porous rock can reduce the mechanical strength of the rock. The interfacial tension between the rock minerals is weakened. This is an important process that can not be overlooked. The solution that the rock is exposed to also has a great effect (Navarro, 1999).

The sandstone used in this project is also used for construction in Marquette, Michigan. In figure 1, a building in Marquette, Michigan illustrates the sandstones use. The lower part of the building is moderately weathered away due to salt used on the roads during winter time. This weathering could also be partially caused by freeze-thaw action (Monuments, 1982)

This project will examine how sandstone will react to different types of fluid corrosion. Three types of fluids will be used. A synthetic seawater, brine, and deionized water will be used. The tests on the sandstone will be run at different temperatures. By raising the temperature, the corrosion process will be sped up. Over time the sandstone should begin to loose its' integrity and break apart. When the grains begin to break apart, that will be the sign that the sandstone has begun weathering.

Sampling and Methodology

The Jacobsville sandstone was collected from discarded material at a construction site in Marquette, Michigan. The large specimen was brought back to the laboratory where it was cut into smaller pieces in order to perform the present set of experiments. The sandstone was cut using a diamond tipped saw. The pieces were cut to a thickness of 1mm or greater. The pieces were cut into a square or rectangle.

After each piece of sandstone was cut, the surface was smoothed by using 600 grit sandpaper. This was performed in order to make the surface as uniform as possible. This will aid in making each piece similar to one another. After smoothing the surface, the sample was placed into an ultrasonic cleaner. This helps to free up any loose particles and dirt that was in the sample. After all the initial preparations the sample was placed into an oven in order to remove all the remaining moisture.

Each sample was weighted to the ten thousandths gram. After weighting, the sample was traced and any distinctive marks that were made prior to weighting were recorded. This was done in order to distinguish the sample from one another. Each sample was photographed under a microscope. Pictures were taken at 1x and 2x magnification. Pictures were taken at the distinctive locations created in the preparation. This will aid in finding the location and comparing the sample before and after the tests.

In order to perform the tests on the sandstone a synthetic seawater and brine had to be created. The amounts of chemicals mixed together, in order to create the synthetic seawater, can be seen in Table 1. Supersaturated seawater, brine, was created by taking the amount of chemicals required to make seawater and multiply that amount by ten. Two batches of seawater were created separately. In order to make them identical, they were both mixed together and placed on a hot magnetic stirrer. This would ensure that all of the remaining solids would dissolve and the solution would be properly mixed. De-ionized water (DIW) was also used as a control.

Chemicals	Amount required (g)	Batch A (g)	Batch B (g)	Brine (g)
NaCl	27.45	27.454	27.454	274.53
CaCl ₂	1.144	1.144	1.145	11.449
MgCl ₂	2.37	2.377	2.376	23.79
KCl	0.761	0.761	0.761	7.06
MgSO ₄	3.38	3.3805	3.381	33.79

Table 1

After all the initial preparations of the sandstone and solutions they are ready to be combined. The samples are placed into either a screw-lid Teflon vessel or a Teflon lined stainless steel bomb container. The screw-lid Teflon vessel containers are used for tests that are run at temperatures of 90°C or less. The Teflon lined stainless steel bomb containers are used in tests that are run at 200°C. Three temperature tests were run during the time of the research; room temperature, 90°C, and 200°C. All of the vessels are capped to prevent evaporation.

At each temperature a container contained one piece of sandstone and any one of the three solutions. At each test multiple containers contained the same solution. The screw-lid Teflon vessels that were run at room temperature and 90°C contained 20g of solution. The Teflon lined stainless steel bomb containers contained 7g of solution. The Teflon bomb containers had only 7g of solution because they are smaller than the regular vessels. This keeps the ratio of solution to air at one-thirds respectively.

The containers were opened at different times. The vessels at room temperature were opened after three months. The 90°C and 200°C vessels were opened on a weekly basis. Each sandstone piece was examined for any loose particles and the results were recorded.

Results and Discussion

The first test that was begun was at room temperature. The samples were left undisturbed for three months in the laboratory. In three months the vessels containing the samples were opened and no change had occurred. The sandstone pieces were still intact and no loose sand particles were present. The only change that did occur was in the brine solution. The flakes are possibly Carbonate flakes that formed during the process of carbon dioxide dissolving in water. During this process carbonic acid is produced and will begin carbonate production (G R Delplerre and B T Sewell, 2002).

Since no results were occurring from the room temperature test, a new batch of samples was put into an oven at 90°C. Running the samples at a high temperature will accelerate the process. The samples at 90°C were examined every week from the time they were put into the oven. In three weeks the only change that occurred was the formation of carbonates in the brine solution. After four weeks there were carbonate flakes present in the seawater solution as well.

Since no significant results were occurring at 90°C another batch of samples was begun at 200°C. These samples only varied in size. At 200°C special containers had to be used. These containers are smaller than the ones used at 90°C. The size of the sandstone put into the vessels was smaller. The thickness remained the same, around 1mm, and the width of the sandstone was around 3-4mm. After one week, each of the samples had grains that broke away from the sandstone. The sample that was in DIW had the most grains that broke off. The seawater and brine solution had around five to ten loose grains. Just like in the 90°C test, the 200°C also had carbonates present in the seawater and brine solution.

Since the results of the experiment were not as expected, another test was performed on the sandstone in order to find out how resistant the sandstone was to salt weathering due to crystallization. The purpose of this research was not to allow crystallization to occur. This test was performed in order to see if the sandstone was more resistant than estimated. The sandstone was cut into 3 cm x 1 cm rectangles. The sandstone was saturated in all three solutions over night at room temperature and then placed in the oven. The sandstone was saturated, with DIW, every three to four days and then dried in the oven at 90°C. Only DIW was added because adding more seawater or brine would add to much residue after evaporation. After one week no break up of grains was present. After two weeks there were loose grains present. After three weeks there was even more grains that broke off. The seawater solution seems to work better at breaking apart the grains because more loose grains were visible. Measurements have not been made yet to find out exactly the amount lost but it is estimated at 3-5% of the original mass was broken off. Both the brine and seawater are in that range and the sample that was exposed to seawater had the higher amount of loss.

At the present time the only tests that have shown results are the 200°C tests. The DIW solution has shown the largest amount of sediment break up. This is highly unusual because the water should not have as much of an effect on the sandstone as the soluble salt solutions would. There is no explanation about higher loss due to DIW at this time. The 90°C and room temperature tests will need more time in order to break up the sandstone. The current results of all the tests can be seen in Table 2. The time and conditions the samples are exposed to are more controlled than what is occurring in natural settings. Only at higher temperatures, when the dissolution process is accelerated, can results be seen.

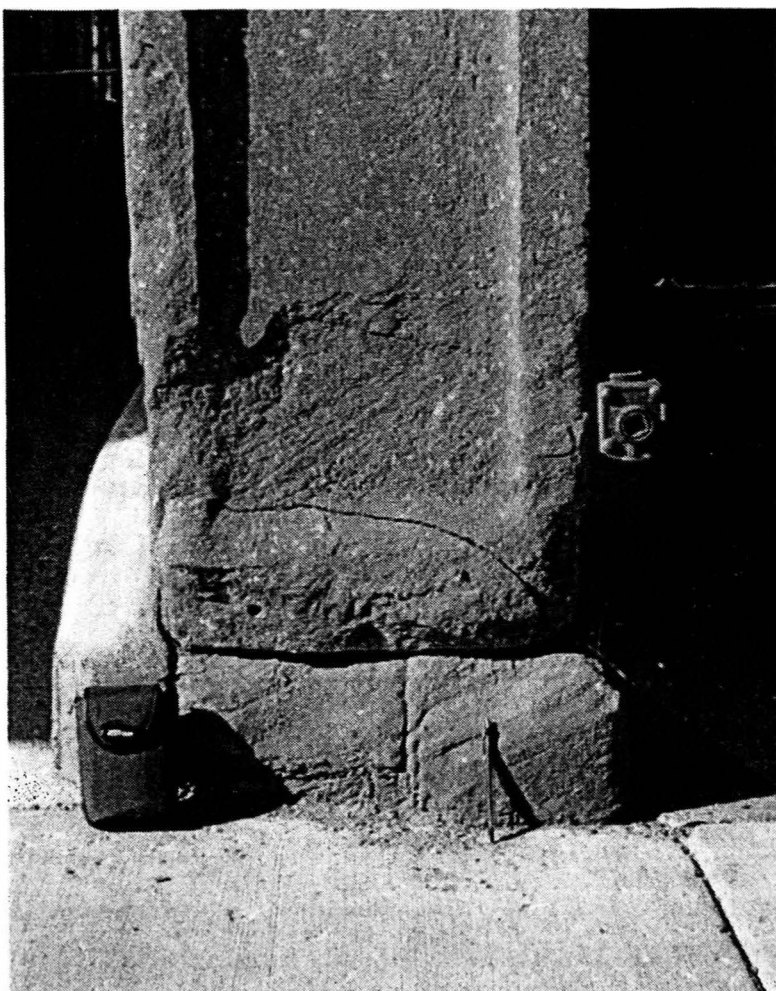


Figure 1- Weathering of Jacobsville sandstone in Marquette, Michigan

Temperature	Solution		
	<i>Seawater</i>	<i>Brine</i>	<i>DIW</i>
Room Temperature			
Vessel 1			No Change
Vessel 10			No Change
Vessel 19			No Change
Vessel 25			No Change
Vessel 34	No Change		
Vessel 35	No Change		
Vessel 36	No Change		
Vessel 43	No Change		
Vessel 44		Small Carbonate Flakes	
Vessel 45		Small Carbonate Flakes	
Vessel 68		Small Carbonate Flakes	
Vessel 73		Small Carbonate Flakes	
90C Test			

Vessel 92	Small Carbonate Flakes		
Vessel 63	Small Carbonate Flakes		
Vessel 109		Large amount of Carbonates	
Vessel 27		Large amount of Carbonates	
Vessel 61			No Change
Vessel 85			No Change
200C Test			
Vessel T	1-2 grains loose		
Vessel K	2-3 grains loose		
Vessel Q		2-3 grains loose	
Vessel U		3-4 grains loose	
Vessel AC			7-9 grains loose
Vessel O			4-5 grains loose

Table 2

Conclusion

Salt weathering is a process that is slowly destroying many of our buildings and monuments constructed out of sandstone. Salt will crystallize when the solution evaporates. The crystals will grow in the porous medium and expand until the matrix will break apart.

Observations on salt dissolution show that this process will take a lot longer as opposed to allowing crystals to grow. The sandstone will also play a vital role in how quickly it can break apart. Well cemented sandstone will hold up better to weathering. The Jacobsville Sandstone is well cemented and holds up against weather better than expected. Due to the strength of the sandstone a side test was performed on samples of the Jacobsville Sandstone. This sample had crystallization take place. Within three weeks the samples in the brine and seawater solution had lost around 3-5% of the grains. This is a large amount considering the timescale.

The current project will continue in order to get more results. All of the samples will be left at the conditions which they are and checked up on at the same intervals. Within a few months more break down of the sandstone will be visible. Weathering is a process that takes a long time in many situations.

Future work will involve looking at the sandstone after more grains will break off. At this point in the project not enough data could be collected by examining the sandstone. Scanning Electron Microscope (SEM) pictures will be taken of the surface of the sandstone. The SEM pictures will show the bonds that hold the grains together and how the different fluids played a role in breaking them apart. The most important thing to get out of the analysis is how the process behaved. Another important thing to look at is the flakes that are forming in the vessels. At this point the most logical explanation would be carbonates. Chemical analysis would be done of the flakes in order to figure out what they are.

Acknowledgements

This work was carried out in the Geochemistry lab of the Department of Geology and Geophysics, University of Missouri Rolla. I am grateful to Dr. David Wronkiewicz for his assistance with some of the laboratory work and for providing me with all the necessary tools to work on this project.

References

Goudie, Andrew. 1995. 'The Nature and Pattern of Debris Liberation by Salt Weathering: A Laboratory Study'. *Earth Surface Processes and Landforms*, Vol. 20, 437-449

Navarro, Carlos. 1999. 'Salt Weathering: Influence of Evaporation Rate, Supersaturation and Crystallization Pattern'. *Earth Surface Processes and Landforms*, Vol. 24, 191-209

G R Delplerre and B T Sewell, 2002. <http://www.physchem.co.za/Inorganic/Carbon.htm>

'Conservation of Historic Stone Buildings and Monuments', 1982. Committee on Conservation of Historic Stone Buildings and Monuments

THE IMPACT OF OCTANT-BASED RELATIVE COLOR DETERMINATION ON FEATURES FOR SKIN LESION DISCRIMINATION IN DERMOSCOPY IMAGES

A research paper presented to the
Electrical and Computer Engineering Department of the
University of Missouri at Rolla for the
Opportunities for Undergraduate Research Experience Program

Jorge Lopez

March 25th, 2005

Abstract

Skin lesion color is one of the main features analyzed in the diagnosis of malignant melanoma, one of the deadliest forms of cancer. Thus, the relative skin color of a lesion is obtained by applying a simple algorithm for different regions of the skin image. Then, color histogram analysis over a set of images was used in order to compute fuzzy logic-based color descriptors of skin lesions to discriminate malignant melanoma from benign lesions in dermoscopy images.

Introduction

In 2002, there were 53,600 new cases and 7,400 deaths estimated from malignant melanoma in the U.S. [1]. That was a 4 percent increase in invasive melanoma compared to the previous year. Melanoma is easily cured if detected at an early stage. Hence, the main goal of this project was to apply optical, machine vision, and images processing techniques to skin tumor images in order to detect key features useful in the diagnosis of skin cancer. The purpose of my project was mainly to assist Kapil Gupta, who a M.S. student is working in this project, in the task of developing a rule-based approach in order to identify fuzzy ratio-based color features [2] from a skin lesion image. The basic algorithm for my work consisted of first finding the center of the skin lesion, and then dividing the image in octants. Then, the average red, green and blue color of the image inside and outside the lesion and this value was then used to create a new mask of the image. Using this mask for each sector of the skin lesion, the relative color of the skin lesion was computed based on the average RGB color in each sector of the skin lesion in the surrounding skin region of the image. The fuzzy ratio feature was computed and

evaluated for skin lesion discrimination comparing the octant-based approach for relative color determination and using the single average RGB value determined from the surrounding skin region [2]. Experimental results are presented for a 512 dermoscopy image data set comparing the two approaches for determining the relative color of the skin lesion for skin lesion discrimination using the fuzzy ratio.

Background

All of the work done in this project is a modification of previous work. The purpose of this work is to investigate a sector-based surrounding skin and skin lesion approach to determine skin lesion relative color for comparison with a single surrounding skin color benchmark approach for computing relative color. The two relative color approaches will be evaluated on fuzzy logic-based color descriptors for skin lesion discrimination.

The ABCD rule actually is a technique to check for asymmetry, border, color, and diameter of a skin lesion [3]. This rule and many other techniques used in the diagnosis of melanoma were actually developed by dermatologist, so one of the purposes of this project focuses mainly on using these rules and techniques created by dermatologist to detect melanoma and apply them in a more accurate and faster way using the aim of computers.

Moreover, it is important to mention that this project focuses mainly in the color of the skin lesion. Thus, one important concept to explain is how the color analysis of the software works. For this code to run successfully, it is important to have as an input the RGB (red, green, and blue) for each pixel of the image, and the border of the image

(border between lesion and skin). All this important information can actually be obtained from three graphic files of the analyzed image. A portable pixel-map graphic file (ppm) is used to obtain information about the RGB, and two portable gray-map graphic files (pgm) are used to obtain information about the border of the image. Then, using this information from the image, the average surrounding skin color value is determined, and a color histogram analysis [4] is created. Finally, the color characteristics of the images are identified from the color histogram and a diagnosis can be obtained by analyzing those histograms.

Octant-based Procedure for Determining Surrounding Skin Color

First of all, it is important to mention that some of the work done by me was first implemented in C++, and it was later implemented in C by Kapil Gupta. Thus, as a first step, the center of the skin lesion was found by determining which pixels were actually considered not skin or inside the border. Then, the following algorithm was implemented.

```
for y = 0 to y_res
  for x = 0 to x_res
    if image[y][x] = Inside_border
      x_c=x_c + x;
      y_c=y_c + y;
      count =count+1;

x_c = x_c / count
y_c = y_c / count
```

Notice that the image can be considered as a plane in the first quadrant of a coordinate system where (y_res) X (x_res) is the resolution of the image. Let the center of the lesion is located at the point (x_c , y_c).

Later, starting at the center, the image was divided into octants of an angle of $45^\circ + (2 \times 5^\circ)$ or 55° , where the 5° angle was used to take care of any calculation error as shown by the following figure.

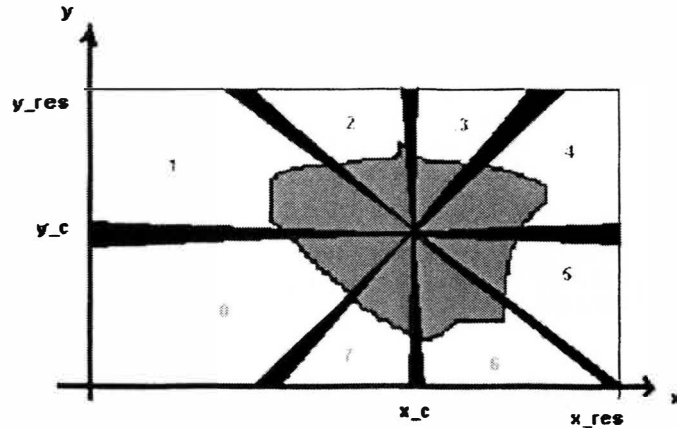


Figure 1: image divided into octants and the intersection of the regions

Notice that the division of the region was obtained by comparing two lines of the form $y = mx + b$ where m is the slope or tangent. Also, notice that the gray area represents the lesion, and the black area represents parts of a region that is intersected or overlapped by the other region right next to it due to a 5° angle as shown by the figure below.

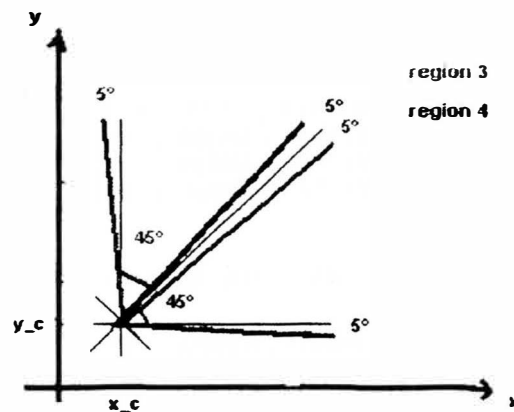


Figure 2: closer look of the angles used for separating into octants

Then, for each octant region, the average RGB values were obtained for the image outside the lesion (skin) for every octant region specified above, as shown by the following algorithm:

```

For octant = 0 to octant = 7
{
    for y = 0 to y_res
    for x = 0 to x_res
        if image[y][x] = skin AND inside octant specified above
            temp_R= image[y][x] + temp_R;
            temp_G= image[y][x] + temp_G;
            temp_B= image[y][x] + temp_B;
            count1 =count+1;

    ave_R [octant] = temp_R / count
    ave_G [octant] = temp_G / count
    ave_B [octant] = temp_B / count
}

```

Thus, from this algorithm, and average RGB outside the lesion was obtained for every pixel inside the specified octant region, so there would be 8 values of the average red, green and blue of the images outside the lesion. Later, in order to obtain the relative RGB, every RGB value for every pixel of the image was subtracted the average RGB and then added 255 (max value for red, green, or blue).

The algorithm used to calculate the relative RGB is shown below:

```

For octant = 0 to octant = 7
{
    for y = 0 to y_res
    for x = 0 to x_res
        if inside octant specified above
            rel_R [y][x] = image[y][x] - ave_R [octant] + 255;
            rel_G [y][x] = image[y][x] - ave_G [octant] + 255;
            rel_B [y][x] = image[y][x] - ave_B [octant] + 255;
}

```

Notice that by using this algorithm, some memory and run-time is actually being wasted due to the fact that the octant regions overlap. Therefore, in order to correct this problem, a new octant region can be specified without including the 5° error angle and instead separate each octant region by 45°.

Thus, it is important to mention that all the steps described up to this point were implemented by Kapil Gupta in C. I was responsible for implementing the remainder of the algorithm. Hence, after that, the relative RGB of the image was mapped into a 3D array of 128x128x128 as shown by the following algorithm.

```
for y = 0 to y_res
for x = 0 to x_res
    tmp_r = rel_R [y][x] / 4;
    tmp_g = rel_G [y][x] / 4;
    tmp_b = rel_B [y][x] / 4;

    img_hist [tmp_r][tmp_g][tmp_b] = img_hist[tmp_r][tmp_g][tmp_b]+1;
```

Notice that `img_hist [][][]` represents the 128x128x128 3D array, which is then used to create the histogram that is a text file that includes information like location in array and value of all the nonzero values of the `img_hist [][][]` array. The algorithm used to write the text file histogram is shown below:

```
for x = 0 to 128
for y = 0 to 128
for z = 0 to 128
    if img_hist[x][y][z] != 0
        write to text file ( x    y        z        img_hist[x][y][z])
```

Finally, a text file containing the names of the list of images that would be analyzed was created (512 images-175 melanomas and 337 benign and dysplastic nevi). Then, the location and name of the text file with the list of images, and the location of the color and border graphic files of the images were specified. After that, the code was compiled and run. Lastly, after the histogram for the 512 images was created, the fuzzy ratio features were computed and lesion discrimination was performed using the fuzzy ratio color feature. The following section overviews the calculation of the fuzzy ratio feature.

Overview of Fuzzy Ratio Feature Calculation

First of all, let \mathbf{B} denote the fuzzy set for relative skin lesion color based on a set of training images [2]. Then let denote the function. $\mu_{\mathbf{B}}(x)$ as $\mu_{\mathbf{B}} = \begin{cases} x / F & \text{for } 0 \leq x < F \\ 1 & \text{for } x \geq F \end{cases}$

[2], where x is the number of hits in a bin over a set of images \mathbf{B} , and F is the bin frequency count. Later, let denote $|\alpha \mathbf{B}|$ as the cardinality of the α -cut related to \mathbf{B} , where

α can be represented as $\mu_{\mathbf{B}}(C(x,y)) \geq \alpha$ where $C(x,y)$ is the relative color bin into which

the skin lesion pixels are mapped [2]. Finally, let $|S(\mathbf{B})|$ denote the cardinality of $S(\mathbf{B})$

[2], where $S(\mathbf{B})$ is the number of nonzero pixels with nonzero membership in \mathbf{B} . Hence,

the fuzzy ratio is defined as $R(\alpha) = \frac{|\alpha \mathbf{B}|}{|S(\mathbf{B})|}$ where the pixels used to compute $R(\alpha)$ are

considered to be inside the skin lesion, so the average color outside the lesion is just used to determine the relative color [2].

Therefore, it can be said that If \mathbf{B} represents the fuzzy train set for benign skin lesion relative color, then $R(\alpha)$ represents how much benign colors within the skin lesion can actually be associated to benign skin lesions for that train set of images[2], so as α increases, $\alpha \mathbf{B}$ contains pixels that are more lightly to be recognized as benign lesion pixels.

Finally, it can be concluded that if a given skin lesion is benign, then $R(\alpha) > T$ where T represents the threshold and it is estimated by computing the true positive or correct melanoma detection (tp), and true negative or correct nevi detection (tn) rates of a training data set. In order to choose an optimal value of T , it has to be iterated through the

sorted ratios of $R(\alpha)$ (from 0 to 1) in increments of 0.001, so that for each T , tp and tn are determined from the training set. Thus, T is chosen so that $tp = tn$. Moreover, it may be possible that tp and tn are not equal for a specified value of T . In that case, if T_i results in $tp < tn$ and T_{i+1} results in $tp > tn$ (or the exact opposite way), then T_i is an optimal value of the threshold T .

Experiments Performed, Experimental Results, and Conclusions

The fuzzy ratio feature was computed for alpha values of 0.1, 0.2, 0.3, 0.4, and 0.5 for 25 randomly generated training and test sets from a dermoscopy image set of 512 images (175 melanomas and 337 benign lesions). The following results were obtained for the average correct melanoma detection (tp) and correct nevi detection (tn) over 25 randomly generated set, where 90% were train images and 10% were test images.

	$\alpha = 0.1$		$\alpha = 0.2$		$\alpha = 0.3$		$\alpha = 0.4$		$\alpha = 0.5$	
	tp	tn	tp	tn	tp	tn	tp	tn	tp	tn
Approach 1	0.821	0.711	0.807	0.695	0.784	0.685	0.771	0.689	0.776	0.704
Approach 2	0.727	0.684	0.706	0.681	0.704	0.68	0.706	0.68	0.701	0.681

TABLE 1: comparison of detection results

Approach 1 is the single average RGB surrounding skin value approach, and approach 2 is the octant-based RGB surrounding skin value approach performed in this project. Thus, the following results were calculated using the fuzzy ratio feature for different values of α and it can be seen that approach 1 has a better detection average than approach 2. In fact, approach 1 is much more accurate when correctly detecting melanoma, but for benign images, both approaches do get close results. However, it is important to mention that a false detection of nevi is much safer than a false detection of

melanoma because the consequences of delaying therapy for melanoma are worse than in unnecessary treatment.

Acknowledgments

First of all, I would like to thank Dr, Stanley for his advice and support, for giving me the chance to work directly with him, and for the experience and skills I learned while working in OURE. Also, I would like to thanks Dr. Stoecker and Dr. Moss for giving me the opportunity of being part of this research group. Finally, I would like to thank Kapil Gupta for his help throughout this OURE project.

References

- [1] Jemal A, Thomas A, Murray T, Thun M. Cancer statistics, 2002. *Ca: a Cancer Journal for Clinicians* 2002;52(1):23-47.
- [2] Stanley RJ, Moss RH, Stoecker WV, Aggarwal C. A fuzzy-based histogram analysis technique for skin lesion discrimination in dermatology clinical images. *Computerized Medical Imaging and Graphics* 27:387-396, 2003.
- [3] Friedman RJ, Rigel DS, Kopf AW. Early detection of malignant melanoma: the role of physician examination and self-examination of the skin. *Ca-A Cancer Journal for Clinicians* 1985;35(3):130-151.
- [4] Faziloglu Y, Stanley RJ, Moss RH, Stoecker WV, McLean RP. Color histogram analysis for melanoma discrimination in clinical images. *Skin Research and Technology* 9:147-155, 2003.

**A Methodology to Assess Critical Infrastructures
and Their Relevance to Missouri**

OURE 2004-2005

Final OURE Report 2005

University of Missouri-Rolla

Nuclear Engineering

Research done by

Ms. Tricia Mattson

In collaboration with

Dr. Akira Tokuhiko

Submitted to Office of Undergraduate and Graduate Studies

On

April 1, 2005


Tricia Mattson

A Methodology to Assess Critical Infrastructures and Their Relevance to Missouri

Tricia Mattson
University of Missouri – Rolla

ABSTRACT

September 11, 2001, a day when thousands of lives were lost under unexpected and unprecedented circumstances, marked the beginning of a difficult national reality; that is, the vulnerability of our society and our infrastructures to terrorist attack. The events of that day have shaken the very foundations of national and the newly coined, “homeland security”. It is apparent that changes need to be made to the national/homeland security infrastructure at all levels. But how will change be brought about and what “roadmap” will we follow?

The research team of Dr. Tokuhiro has been studying complex social-technological issues. We are especially interested in how society will protect its sensitive materials and installations in the post-9/11 environment. One promising way appears to be an approach based on “eigenmetrics”; that is, largely on time and countable arguments (“numbers”) that apply to local, state and national security issues. Our approach provides a foundation, beyond endless discourse. The project presently consists of surveying the *9/11 Commission Report* and the *National Response Plan*. We will extract the overarching time- and number-scales from these reports and provide relevant examples for the State of Missouri.

INTRODUCTION

After the terrorist attacks of 9/11, the government went into a frenzy seeking answers and trying to build a plan that would prevent events of the same magnitude from occurring again. The *National Strategy for Homeland Security*, the *National Strategy for the Physical Protection of Critical Infrastructures and Key Assets*, the *National Incident Command System*, the *9/11 Commission Report*, and the *Initial National Response Plan* provided the fundamental ideas and drafts of the final *National Response Plan*. This comprehensive plan provides a template for any disaster that could occur on U.S. soil. However, the plan is based on the assumption that every state has an integrated organization, communication capabilities among all critical infrastructure, key asset, and emergency response entities, and an incident command system. There is also no clear way of enforcing the plan among states. Missouri is one of the states not yet ready to implement the *National Response Plan*. Missouri doesn't quite meet the assumptions of the plan, however, Missouri's homeland security program is about average compared to other states. On all levels—national, state, and local—the *National Response Plan* is going to take a lot longer than originally expected to fully implement.

National Strategies

On October 8, 2001 President George W. Bush established the Office of Homeland Security along with its first responsibility of producing the *National Strategy for Homeland Security*. This strategy would be the first in a string of documents that analyze the state of homeland security and make recommendations for improvement.

The *National Strategy for the Physical Protection of Critical Infrastructures and Key Assets* focuses on one of the critical mission areas outlined in the *National Strategy for Homeland Security*: protecting critical infrastructures and key assets. Key assets include national monuments and icons, government facilities, and nuclear power plants. The *National Strategy for the Physical Protection of Critical Infrastructures and Key Assets* gives the Nuclear Regulatory Commission (NRC) the responsibility of developing a standard methodology for conducting vulnerability and risk assessments, improving the capabilities of nuclear power plant security forces, and enhancing public outreach and awareness programs and emergency preparedness programs. (NUCLEAR POWER PLANTS 74) This document serves as a connection between the *National Strategy for Homeland Security* and the *National Response Plan* (NRP).

9/11 Commission Report

In late 2002, President Bush formed the 9/11 Commission on Terrorist Attacks Upon the United States (9/11 Commission). The Commission's purpose was to complete a full report of findings, analysis, and recommendations surrounding the attacks of 9/11. On July 22, 2004 the Commission released the 9/11 Commission Report. The report outlined the events surrounding the World Trade Center (WTC) attack and made bold conclusions as to why the tragedy was allowed to occur. Two of the conclusions can be linked to nuclear security. These problematic areas are lack of an integrated communications system and lack of an incident commander (IC). If a nuclear disaster were to occur today, an effective communications system and an IC would be necessary to minimize the aftermath of the attack.

In terms of eigenmetrics, numbers can be extracted from the 9/11 Commission Report and applied to different situations on national, state, and local levels. The following numbers can be extracted for the WTC:

	total amount	initially responded
FDNY members	11,000	235
FDNY engine companies	205	21
FDNY ladder companies	133	4
NYPD members	40,000	922

elevators per tower	99
acres per floor	≈1
floors per tower	110
height of tower (ft)	1350

length of walls (ft)	208
number of central stairwells	3
number of windows	21,800
number of emergency exits	800
number of office workers	50,000

These numbers can possibly be applied to an incident on the state or local level and compared to highlight inefficiencies in pre-event, event, and post-event phases of an incident.

Incident Command System

The 9/11 Commission Report states, "If New York and other major cities are to be prepared for future terrorist attacks, different first responder agencies within each city must be fully coordinated, just as different branches of the U.S. military are. Coordination entails a unified command that comprehensively deploys all dispatched... first responder resources." (HEROISM AND HORROR 321)

Recent military operations in Afghanistan and Iraq have been steady and successful, especially compared to the military's prosperity in the Vietnam War and the First Gulf War. The Goldwater-Nichols Department of Defense Reorganization Act of 1986 is responsible for this change in the military's efficiency. The Goldwater-Nichols Act passed because of previous problems of rivalry among different branches of the military in the Vietnam War and the Iranian hostage rescue mission of 1980¹. The act unified military responsibilities under one Chairman of the Joint Chiefs, creating a unified command or an "incident commander" for the military.

A similar type of incident command was used on September 11th at the Pentagon and presided over all of the emergency responders and regions involved. Of all local, regional, state, and federal agencies responding to the Pentagon attack, one incident commander was quickly established to take control of rescue and relief efforts. While it is impossible to compare the attacks on the Pentagon and the WTC, it is obvious to see that the presence of an incident commander, organization, and communication improves emergency response by magnitudes.

The definition of Incident Command System (ICS) is the combination of facilities, equipment, personnel, procedures, and communications operating within a common organizational structure, designed to aid in domestic incident management activities. The ICS should have a command post somewhere near the location of the incident and communication capabilities with all of the emergency relief parties. For maximum efficiency of emergency response during an incident, it is necessary to establish an ICS. It is therefore necessary that planning for the execution of incident command systems should be implemented over the entire nation. Both the *9/11 Commission Report* and the *National Response Plan* recognize this need.

¹ Definition taken from Wikipedia's Goldwater-Nichols Act, 27 Mar 2005, at http://en.wikipedia.org/wiki/Goldwater-Nichols_Act

Homeland Security Presidential Directive - 5

The *Homeland Security Presidential Directive* (HSPD-5) was published to establish a single, comprehensive approach to domestic incident management. HSPD-5 made the following demands of the Homeland Security Secretary, Tom Ridge: publish an *Initial National Response Plan* by April 1, 2003. This was accomplished as a draft for the final *National Response Plan*.

By request of the HSPD-5, the *National Incident Management System* document was issued by Secretary of Homeland Security, Tom Ridge, to provide a standardized national plan to help Federal, State, and local governments and private sector organizations to work together in the event of a domestic incident like a terrorist attack. State, local and tribal governments to work together effectively and efficiently to prepare for, prevent, respond to, and recover from terrorism.

National Response Plan

In December 2005, after the establishment of the *National Strategy for Homeland Security*, *National Strategy for the Physical Protection of Key Assets and Critical Infrastructures*, *Presidential Directive for Homeland Security – 5*, *National Incident Management System*, and *9/11 Commission Report*, the United States Department of Homeland Security established a comprehensive template for all domestic emergency response efforts called the *National Response Plan*. This plan provides the framework for response to any possible domestic incident. It affirms the use of an incident command system, the establishment of an organization among all levels (national, state, and local), the establishment of a working communications system between all critical infrastructure, key asset, and emergency response entities.

The purpose of the NRP is to establish a comprehensive, national, all-hazards approach to domestic incident management across a spectrum of activities including prevention, preparedness, response, and recovery (NRP 2). The plan explicitly states the need for an integrated organization of all critical infrastructure, key asset, and emergency response entities, an incident command system, and an integrated communications system. Without this type of system, none of the Emergency Support Function Annexes, Support Annexes, or Incident Annexes established by the NRP to provide incident-specific support would prove to be useful. Together, the NRP and the NIMS integrate the capabilities and resources of various governmental jurisdictions, incident management and emergency response disciplines, nongovernmental organizations, and the private sector into a cohesive, coordinated, and seamless national framework for domestic incident management (NRP 1).

The NRP establishes the Nuclear/Radiological Incident Annex. This annex delegates the mitigation and consequences responsibility to the owner of the nuclear/radiological facility involved in the accident. They are responsible for notifying the state and local

government and containing any radiation. Any owner of a nuclear/radiological facility can request help directly from the United States Department of Homeland Security.

The greatest shortfall of the NRP is there is no entity to ensure states will implement the organization the NRP assumes. The Department of Homeland Security is responsible to make sure all annexes are fully functional and being used properly, but they have no role in making sure states have an organizational structure or means of communication throughout the structure.

Establishment of organization/integration among levels

The national level includes all national governmental bodies, the president and Congress. The national level is responsible for helping to fund clean up efforts, analyzing the situation and dealing with the psychological effects the disaster would have on society. This level encompasses all critical infrastructure, key asset, and emergency response entities in all of the state levels.

The state level includes all state government bodies. The state is responsible for making sure local first responders are being timely and efficient, distributing federal funds to appropriate local and state entities, and relaying information and implementing security policies to the local entities.

The local level includes all first responders, fire fighters, police officers, and emergency management personnel. The local level responders are the first on the scene of the incident, and are the last to leave the scene. It is the quickness of efforts from the local level that will minimize the aftermath of the disaster.

There needs to exist an integration and coordination of all levels. This organization will reduce redundancy of actions, put all efforts in unison with one another, and increase the efficiency of the operation as a whole. In order to keep and maintain a functional organization below the state level of all critical infrastructure, key asset, and first responder entities, it is necessary to hold semiannual meetings, sustain a fusion center (usually the state highway patrol agency), and have entities report to the state homeland security office frequently. In order to maintain a working organization below the national level, it is important that the federal government establish clear and concise homeland security laws and orders. If the state is uncertain about certain documents or orders, nothing will get done. For example, the national government has implemented the National Response Plan as the core, comprehensive, operational plan for domestic incident management, but the requirements for state execution of the plan are unclear.

Evaluating an Event in terms of Phases

In addition to evaluating security on the national, state, and local levels, it is valuable to evaluate an attack in terms of time phases. An attack can be broken into pre-event, event, and post-event phases.

The pre-event stage includes planning, funding distribution, training, integration and information sharing among common entities, use of an integrated organization of critical infrastructure, key asset, and emergency response entities, and the establishment security policies. The pre-event time phase deserves greater attention considering the actions taken during this phase can alter the other two phases significantly. For example, a skydiver is in greater danger if he were to jump out of a plane without a parachute and having ambulances on site, than if he were to jump out with a parachute and a Band-Aid. Having the parachute will most likely eliminate the need for first aid. In comparison, having more funds and time spent with the pre-event time phase will provide a wall of protection. Only if a terrorist attack cannot be prevented in the pre-event time phase, will the incident leak through to event and post event.

The event stage includes use of funding, detection, first responders, and establishment of an ICS. This is the phase that determines whether the terrorist attack will be success or a failure. The use of funding, planning, and training is tested during this phase. The event phase is usually the shortest phase in terms of a timescale.

The post-event stage includes clean-up, containment, analysis of event, public communications, and restoring public confidence. This phase is hard to predict because it depends completely upon the success of the pre-event and event phases.

This method is especially useful when analyzing risk. The risk that something will occur in the event stage is totally dependent upon what happens in the pre-event stage. The actions that take place in the post-event stage are dependent upon the event stage, and therefore the risk is dependent upon the pre-event stage.

Nuclear Risk Analysis in Time Phases

Time Phase	Pre-event	Event	Post-event
Risk Analysis	Probability of specific accident scenarios	Potential radiation release from the plant	Potential public health consequences

Using a chart like this can help in analyzing the probability of an event occurring and determine how big a risk the situation carries.

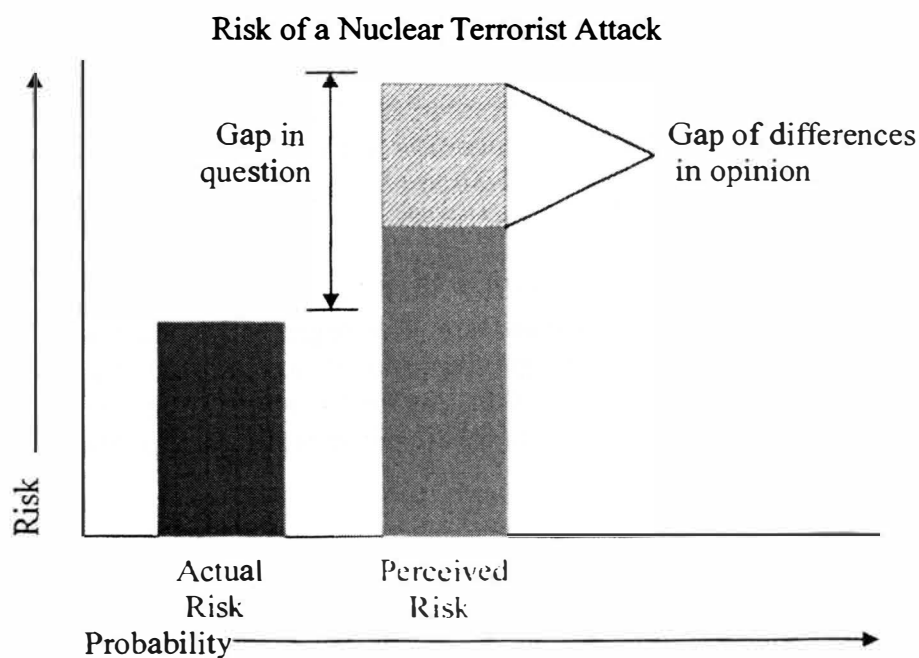
Importance of Public Relations

Aside from the recommendations made in the 9/11 Commission Report and the strategies established in the National Response Plan, there are other, less direct methods for fighting against nuclear terrorism. Nuclear terrorism is the use or threatened use of a nuclear mechanism against civilians with the purpose of instilling fear in societies for political or religious reasons. This definition encompasses the use (or threatened use) of nuclear weapons, radiological dispersion devices, or nuclear reactors as weapons. Using this definition to isolate the root of nuclear terrorism, the authors have evaluated a different approach to preventing a terrorist attack on a reactor.

A more overlooked option for fighting nuclear terrorism is decreasing the desirability of nuclear reactors for terrorists. We have to ask ourselves, if society gains a better understanding of nuclear safety, could that itself decrease the desirability of nuclear reactors to terrorists? It is the opinion of the authors that gaining public acceptance would significantly decrease the risk of nuclear reactors as terrorist targets.

A better understanding of nuclear safety by the public would increase reactor credibility. Improving the credibility would take definition out of nuclear terrorism. This is because once the public understands the risk of a terrorist using a nuclear plant against society, there will be less of a psychological scare factor for the terrorist to use. This would make nuclear reactors less desirable for a terrorist attack.

One way to increase reactor credibility is to reduce public perceived risk. Nuclear safety is numerically represented by the term “risk” which is very subjective; each person perceives it differently. Perceived risk is larger than actual. There needs to be a reduced gap between perceived and actual risk. This would enhance public acceptance. Increasing actual risk to close the gap would obviously be counterproductive, so there needs to be a decline in perceived risk. The following graph depicts the situation described:



The question is how can public perceived risk be decreased? To answer this question risk measurements must be analyzed. Nuclear risk assessment involves likelihood and probability. For example, if the likelihood that an accident will occur is great, so is the risk. There is a probability that a smoker will develop some sort of lung-related disease at some point in their life. The bigger the probability for the disease, the bigger the risk the smoker is taking for contracting the disease. If the general public can recognize there is a

small likelihood or probability of a nuclear attack occurring, the corresponding risk would also be small. Helping society recognize this idea can be accomplished by several means:

- Increasing political support
- Handing out public educational tools (informational pamphlets, videos, etc.) to areas surrounding reactors
- Holding press conferences
- Conducting lectures and forums open to the public
- Taking a grassroots initiative
- Gaining media cooperation

Homeland Security in Missouri

Even though the Missouri Homeland Security Office was the first state office established after 9/11, Missouri still has a long road ahead in improving homeland security. Missouri is in the very preliminary stages of implementing the National Response Plan. There are no enforcing entities to guarantee full implementation for Missouri, and there needs to be a better communication of the plan between national, state, and regional levels. The basic roots of Missouri's homeland security needs will come from full implementation of the NRP.

In Missouri, more focus needs to be placed on the pre-event phase. Missouri is lacking in efforts made in the areas of: distribution of funding, integration and information sharing among common entities, and use of an integrated organization of critical infrastructure, key asset, and emergency response entities.

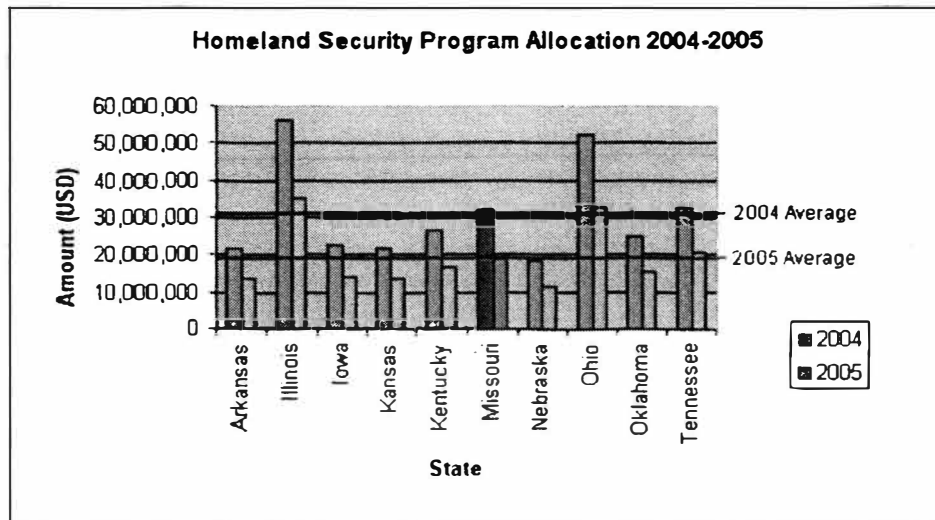
First, there needs to exist an organization among all entities in Missouri involving a state key asset, critical infrastructure, or emergency response team. This organization must be arranged so actions can be streamlined to appropriate groups or people in the event of an emergency. The establishment of this organization would allow for Missouri to improve integration and standardization among common entities, funding distribution, and public relations.

Once the organization is established, there needs to be semi-annual collaborative meetings of common entities. For example, one of these collaborative meetings would include all groups that deal with nuclear materials. Representatives from UMRR, MURR, Callaway, Cooper, and Fort Leonard Wood would attend the meeting to share information and discuss pertinent security issues. These information-sharing sessions would help the entities standardize their safety and emergency plans.

Missouri receives \$125 million in federal funds for homeland security. Approximately 20% of federal funds are supposed to support homeland security on the state level. The remaining 80% of funds are supposed to support homeland security on the local level. Missouri has spent less than 25% of this federal grant money. The reason for the inefficiencies in grant spending is largely due to the lethargic distribution of funds across

both the national to state levels and the state to local levels. If Missouri had an organization, funds received from the government can be allocated and streamlined to appropriate groups faster and more efficiently. An example of an area of funding distribution that needs improvement is Missouri's development of the Joint Information System established in NIMS. The Missouri Homeland Security Annual Report for 2003 states that one of the additional needs toward ...for the department is "The State should consider taking the first steps toward establishment of a Statewide Communications system." Nothing has been done since the publication of the report in terms of establishing a statewide communications system because no organization exists among the levels of state key asset and critical infrastructure entities. There are no defined groups to distribute communication services and equipment.

Missouri does receive enough funding from the government to ensure a safe place for residents. \$20 million of the total comes from the Homeland Security Grant Program



NOMENCLATURE

Initial National Response Plan (INRP) – document published by the Department of Homeland Security as the first step in aligning incident management response and actions between all Federal, state, tribal, local, and private communities. Later to be superseded by the final National Response Plan

Nuclear Regulatory Commission (NRC) - The U.S. Nuclear Regulatory Commission (NRC) is an independent agency established by the Energy Reorganization Act of 1974 to regulate civilian use of nuclear materials.

Missouri Security Panel – A governor appointed (Executive Order 02-15 and Executive Order 02-16) panel organized to examine Missouri security and propose recommendations for improvement in communication, security of critical infrastructures and public safety

ACKNOWLEDGEMENTS

Dr. Tracia (West) Love
Sandia National Laboratories
University of Missouri-Rolla

Michael Chapman
Missouri Homeland Security Director
Missouri Homeland Security Office

Dr. Akira Tokuhiro
Assistant Professor Nuclear Engineering Department
University of Missouri-Rolla

REFERENCES

- The Nuclear Energy Institute, *Safety Benefits of Risk Assessment at U.S. Nuclear Power Plants*, March 2002, <<http://www.nei.org/doc.asp?docid=805>>.
- The White House, February 2003, *National Strategy for Homeland Security*, <<http://www.whitehouse.gov/pcipb/physical.html>>.
- The White House, *National Strategy for the Protection of Key Assets and Critical Infrastructures*, February 2003, <http://www.whitehouse.gov/pcipb/physical_strategy.pdf>.
- Federal Emergency Management Agency, *National Incident Management System*, March 1, 2004, <http://www.fema.gov/nims/nims_compliance.shtm#nimsdocument>.
- Missouri Homeland Security Office, *Missouri Strategy for Homeland Security*, November 17, 2004, <<http://www.homelandsecurity.mo.gov/StateStrategy111704.pdf>>.
- United States Government Printing Office, *9/11 Commission Report*. July 2004, <<http://a257.g.akamaitech.net/7/257/2422/05aug20041050/www.gpoaccess.gov/911/pdf/fullreport.pdf>>.
- U.S. Department of Homeland Security Office for Domestic Preparedness, *Fiscal Year 2005 Homeland Security Grant Program*, <<http://www.ojp.usdoj.gov/odp/docs/fy05hsgp.pdf>>.
- U.S. Department of Homeland Security Office for Domestic Preparedness, *Fiscal Year 2004 Homeland Security Grant Program*, <http://www.ojp.usdoj.gov/odp/docs/fy04hsgp_appkit.pdf>.
- U.S. Department of Homeland Security Office for Domestic Preparedness, *Fiscal Year 2003 State Homeland Security Grant Program – II*, <<http://www.ojp.usdoj.gov/odp/docs/fy03shsgp2.pdf>>.
- U.S. Department of Homeland Security Office for Domestic Preparedness, *Fiscal Year 2003 State Homeland Security Grant Program*, <<http://www.ojp.usdoj.gov/odp/docs/ODPApplication.pdf>>.
- U.S. Department of Homeland Security Office for Domestic Preparedness, *Fiscal Year 2002 Domestic Preparedness Grant Program Application Kit*, <<http://www.ojp.usdoj.gov/odp/docs/02odpkit.pdf>>.

**PROGRESS ON THE ORIGIN OF PEGMATITE DIKES AND PODS IN THE MOUNT
SHERIDAN GABBRO, OKLAHOMA**

Andrew McEllen

Project Advisor Dr. Hogan

March 25, 2005

ABSTRACT

The Mount Sheridan Gabbro of the Wichita Mountains of south western Oklahoma contains dikes and pods of a coarse grained pegmatite. Initial field work was carried out and samples collected. All samples have been slabbed with a rock saw and described. These samples reveal spectacular examples of the minerals amphibole, feldspar, quartz, and apatite and zircon. The minerals apatite and zircon were investigated using the SEM as part of a class. From these slabs, representative examples have been selected for making thin sections. These are prepared by a commercial lab and I am awaiting their return. I can then complete my descriptions with a petrographic microscope. Rock powders have been prepared for geochemical analyses pending installation of the LAICPMS at UMR. I will also complete geochemical analyses of individual minerals using this equipment and the thin sections.

INTRODUCTION

The Mount Sheridan Gabbro of the Wichita Mountains of south western Oklahoma contains dikes and pods of a coarse grained pegmatite (Fig. 1). Dikes of the material can be found throughout the body of rock, but with greater abundance of large dikes in the middle parts of the pluton with some over one meter in thickness. The dikes exhibit clear cross-cutting relationships with the gabbro. Pods of the material are common in the lower and middle areas of the pluton and are commonly intimately associated with the gabbro.

These initial observations suggest two possible hypotheses for the origin of the pegmatite. Are these pegmatites derived from Gabbro by extreme fractional crystallization? In this model the pegmatites form by the coalescence of pods of felsic material into dikes due to filter pressing of the gabbro. Are the pegmatites the result of a separate intrusive event? There is a large amount of granite which was emplaced around the gabbro. The pegmatite magma may have had its source from one of these granites and intruded into the gabbro. By establishing a crystallization age on these dikes, the minimum age of the gabbro's crystallization can be constrained.

The goal of this project is to test these hypotheses. To do this, the distribution of pegmatite in the Mount Sheridan Gabbro was mapped. I have completed one field season, and based upon my initial result I am planning on a second field season this summer. Samples have been collected for petrographic and chemical analysis. Unfortunately, due to delays with an outside company and delays in installation of the LAICPMS several portions of the project are still needed to test the hypotheses. Although I have described in detail hand samples and sawed slabs, a complete mineralogical description of the pegmatite using thin sections and a petrographic microscope must still be done. Interpretation of whole rock chemical analyses done by a commercial lab cannot be done yet. Once thin sections are returned from the commercial lab, a visit to use the electron microprobe facilities at the University of Oklahoma for compositional characterization of minerals will hopefully be made. When the new LAICPMS instrument at UMR is installed, an attempt to determine the age of crystallization for these dikes will be made.

FIELD WORK

During the first to fourth of June 2004 field work for this project was conducted in the Wichita Mountains of Oklahoma. During this excursion, Dr. Hogan, Daniel Lasco and I made several trips to the mountain to collect data and samples for Daniel Lasco's masters research and this OURE from the Mt Sheridan Gabbro and its associated pegmatites. On the mountain, each outcrop was recorded using GPS. All pegmatite dikes were measured using a Brunton compass to obtain their orientation of each dike present. In addition, the thickness of each dike was recorded. Dikes and pods were classified based on amphibole characteristics and rock texture; small amphibole pegmatite dikes (SAPD) (Fig. 1), combed small amphibole pegmatite dikes (SACP) (Fig. 2), large amphibole pegmatite dikes (BAPT) (Fig. 3), combed large amphibole pegmatite dikes (BAPC) (Fig. 4), hair line dikes (HLD) (Fig. 5), and granitic dikes. Samples were taken of any dike which had little weathering, had good exposure, and were representative of an outcrop. In addition some samples were taken of dikes which appeared to have unusual compositions or positions in the pluton.



Image 1: SAPD dike, this material is commonly found in the smaller dikes (3-20cm) and pods and is typified by a relatively even distribution of blocky amphibole crystals

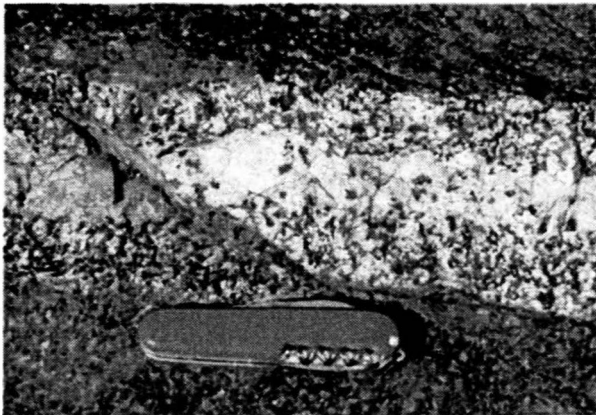


Image 2: SACP dike, composed of a pegmatite which that is enriched in amphibole near the contact with the Gabbro, while the inner portion of the dike is filled with a more felsic or SAPD material. Like the SAPD type dikes and pods, all amphiboles in these dikes are of the small blocky variety.



Image 3: BAPT dike, composed of a pegmatite characterized by large, hollow, tabular amphiboles with little or no comb of large tabular or small blocky amphibole crystals on the walls of the dike.



Image 4: BAPC dike, dikes containing large, hollow, tabular amphibole crystals with a comb of small blocky and tabular crystals protruding into the dike from the walls.

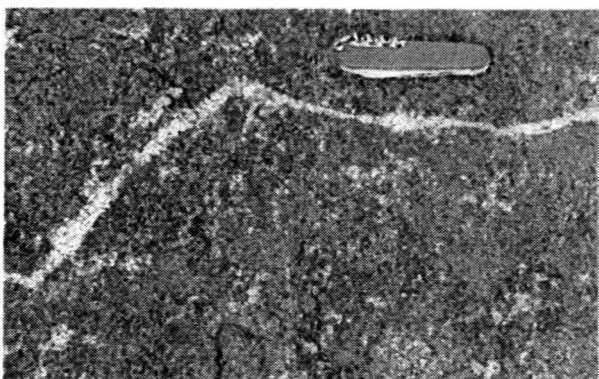


Image 5: HLD type dikes are small, filled fractures. These dikes are characterized by small width and lack of amphiboles.

SAMPLE PREPARATION

Once the samples were returned to the lab they underwent preparation for analysis. Each sample was cut into slabs approximately one centimeter thick using a Hillquist slab saw. The slabs were then examined and the most representative and unusual areas were cut into thin section blanks; matchbook sized pieces of stone, using a Felker cutoff saw. The remaining slabs were polished using five stages of grinding on a lap in order to remove saw marks.

Two of the samples were large enough for whole rock chemical analysis. The original samples were cut into slabs, and blanks for thin sections were extracted and a set of representative slabs were set aside. For chemical analysis, the rock must first be reduced to a powder form. In order to reduce a sample to the desired grain size, several steps are taken. First the sample is broken by hammer into pieces half the size of a fist or smaller. In addition, the weathered material on the samples was removed using the hammer to prevent contamination from recent chemical changes in the sample. The broken fragments are then placed into a Bico Inc. jaw rock crusher to reduce the size of fragments to less than ½ centimeter on an edge. At this point the material is small enough that it can be introduced into a tungsten carbide shatter box. After several minutes in the grinder the material is a rock flour of the proper size for chemical analysis. The thin section blanks and whole rock chemical samples were sent off to a company in December.

ANALYSIS

Until thin sections and chemical samples are returned, little more can be done to analyze the samples at this point in time. Some analysis was done using the JEOL T330 on samples collected and made into polished sections by Dr. Hogan several years ago. Standardless EDS x-ray spectra were taken for several accessory minerals. In addition, several EDS maps were produced of pegmatite samples (Fig. 6).

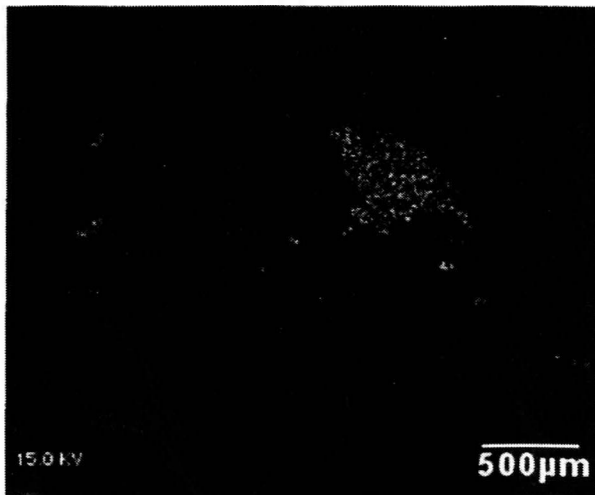


Image 6: Compositional false color eds map of pegmatite polished section.

Once the thin sections returned by the outside company, more analysis will be done to complete this project. The thin sections must be polished before they can be analyzed using transmission light microscopes and before they can be analyzed for compositional variation with the electron microprobe facilities at the University of Oklahoma. The new LAICPMS instrument at UMR will be used for an attempt to determine the age of crystallization of these dikes.

OBSERVATIONS

Visual analyses of slabs taken from samples collected for this project suggest that the majority of pegmatites are genetically related. There is a smooth transition in the groundmass texture as well as amphibole types and quantities between each type of pegmatite, ranging from SAPD type to BAPC dikes. The granitic type dikes are variable in texture and amphibole types, with some appearing to be related to pegmatites, while others do not. Dikes have a preferred orientation in the gabbro, indicating a uniform stress regime at the time of emplacement. The distribution of dikes is more complete than first suspected; nearly all outcrops in the gabbro had some pegmatites in them. The pegmatites appeared to have a decrease in amphibole concentrations, and increase in amphibole crystal size with increased elevation in the Gabbro.

CONCLUSIONS

Preliminary field observations and description of hand samples and sawed rock slabs has been used to recognize and describe distinct types of pegmatite in this gabbro. Several of these pegmatite occurrences appear to be texturally related. This suggests that the different types of pegmatite represent sequential stages in the segregation of felsic magma to form first pods and then eventually dikes. In order to more fully develop my model for pegmatite formation I would like to make additional field observations and analyze thin sections and rock powders.

NOMENCLATURE

Dike: Tabular body of igneous rock that cuts across a structure of massive rocks.

Pod: Small body of pegmatite, usually between 45cm and 5cm in their longest direction.

Pods are normally ellipsoid in shape, but often times irregular. They are filled with SAPD type pegmatites, and some times lack a definite boundary with the host gabbro.

LAICPMS: Laser ablation inductively coupled plasma mass spectrometry is a technique used for the in place analysis of trace elements in solid samples.

EDS: Energy Dispersive Spectroscopy technique on a SEM

Acknowledgements

I would like to thank my advisor Dr. Hogan for his help on all aspects of this project, Daniel Lasco for his help in the field and insights into this area and the OURE program for funding.

NetExaminer: A Network Visualization Tool

Justin Miller

Abstract

The purpose of NetExaminer is to provide a tool that can visualize the condition of a network without communicating with the network being monitored. The application is written for operating systems that support wxWidgets, a cross-platform GUI toolkit. MySQL was used to provide the data for NetExaminer. Whereas most tools for gathering and displaying security related information available today display data in a readout form, NetExaminer attempts to take the data and display it graphically. The NetExaminer software takes data in from MySQL and generates a list of hosts that matches a pre-defined dynamic criteria. The project has been a great success, and the application will soon be able to isolate defective and volatile hosts from any network that is being monitored by NetExaminer's data aggregation software.

Keywords

network visualization, network monitoring, graphical user interface, MySQL applications, wxWidgets

Introduction

Certain tools already exist to provide low-level monitoring of network conditions. Tools such as Ethereal provide packet-level monitoring, but with the sheer quantity of information available on a network, it is difficult to discern the state of security on a network with simple data observation. By combining tools that are capable of aggregating network traffic data and the NetExaminer application, the process of isolating dangerous hosts is simplified.

Requirements for Operation

The current version of NetExaminer requires a machine with a working compiler (GCC), wxWidgets (libraries and headers), MySQL (if database is not hosted elsewhere), and the X graphics system. A database must be established to contain the data acquired by intrusion detection systems (IDS) or port-scanning software.

Data Acquisition

The data necessary for NetExaminer can be retrieved in many ways. NetExaminer operates from data presented in its MySQL database, so examination of real-time or logged data can be achieved by simply modifying the MySQL database.

NetExaminer User Interface

The overall interface to NetExaminer is centered around the primary window. Upon program startup, each window is kept in memory and hidden from the user, allowing for fast access to all windows. Windows are also kept open to allow for communication between

windows, allowing for new information to ripple through each of the windows as it is added. All data once retrieved from the MySQL database is stored in internal data structures within memory to allow for fast access to data. Since all data is retrieved at once, concurrency issues are all but eliminated, due to the locking of data in the database while the query to the database server executes.

Expandability by Design

A database schema can vary from design to design. NetExaminer was designed therefore to operate off of a small set of data, with the ability to integrate more data as it is needed. While NetExaminer requires a database with specific table structure, not every field is required, allowing for expandability (source code is freely available to expand on the original design), in addition to the ability to not use certain fields. Due to indexing, there is a certain amount of information that NetExaminer needs to operate, fields such as IP address would be necessary for correct operation.

Speed Through Open Communication

Windows inside NetExaminer can communicate via adapters (pointers) between the windows, with the main window containing the primary data structures that all windows need to output data. Through the use of adapters, each window can access any piece of data that is used throughout the application, and changes made through the adapters apply to the entire application. This means that if a user of NetExaminer needs to modify a username, for example, the rest of the application is effected, and the username will appear different in all windows.

Figure 1: Data Flow in NetExaminer

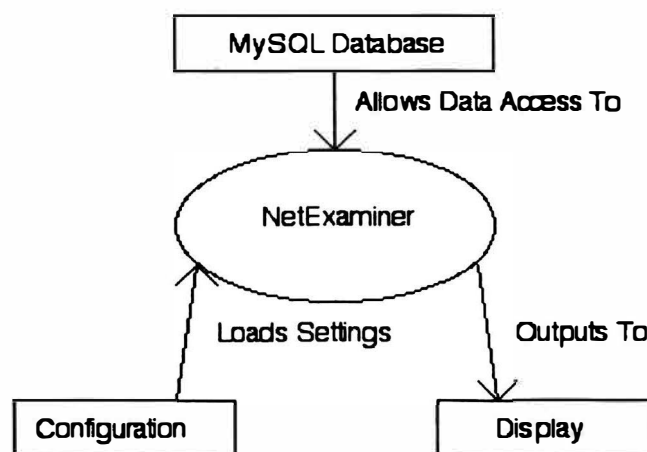


Figure I shows data flow through NetExaminer. Configuration data is loaded from the configuration system (a series of configuration files are read and processed) and MySQL calls are made to access a MySQL database that contains data necessary for NetExaminer's operation. The results obtained from the MySQL database are stored internally and processed by NetExaminer. The processed data is then displayed on the screen.

NetExaminer Configuration

NetExaminer is designed for maximum configurability, and because of this the input must also be configurable.

Cross-Platform Compatibility

By virtue of being written using the wxWidgets toolkit, the NetExaminer application is inherently cross-platform with only a few modifications and a recompile. However, the primary target platform of Linux has presented an excellent alternative for those that do not wish to port it to their target platform. The NetExaminer application can be forwarded over a network using SSH and X, which means that any platform that supports X clients (Windows, OS X, BSD, Linux) can view the application remotely. Examples of this are available in the Screenshots section.

Conclusion

Generic security visualization tools are surprisingly absent from the commercial and free software markets. The open-source community has many free tools for data aggregation, tools such as NMAP (port-scanner), SNORT (lightweight IDS), and Ethereal (packet sniffing). These tools are all excellent resources and work fine for smaller networks, but interpreting the flat log files that these tools generate can be cumbersome for thousands of hosts. With NetExaminer, it is possible to view thousands of hosts, and look only at hosts or groups of hosts that are threatening the network. The modularity of both the configuration and display sections allows for quick changes to both input and output in NetExaminer.

Nomenclature

GUI

GUI is an acronym for Graphical User Interface, and involves the use of a mouse or other input device to navigate a screen interactively, as opposed to a CLI (command line interface), in which data is entered through a keyboard. A GUI toolkit can be used to quickly create applications, and a cross platform GUI toolkit is used to generate applications that can be easily rebuilt on another platform.

Packet-Level Monitoring

Packet-Level Monitoring refers to monitoring traffic across a network at the packet level. Packets are crafted pieces of data that are sent across a network from a source host and decoded at the target host.

Open-Source

Open-Source in the realm of software generally applies to software that has its source code openly available to the public, and does not necessarily imply free use, though in many cases Open-Source is also free.

Intrusion Detection System (IDS)

An intrusion detection system is used to track intrusions made on a network. When coupled with monitoring or an intrusion response system, an IDS can isolate attackers and remove or continue monitoring the intrusion.

Linux

Linux kernel development started in 1992 when Linus Torvalds, a Finnish computer science student, released it to the world on a Usenet group. The Linux kernel is now central to numerous Linux distributions, such as Red Hat, Slackware, SuSE, and Debian. Distributions package tools such as compilers and desktop environments make it easy for developers, users, and server administrators to use. (I)

SSH

SSH stands for secure shell. SSH is essentially a protocol for secure data transmission over a network.

X

X windows is a collection of applications and protocol used as a base for graphical user interfaces on a variety of platforms, including Linux distributions and *BSD releases.

MySQL

MySQL database software is freely available (including source) at <http://www.mysql.com>. The software is open-source, and is scalable from a small office environment to the corporate level. The wide-spread adoption of MySQL and its inclusion in almost every major Linux distribution. (II)

wxWidgets

Julian Smart created what would become wxWidgets in 1992 to facilitate cross-platform development to avoid the high costs associated with commercially available cross-platform development tools. (III)

Ethereal

Ethereal was originally authored by Gerald Combs, and has since been contributed to by numerous individuals and corporations. Ethereal can analyze data from a network or from a captured file on disk. (IV)

Acknowledgments

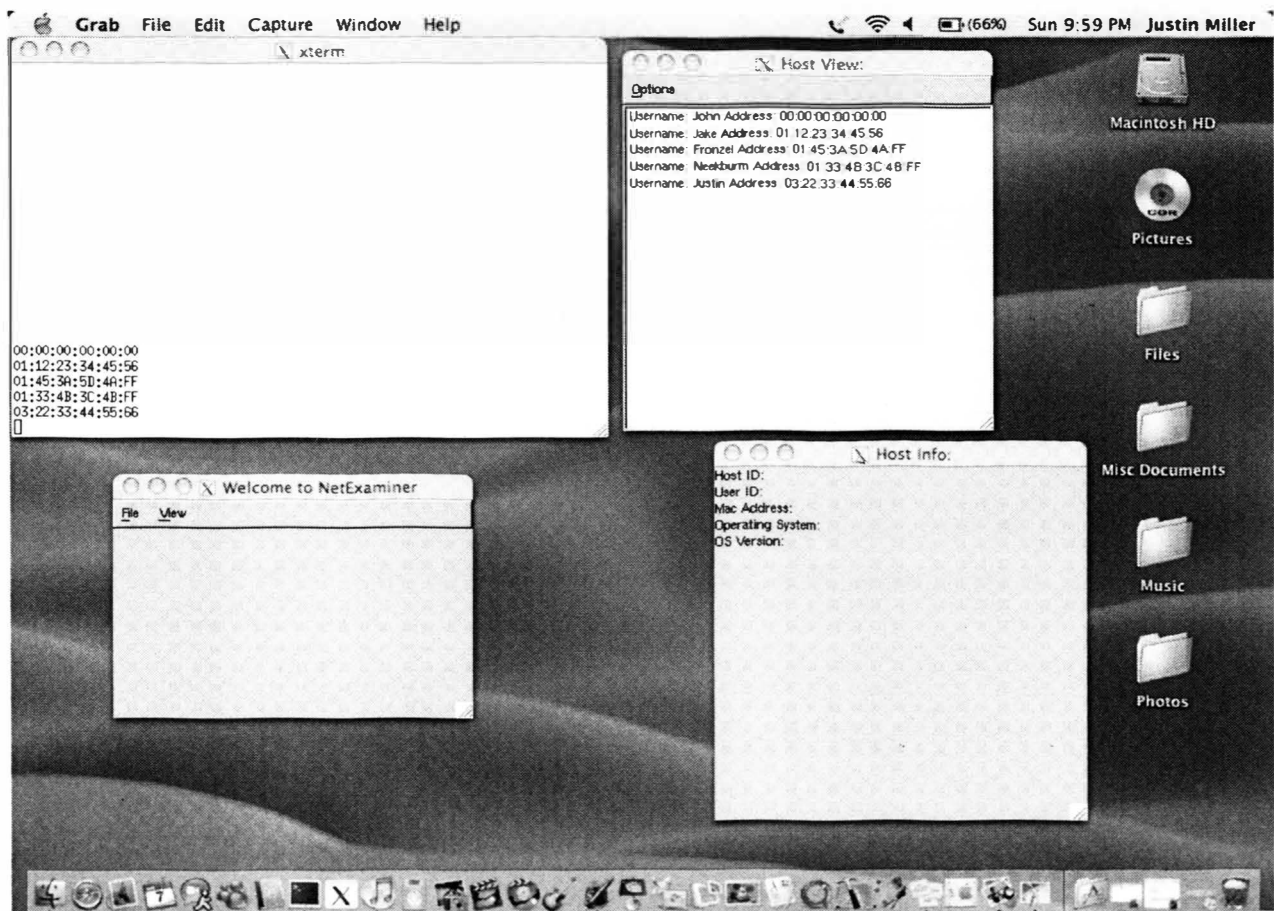
I would like to thank my faculty advisor Dr. Daniel Tauritz (CS) and our partner in the IT department Mr. Brian Buege (Director of Networks and Computing for UMR) for both financial support and research assistance.

Future Work

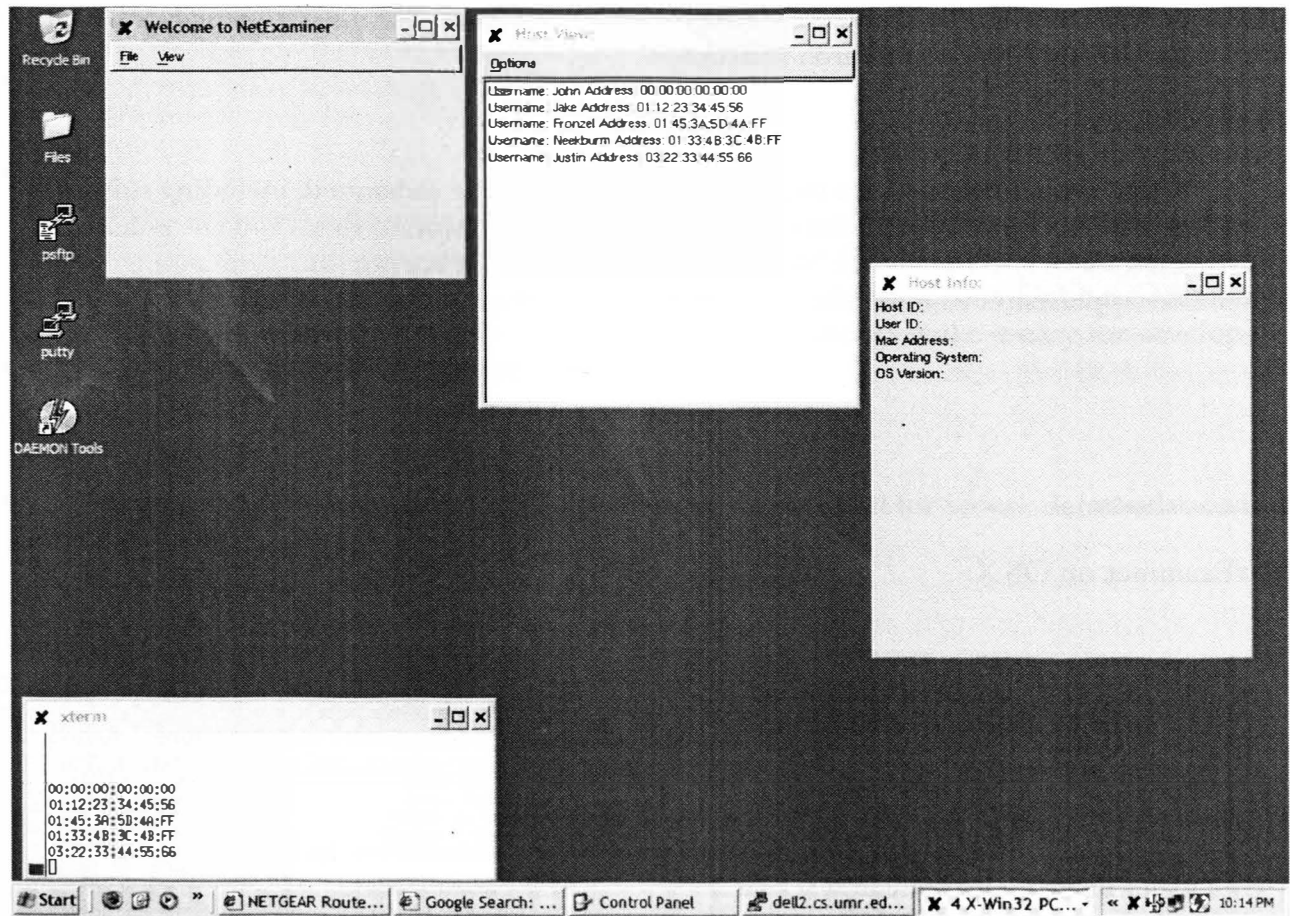
There are numerous ways that NetExaminer could be enhanced, including support for XML(for configuration and data formats), 3d representation of data, and the construction of a database specifically for NetExaminer that would allow for fine tuning of the NetExaminer application to meet the specific needs of a corporation or organization.

Screenshots

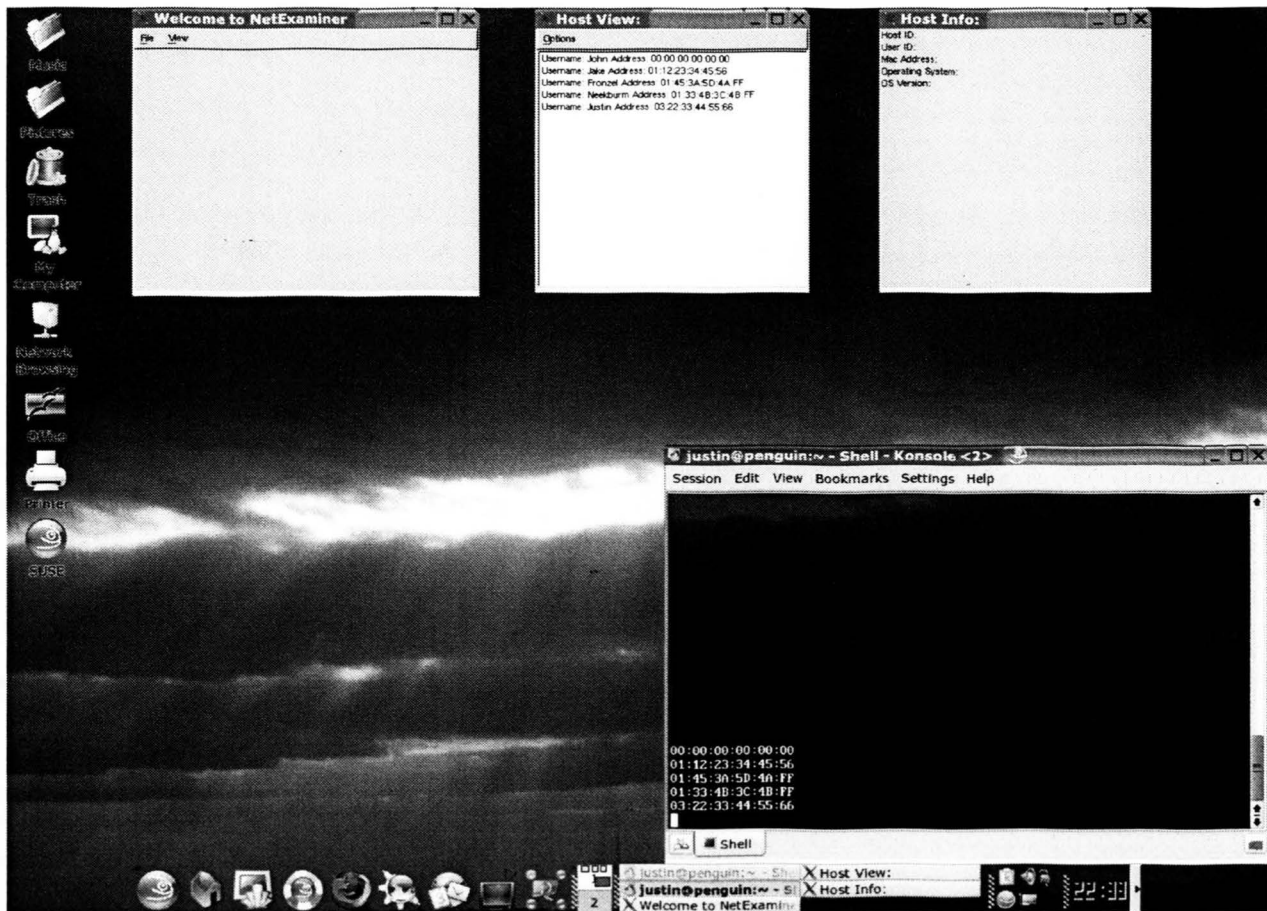
NetExaminer on OS X:



NetExaminer on Windows XP:



NetExaminer on SUSE Linux 9.2:



References

1. Linux International - <http://www.li.org>
2. MySQL - <http://www.mysql.com>
3. wxWidgets - <http://www.wxwidgets.org>
4. Ethereal - <http://www.ethereal.com>

Mobile Telephone Detection

Benjamin Moss and Todd Hubing

April 1, 2005

Abstract

A common threat to military personnel in Iraq is the use of unconventional warfare. Improvised explosive devices (IEDs) are crudely fashioned using explosives wired to consumer radio electronics. Garage door openers, two-way radios, and mobile telephones are a small sampling of the devices used in IEDs. The diverse nature of these devices makes it difficult to preemptively detect an IED using traditional means. Various methods of mobile phone detection are investigated, taking into account the type of phone and the available detection equipment. Specifically, a first generation mobile phone is detected using an oscilloscope and MATLAB.

Introduction

Traditional military munitions are very expensive and can be difficult to obtain for non-military enemy forces. The improvised explosive device is a cheap alternative often employed by Iraqi insurgents. IEDs vary widely in design, size, and complexity based upon the resources the designer has available. Detecting an IED is a difficult task that must take into account many more variables than detecting standard munitions.

A mobile phone detector by itself is not particularly useful in detecting an IED due to the ubiquity of cell phones. Most cell phone usage by residents is legitimate; very few are used to create an IED. The location and context of the detected mobile phone is necessary to determine if a threat is present. A military convoy moving along an open field might detect a cell phone fifty meters ahead near a group of rocks. A cell phone detected in such an unanticipated location could alert the convoy to a possible upcoming danger. In comparison, detecting ten cell phones in a crowd of people is meaningless. A directional antenna is thus a useful part of an effective detector.

The goal of the overall project (which is much wider in scope than this paper) is to design a system that can detect any unexpected consumer radio receiver or transmitter from a safe distance. Although transmitters are easy to detect, they can often only be detected while they are transmitting – the point at which the IED explodes. Therefore, a primary goal is to detect active receivers. Receivers contain local oscillators at either the carrier frequency or a lower intermediate frequency to demodulate the incoming signal. This oscillator frequency is radiated unintentionally and can sometimes be detected with sufficiently sensitive equipment.

Fortunately, this level of sensitivity is not required to detect a cell phone. Cell phones periodically transmit a burst of information to a base station to verify that the phone has not moved into a region covered by another base station. The long-term goal of

this aspect of the project is to detect and count the number of active cell phones of any type within a region. This technology, when fully functional, can be adapted to detect other radio sources.

An oscilloscope coupled with MATLAB was initially used as the mobile phone detector. The project is constantly evolving at a fast pace to incorporate the latest in receiver technology, and currently a highly sensitive receiver is being adapted to use in place of the oscilloscope. The receiver is approximately the size of a hard drive, uses little power, and is better suited to the task of cell phone detection than a bulky oscilloscope.

Background and History of Mobile Phones

FIRST GENERATION

The first practical cell phone system came into use in 1982. Bell Labs implemented the Advanced Mobile Phone System (AMPS) in the United States. Similar networks were installed in Europe and Japan under different names. Each regional cell is 10 to 20 km in diameter.² These cells can be approximated by a honeycomb structure of connected hexagons (see Figure 1). A mobile phone in a given cell uses two channels out of a set of channels allocated for the cell. No two adjacent cells share the same set of channels. With this scheme, the channel sets can be reused if cells using the same channel sets are far apart.

As a traveler with a cell phone moves from cell 'a' to cell 'b', base station 'a' notices that the signal from the phone gets weaker. Base station 'a' communicates with the other base stations and transfers the phone connection to the station receiving the strongest signal, which would be base station 'b'. If a single cell gets overloaded (at a large sporting event, for instance), it can be further split into smaller cells by using temporary base stations.

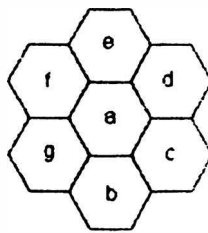


Figure 1: Cell model

In AMPS, frequency division multiple access (FDMA) is used. This means that each mobile phone has a full duplex channel. The full duplex channel consists of a receive channel and a transmit channel, each 30 kHz wide. These two channels are unique to each cell phone within a cell. The mobile to base station channels (transmit channels) are between 824 and 849 MHz, and the base to mobile channels (receive channels) are between 869 and 894 MHz.¹

SECOND GENERATION

The second generation of mobile phones introduced digital communications. One of the second generation systems popular in the United States is D-AMPS, or Digital AMPS. This system is backwards-compatible with AMPS so that both first and second generation phones can operate within the same cell. The bandwidth allocations are identical; D-AMPS phones use the same 30 kHz channels at the same frequencies using the FDMA method. A further advantage of D-AMPS is that three users can share a single channel at the same time by using “time division multiple access” – the time domain counterpart for FDMA. With TDMA, each mobile phone has a specified time slot to transmit its data. TDMA cannot be used effectively in analog systems because the data cannot be compressed to fit into a smaller time slot.

Another second-generation system called GSM (Global System for Mobile communications) also uses a digital FDMA/TDMA scheme. GSM uses a much wider channel of 200 kHz, allowing higher data transfer rates for each user.¹

THIRD GENERATION

The third generation of mobile phones uses “code division multiple access” (CDMA). Instead of using FDMA, where each phone has one or more unique discrete channels, a CDMA phone is allowed to transmit over its entire spectrum. Collisions are not treated as lost data with a CDMA implementation; signals are assumed to add linearly. Due to the spread-spectrum nature of a CDMA phone, it is much harder to detect than second or first generation phones. Detection of a CDMA phone is a long-term goal of this project.

Mobile Phone Detection

There are multiple techniques for mobile phone detection depending upon the desired results and available test equipment. Initially a spectrum analyzer was used to try to detect a Nokia first generation (AMPS) phone. The phone was turned on but the user was not engaged in a call. The spectrum analyzer could not sweep fast enough to properly capture the small burst transmitted by the phone, as was expected. A digital oscilloscope is a more appropriate tool because it can capture data after being triggered by a certain input signal.

OSCILLOSCOPE

An Agilent Infinium digital oscilloscope was connected to a small omnidirectional cone antenna. The oscilloscope was also connected to a computer through its IEEE-488 bus (also known as GPIB). The computer was running MATLAB version 6.5 under Microsoft Windows XP.

The purpose of the setup is to have the oscilloscope continually triggering on the small bursts of data radiated by nearby cell phones. After each burst the oscilloscope

transfers its data to the computer for analysis. The computer interprets the data and counts the number of unique detected phones based on the transmitting frequency.

The MATLAB script initially resets the oscilloscope to its default state to avoid inconsistent data due to different settings. The script then sets the trigger to 765 mV (determined empirically) on the rising edge of the input signal. The oscilloscope is constantly polled until it reports that the trigger conditions have been met by a signal. 50 nanoseconds of data is transferred to the computer, where MATLAB plots the data and determines the peak frequency of the signal. An example of a received signal is shown in Figure 2 and Figure 3. This is the signal that the Nokia phone sends to the base station after being powered up.

Before the script was fully able to distinguish between different cell phones, the UMR EMC Lab obtained sophisticated receivers built by DRS, Inc. The mobile phone detection project is intended as a stepping stone for more sophisticated detection systems, so it was not crucial to fully finish the setup before moving on. The script was not developed to the point where it could properly distinguish between similar phones, and it was only used on AMPS first-generation phones.

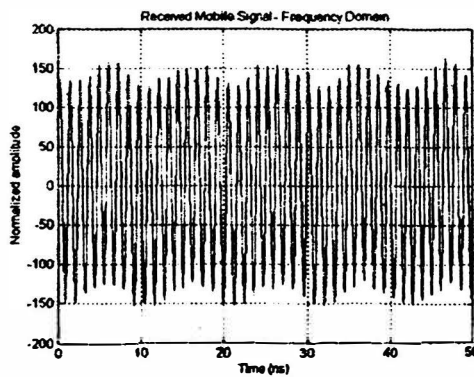


Figure 2: Received 834 MHz Mobile Signal (time domain)

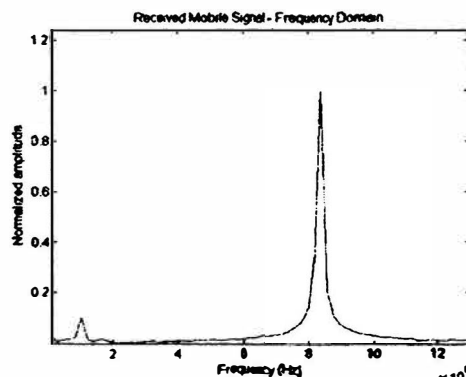


Figure 3: Received 834 MHz Mobile Signal (frequency domain)

DRS RECEIVERS

The next step in the project is to adapt the new DRS receivers to function in place of the oscilloscope. This effort is currently underway. The functionality of the receiver should allow more accurate detection of mobile phones and other electronic devices.

Directional Headphones and Audio Downconversion

As mentioned in the introduction, a directional antenna is a necessity for practical usage of an IED detector. A more imaginative method of direction finding was also attempted.

If radio signals were acoustic vibrations instead of electromagnetic waves, they would be far above the audio range of the human ear. It is possible to digitally scale a

signal down from a radio frequency to an audio frequency so that it can be heard. With two antennas connected to the oscilloscope and each received signal rescaled to one headphone, it is possible to listen to the same radio signal from two different antennas at the same time; one in each ear. The audio signal is not technically “real time” – that is, the audio signal is many times longer than the associated radio signal. 10 microseconds of radio signal can be rescaled to one second of audio. If this process is repeated in succession, the illusion of real-time audio can be created.

The advantage of having two antennas is that the phase of the received signal is different for each ear. The human ear uses a phase difference as one of the factors in determining the direction of a noise source.

Two omnidirectional cone antennas were connected to the oscilloscope. The antennas were spaced appropriately so that in the rescaled signal the antennas would seem to be as far apart as two human ears. A cordless phone was used as a radio source. Data was captured using the oscilloscope and sent to MATLAB to be rescaled. The PC sound card was used to play the rescaled audio through the headphones. Unfortunately, I could not hear a direction change through the headphones as the antenna was rotated with respect to the cordless phone.

A simulation in MATLAB was made to see if it was possible to detect a phase difference through the headphones. The phase of a sine wave was slowly changed for one headphone with respect to the other. The simulation can be thought of as a trumpet player slowly walking around an observer in a circle. The magnitude of the sinusoid changes minimally for each ear, but the phase of the wave changes significantly. I was never able to determine the direction of a randomly placed trumpet player with the headphones I was using.

Further research on the Internet revealed that special binaural microphones are used to synthesize locational audio signals, and the phase must very carefully be preserved to avoid distortion. The human ear also takes into account the effects of the human head on sound waves (an aspect that was neglected in the simulation). It is possible that we will continue this research in the future. The goal was to design a receiver such that the user could determine the source of a signal based upon his own sense of hearing instead of relying upon instrumentation.

Conclusion and Encountered Problems

A majority of my time working on the project was spent familiarizing myself with the equipment and its associated software. Although I have made many measurements in the past using the test equipment in the lab, I have rarely needed to design my own test setups. Small setup details that are conceptually simple can take a many hours to implement successfully. For instance, the initial mobile phone measurements were made inside the anechoic chamber to reduce the effect of background interference on the data. Although the antenna connected to the oscilloscope was sitting less than six inches from the Nokia mobile phone, no signal could be detected above the noise floor. A Motorola Startac third generation phone could clearly be detected with a graph similar to Figures 2 and 3 (which is not an appropriate graph for a CDMA phone). It was determined that the Nokia phone was not transmitting because it did not receive a signal from a base station. The phone did not waste power transmitting when a station could not be reached. Opening the door of the chamber solved the problem. The Motorola phone was not

transmitting using CDMA mode for the same reasons. When the Motorola phone could not communicate using the CDMA method, it used the AMPS method as a backup, generating an FDMA signal.

The DRS digitizer transfers digital data to the computer through an IEEE-1394 (Firewire) interface. Unfortunately, MATLAB does not have support for low-level Firewire transfers. A program is currently being written to act as an intermediary between MATLAB and the receiver to allow the data to be transferred. This driver program should be completed in the near future.

Although the detection of the above mobile phone is very rudimentary, the new receivers and subsequent software should be many times more adept at the task of device detection. The first step is always making the hardware work with a simple test case. It is difficult to form definite conclusions about the project at this stage.

The OURE funds for this project were used for me to attend the 2004 IEEE International EMC Symposium in Santa Clara, CA. The symposium gave me an opportunity to learn about basics in EMC engineering including circuit board design, component placement, techniques for determining causes of EMI, and computer modeling methods.

Nomenclature

EMC – Electromagnetic Compatibility - a general term to describe the engineering practice of ensuring that a device does not create or suffer from unintentional electromagnetic interference.

EMI – Electromagnetic Interference.

IED – Improvised Explosive Device – pejoratively, a homemade bomb.

AMPS – Advanced Mobile Phone System – a first generation mobile phone service.

GSM – Global System for Mobile communications – a second generation mobile phone service.

FDMA – Frequency Division Multiple Access – dividing a frequency spectrum into discrete channels to share the available radio spectrum.

TDMA – Time Division Multiple Access – allowing several users to share the same frequency by dividing it into multiple time slots.

GPIB – General Purpose Instrumentation Bus, formally IEEE-488 – a data protocol to communicate to and from measurement equipment.

Firewire – Also known as IEEE-1394, another data protocol designed rapidly transfer data from node to node.

Equipment

Agilent Infinium 54855A 6GHz, 20GS/s digital sampling oscilloscope

Nokia NHA-3NA AMPS mobile phone

Cone antenna – constructed by EMC lab, receives signals well at 1 GHz

Acknowledgments

I would like to thank Dr. Hubing and Dr. Beetner for recruiting me for this project, for teaching me about the art of EMC, and for giving me the opportunity to attend the symposium. I would also like to thank Xiaopeng Dong, Haixiao Weng, and Michael Noll, for showing me how to use the test equipment in the wee hours of the night; and Vimal Ambat, for helping me with the oscilloscope measurements.

References

¹Tanenbaum, Andrew S. Computer Networks. 4th Ed. Upper Saddle River, NJ: Prentice Hall PTR, 2003.

| ²Ziener, Rodger E., and Roger L. Peterson. Introduction to Digital Communication. 2nd Ed. Upper Saddle River, NJ: Prentice Hall, 2001.

Tests on the Relationship between the Oxide Thickness of CMOS Chips and Their Resistance to Neutrons

Justin Munson
Will Li

April 1, 2005

UMR – OURE Final Report

Abstract

The effect of neutron bombardment on the performance of selected COTS (commercial-off-the-shelf) logic chips was examined, and a test procedure was developed. Possible improvements of the test are also discussed. The chips tested were ST Microelectronics M74HC08 (oxide thickness of 550Å), Fairchild Semiconductor 74AC08 (oxide thickness of 250Å), and Texas Instruments SN74AHC08 (oxide thickness of 185Å). The chips were exposed to a neutron fluence of around 1.674×10^{15} n/cm², and received a gamma exposure of about 5 Mrad. Slight change was seen in the operation of the TI and Fairchild chips, and significant change was seen in the ST Microelectronics chip. These changes in device operation would become a factor primarily at high frequencies.

Introduction

From a cost standpoint, COTS (commercial-off-the-shelf) parts are preferred over more expensive parts designed for radiation environments. In an effort to cut costs, it may be possible to use COTS parts in some radiation environments if the effect of radiation on these COTS parts is known [2].

For this study, three logic gates, each with a different oxide thickness, were exposed to neutrons. Oxide thickness was previously shown to affect the resistance of these logic gates to gamma irradiation [1]. In the previous study, thin oxides were less affected than thick oxides, since the amount of energy deposited by ionizing radiation is proportional to the oxide thickness. It was initially assumed that the chips would have similar behavior under neutron exposure, since the number of neutron interactions would similarly be proportional to the oxide thickness.

The test designed used an oscilloscope to measure key features of the output of the logic gate. Key features include the rise time and peak amplitude of the signal. The rise time is important since longer rise times require slower operation frequencies. The peak voltage is important since a low output voltage may not be readable by components further down the signal chain. The largest changes were expected to be seen in the rise time of the chip.

Experimental Procedure

Irradiation Procedure

The logic gates were tested for cumulative effects by exposing them to neutrons using a pneumatic delivery system. The gates were sent down to the reactor while the reactor was at 200 kW, and remained there for 15 minutes, at which time the reactor was shut down. Since the gates become radioactive during the irradiation, they remained in the core for a sufficient amount of time to allow them to decay to a level safe for handling.

During the irradiation, the chips received both neutron and gamma exposure. After removal from the core, the chips were allowed more time to decay for added safety. The chips received a neutron fluence of approximately $1.674\text{E}15 \text{ n/cm}^2$. The gamma exposure, assuming an intensity of 10,000 kRad/hr of gammas during high power operation, was about 2500 kRad during the 15 minute neutron exposure, plus around an additional 2500 kRad received while decaying in the core after shutdown. It was shown in an earlier study [1] that this level of gamma exposure would have little effect on the TI (185A) and the Fairchild (250A) chips, and would result in around a 20% increase in rise time for the ST Microelectronics (550A) chip.

IC Test Procedure

The testing consisted of applying +5V to the V_{cc} pin as well as one input to one gate. The other input of the same gate was connected to a signal generator which generated a +5V logic pulse of a set frequency. Two of the other gates were grounded, and the fourth was left with no connection¹. Ideally, a definite rise time and peak voltage would be measured for the gate output. The test setup used caused the output measured to oscillate several times before settling onto a steady on state. Due to time constraints, it was decided to measure the change in this waveform rather than to develop a test setup that would produce a more ideal output. This waveform was reproducible, and comparisons using this waveform should give good qualitative data. Below is an example of the waveform, with the measured points shown.

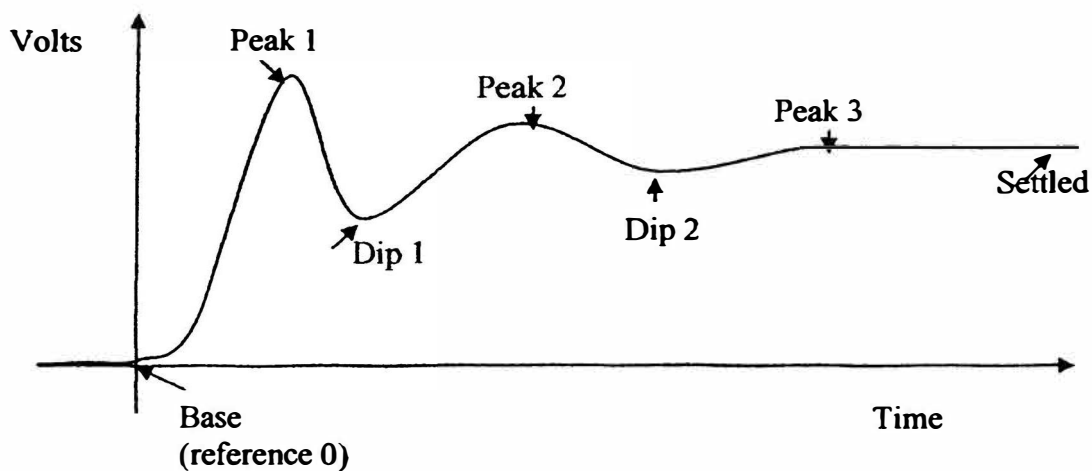
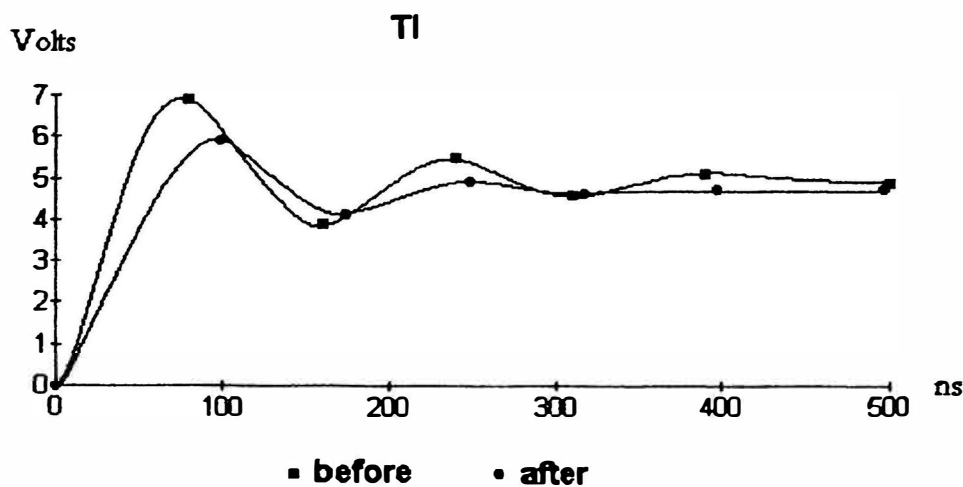


Figure 1 - Typical recorded waveform

¹ This gate originally was going to be used for a separate concurrent test, which was not performed. It was used to verify the results of the ST Microelectronics chip following exposure, and showed a similar result.

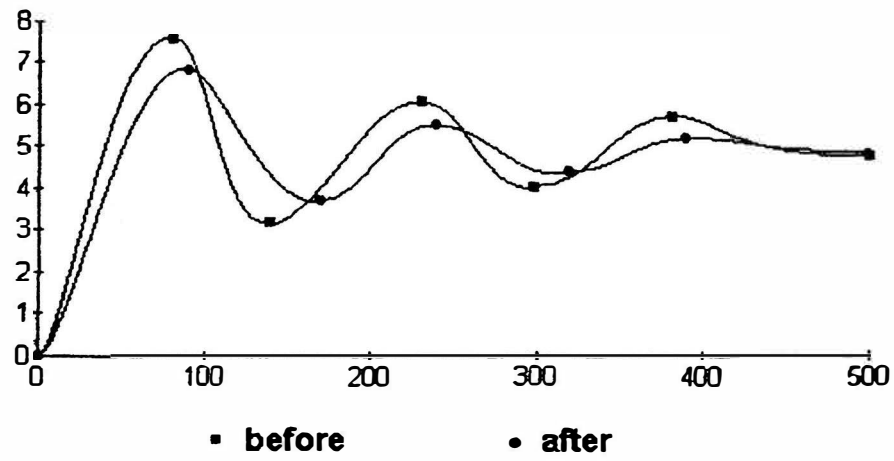
Results

Neutron exposure caused the oscillations to smooth out to varying degrees. The effect was slight in the Texas Instruments (185A oxide) and the Fairchild (250A oxide) chips and was very pronounced with the ST Micro (550A oxide) chip. In fact, the ST Micro chip was smoothed out enough that the measurement method used for the other two chips would not have given usable results, and instead the rise time of the signal was measured directly². The smoothing of the oscillations in the voltage is likely due to an increase in the rise time of the chip. In the following plots, the solid line is added for visual reference only.

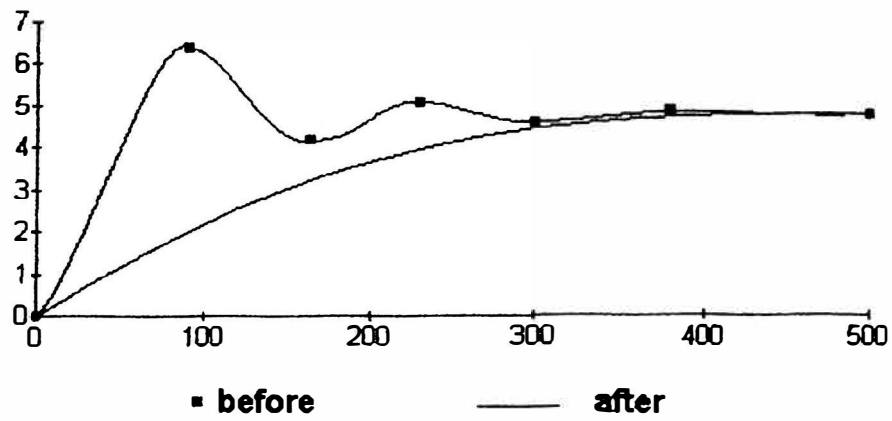


² This rise time is particular to this setup, as is the waveforms for the other chips. These waveforms are however indicative of the operation of the chip independent from the test setup.

Fairchild



ST Micro



Conclusions

The oscillatory nature of the output suggests a fairly short rise time before irradiation. The most affected chip, the ST Microelectronics (550A) chip, had a considerable increase in rise time. This increase was much more than the ~20% increase expected from 5 Mrad of gamma exposure [1]. Definite statements about the two thinner oxide chips (TI and Fairchild) are more difficult due to the shape of the output, but it is assumed they underwent similar damage, but to a lesser degree than the ST Microelectronics chip.

The test could be improved by changing the test setup to eliminate the oscillations in the chip output. This would allow exact measurements of the rise time to be made. This test could also be modified to allow continuous measurements to be made while the chip is being exposed to neutrons.

References

- [1] Tokuhiro, Akira T.; Bertino, Massimo F.; Smith, Scott C.; Dharavat, Hiten P.; Munson, Justin M.; Farmer, John; Pecht, Michael; Das, Diganta; "Tests on the Relationship between the Oxide Thickness of CMOS Chips and Their Resistance to Gamma Radiation."
- [2] Tokuhiro, Akira T.; Bertino, Massimo F. "Radiation Resistance Testing of MOSFET and CMOS as a Means of Risk Management"

Appendix – Raw Data

Before Irradiation		3-11-2005						
Chip		Base	Peak 1	Dip 1	Peak 2	Dip 2	Peak 3	Settled
TI - H	Volts	0	6.9	3.9	5.5	4.6	5.1	4.9
	nanosec	0	80	160	240	310	390	
ST - G	Volts	0	6.4	4.2	5.1	4.6	4.9	4.8
	nanosec	0	90	165	230	300	380	
F - Y	Volts	0	7.6	3.2	6.1	4	5.7	4.8
	nanosec	0	80	140	230	300	380	

After Irradiation		3-29-2005						
		200 kW		15 min		Bare Rabbit		
Chip		Base	Peak 1	Dip 1	Peak 2	Dip 2	Peak 3	Settled
TI - H	Volts	0	6	4.2	5	4.7	4.8	4.8
	nanosec	0	100	175	250	320	400	
F - Y	Volts	0	6.8	3.7	5.5	4.4	5.2	4.8
	nanosec	0	90	170	240	320	390	
ST - G	Rise	241 ns						
	Volts	5.022						

Opportunities for Undergraduate Research

Submitted March 25, 2005

Molybdenum Adsorption on Iron Oxides

Lead-Succimer compounds in Chelation Therapy

Submitted by

Jacob Naeger

Advised by

Dr. Charles C. Chusuei

Abstract

For this research opportunity, two different projects were performed. Much time and effort was put into each project both over the summer of 2004, the winter semester 2004, and spring 2005. Various challenges were present with each experiment. These challenges did not prevent learning and research success however. Through the work, much knowledge was discovered despite numerous unfortunate setbacks. This paper chronicles the results from each experiment. In each proceeding section, two subsections indicate discussion and results from each individual experiment.

Introduction

As an undergraduate student, I had many different reasons for deciding to work on this research project. One reason would be that a respected former professor of mine once told me that there was more to getting a degree than passing classes, and the time spent out of the classroom working research is an invaluable way to learn and impress your knowledge on others. On top of this, my pure love for chemistry and applied science led me to want to work on a project such as this. My advisor for the project presented me with my first research opportunity, and I accepted. Finally, the nature of being a college student requires a job of some sort to maintain financial balance during the scholastic year. Working on a project enabled me this opportunity as well.

This paper contains results and analysis from two experiments. The first experiment involved molybdenum concentration analysis. Molybdenum is thought to be a potential reason for bovine and livestock disease in the United States. Molybdenum is found in varying concentrations the ground, as it binds to iron oxides in the soil. X-ray photoelectron spectroscopy (XPS) was used to analyze two different sets of iron oxide samples and detect molybdenum concentration levels. In attacking this problem, the different iron oxide samples of magnetite and goethite were observed. These samples were prepared outside the Chusuei lab with two variables: Exposure time to Molybdenum, and pH. Molybdenum concentration was measured based on the scans provided by the XPS machine.

A second experiment involved lead-succimer compounds, and their relation to lead poisoning victims in chelation therapy. Succimer is a compound used to treat lead poisoning, but phosphate found in the body could potentially interrupt the treatment. This, in theory, could prevent correct healing in lead poisoning victims. Phosphate is naturally occurring in the human body, but concentration of phosphate can increase based on a persons diet and eating regiment. For example, soft drink beverages contribute to increased phosphate concentration in a human being.

Molybdenum Concentration Research-Basis of Experiment

Several studies have been done in the past pertaining to the adsorption of various elements on oxide minerals. Arsenate, phosphate, and molybdate compete for adsorption sites on soil mineral surfaces¹. The minerals that control the adsorption include Iron and Aluminum oxides, respectively. Two common iron oxides that hold adsorption sites are goethite and hematite.

In previous studies, liquid samples of synthetic goethite and another oxide, gibbsite was used for testing¹. In these studies, it was shown that the minerals arsenate, phosphate and molybdate compete for adsorption sites in the iron oxides. X-ray diffraction analysis was used to study and reveal the results of these experiments. The analysis technique showed that the adsorption occurred as a result of an inner-sphere complex. This form of adsorption is referred to as ligand exchange². An inner-sphere complex, by definition, is a complex with no water between the adsorbing ion and the surface functional group². This is indicated by a highly increased negative surface charge on the anion¹.

As there are multiple minerals that compete for adsorption sites, molybdenum was the specific element studied in this research project. In the past, it has been speculated that soil with a high concentration of molybdenum could cause harmful health defects in cattle and other livestock vital to American society. Gaining knowledge about why this molybdenum exists so readily in certain soils would be helpful in saving cattle and livestock from the health problems they have experienced due to over-exposure to molybdenum.

Experimentally, when an iron oxide solution was presented with molybdenum, the adsorption was extremely dependent on the pH of the solution^{1,2}. As the solution pH was increased, the amount of molybdenum adsorbed significantly decreased. It was shown that greater than 95 percent of the molybdenum adsorbed occurred at a pH level of 4.0 or lower. Any higher, and other minerals (phosphate, arsenate) competed with the molybdenum adsorption.

Figure 1

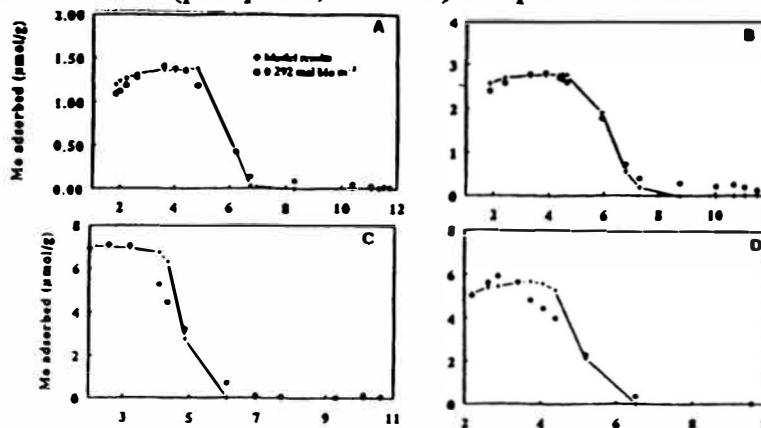


Figure 1 shows the pH dependence of molybdenum adsorption

The strong dependence on pH necessitates a point of zero charge (PZC). The PZC is defined as the pH value where there is no net particle charge. Specific adsorption of anions onto minerals such as oxides shifts the PZC to a more acid pH value². In the liquid solutions studied, it was shown that molybdenum adsorption on the surface of the iron oxides goethite and gibbsite lowered the PZC of the iron oxides.

This information prompts questions. Most specifically, where and why in the U.S. is the pH level of soil suitable for high levels of molybdenum adsorption? Also, if molybdenum adsorbs at only low pH levels in solution form, how would it bind to the iron oxides in solid form? No significant studies of molybdenum adsorption had been done on solid samples. The primary focus of this research experiment was solid samples of iron oxides.

Molybdenum Concentration Research-XPS Analysis Description

In order to gain understanding on molybdenum adsorption on solid iron oxide samples, x-ray photoelectron spectroscopy (XPS) was used. XPS is a surface analyzing technique. X-rays are fired on the surface of a solid sample. These x-rays remove electrons from the surface of the sample. An analyzer attached to the main chamber of the x-ray gun collects the electrons. A computer program monitors the resulting removal of electrons. The program yields graphs, which are referred to as "scans." These scans show peaks for corresponding elements that exist on the surface of the sample.

XPS is a highly sensitive surface analyzing technique. It views only as deep as 10 angstroms onto the surface of a sample. Therefore, sample purity is highly important, as any contamination will potentially ruin the data shown on the scan. As the machine is operating, multiple different scans are possible. The machine and scanning program can search for all the elements on the entire surface, which is known as a surface scan, or, searches can be done for each individual element believed to be present.

Each individual peak can be interpreted differently. The area under the curve of a peak indicates the relative amount of that element present. When each elemental peak area is measured and compared, an observer can fully measure and plot the amount of each element present relative to the other elements. In this way, one can see the predominant elements in the sample.

Preparing for an XPS sample analysis is a tedious and often difficult process. The sample must be kept clean and free of contaminants from the time it is prepared to the time it enters the x-ray chamber. In order to assure purity, the sample is handled with special instruments then mounted onto the XPS probe. The sample is first mounted onto a small piece of foil-like material. The foil is attached to two small tongs. These tongs are attached to the long cylindrical XPS probe. The probe, with the sample on the end, is then guided into the x-ray chamber. However, the sample can't be pushed straight into the x-ray chamber. XPS is dependant on low pressures, and the x-ray chamber must be kept at a perfect vacuum. Therefore, the sample must pass through a series of antechambers. These antechambers have vacuum pumps attached to them. Once a

sample enters each chamber, the chamber is pumped down to a pressure of roughly one pico-torr. It takes about one full hour to take a sample from atmospheric conditions into the x-ray chamber. Once inside the chamber, the x-ray gun must be powered up for use. Once operational it can take the XPS machine as long as an entire day to perform all necessary scans on a sample.

Molybdenum Concentration Research-Data and Results

For this research project, ten samples were observed. Five of these were samples of goethite and five samples of hematite. Both goethite and hematite are iron oxides that at certain pH values are thought to adsorb high levels of molybdenum. In order to test the previous studies that showed high molybdenum concentration at low pH levels, the samples used in the experiment contained varying pH levels. In addition to the varying pH levels, each sample was exposed to molybdenum at various times.

As the samples were scanned, it was noticeable that the molybdenum peaks were much stronger and more present in the samples with low pH levels. This was most noticeable in the goethite samples where previous studies had indicated. It was much more difficult to see the effect of adsorption exposure time on the samples. Unfortunately, as we were nearing the end of our sample analysis, the XPS machine in the surface chemistry lab experienced operational problems. Suitable replacement parts could not be identified in time to complete the scans. Because it was thought that the machine was not working entirely properly from the start of the research project, all data collected could not be assumed correct. For this reason the experiment had to be canceled prior to completion.

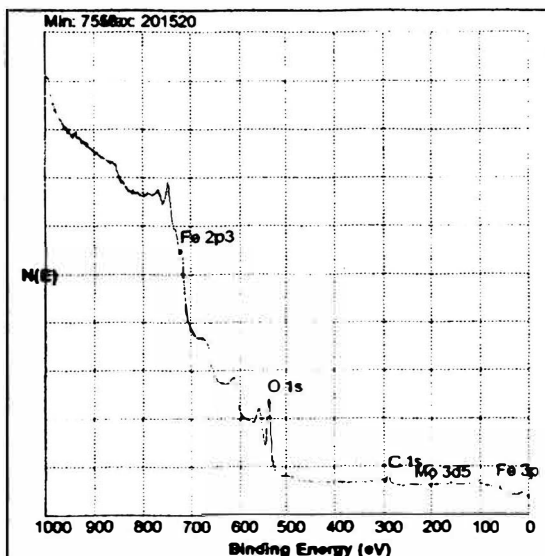


Figure 2 Molybdenum-Goethite Survey Scan

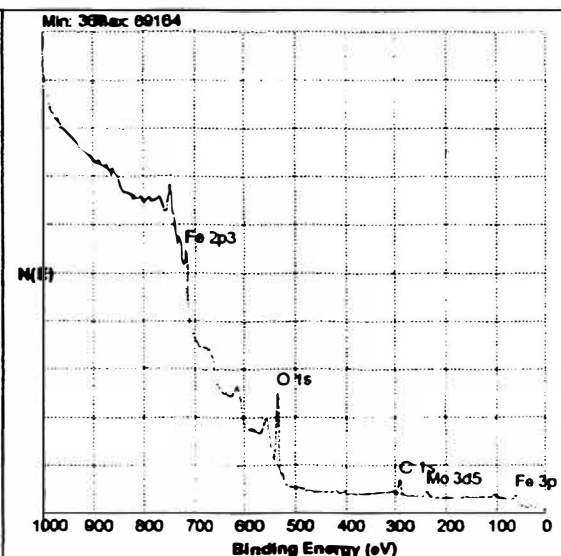


Figure 3 Molybdenum-Goethite Survey Scan

Lead-Succimer Compounds Chelation Therapy-Experiment Basis

This experiment pertained to chelation therapy and its role as a cure for lead poisoning patients. Chelation therapy for metal intoxication has been practiced for decades. The benefit of chelation therapy is that it can increase the urinary excretion of harmful metals³. In the present, succinic acid, particularly DMSA (2,3-dimercaptosuccinic acid) has been used for the treatment of lead poisoning. However, because of its slight solubility of water, DMSA must be present in extremely high concentrations to be effective. At these high concentrations, DMSA can cause harmful side effects in the human body. Was it possible other compounds in the human body interfere with the effectiveness of DMSA?

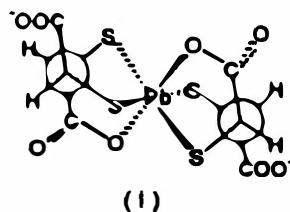


Figure 4



Figure 4 represents predicted chemical structures of DMSA binding to lead

As before in the case of molybdenum studies, numerous studies of succimer-lead compounds have been done. However, almost all of these studies were done on solutions of succimer-lead compounds. These experiments found competing ligands in the solution³. Possible competing ligands believed to interfere with the succinic treatment were forms phosphates.

Phosphates are naturally occurring in the human body. Our daily intake of food and beverages can increase the level of phosphate in the body. This experiment was designed to find the amount of interference associated with varying levels of phosphate I in lead-succimer compounds. If too much DMSA was harmful to the human body, and DMSA has trouble disassociating in the human body anyway, perhaps a more proper diet and nutrition regiment for lead poisoning patients could increase the effectiveness of DMSA by eliminating competing ions. If phosphate was proved to interfere with the attachment of DMSA to lead, then perhaps the success of chelation therapy could be improved through diet.

Lead-Succimer Compounds-Glove Box Usage

Following the XPS machine failure, and because XPS research was the main form of research conducted in the surface lab, the new project could not be XPS dependant. In the first research project, an outside chemist prepared samples and we analyzed them in the Chusuei lab. Thus, I gained the experience of operating an XPS machine. For the second research project, we would prepare different samples, and rely on the materials research center (MRC) to analyze the samples with their XPS machine. To prepare the samples, a glove box was used.

A glove box is a container closed to the atmosphere that contains a glass front. Two gloves protrude from the front of the box. The user puts his hand inside the gloves and into the box to conduct experiments. The purpose of this container is to keep contaminants, such as carbon dioxide, from entering the environment in which samples are prepared. The glove box contains valves that allow for inert gas to be passed through. Typically, Nitrogen gas is used as an inert to purify the box from carbon dioxide.

Similar to what was discussed about antechambers and low-pressure environments for the XPS machine, a glove box contains an antechamber. However, the objective of this antechamber is not to keep a perfect vacuum as in the case of an XPS machine. This antechamber is for passing samples and supplies in and out of the box while a researcher conducts experiments. The antechamber can be accessed without exposing the entire inside of the glove box to the outside air. Once a sample or instrument is placed inside, the antechamber door is closed. Then the antechamber is purged of all gases by the nitrogen flow. After a period of time, a door inside the glove box is opened. This door connects the main chamber of the glove box to the antechamber. Thus supplies can be passed in and out of the glove box through the antechamber without admitting carbon dioxide into the glove box.

On the following page, I have included some pictures of myself working with chemicals inside the glove box. I have also included a picture of all the tools, supplies and instruments used inside the glove box. Inside the glove box you see a centrifuge that was used to separate the precipitate. Also inside was a pH meter that is out of view. The other supplies include HPLC water (pure water used to clean glassware and perform dilutions), test tubs, beakers, filters, spatulas and a special pipet makes measuring small amounts of fluids extremely easy. In the other picture you can see me standing next to the antechamber on the box. Inside the box in this picture is the antechamber door that has a hinge and knob on it. The tank I am standing next to is the nitrogen tank that purifies the air inside the antechamber and glove box. Plastic tubes connect the nitrogen tanks to various valves on the box exterior.

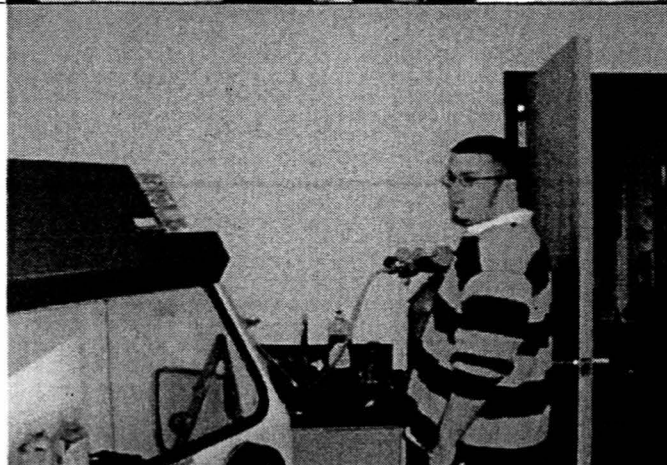
Picture 1

Working in the glove box



Picture 2

Adjusting pressure of inert gas



Picture 3

Glove Box Supplies and Equipment



Lead-Succimer Compounds-Data and Results

The samples we prepared in the glove box were lead-succimer samples with differing concentrations of added phosphate. Four samples were prepared. A control sample containing no phosphate was first prepared. This sample contained three milliliters of lead and three milliliters of succimer. A buffer solution to adjust the pH was also added. Solubility occurred at acidic pH levels, so sodium acetate was initially used as a buffer due to its non-reactive properties when combined with lead. However, the sodium acetate was far too weak in the volume of solution being used to lower the pH to a proper level for solubility. A new acid was required, but one which did not react with lead to form a precipitate. Hydrochloric acid (HCL) was tried, but HCL reacts with lead forming a precipitate. This would not be effective in this particular experiment. Acetic acid was a possibility, but in its dilute form, acetic acid would not be strong enough to lower the pH of the solution without adding significant volume. Glacial acetic acid (pure acetic acid) would be required to properly lower the pH without contributing unnecessary volume.

Once the proper acid was found, experiments were continued with the new mechanism. The control would again contain equal amounts of succimer and lead in solution. Glacial acetic acid was used to adjust the pH of the control solution until the solution turned yellow indicating a precipitate. This solution was centrifuged until the precipitate was separated out of the solution. This precipitate was extracted using a filter process and then placed in an incubator to properly dry.

Three other experiments were conducted. Each experiment, like the control, consisted of equal parts of lead and succimer. However, for each run, a different concentration of phosphate was also added. For the first run, 300 mM (milli-molar) phosphate solution was used. The phosphate was added in equal proportion to the succimer and lead. This phosphate solution was prepared in the lab, and then passed through the antechamber into the glove box. Once inside the glove box, it could be diluted for the other samples using HPLC water.

The second run again consisted of equal parts of succimer, lead, and phosphate. However, for this run, 200 mM phosphate solution was used. The third run was done with 100 mM phosphate solution. As with the control, each subsequent run was brought to the proper pH level using the acetic acid. All samples were brought to the exact same pH, with error being roughly .01 percent. All samples were centrifuged, filtered, and dried in the exact same manner as the control. The experiment data and observations are included as an attachment to this report.

Once properly dried, the samples were mounted on XPS slides in the manner described for the molybdenum experiments. These samples were sent to the MRC for XPS analysis. Upon receiving the XPS data from the MRC, a problem was very noticeable. The XPS printout from the MRC showed phosphate present in the control.

This was not in the experiment mechanism and is not readily explained. Perhaps the control was contaminated in some way. Perhaps the samples were mislabeled in the laboratory. One final possibility could be error in XPS operation from the operator at the MRC. Regardless of the source of the error, countless lab hours were lost in this disaster. The data from the MRC was not usable and revealed no useful information.

Despite the setback, a new control was prepared. The new control followed the same steps as the original control, and extra care was taken to assure purity. The same chemicals were used in the same proportions in the same manner. Once again, the control was centrifuged, filtered and dried. It was mounted properly under the vision of Dr. Chusuei and was once again sent to the MRC. As before, only problems came back. The XPS operator at the MRC admitted using an incorrect analysis technique. The XPS operator used the wrong function of the machine to analyze the samples on both occasions. Due to the fact that deadlines are present in the modern world, this experiment could not be continued. New samples could not be prepared in time for the deadline of this report.

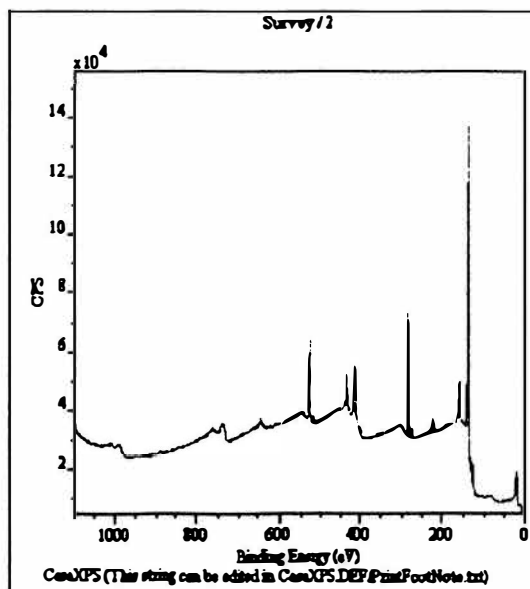


Figure 5 Survey Scan of Lead-Succimer Sample

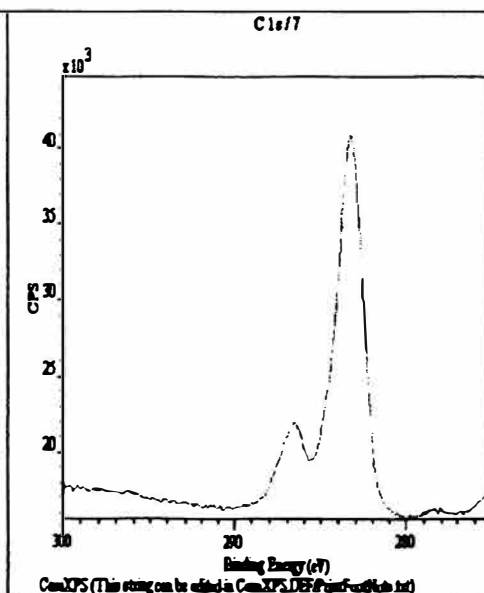


Figure 6 Individual Phosphate peak scan

The first of these scans represents the overall elemental content of the surface of the control experiment. The second scan is a scan of the element phosphate. This is an individual scan done on the element phosphate for the control experiment. As stated, phosphate should not have been present in the control. This scan indicates otherwise.

Summary

The results and experiments studied in this project clearly show the value and versatility of XPS analysis. It truly is a multi-faceted technique that can be used in a variety of ways. It is very effective when used properly. I benefited extremely from learning both how to operate and XPS machine, and how to prepare samples for XPS analysis. Despite the disappointing end of each project, the skills I learned were invaluable in furthering my knowledge as a chemist and engineer.

Acknowledgements

Dr. Charles C. Chusuei

Department of chemistry at UMR

Rob Hull

Graduate Student, Department of Chemistry at UMR

Dr. Terry Bone

Department of chemistry at UMR

Dr. Nuran Ercal

Department of chemistry at UMR

Mike Webb

Under-graduate student at UMR

References

1. Manning, Bruce A. "Modeling Competitive Adsorption of Arsenate with Phosphate and Molybdate on Oxide Minerals." *Soil Science Society of America Journal*. Vol. 60, 1996 pgs 121-131
2. Goldberg, Sabine. Su, Chunming. Foster, Harold. "Sorption of Molybdenum on Oxides, Clay Minerals, and Soils." *Adsorption of Metals by Geomedia*. Pgs 405-425
3. Fang, Xiaojun. Fernando, Quintus "Stereoisomeric Selectivity of 2,3-Dimercaptosuccinic Acids in Chelation Therapy for Lead Poisoning." *Chemistry Res. Toxicology*. Vol. 8, 1995 pgs 525-526

Engineering Management: Student and Alumni Perspectives

**Vaishalee Naruka
Department of Engineering Management
University of Missouri – Rolla**

**Advisor:
Dr. Stephen Raper**

**Department Chair:
Dr. William Daughton**

Engineering Management: Student and Alumni Perspectives

Abstract

Engineering Management which is considered to be a “non-traditional” field of engineering has a long history of attracting high caliber students regardless of some negative perceptions. This study was done at the University of Missouri – Rolla through focused interviews of forty current students and ten alumni in industry. The objective was to find out what motivated these students to pursue Engineering Management as a discipline, their perceptions and their success in industry compared to “traditional” engineers. This study showed that Engineering Management students just like others, choose a career path that satisfies their needs. These students tended to like technical field, but they also desired to combine it with a more people oriented approach. Engineering Management discipline is fairly new and although, is being widely accepted, it still faces some challenges due to ignorance. Nonetheless, industries recognize Engineering Management as a much needed discipline.

Introduction

Engineering Management is relatively new among other engineering programs. “The Engineering Management program at the University of Missouri – Rolla began as an interdisciplinary M.S. program in the fall of 1965, and as a B.S. program two years later. It was established as a full Department of Engineering Management in the school of Engineering July 1, 1968.” (Daniel, 1) Engineering Management is considered “non-traditional” as it focuses less on technicality and highlights communication and people orientation compared to other engineering fields. This sometimes, is the reason for it to be thought of as “less” of an engineering compared to other more “traditional” ones like Mechanical or Electrical Engineering. Yet, Engineering Management at the University of Missouri – Rolla has a long history of success in attracting high caliber students and industry has found Engineering Management very desirable, especially since

“It is often remarked that engineers communicate and express themselves poorly – this not only limits their effectiveness in the technical sphere, but can seriously prejudice their success as managers. Sir Peter Walters, who began his BP career in the supply and development department when he was 24, rose to be Chairman of the company and, in 1986, president of the Institute of Directors. He has said that he first came to the attention of senior management through the ability to write a good report. A specialist may do brilliant original work in isolation, but if it is to have any practical application and benefit to the community, the ideas must be spread. They will be recognized and adopted in direct proportion to the clarity with which they are expressed.” (Johnston, 93-94)

Formatted: Indent: Left: 0.5",
Right: 1"

The study was done at the University of Missouri – Rolla through focused interviews of thirty current Engineering Management students, ten “traditional” (non Engineering Management) engineering students and ten alumni in industry with Engineering Management degrees. The purpose of the study was to find out what motivates a student to pursue Engineering

Management as a discipline? What are their perceptions and perspectives of the degree while on campus? Do they consider themselves to be different than a traditional engineering student? How well does the degree prepare them for success in industry and do they compete well with "traditional" engineers in their industry environment? Interviews were conducted to collect data to see the response pattern, and to help understand the discipline as well as aid in efforts to develop focused marketing and recruitment materials.

Procedure and Analysis:

The participating students and alumni were recruited at the University of Missouri-Rolla through phone, emails and class announcements. These participants were from three different categories: Thirty Engineering Management undergraduates, ten non-engineering management undergraduates and ten alumni who graduated with a degree in engineering management. The reason for these different categories was to get different perspectives of engineering management. Not much emphasis was given on equalizing male to female ratio for this study as in general male to female ratio is 3 to 1 at the University of Missouri – Rolla (<http://www.umsr.edu>). An attempt was made to keep the class ratio even through recruitment, but more importance was given to "randomness" for the fairness of the sample.

An hour long interviews were conducted to find a set of questions that would get students' response to show some kind of a pattern [Appendix A]. Based on those questions survey forms were created [Appendices B & C] and given out to other Engineering management undergraduates. Also, a lot of them were interviewed and were asked about their inducement in choosing this area as their field of study and how they perceive it. They were also asked what they think about others' perception. To make sure what they feel is in fact the general perception of engineering management by others, ten non-engineering management students were interviewed and their responses were matched against what Engineering Management students had commented.

~~Deleted:~~

~~Deleted:~~ asked

~~Deleted:~~ ed.

Responses that reflect majority of students' feelings are included with the data. Some other common ones can be found in Appendix D.

~~Deleted:~~ The data was cross-checked.

Engineering management alumni were questioned about how they compare themselves against other "traditional" engineers and if they feel the discipline prepared them enough for success in industry.

The first question participants were asked was, "What motivated them to pursue engineering management as a discipline?"

~~Deleted:~~ An hour long interviews were conducted.

A senior responded to this question as, "It's the best of both [Engineering and Management] worlds."

A junior replied to the same question by saying:

"It was an easier degree. I could graduate faster."

Motivation

	Alumni (total: 10)	Students (total: 30)
Higher Status (position in the company)	30%	23%
Higher Salary	10%	30%
Time flexibility	10%	7%
Career flexibility	50%	40%

Table 1

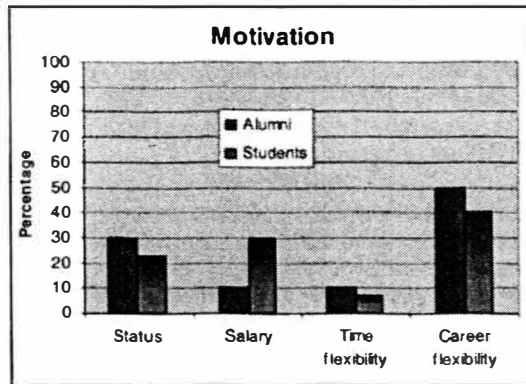


Figure 1

The data was collected and compared against different options and Figure 1 shows a comparison of the responses by alumni and students. According to the majority of alumni and students, *career flexibility* was their number one reason for choosing engineering management as a career. Although, students valued Salary as their second most important reason whereas, alumni seemed more inclined towards status.

Next question asked was, "What are their perceptions and perspectives of the degree while on campus and what do they think others' perceive it as?" Majority of our respondents agreed that whereas they consider engineering management as a great program that bridges the gap between business and engineering worlds, "traditional" engineering majors think of it as a "fall back" program.

A Mechanical Engineering said, "I thought about Engineering Management once, but decided against joining it as most of my friends thought of it as a sissy program."

An Engineering management junior replied, "I really like what this [Engineering management] department does and is doing for me, but the stereo-type really irritates me."

Deleted:

An Engineering management sophomore answered:

"When they make fun of my discipline, I tell them to call me whatever they want now, but in ten years I will be bossing them."

Another common response was:

"Everyone thinks EMAN [Engineering Management] is an easy major, but we still take the same general courses other students struggle with at UMR [University of Missouri – Rolla]. Same people even struggle in the actual EMAN courses if they don't have a head for business practices." says another Engineering Management junior.

A few students mentioned that this negative perception or rather misconception came because a lot of "traditional" engineering students changed their majors and joined engineering management discipline when they found their respective engineering program to be hard.

Where most of the students had slightly different approaches to their answers, majority mentioned something related to how people perceive Engineering management as a "cop out" program that is for those "who can't hack real engineering programs". However, respondents believed that engineering management is just a different program that requires interpersonal skills and leadership qualities and to those who do not possess these qualities it might seem the hardest program.

To find out if others' [non engineering management/traditional engineering students] truly perceive engineering management as learned above, the same questions were asked to non engineering management students.

A mechanical engineering junior responds, "I personally believe that most of the engineering management students are those who can't deal with real engineering, but still want to be called an engineer."

Another response was from an Electrical engineering sophomore, "I really don't understand the point of engineering management. If I was an employer and needed someone to manage my company, wouldn't I hire someone who not only has a real management degree like MBA, but also a hardcore technical base?"

A senior from civil engineering department mentioned, "I think that all the confusion in industry is because of these engineering management people who think they know everything and they are better than everyone else, but the truth is when a bridge falls it's rarely our fault. It is usually because some genius engineering management messed up in translating. I like to think of them as Jack of everything and master of nothing."

Out of Department students' perception

Positive comments	10
Negative comments	80
Neutral comments	20

Formatted Table

Table 2

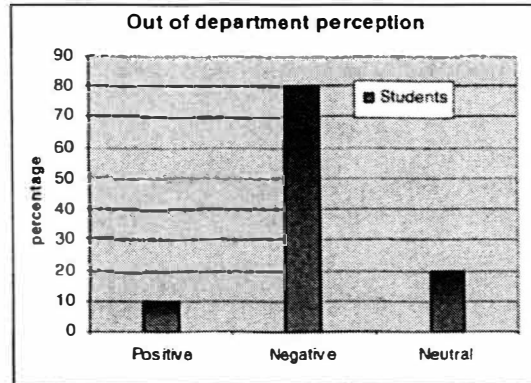


Figure 2

Out of 10 out-of-department students, 20% had no opinion because they believe they did not know enough. Other 10% answered in favor, saying,

"I think they deserve some respect for who they are and what they do. It's just a different career path and it's wrong to be so critical about it."

When alumni were asked the same questions, they all agreed with a '98 engineering management graduate who is working in industry currently:

"I feel that Engineering Management is the meshing of an engineering background with a business mindset. While EMAN [engineering management] does not fully train you in either an engineering degree or a business degree, it prepares you to make these two worlds meet. Engineers often cannot communicate clearly and business majors often can not relate the technical side of a company. Our degree allows us to make these two worlds successfully work together."

Further questioning included, "If they really consider themselves to be different than a traditional engineering student and how?"

Most participants responded, "Yes" and added "only because we are better in interpersonal skills."

A freshman adds, "I think we are as good as other traditional engineers. We take all the basic engineering classes, educating ourselves about engineering. Plus, we also enhance our learning with more versatility."

Looking at the engineering management curriculum it became clear that they indeed take basic engineering courses just like most engineers. Robert Shaw, past president of Engineering Institute of Canada said, "I believe, that the key mission of the engineer in these radically changing times is to improve productivity. He must provide the energy and tools we need; he must innovate, research, develop and transfer technology from the laboratory bench to field and factory." (2) And this is exactly what engineering management program is all about.

Next question was, "How well does the degree prepare them for success in industry, and do they compete well with traditional engineers in their industry environment?"

| Although most of our student participants believed that the degree was preparing them very well with some real life experiences as they worked in teams and did a lot of group projects, most accepted that they have only heard that Engineering Management students get jobs quickly and they excel in what they do.

To get a more reliable and first hand response, inquiry turned towards alumni.

"I feel that EMAN [Engineering management] gives its students the necessary skills and knowledge to succeed in the industry. I found that EMANS do very well when competing with traditional engineers, because they are more flexible and can communicate better." said one alumnus.

Another alumnus replied, "I would say we do relatively well. Most of my engineering management friends already have a job, whereas, some traditional engineering friends of mine are still looking."

Also, at the first annual conference of the American Society for Engineering Management Paul F. Chenea, Vice President in Charge of General Motors Research Laboratories Warren, Michigan said, "Although most of the major engineering societies have management divisions, there has been a growing need for a separate engineering management society which recognizes this profession as a specific discipline requiring special knowledge and skills." (American Society for Engineering Management, 1), which supports that engineering management program is much needed in industry.

Study went further to find out after so many positive responses why engineering management is still a small department. Participants were asked numerous questions like why they preferred this department or how their families responded to this decision of theirs, etc.

In response to the first questions, most participants admitted that People orientation was the major reason why they chose this discipline over others.

Preference		
	Alumni	Students
People orientated	40	47
Communications	10	20
Problem solving	40	13
Broad range	10	13
Easy		7

Table 3

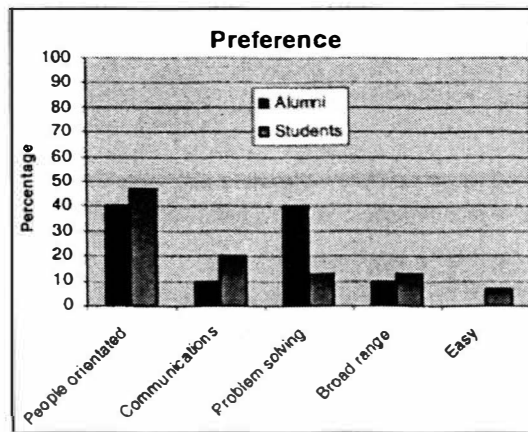


Figure 3

For alumni their second most important reason was *problem-solving* skills, whereas students preferred *communications*. Engineering Management has an all rounded approach to it including broad range of emphasis students can choose from.

In addition, most student participants acknowledged all the support they have from friends and families, but some accepted that people make fun of them and want them to change their discipline.

"My parents are happy because they are both Engineers, so they thought this department was perfect for me. I was excited because this department was exactly what I wanted." said a sophomore.

"They are somewhat supportive, some say, "get a real degree", but I love it and that's what matters" said a freshman

In contrast, most alumni mentioned either their families did not know about engineering management program or was plainly not supportive of it.

"My dad thought, I needed to change it [engineering management discipline] in order to find a job." said an alumnus.

"They were just happy to know that I was going to graduate. They said, "Thank God, Graduation is in his future!" said another.

Family support

	Alumni	Students
Yes	20	57
No	50	17
don't know	30	26

Table 4

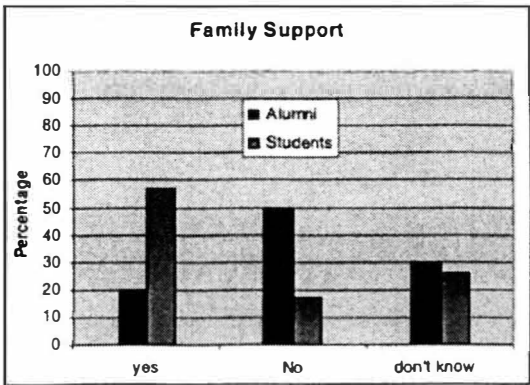


Figure 4

When data was compiled and pattern was generated, it was apparent that most alumni's parents were less supportive than the parents of current students.

Conclusion

The interviews were conducted and all the data was collected to see the common patterns that confirmed that negative perception about engineering management still exists, although people are becoming increasingly aware of the program and now have more respect for it.

The study showed us different perspectives and opinions. Most of engineering management students think that engineering management is a great program that is not only teaching them actual engineering, but also developing their personality all-rounded. They think of themselves as just an engineer if not more than other "traditional" engineers, but they also consider themselves people-oriented. Majority of our participants were motivated by time flexibility, career flexibility, money or high position. They all like technicality, but also wish to enhance it with some interpersonal skills. Participants mentioned communication and problem-solving skills being another reason why they got interested in engineering management. Students also mentioned engineering management might be easier for some who think communication and management classes are easier than the hardcore "traditional" engineering classes, but to those who do not have good interpersonal skills or business mind, it might as well be the hardest. A lot of alumni confirmed that engineering management is indeed very popular in industry and most students get jobs easily. They also tend to get a better salary.

Deleted: status

The whole misconception about engineering management exists due to a lack of knowledge about the program. A lot of students who seem to like it or could possibly be really good at it, just never give it a shot because families and friends still have a negative perception and the peer pressure is a lot to deal with. Looking at the pattern from alumni interviews, it seems like slowly engineering management program is getting popular as people are learning more about it. Pattern shows that in few years engineering management will be as well-liked as other "traditional" engineering if not more. Industry is already learning the qualities an engineering management can bring right from the start. At the same time, society is also being familiarized with the program and is getting ready to accept it. Either way, our engineering management students care only about how they feel and what all they can do with their *multitalented* degree.

Acknowledgement

Dr. Stephen A Raper, associate professor, University of Missouri - Rolla

Dr. William J. Daughton, Professor/chairman, University of Missouri – Rolla

Deleted: -

Reference

Babcock, Daniel L. "An engineering management program comes of age" *American Society for Engineering Education*. (1973): 1

"Engineering Management in Radically changing times" 24th *Join Engineering Management Conference*. (1976): 2

Johnston, D L. "Management for Engineers" United Kingdom: Peter Peregrinus Ltd, 1987

University of Missouri-Rolla FAQs. University of Missouri – Rolla. Nov 25, 2004

<http://www.umsr.edu/index.php?id=379&type=98>

Formatted: Centered

Formatted: Centered, Right: 0"

APPENDICES

Appendix A

1. What is your status at school? (Freshman, sophomore, alum, etc.)
2. What do you like about Engineering Management?
3. Why did you want to major in this department?
4. How did you hear about Engineering Management? What was your first reaction?
5. What kind of students does Engineering Management attracts?
6. Did you switch from some other department/major? If yes, what was your major? When and why did you decide on switching?
7. What do you think Engineering Management is all about? Please describe. Sometimes it gets really hard to explain people what Engineering management is about, what they do, why we need this department etc.
8. When did you find out about EMAN? Do you think it's as known as some other traditional engineering programs? Why /why not?
9. Some people consider EMAN as an invisible/imaginary/not-real engineering/stupid engineering/easy degree. What do you have to say about that? Where does this perception come from?
10. How would you describe EMAN?
11. What are the qualities/skills that make a good EMAN?
12. Have you heard any negative/positive comment about Engineering Management?
13. How do you feel about the negative perception about this department and how did you overcome it?

Formatted: Centered, Right: 0"

Formatted: Right: 0", Numbered +
Level: 1 + Numbering Style: 1, 2, 3,
... + Start at: 1 + Alignment: Left +
Aligned at: 0.25" + Tab after: 0.5"
+ Indent at: 0.5"

Formatted: Bullets and Numbering

Formatted: Indent Left: 0.25",
Right: 0"

Formatted: Centered, Right: 0"

Appendix B

Interview Questions

Formatted: Centered

Formatted: Bullets and Numbering

1. What's your status at school? Freshman, sophomore etc.
2. How and when did you hear about this department?
3. What was your first reaction about the Department? (Any stereotypes you came across)?
4. Did you switch from some other department/major? If yes, what was your major? When and why did you decide on switching?
5. What do you think Engineering Management is all about? Please describe. Sometimes it gets really hard to explain people what Engineering management is about, what they do, why we need this department etc.
6. When did you find out about EMAN? Do you think it's as known as some other traditional engineering programs? Why /why not?
7. Some people consider EMAN as an invisible/imaginary/not-real engineering/stupid engineering/easy degree. What do you have to say about that? Where does this perception come from?
8. If you had to recruit someone in this department what would you tell them?
9. If you had to generalize the type of students we have in EMAN, what would you say?
10. What motivated you to become an EMAN? Status, money, time flexibility, career flexibility, other _____?
11. What's your perception of EMAN?
12. How do you think others in and outside the department (EMAN) perceive it as?
13. Do you consider yourself to be different from a traditional engineering student? In what ways? How do you feel about it?
14. How well does the EMAN degree prepare students for success in Industry? Do EMANS compete well with traditional engineers in their industrial environment?
15. Why did you choose this discipline? People oriented, communications, problem solving, other _____?
16. What are your plans after graduation?
17. Where do you see yourself in five years?
18. How will your degree in EMAN fill into your goals?
19. How did your friends and family respond to your decisions of being an EMAN? How did you react?
20. How would you describe EMAN?
21. What are the qualities/skills that make a good EMAN?
22. How do you feel about the negative perception about this department and how did you overcome it?

Appendix C

Questionnaire

Formatted: Centered, Right: 0"
Formatted: Centered

Name: _____ (Optional)

1. Are you an Engineering Management student? Yes/No _____ (major)
2. Are you a Male/Female _____
3. School Status: Freshman/Sophomore/Junior/Senior/Super senior/Alumni _____
4. What motivated you to be an EMAN? Status/Money/Time flexibility/career flexibility/other _____
5. Why did you choose this discipline? People oriented/communications/problem solving, other _____
6. What's your perception of EMAN?
7. How do others perceive it as? Please try to use direct quotes.
Negative: _____
Positive: _____
8. What are the qualities/skills that make a good EMAN?
9. How did your friends and family respond to your decision of joining EMAN?
10. Some people consider EMAN as an invisible/imaginary/not-real engineering/stupid engineering/easy degree. What do you have to say about that? Where does this perception come from?
11. How do you feel about the negative perception about EMAN dept? how did you overcome?
12. If you switched from a different major? What major was it? When and why?
13. Do you consider yourself to be different from a traditional engineering student? In what ways? How do you feel about it?

Formatted: Bullets and Numbering

Formatted: Centered

Appendix D

<u>Positives comments</u>	<u>Negatives comments</u>	<u>Qualities/skills for a successful Engineering Manager</u>	<u>Suggestions for Recruitment</u>
<p><u>"We get the best of both worlds"</u></p> <p><u>"It's interesting"</u></p> <p><u>"Easy major"</u></p> <p><u>"...Emans are needed to coordinate projects and maintain the peace between civilians and engineers."</u></p> <p><u>"You will go far in life"</u></p> <p><u>"It's easy and pays good."</u></p>	<p><u>"You're not a real engineer"</u></p> <p><u>"It's the easiest one at UMR."</u></p> <p><u>"In all honesty, I think it's really not needed."</u></p> <p><u>"Emans are outgoing, fun spirited and not afraid of skipping homework to go to the bar. May be b/c they think they can cope up."</u></p> <p><u>"Eman is more of a concept based learning process while the other majors have more of a technical emphasis. Plus, most- ummm...how would you say – less than bright students – tend to migrate toward Eman and seem to thrive."</u></p> <p><u>Where leaders are made</u></p> <p><u>"It is easy to get."</u></p> <p><u>"If you can't do something else, you go to Eman"</u></p> <p><u>"...bunch of sissies"</u></p>	<p><u>Outgoing, social, organized, adaptable</u></p> <p><u>Common sense,</u></p> <p><u>Business oriented</u></p> <p><u>Leaders,</u></p> <p><u>Fun spirited</u></p> <p><u>Good listener,</u></p> <p><u>Good organizer, good problem solver</u></p> <p><u>Status, Money, time flexibility,</u></p> <p><u>Career flexibility</u></p> <p><u>Intelligent, enterprising</u></p> <p><u>Active on organizations</u></p> <p><u>Morals, respect</u></p> <p><u>Like to Plan, Organize, control</u></p> <p><u>Technical skills, leadership skills, communication skills and organizational skills</u></p> <p><u>Communications, problem solving, broad field,</u></p> <p><u>Humbleness</u></p>	<p><u>"I would tell them that it's a great degree if you like technical things, but want to interact with more people and be in office atmosphere instead of on the factory floor.</u></p> <p><u>Career flexibility,</u></p> <p><u>"Opportunity to gain high management status"</u></p> <p><u>Money</u></p> <p><u>"I would tell them that they would have a much broader degree that is more people oriented than technically oriented."</u></p> <p><u>"...Eman is where leaders are made"</u></p> <p><u>"...If you have any interest in business or entrepreneurship it is a great avenue to build technical knowledge and grow your people and business knowledge."</u></p> <p><u>Time flexibility,</u></p> <p><u>career flexibility,</u></p> <p><u>broad field,</u></p> <p><u>Reasonable graduation time</u></p> <p><u>High position</u></p>

Formatted Table

The Impact of RFID Technology on Supply Chain Management

Nguyet Nguyen, Department of Information Systems & Technology, School of Management and Information Systems, University of Missouri-Rolla, Rolla, MO 65409

Faculty Advisor: Dr. Bih-Ru Lea, School of Management & Information Systems, University of Missouri – Rolla, Rolla, MO 65401, email: leabi@umr.edu

Abstract

Supply Chain Management is an important criterion to companies' success today. However, Supply chain visibility certainly is a significant supply chain issue. Inventory invisibility and inventory imbalance caused companies to lose a lot of profits nowadays. With Radio frequency identification (RFID) technology, supply chain management can improve efficiency. RFID technology can help reduced supply chain costs, increase efficiency and inventory visibility. In recent years, one of the most advancing technologies is RFID technology. Journals, articles, television shows, and papers are talking about the potential benefits of RFID. This research paper will help you to understand what RFID is, how it works, and the benefits throughout the supply chain.

1. Introduction

Supply Chain is a process of optimizing the delivery of goods, services, and information from the supplier to the customers (Kinsella, 2003). Supply chain management (SCM) is the major concern of all of the companies today as they strive for better quality and higher customer satisfaction (Mentzer et al. 2000; Chopra and Meindle 2001). To bring the supplier, the distributor, and the customer into one united process, a strong and efficient supply chain management is needed (Laudon and Laudon, 2001; Youngdahl 2000). The manufacturers, suppliers, transporters, warehouses, retailers, and customers are involved in a dynamic, but constant, flow of information, products, and funds (Simchi-levi et al. 2000). According to a recent Deloitte Consulting Survey, 91 percent of North American manufacturers rank supply chain management as very important or critical to their companies' success; however, only 2 percent of the manufacturers rank their supply chains as world-class (Gulisano 2000). The supply network is like Supply chain management or the supply web because they all show how each unit interacts with the others. The suppliers and distributors that were once adversaries are now becoming partners in order to improve both corporations (Gryna 2001). Managing the series of events in this process is called supply chain management. Effective management must notice all the different pieces of this chain as quickly as possible without losing any of the quality or customer satisfaction, while still keeping costs down (Craig 1996; Shin et al. 2000).

Successful implementation of supply chain management can do the following: help cut costs (Mainardi et al. 1999), increase technological innovation (Hult et al. 2000), increase profitability and productivity (Gryna 2001), reduce risk (Chase et al. 2000), and improve organizational competitiveness (Fisher 1997; Christopher 2000; Spekman et al. 1994; Wisner and Choon 2000). However, supply chain management does encounter several obstacles. Some of these obstacles are: an increasing variety of products, decreasing product life cycles, more demanding customers, globalization, and difficulty executing new strategies (Chopra and

Meindlc 2001). According to a recent survey, 95 percent of Fortune 500 executives said their companies should be more focused on global supply chain management; however, only 45 percent have actual programs in place. The misleadingly optimistic of these companies are working on only one piece of the total supply chain (Gulisano 2000).

Inventory visibility, or blindness is a major problem facing a supply chain (Spiegel, 2003; Gladson, 2003) and has been contributing to product theft. It is reported that most of product theft occurs in the supply chain prior to goods reaching the retail store and is typically account for about 2 percent of revenue for consumer goods (Kinsella, 2003).

Inventory visibility also causes product unavailability in a supply chain (Green, 2004). Out-of-Stock is another major issue that occurs due to the problem of product unavailability. According to a Supply Chain Europe Article, 7.1% of products are unavailable on store shelves. It is responsible for losses in sales, losses of customers, and losses of profits across the industry. Customers often choose a similar product from other suppliers when the products they want are not available. If the manufactures and retailers keep letting consumers down on products they want to buy, they increase the chance of forcing people to walk out of the store empty-handed or with substitute products from rival companies. Study reports that 70% of shoppers prefer different product, with the other 30% leaving the storey. (Tierney, 2004).

An inventory imbalance is another problem in supply chain that is caused by inventory visibility (Gladson, 2003). Because of weak coordination of orders and shipments between manufacturers and retailers, serious inventory imbalance starts to buildup. Companies today often experience either excessive inventory or inventory shortage or both. The inventory is invisible in the company's own internal supply chain and its trading partner. The supply chain managers cannot detect how many items are in a container warehouse as well as if they are the correct items. The companies are experiencing unbalanced shipments. The managers fail to forecast correctly on the amount to ship from one retailer to another and determe of the new stocking levels in a retail network (Spiegel, 2003).

In conclusion, theft of products (Kinsella, 2003), product unavailability (Green, 2004), and imbalanced inventories (Gladson, 2003), caused by inventory visibility are bringing the companies down. They are major problems in supply chain that need to be fixed right away.

RFID is a new wireless electronic identification technology that uses radio frequency signal to read on RFID tags. RFID systems have been reported to provide some remedies to problems facing a supply chain and to improve supply chain management performance

This paper describes the problems and difficulties that supply chain is facing and provides solution to supply chain's problems. With supply chain problems arise, companies' costs are increasing and also lost in sales are increasing. RFID technology can help improve accuracy in tracking and tracing goods, and inventory visibility. This paper is a guide to understand what RFID is, how it works and its benefits to the supply chain.

2. RFID Overview

RFID is a new wireless technology used to receive, store and transmit information. RFID technology uses radio waves to identify the object. The RFID system includes two components. First, is the transponder which is located on the object to be identified as you see in Figure 1 and Figure 2. Second, is the reader, which is used to read and write the signal (Finkenzeller, 7). There are two types of transponders. The first type is a passive tag. Passive tags do not contain batteries. They stay interactive and only activate when the readers transmit radio frequency to

them and give them energy. Therefore, passive tags can only be read in short distances. The second type is active tags. Active tags need batteries and can be read from hundreds of feet away. Active tags include transmitters that send back information. They can be reprogrammed with data and read at a distance of 100 feet or more. A passive tag costs 50 cents or less while an active tag would cost about as much as 50 dollars each (Sawyer, 2004).

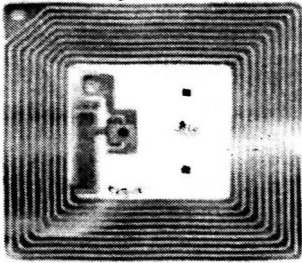


Figure 1 Source: Rappold, 2003

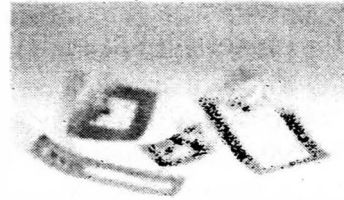
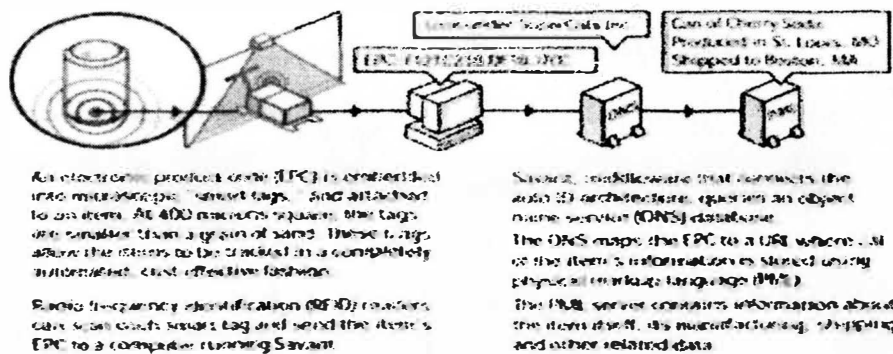


Figure 2 Source: Robert, 2000

2.1 RFID Systems and Advantages of RFID

Since we all know what RFID is, how RFID works is describing in the following manner: Electronic Product Code (EPC) is embedded into the RFID tags. EPC contains data such as a SKU (Stock Keeping Unit) number, cost, date of manufacture, date of shipping, etc. The RFID readers scan each tag and exchange its EPC with the readers. That reader then sends the EPC to a computer database, as Figure 3 (Atkinson, 2004).



Courtesy The Auto-ID Center. Copyright 2002 XPLANE.com

Figure 3

Source: Rappold, 2003

Unlike bar codes, RFID tags don't require manual scans to be tracked. Instead, at the pallet and carton level, tagged pallets can automatically transmit the time and date they pass through the warehouse door (Tesoriero, 2004). Shippers can know exactly how many units are in shipment, what they are, where they came from, and when they entered transit by placing an RFID tag on every unit in a shipment. By using RFID, some companies are already reducing the number of suppliers and yielding cost savings along with many other benefits (Atkinson, 2004).

Product availability is one of the benefits of using RFID. RFID increases accuracy in tracking and tracing goods in the containers that hold them. This gives more options for

placement and increased resistance to moisture. It also makes ability to actively transmit information and save labor (Calkins, 2004).

Improvement in theft reduction is another benefit of using RFID. RFID can reduce theft by tracing goods more effectively through the supply chain all the way to the retail shelf, which results in better inventory invisibility. It reduces the opportunity for theft to go undetected. Moreover, it also provides valuable information to track down theft, while deterring future theft. According to a P&G report, it is estimated that counterfeiting costs the company \$500 million annually. By using RFID, it can embed unique product identifiers placed on all products can quickly establish theft. Therefore, RFID can save the companies a lot of money (Kinsella, 2003).

With RFID, the manufacturing suppliers can improve their operational efficiencies. RFID technology can improve in shipping, receiving, and other handling activities that take place in a supply chain. Goods can be moved around faster, cheaper and more accurate. RFID readers decrease reading errors and require less manual labor. They are faster at reading huge quantities of information than other manual methods currently used for shipping, handling, and receiving. Moreover, RFID tags can make recall operation easier (Lapide, 2004).

RFID can also help improve multi-tier forecasting methods. Multi-tier forecasting methods are a way to make accurate forecasting on demand, which can be better forecasted if one understands what is going on in the supply chain after products are shipped to customers and until the final consumption of the products. That understanding can then be used to: develop a quantitative downstream model of manufacturer demand as a function of warehouse, withdrawals, and consumption; estimate historical consumption and use it to forecast in the future; and use both quantitative downstream model and consumption forecast to forecast demand of the upstream manufacturer as show in Figure 4.

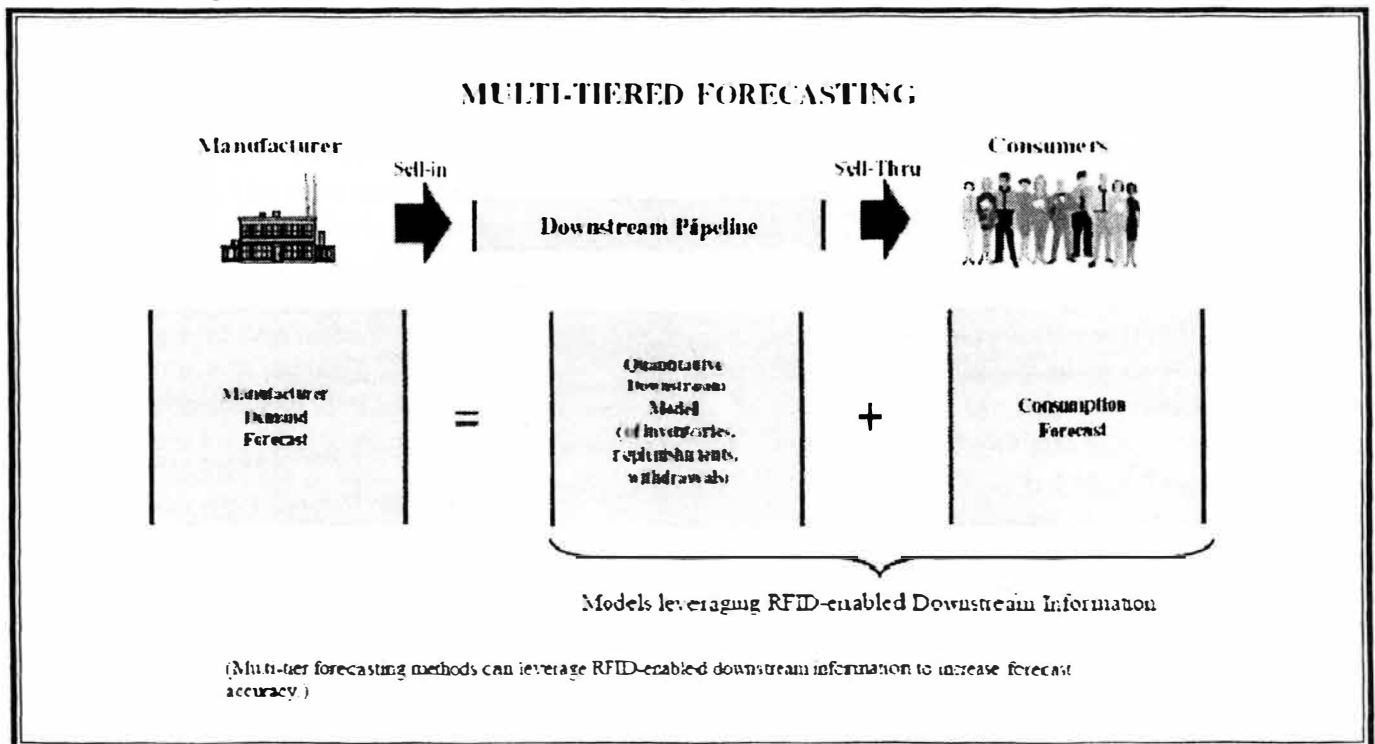


Figure 4 RFID and Multi-Tier Forecasting

Source: Lapide, 2000

RFID technology will make it easier to assemble vast quantities of accurate downstream data as an input to this type of multi-tier forecasting process. The data can include warehouse inventories and withdrawals, product consumption, and inventory replenishments. For instance, Wal-Mart is promising its suppliers information on products as they arrive and leave the warehouses (Lapide, 2004).

2.2 Current RFID Applications

RFID is not only used to improve supply chain management, it can also be used for a variety of different purposes such as, transportation, personal identification, and medical applications.

Public transport is one of the applications that have a great potential for use of RFID. According to Czako, in Europe and the USA traffic association is still operating at a huge loss, sometime at 40% turn over. Using RFID can improve public transport companies and users by eliminating daily income calculation, reducing operating cost, maintenance cost of sellers' dispensers, ticket devaluers, expressive statistical data, and reduce the need for subsidies due to low cost reduction (Finkenzeller, 2003).

RFID is also used for animal identification. It is used for tracing the origin of animals and for the control of epidemics. There are four basic procedures for attaching the tags to the animal: collar tags, ear tags, injectible tags, and so-called bolus.

Container identification is also a use for RFID. Gas and chemicals are transported in high quality rented containers. Serious consequences can occur by selecting the wrong bottle during refilling or use. A clear identification system can help to prevent product sealing errors. Barcodes are used by a large proportion of containers supplied today. However, a barcode is not reliable enough and its short lifetime causes high expense. RFID has a higher storage capacity and longer lifetime than barcodes. Further more, additional information can be attached to containers such as, owner details, contents, volumes, maximum filling pressure and analysis data, and security mechanisms can be used to prevent unauthorized writing or reading of the stored data (Braunkohle, 1997).

The cost of waste disposal is increasing because of increasing environmental legislation. With automatic measures of the amount of waste produced, it can help distribute the cost more fairly. For this reason, the RFID system can maximize the use of communal waste disposal; therefore, replacing the flat rate charge for waste disposal with a charge based upon the quantity of waste produced (Finkenzeller, 2003).

The RFID is also used for patient identification. Many hospitals, the Massachusetts General Hospital Blood Transfusion Service, for instance, has been using the RFID during blood transfusions. Passive RFID tags are inserted in the patient wristband, and similar tags are embedded into the blood-bag labels used when blood is assigned to an individual recipient. Then software is used to verify the match between patient and blood tag. With RFID systems, many serious errors can be eliminated (Butalla, 2004).

2.3 Successful Cases of using RFID

RFID has not only been used widely, but also has been used successfully for many companies. Wal-Mart and Procter & Gamble are the early adopters and are starting to receive the efficiencies from RFID technology (Mohamed, 2004). Moreover, in Mercedes Benz's

Tuscaloosa factory in the USA, RFID is used for the identification of skids bodies (Schenk, 1997). The J.M. Schneider meats Company, the largest meat companies in Canada, is using RFID system successfully for product identification and tracking because the barcode system cannot be used due to high temperatures of above 100C. The RFID tags are placed on the individual shelves and data such as the location of the shelves, meat type and weight data, is written to the tag (Escort, 1998c). Marks & Spencer Company also used RFID technology on their men's suits, shirts, and ties at its High Wycombe store. The RFID tags let Marks & Spencer check stock deliveries to count inventory quickly in its stores, and depots. To keep low prices, they use passive tags with limited information such as size, style and color (Butalla, 2004). RFID has even spread out to the pharmaceuticals area. According to Butalla, the FDA (Food and Drug Administration) has recently expected to use RFID for the fight against counterfeiting. RFID technology is a reliable track and trace system, thus would help secure the integrity of the drug supply chain by providing an accurate drug pedigree. In addition, Delta Air Lines also used RFID to run a pilot test and correct misplacement of baggage. (Butalla, 2004).

3. Problems with RFID

RFID is going to change the way companies do business. It makes it easier than ever before to track and trace specific items throughout the supply chain. However, there are still some obstacle issues. The obstacles to widespread RFID adoption are privacy, political and technical.

3.1 Consumer Concerns about Privacy

Because of the widespread use of RFID, the consumers worry about their privacy. They claim that their lives will be invaded by state and global corporations if they allow this technology to expand. Some of these concerns are reasonable. If RFID technology tracking is misused by unethical people or companies, the results could be harmful. However, while these fears are understandable, they can be successfully addressed. Consumer groups are working to ensure the safest practices for this new technology. The individual shopper can put control in their hands through a combination of technological safeguards, regulations and sensitivity to consumer concerns. This way, retailers can enjoy the business advantages of RFID, while consumers can enjoy an improved shopping experience (Calkins, 2004).

Despite the concern of consumers, RFID offers ways to make shopping easier, quicker and safer. Smart shelves and automated checkouts are in a progress to make customers' shopping life better. Smart shelves can detect how many items are on them and can also check for correct items. Electronic shelf labels assure that the price given on the label is the same as the checkout, and the labels are updated immediately as prices change. The Intelligent Scale identifies and weighs the product and prints out an RFID sticker for the item. If the customers are concerned about privacy, they have the option of deactivating the RFID tags on their items by placing the items on the De-Activator after the customer check out of the store. In addition, the customers are no longer waiting in check-out lines. And at home, smart fridges that warn you when you are running short on necessary items or propose a meal or recipe based on what you have got at home (Lillo, 2004).

3.2 Technical Problems

The RFID signal, which is the tendency of liquids to absorb electromagnetic energy, is part of the technical problem. Everything will work fine, if you are operating an RFID network in your warehouse in a controlled test environment. But, if you have 75 cases of beer, for example, on a pallet rolling by a reader at 10 mph, the reader might only pick up the cases of beer on the outside of the pallet and there is a good chance that the cases on the inside will not be read. The range of the reader is short, the forklift is going too fast, and the cases in the middle are concealed behind too many other cases of beer for their tags to be accurately tracked. As you see, if the RFID has problems with passing through beer, it will probably have problems with liquid soap. However, there is a solution to this problem. High-power reader and a low-power tag will solve the problem. Passive tags have no power of their own. They are only active when interrogated by a reader and reflect back that reader's wake-up signals (Schwartz, 2004).

Another obstacle is the problem with placing RFID tags. Large retailers and their suppliers are facing a significant engineering challenge as they begin tagging cases and pallets. According to Rupert Ralph, his team has tested RFID tags on pallets and found that the technology can fail if applied inappropriately. In addition, the tags are vulnerable to wear and tear in the warehouse that could render them unreadable once they reach their destination. The metal mass of the forks can cut off the signal to the tag or reduce the read distance. According to Rupert, two tags could be needed to ensure a drive-through read at a dock door. Tag placement has emerged as an important factor for both case and pallet tagging in every pilot conducted so far. Rupert adds that the goal of his study was to alert companies to these issues before they even begin their pilot programs. However, as long as the tag is placed properly, it is readable and it can be placed anywhere on the load. They can be placed on the pallet itself, on the last carton on the pallet, or even on the stretch wrap, as in Figure 5 (Albright, 2004).

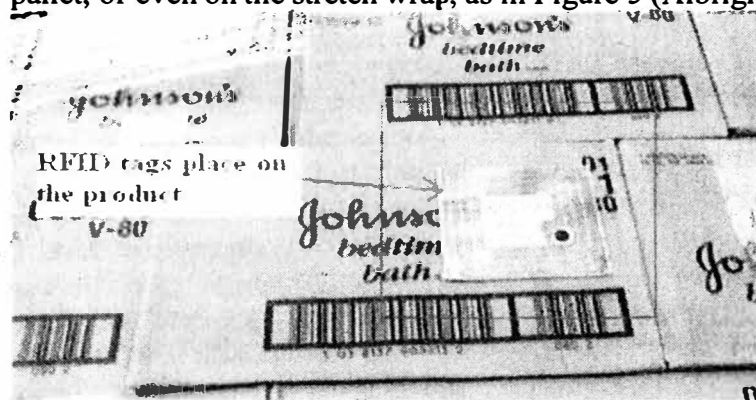


Figure 5. A tag placed on products

Source: Kinsella, 2003

3.3 Problems with Wal-Mart and Its 100 Suppliers

Wal-Mart announces that it requires all suppliers to put RFID tags carrying Electronic Product Codes on pallets and cases by the end of 2006. However, some of the larger suppliers are concerned that they do not have enough time to meet the deadline.

3.3.1 Problem in China

China is a huge manufacturer and is one of the top suppliers of Wal-Mart. It is reported that Wal-Mart already buys about \$15 billion in goods a year from China and now is pushing its global suppliers to adopt RFID, because it believes that applying RFID technology will save billions annually through improved efficiency. In some cities, like Shanghai and Beijing, it has already been applied to smart cards that can be used to pay subway tolls or taxi fares. However, to apply the RFID-visibility into the supply chain is to threaten too quick adoption. The Chinese government is cautious of adopting a foreign standard, and has indicated that the frequency range of passive tags chosen by the United States, Europe, South Korea and Japan conflicts with current frequency allocations. The nation still struggles in debate over how its standard should look. Nevertheless, China could allow companies to use RFID tags and readers that are similar to a particular region's standard, but just within the factory. By doing that, China could satisfy the demands of its important trade partners and still have a separate standard that works in this country (Cledenin, 2004).

3.3.2 Problems in E. & J. Gallo Winery.

E. & J. Gallo Winery is another big supplier that is required to ship RFID tagged cases and pallets to Wal-Mart's distribution centers by January 2006. Yet the complicated issues ahead for Gallo show why requirement of applying RFID technology is not easy to meet. According to a recent survey conducted by analyst firm, Forrester, the main problem for suppliers is the cost of implementation. Forrester estimates the total price tag to launch and maintain an RFID program for one year could cost a typical Wal-Mart supplier more than \$9 million dollars. Since most states require that wine and liquor be sold through distributors, Gallo needs to bring its some 480 distributors into the project and problems arise. For more complication, those distributors often put wines from multiple companies on the pallets they ship to retailers. Thus, the responsibility of the identification for the case and the mixed pallets is a big issue here (Sullivan, 2005).

Another part of the problem is the RFID rate is slower than today hype's suggests. The reason is some stores still rely on paper orders, the post office and the fax machine. Some shops view RFID as a representation for an incremental improvement over current technologies. Bar codes already provide substantial data with an existing set of standards and a high level of accuracy. RFID tags can be read with reduced labor cost, but some companies do not really want to spend very much on reading bar codes. If RFID only enables collecting data that is not actually used fully or effectively, then industry probably hasn't gained much. It is, business practice, not technology, that the primary key to supply-chain superiority. Recent Capital Consulting & Management Inc. (CCMI) survey found that only 20 percent of companies that invested in supply-chain-related information technology systems over that past few years could achieve a return on investment from these IT systems (Elliff, 2004).

However, as applications increase and the price of RFID labels falls, all kinds of further benefits arise, such as more and better in-store product information, and assurance of product authenticity (reduction in counterfeiting). And with the huge motivation now behind RFID in supply chain management, its extension to stores is likely to continue. Retailers can achieve significant business efficiency gains, more convenience, more enjoyable shopping and systems better tailored to their needs (Calkins, 2004).

4. Conclusion

RFID technology can bring benefits in improving efficiency in supply chains, providing issues of cost, and standards can be resolved. Innovative uses of RFID technology benefits supply chain from reducing out-of-stock items, cutting headcount, gaining better visibility, and preventing counterfeit and theft. In addition, RFID not only move beyond the supply chain, it also enters other business and consumer use. It can be used for almost every business such as transportation, personal identification, and medical (Lapide, 2004).

Unfortunately, there are some problems with this new technology. As RFID is using widely, the consumers concern about their privacy is one of the problems. Another problem is technical problems such as RFID signal, where to place tag. Moreover, high cost of RFID tags and lack of standards are another problem.

To get the maximum benefits of RFID technology, companies must understand the technology. According to the Engineer journal, some of following advice will help to improve the use of RFID:

First, start to learn how best to employ RFID in your environment by limited trials. Second, increase the complexity and scale in the phases of trials. Third, be prepared to make process changes to fit the technology and take advantage of its key benefits. Fourth, develop a strategy from the beginning for capturing and managing the data generated by RFID tags. Last, employ a cross-functional team to shape, operate, and measure the initiative (Kinsella, 2003).

And before contemplating an RFID strategy, according to Rappold, you should: First, understand what customers truly want, how they buy and use the product, and the lead-time they expect for product deliver. Second, the firm must have the physical capability to take advantage of the additional information. Firms with unpredictable equipment, unreliable manufacturing processes, long supplier lead-times, and facilities with long and variable flow times have little to gain from RFID. Third, RFID systems will create a lot of data quickly. The firm must have the information basic to store, transmit, and process the data across the organization and to its suppliers.

Acknowledgement

I have gained valuable experiences and knowledge through conducting scientific research over the past year. I gratefully acknowledge Office for Undergraduate Research OURE for providing the opportunity to expand my horizons through research. I would like to thank Dr. Bih-Ru Lea, my faculty advisor and mentor, for her support, encouragement, and guidance.

Reference

1. Atkinson, William; July 2004; Tagged: The Risks and Rewards of RFID Technology; Risk Management; 51(7), 12-17.
2. Butalla, Laura; Jun 2004; The hottest trends in smart labels & packaging; Converting Magazine; 46-47.
3. Calkins, Bill; September 2004; The Great Debate; Greenhouse Grower; 44 – 48.
4. Chase, R.B, Jacobs, R.F; 2000; Operations Management for Competitive Advantage; Irwin Publishing Co.; Chicago, IL;30-45.
5. Chopra, S. and Meindle, P.; 2001; Supply Chain Management: Strategy, Planning, and Operation; Prentice Hall, Inc., Upper Saddle River, NJ; 1-24.

6. Clendenin, Mike; October 25, 2004; China mulls proprietary; Electronic Engineering Times; 1-4.
7. Craig, T. February 23, 1996; Supply Chain Agility: Inducing World Class Performance for the 21st Century; 1-2.
8. Elliff, Scott; September 2004; RFID: maybe not the 'next big thing'; Journal of Commerce; 1-2.
9. Finkenzeller, Klaus; 2003; RFID Handbook: fundamentals and applications in contact less smart cards and identification, translated by Rachel Waddington, 2nd ed, Wiley; 20-23.
10. Fisher, M. March; April 1997; What is the Right Supply Chain for Your Product? Havard Business Review, 105-116.
11. Gladson, Ted; March 2003; No stock, no sale, no business; Aftermarket Business, 113(3), 6.
12. Green, Martin, December 2004, Availability on the shelf: the last great challenge for Retail; Logistics and Transport Focus; 6(10), 22.
13. Howe, Amanda; October 2004; The implications and benefits of RFID; Retail World; 34-35.
14. Kinsella, Bret; November 2003; The Wal-Mart Factor; Industrial Engineer; 32-37.
15. Lapide, Larry; Summer 2004; RFID: What's in it for the forecaster? The Journal of Business Forecasting Methods & Systems; 23(2), 16.
16. Laudon, K.C. and Laudon, J.P.; 2001; Essentials of Management Information Systems: Organization and Technology in the Networked Enterprise; Prentice-Hall, Upper Saddle River, NJ; 80-94.
17. Lillo, Andrea; January 2004; Store of the Future is here today; Home Textiles Today; 25(19), 11.
18. Mainardi, C.A., Salva, M., and Sanderson, M; 2nd Quarter 1999; Label of Origin: Made on Earh,. Strategy Management Competition; 20-28
19. Mentzer, J.T., Foggin, J.H., and Golicic, S.L.; September 2000; Collaboration. Supply Chain Management Review; 4(4), 52-60.
20. Mohamed, Arif; November 2, 2004; RFID poised to move beyond supply chain ; Computer Weekly; 22-23.
21. Rappold, James; November 2003; RFID: The Risks of RFID; Industrial Engineer; 37-38.
22. Roberts, Simon; March 2003; Tracking medical devices via RFID; Frontline Solutions. 12(2), 54.
23. Sawyer, Tom; December 13, 2004; Researchers Are Getting Serious About Electronic Tracking Tags; 253(23), 28.
24. Schwartz, Ephraim; November 29, 2000; RFID: Look before You Leap. InfoWorld; 26(48), 16.
25. Simchi-levi, D., Kaminsky P., and Simchi-levi, E.; 2000; Designing and Managing the Supply Chain; Irwin McGraw-Hill Companies, Inc., Boston, MA; 15-165.
26. Spiegel, Robert; September 2003; Blind spots. Logistics Management (2002); 42(9), 49.
27. Tesoriero, Heather Won; Nov 16, 2004; Radio ID Tags Will Help Monitor Drug Supplies. Wall Street Journal (Eastern edition). D.9.
28. Youngdahl, W.E; 2000; Supply Chain Management; John Wiley & Sons, Inc.; Toronto, Canada; 60-82.
29. Sullivan, Laurie. January 2003. RFID: The Plot Thickens. InformationWeek; (24), 3.
30. Wu, Jianghua; May 2005; Quantity flexibility contracts under Bayesian Updating; Computers & Operations Research; 32(5), 12.

**Cultural Mindset Concerning Water:
Ongoing Research in Lemoa, Guatemala**

Moya O'Berry

Jim Martin, Ph.D.

Dept. of Psychology

Curt Elmore, Ph.D.

Dept. of Geological Engineering

Abstract

Attitudes and behaviors regarding water consumption were investigated in two rural indigenous communities in the central highlands of Guatemala. Results indicated that residents of a community at which a deep (245 m) well had been installed were more favorably disposed toward well water. Directions for future research include education for the local residents about their water sources and the link between illness and contaminated water, thereby leading to greater usage of the well. Implications for collaboration between engineering and social science approaches are discussed.

Cultural Mindset Concerning Water: Ongoing Research in Lemoa, Guatemala

In 1999, the World Health Organization reported that annually, there are 2.2 million diarrhea-related deaths, with contaminated drinking water being a direct factor.

Guatemala is a specific country where this is a dilemma. Many people, especially children under the age of five, are greatly impacted by this continuing problem.

Although water is Guatemala's most abundant natural resource (Annis & Cox, 1982), there is difficulty in transporting water to the areas where it is most needed (Bovay Engineers and CNPE, 1976). A perfect example is that of the orphanage in Lemoa, Guatemala.

The Hogar de los Ninos orphanage in Lemoa, Guatemala experienced water shortage when relying on existing water sources in the town. Addressing this need, Dr. Curt Elmore from the University of Missouri at Rolla came to Lemoa in March of 2002 and drilled a deep water well (800 ft). Besides providing an abundant amount of water, the well water did not need any form of treatment. This was a great provision for the orphanage considering that clean water is especially vital for the children. Because of the excess supply of well water, it was acknowledged that sharing the new resource with the town would be helpful to others.

In March of 2003, Dr. Elmore took a class of engineering students to Lemoa to install a water-extension system; this would help to sustain many more than just those at the orphanage. A water spigot was installed outside of the orphanage for public usage. The spigot was metered to keep track of the amount of water being utilized. Data collected from the meter showed that approximately one family's worth of water was being used.

As researchers, this poses an interesting question. Why would so few people be using the spigot if it provides pure water free of charge to anyone who wants it? This question fueled the trip to Guatemala in 2004 by Dr. Jim Martin and Moya O'Berry, a psychology professor and student at UMR, respectively. We believed that the mindset behind these decisions is what we needed to uncover. Previous research has shown that the installation of superior apparatus or institutional mechanisms to deliver safer water to rural areas does not ensure that inhabitants of such areas will immediately abandon water consumption habits they may have observed for generations (Kroutil & Eng, 1989).

Realizing the general need to explore this culture's water drinking attitudes and behaviors, yet implement it with a specific plan, a survey was constructed for the purpose of gathering information on personal water habits and usage. The survey was made both for the Lemoan residents, especially those living near the well water source, and those in another town removed from the well source. The survey was made to address the following research questions:

We wanted to know if residents related illness to water. As cited earlier, the World Health Organization reported deaths numbering in the millions due to diarrhea-related sickness, where contaminated water is a direct factor. Our rationale: How accurate are peoples' perceptions of risks associated with water?

Our second question is if they believed their current water source was safe. Our rationale: Why should people switch water sources if they believe their current source is safe?

We also wanted to get a general idea of peoples' opinion of well water. Our

rationale: Would prior experience with unclean well water have an effect on their attitudes toward well water? Has the Hogar well impacted Lemoa residents' attitudes?

Method

Participants

Sample 1. Twenty-one residents (16 women, 5 men, age: $M = 39.48$, $SD = 15.68$) of Lemoa, a small village in South-central Guatemala, were selected based upon their proximity to the new water source (spigot). Most of our participants were women. This is likely to be due to the time of day we collected our data; most of the men were working. Women are the ones that gather water for the family and stay home during the day, so we wanted to talk to them. As compensation, they were given five quetzals (Q5).

Sample 2: Thirty residents (19 women, 11 men; age: $M = 36.00$, $SD = 12.76$) of Camancaj, a village to the southwest of Lemoa, were surveyed. Respondents were recruited at the Salud y Paz medical clinic, where they were waiting for routine dental examinations. They were also paid five quetzals for participating.

Materials

A 32-item questionnaire was developed after reviewing previous research in water consumption behaviors and attitudes [Gregory & DiLeo, 2003]. It was translated into Spanish and then back-translated into English. The two versions agreed nearly perfectly. Dimensions included: (a) primary sources of water currently used; (b) source of parents' water; (c) whether anyone in their family had been sick from drinking water; (d) whether they believed their current source of drinking water was safe; and (e) what their opinion was of well water.

Procedure

The surveys were made before the trip to Guatemala. Upon arrival, we hired members of the Chichicastenango volunteer fire department to serve as translators (English/Spanish/Quiche) at both data collection sites.

The first wave of data collection occurred at Lemoa. Initially, we piloted the survey on a group of three female employees from the orphanage. We then had to reduce our survey from 32 questions to 11 based on their responses. They had trouble answering all the questions as they thought many of the questions were repetitive. Once we revised our survey, we hired a well-known local to lead us around to peoples' houses. This was for guidance and to make the people more comfortable talking to us. Our translator also conversed with participants and explained that we were gathering data on their water usage habits. Any questions that arose were answered and then the survey was administered. Responses to open-ended questions were recorded verbatim, allowing for coding to be done later. After finishing the survey, the participants were paid (Q5) and thanked for their time. The second data collection site was at Camanaj, and similar procedures were used.

Results

Statistical Procedures

After gathering the data, it was coded and put into categories. Open-ended responses to structured questions were coded dichotomously such that "yes" responses were coded "1," and "no" responses were coded "2." Responses were coded by raters from the context of the answers. For example, where a respondent reported that well water is "ok," it was coded "1," implying that it was good. If a respondent reported that well water was "dirty," it was coded with a "2," implying that it was bad.

Means and standard deviations for both samples are reported in Table 1.

Independent sample t-tests were employed to investigate the three research questions.

These results are reported in Table 2. Lemoa residents reported less family illness due to contaminated water than Camancaj residents ($t(49) = 2.012, p = .05$). The groups did not differ in their perceptions of the safety of the water they currently use ($t(49) = .154, p = .878$). However, significantly more Lemoa residents reported that well water is safe for consumption ($t(49) = 2.418, p = .019$).

Discussion

The goal of our research was to determine whether residents related illness to contaminated water, their perception of the safety of their water, and their opinion of well water. We surveyed people living near the well in Lemoa and also residents of Camancaj. We found that many people living in Lemoa reported less sickness due to contaminated water than those living in Camancaj. The groups did not differ in their perceptions of the safety of the water they currently use. Also, significantly more Lemoa residents reported that well water is safe for consumption.

The Camancaj respondents, with no access to deep-drilled, sanitary wells, were more suspicious of well-water than were the Lemoa residents. It appears that the well has had a significant impact on the residents of Lemoa. They reported that well water is safe for consumption, whereas Camancaj residents do not have the same opinion of well water. This may be due to only good reports from those using the Hogar well, while people from Camancaj may have experienced bad water coming from wells if they have been dug too shallow and get contaminated.

These findings are important because they give us a glimpse into a cultural difference between Guatemala and the U.S. Although other water intervention systems have been tried for other rural Guatemalan towns, drilling deep water wells seems more logical and sustainable when compared with other systems. For example, having people mix chemicals with their water (Rangel, Lopez, Mejia, Mendoza & Luby, 2003) is a good short-term solution. However, these chemicals can become bothersome, sources can run dry, or people tire of using them. Another intervention is that of educating people to boil their water. It is widely recommended that people boil water for at least 20 minutes, however, when wood is the residents' meager source for heat, people become impatient and do not usually boil their water for the complete 20 minutes.

From the data, it would seem that education is necessary before Guatemalans will realize the benefit of deep well water. Unless they link sickness with contaminated water and are informed of the safety of different sources, it would not be reasonable for anyone to assume that they would be compelled to use the new water source. Similar strategies have been implemented in communities in Sub-Saharan Africa where social marketing and motivational interviewing were combined to induce people to employ safe water treatment and storage methods (Thevos, Olsen, Rangel, Kaona, Tembo, & Quick, 2003).

Limitations of the present study: 1) Only descriptive data has been obtained. It cannot be inferred that the deep well impacted Lemoans' attitudes without experimental study, which is not possible under the circumstances. 2) Our study is limited by the small sample size. Residents had to be individually interviewed, due to the low levels of literacy.

More research would be helpful in finding the best ways to educate the people about their water, and learn how well water can best be delivered to people from more than just a spigot. Some residents mentioned that they would like to pay for the well water, so that is another area that should be looked into.

One of the most daunting challenges to be overcome in future research and fieldwork is the mindset that we can come in and change the well-established patterns of a society just by telling people that it would be better for them. They may be suspicious of our intent or expect more from us than is deliverable. Much time and effort may be required to earn a good rapport with the people and have credibility in their eyes.

There are also disputes over water sources and who rightfully owns them, and this can be a real problem if pipe systems would need to be used. When a pipe runs through someone's property, they feel they have a right to that water, so how would you transport water without causing an uproar?

Typically, most interventions have involved either an engineering or a social approach. In the present study the investigators combined these, leading to better understanding of the problem and what can potentially be done to solve it. Combining the practical and people-oriented strategies can be difficult, but will ultimately lead to a more widely-accepted solution.

References

- Annis, S., & Cox, S.B. (1982). The integration of small-scale irrigation and village potable water systems in Guatemala. *Water Supply & Management*, 6, 455-464.
- Bovay Engineers, Inc. and Secretaria del Consejo Nacional de Planificacion Economica (CNPE) (1976) *Pr-feasibility Study for a Master Plan for the Protection of Guatemala's Renewable Natural Resources*, Vol. 3, *Water*. CNPE, Guatemala.
- Gregory, G.D., & DiLeo, M. (2003). Repeated behavior and environmental psychology: The role of personal involvement and habit formation in explaining water consumption. *Journal of Applied Social Psychology*, 33, 1261-1296.
- Kroutil, L.A., & Eng, E. (1989). Conceptualizing and assessing potential for community participation: A planning method. *Health Education Research*, 4, 305-319.
- Rangel, J., Lopez, B., Mejia, M.A., Mendoza, C., and Luby, S., (2003). A novel technology to improve drinking water quality: a microbiological evaluation of in-home flocculation and chlorination in rural Guatemala. *Journal of Water and Health* 01.1, pg 19.
- Thevos A.K., Olsen, S.J., Rangel, J.M., Kaona, F.A., Tembo, M., & Quick, R.E. (2003). Social marketing and motivational interviewing as community interventions for safe water behaviors: Follow-up surveys in Zambia. *International Quarterly of Community Health Education*, 21, 51-65.
- WHO 1999 *Guidelines for Drinking-Water Quality*, 2nd edition. World Health Organization, Geneva.

Table 1. Descriptive Statistics

	Sick		Safe		Well water	
	M	SD	M	SD	M	SD
Lemoa	1.90	0.301	1.24	0.539	1.24	0.436
Comanchaj	1.67	0.479	1.17	0.379	1.57	0.504

NOTES: $N = 21$ (Lemoa); $N = 30$ (Comanchaj)

Sick: Has any family member ever been sick from unclean water?

Safe: Do you believe the water your family uses is safe?

Well water: What do you think about well water (*lit.* water that comes out of the ground?)

Table 2. Test for Equality of Means of Water Attitudes between Lemoa and Camanchaj Residents.

	t	df	Std. Error Difference	95% Confidence Interval of the Difference	
				Lower	Upper
Sick	2.012*	49	0.118	0.000	0.476
Watersafe	0.154	48	0.108	-0.200	0.234
Wellsafe	2.418*	49	0.136	0.056	0.602

*p < .05

New Technology Does Old Tricks

Ryan Parish

ABSTRACT

The purpose of this project was to create an interactive slide rule accessible over the Internet, usable to illustrate both the principles behind logarithms and how to use a beautiful but obsolete piece of technology. To see this project in action, visit it on the web at <http://web.umn.edu/~ouresr/SlideRule/SlideRule.htm>.

INTRODUCTION

Throughout history, Scientists, Accountants, and Engineers have always needed to be able to do large amounts of computing quickly and reliably. Operations like square roots, logarithms, and even multiplication and division can get very tiresome quickly, and errors in computation can also build up if one is doing large amounts of calculating by hand.

John Napier first developed the mathematical principles behind the Slide Rule in 1614. He was the first to discover logarithms and their properties, especially that $\log(x) + \log(y) = \log(x \cdot y)$. 6 years later, Edmund Gunter used these to construct the first Slide Rule, which consisted of only what we later called the C scale, along with a crude way of tracking distance. In 1630, William Oughtred added another scale, enabling easier computation that could be obtained by sliding the two scales back and forth. Later slide rules had many more scales, and could be found in circular form as well.

Ironically, what I am using to demonstrate the awesomeness and power of the slide rule is in many ways the descendant of the calculators that killed the slide rule in the first place. The computer program that runs the slide rule has more degrees of accuracy than the most powerful slide rule ever made, and can solve equations far quicker than even the most skilled humans can match.

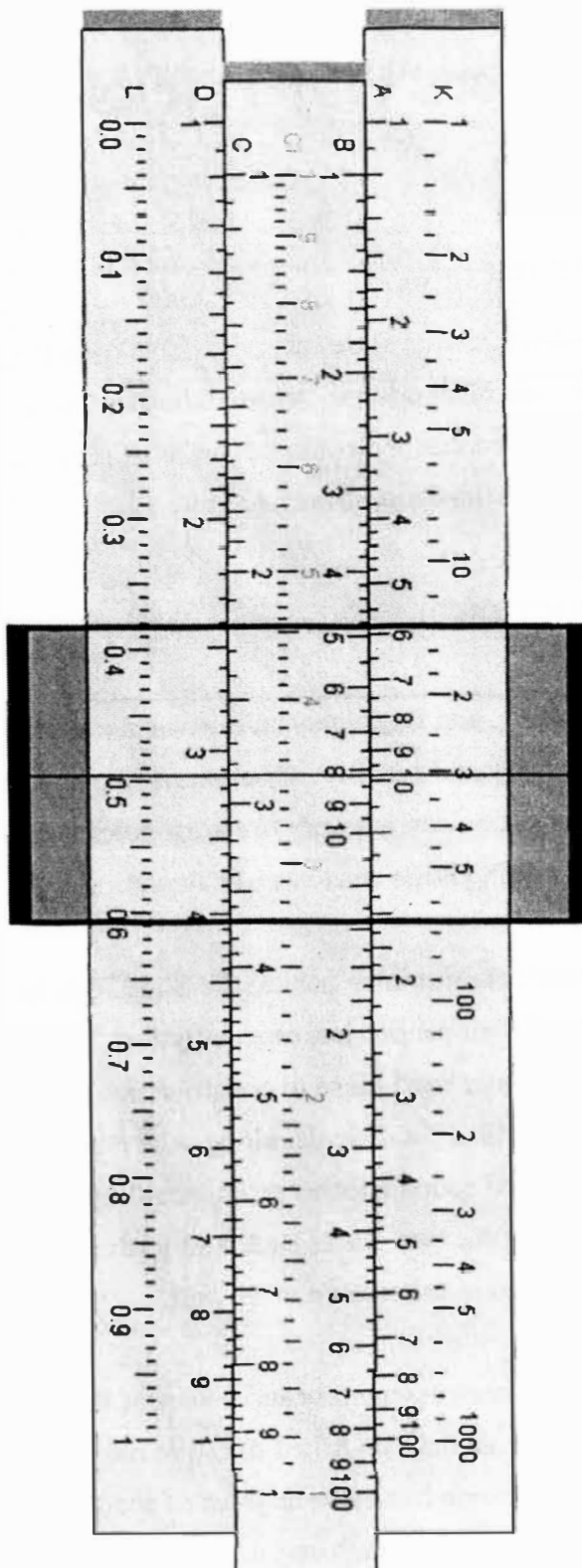


Figure 1: The Slide Rule

This is the slide rule that you will see when you go online to visit my project.

Note that it has 7 Scales, each labeled with a different letter. Also note the center slide which can move back and forth independently of the other two.

The line going through the black box in the middle is the indicator. It is a line that can slide back and forth to measure scales relative to each other.

ABOUT THE SLIDE RULE

Slide rules consist of many different scales, each labeled with a different letter (or letters, such as the CI scale). While each scale has the same length, the scales measure different ranges of data and measure the length differently. The Slide Rule I created has 7 scales that can do 9 different operations. (See Figure 1). Other slide rules besides mine may have more or fewer scales, which would enable them to perform different functions.

The scales that my slide rule has, in order from top to bottom are:

K is a logarithmic scale going from 1 to 1000.

A is a logarithmic scale going from 1 to 100

B is a logarithmic scale going from 1 to 100 on the center slide.

CI is a logarithmic scale going from 10 to 1 on the center slide.

C is a logarithmic scale going from 1 to 10 on the center slide.

D is a logarithmic scale going from 1 to 10,

and L is a metric scale going from 0 to 1.

Because of this setup, the scales are all related in mathematically significant ways.

If all the scales are aligned,

(1) $10^L = C = D$.

(2) $10 * 10^{-L} = CI$.

(3) $100^L = A = B = C^2 = D^2$

(4) $1000^L = K = C^3$

Therefore, (5) $\log(C) = \log(D) = L = \log(A)/2 = \log(B)/2 = \log(K)/3$

The operations that you can perform with this slide rule are: Multiplication, Division, Squares, Square roots, Cubes, Cube roots, Logarithms, Powers of 10, and Multiplicative inverses.

HOW IT WORKS AND WHY

Notation: for all positive real numbers x , I use the notation (6) $x = X \cdot 10^{E(x)}$, where X is a real number in $[1,10)$ and $E(x)$ is an integer such that the equation holds.

For negative x , (7) $x = -X \cdot 10^{E(x)}$ instead of $X \cdot 10^{E(x)}$.

One can use D, A, and K to find the squares, square roots, cubes, and cube roots of numbers.

Finding Squares:

For any non-zero x , X will be on $[1,10)$. Furthermore, (8) $x^2 = X^2 \cdot 10^{2E(x)}$. Since the A scale is equal to the square of the D scale, and X is on the D scale, we can use the indicator to find X^2 . Then we double the E value of x and we have found the square of x , that is, $X^2 \cdot 10^{2E(x)}$.

Finding Square roots:

Let q be a non-zero real number, and let Q be in $[1,100)$, and $E(q)$ an even integer such that (9) $q = Q \cdot 10^{E(q)}$. To find the square root of q using our scale, we begin by finding Q on the A scale. We use our indicator to find the square root of Q by checking the indicator's value on the D scale. Since (10) $\sqrt{q} = \sqrt{(Q \cdot 10^{E(q)})}$, we have found the square root of q .

Finding Cubes:

For any non-zero x , X will be on $[1,10)$. Furthermore, (11) $x^3 = X^3 \cdot 10^{3E(x)}$. Since the K scale is equal to the cube of the D scale, and X is on the D scale, we can use the indicator to find X^3 . Then we triple the E value of x and we have found the cube of x , that is, $X^3 \cdot 10^{3E(x)}$.

Finding Cube roots:

Let c be a non-zero real number, and let C be in $[1,1000)$, and $E(c)$ an integer multiple of 3 such that $c=C*10^{E(c)}$. To find the cube root of c using our scale, we begin by finding C on the K scale. We use our indicator to find the cube root of C by checking the indicator's value on the D scale. Since the cube root of c is equal to the cube root of $C*10^{E(c)/3}$, we have found the cube root of c .

Finding Logarithms:

For any non-zero x , X will be on $[1,10)$. Furthermore, we know that L is equal to the log of D . Therefore, We can place the indicator at the value of X on D and the value at L will be equal to the log of X . Since (12) $\log(x) = \log(X)+E(x)$, we can find the log value of x .

Finding Powers of 10:

Suppose we want to find 10^p , where p is a real number. Then for all non-zero p , $p=I+P$, where I is an integer and P is in $[0,1)$. Then P is on the L scale, and we can find 10^P by taking the indicator to the L scale and then checking its value on the D scale. Since (13) $10^{(I+P)}=10^P*10^I$, we have found the power of 10 for which we are looking.

Finding Inverses:

Suppose we want to find the reciprocal of $x=X*10^{E(x)}$. We know that the C scale is equal to 10^L , and the CI scale is equal to $10*10^{-L}$. Therefore $1/C=CI/10$. So we can take the indicator, put it over X on the C scale, and find $10/X$ on the CI scale. Since (14) $1/x=1/X*10^{-E(x)}=10/X*10^{-(E(x)-1)}$, we can use the slide rule to find reciprocals as well.

Although Multiplication and Division are the more basic operations with a slide rule, they are more complicated than the others mentioned, so I have saved them for last here.

Multiplication:

Suppose we are given (15) $y=Y*10^{E(y)}$ and $x=X*10^{E(x)}$. We can use the slide rule to find the product of X and Y.

The Easy Way:

We know that (16) $y*x=Y*X*10^{E(y)+E(x)}$. Since $100^L=A=B$, If X is on the A scale, and Y is on the B scale, then the distance from 1 to X on the A scale + the distance from 1 to Y on the B scale is equal to (17) $\log(Y)/2+\log(X)/2 = \log(XY)/2$ on the L scale. Going back up to the A scale we find that $\log(XY)/2$ on the L scale is equal to $X*Y$ on the A scale. This means that if we offset the B scale by the distance from 1 to (X) on the A scale, that the value of Y on the B scale will be equal to the value of (XY) on the A scale.

The Better Way:

We know that $y*x=Y*X*10^{E(y)+E(x)}$. Since $10^L=C=D$, If X is on the C scale, and Y is on the D scale, then the distance from 1 to X on the C scale + the distance from 1 to Y on the D scale is equal to (18) $\log(Y)+\log(X) = \log(XY)$ on the L scale. Since $\log(XY)$ on the C scale is equal to $\log(X)+\log(Y)$ on the L scale, we know that if we slide the 1 of the C scale to the value of X on the D scale, then the value at Y on the C scale will be equal to the value of $X*Y$ on the D scale. Therefore we can find the value of $X*Y$ and use it to find the value of $x*y$, using the formula $x*y=X*Y*10^{E(x)+E(y)}$.

Note: Often $X*Y$ will be off the scale. When this is the case, place the 10 of the C scale onto X of the D scale, and then look at the value of the C scale at Y. Directly under this will be the value $(X*Y)/10$. This works because $\log(X)+\log(Y)-\log(10)=\log(XY/10)$.

Division:

Not surprisingly, the Slide Rule can be used to solve x/y , too.

The Easy and Better way for Division:

We know that $(19) x/y = X/Y * 10^{E(y) - E(x)}$. We find the value of X on the D scale, then place Y on the C scale directly above it. Since $\log(X) - \log(Y) = \log(X/Y)$, where the value of 1 is on the C scale will also be the value of X/Y on the D scale. Once we have X/Y, we find x/y by $x/y = X/Y * 10^{E(y) - E(x)}$.

Note: Often X/Y will be off the scale. In this case, look at the value of the D scale where the C scale is 10. Since the Value there is equal to $10 * X/Y$, We can divide that number by 10 to get X/Y.

For examples go to <http://web.umn.edu/~ouresr/SlideRule/SlideRule.htm>. Type the equation into the calculator you will find there and you will see a diagram showing how to solve your problem, along with a brief explanation.

ABOUT THE CODE

My Slide Rule Program was based off code written by Matt Battles a year earlier. In the original code, Matt created a slide rule similar to the one in my program, with the ability to slide the indicator and the center scale back and forth. There was not any indication, however, of how to use the slide rule. I originally changed the slide by replacing his scales with (I believed) more useful ones. I kept the C, D, and CI scales, but added the K, A, B, and L scales. The L scale especially I thought was important, because it illustrates the logarithms behind the slide rule much more effectively. I also changed the way the graphics displayed to make the display less jerky and update quicker. I also added the entire calculator, as well as the calculator's interface with the rest of the program. All of my work was done with Java using the free NetBeans compiler provided by Sun Microsystems, Inc. While the code will (in theory) run on all browsers, I have experienced some difficulty in that regard, as different browsers will interpret the same program differently. I tested this code using Mozilla, so I know that browser will show it properly. Internet Explorer will not, at this time, show the applet correctly.

NOMENCLATURE

Indicator: A line that slide back and forth across the Slide Rule, allowing for accurate measurements between non-adjacent scales.

Scale: A way of measuring distance. The slide rule has many different scales, some of the logarithmically based.

It is assumed that all logarithms are base 10.

ACKNOWLEDGMENTS

I would like to acknowledge Matt Battles, who gave me the idea to do all of this, and Dr. Roe, my adviser for this project and my Mathematics degree, who has provided me with lots of help over the years.

REFERENCES

“Learning to Use The Slide Rule”, Kueffell & Esser Co. © 1961.

A copy of the code behind this project is in the hands of my adviser, Dr. Roe. It is freely available to any University of Missouri-Rolla faculty or OURE officials.